



Durham E-Theses

Design and application of bifunctional organic catalysts

Arnold, Kenny

How to cite:

Arnold, Kenny (2008) *Design and application of bifunctional organic catalysts*, Durham theses, Durham University. Available at Durham E-Theses Online: <http://etheses.dur.ac.uk/2514/>

Use policy

The full-text may be used and/or reproduced, and given to third parties in any format or medium, without prior permission or charge, for personal research or study, educational, or not-for-profit purposes provided that:

- a full bibliographic reference is made to the original source
- a [link](#) is made to the metadata record in Durham E-Theses
- the full-text is not changed in any way

The full-text must not be sold in any format or medium without the formal permission of the copyright holders.

Please consult the [full Durham E-Theses policy](#) for further details.

Design and Application of Bifunctional Organic Catalysts

The copyright of this thesis rests with the author or the university to which it was submitted. No quotation from it, or information derived from it may be published without the prior written consent of the author or university, and any information derived from it should be acknowledged.

A thesis submitted to Durham University for the degree of Ph.D.

Kenny Arnold

Department of Chemistry

2008



18 APR 2008

Declaration:

I confirm that no part of the material offered has previously been submitted for a degree or qualification at this or any other university or institute of learning.

To my parents and sister

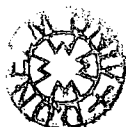
Acknowledgement

Firstly, I would like to thank my supervisor Dr. Andy Whiting for his guidance, advice and support. In particular, the encouragement to attend and present at workshops and conferences has proven to be an excellent opportunity to further my personal and professional development. I would also like to express my appreciation to my GSK supervisor Bryan Davies, who has provided an alternative viewpoint to solving problems that I encountered, and has been very helpful throughout.

I would like to acknowledge the analytical services at Durham. In particular: Dr. Andrei S. Batsanov for performing X-ray crystallography; Dr. Alan Kenwright, Catherine Heffernan and Ian McKeag of the NMR service; Dr. Mike Jones, Lara Turner and Jackie Mosely of the mass spectrometry service; and Jarika Dostal and Judith Magee from elemental analysis. I would also like to thank Emma Smart and Judith Magee for letting me borrow items at short notice from the undergraduate laboratory, and Richard Hudson from ReactArray for his prompt and effective assistance in solving issues that arose with our synthesis workstation. I would like to acknowledge the efforts of the Lab Automation team at GSK, in particular: Adrian Bateman, Sharon Bell, Toby Broom, Kathy Harwood and Dan Tray, for their help with matters relating to Design of Experiments and HPLC.

I must also thank past and present members of the Whiting group for their support and assistance over the last three years. Particular thanks go to Dr. Christophe Grosjean, Dr. Damien Héroult, Dr. Richard Giles, Dr. Steven Twiddle, Dr. Carl Thirsk, Dr. David Jay, Jon Knowles and Karel Aelvoet.

ABBREVIATIONS.....	3
ABSTRACT.....	5
1. DIRECT CATALYTIC AMIDE AND ESTER FORMATION FROM UNACTIVATED CARBOXYLIC ACIDS.....	6
1.1 INTRODUCTION	6
1.2 DIRECT AMIDE FORMATION FROM CARBOXYLIC ACIDS AND AMINES.....	6
1.2.1 <i>Thermal methods</i>	6
1.2.2 <i>Catalytic amide condensation</i>	9
1.2.2.1 Arylboronic acid catalysts	9
1.2.2.1.1 Amidation with chiral substrates.....	10
1.2.2.1.2 Mechanistic considerations	11
1.2.2.1.3 Carboxylic acid condensation with ureas	12
1.2.2.2 Boric acid and boric acid ester mediated amide condensation	12
1.2.2.3 Other catalytic amide condensations	13
1.2.2.3.1 Pyridine boronic acids	13
1.2.2.3.2 Titanium and antimony mediated amidation	14
1.2.2.3.3 Amide formation at the interface of micelles of fatty acid salts ..	15
1.3 DIRECT SYNTHESIS OF ESTERS FROM CARBOXYLIC ACIDS AND ALCOHOLS	15
1.3.1 <i>Introduction</i>	15
1.3.2 <i>Boronic acid catalysed esterification</i>	16
1.3.3 <i>Metal-based catalysts for esterification</i>	18
1.3.3.1 Nickel, iron and titanium	18
1.3.3.2 Hafnium, zirconium and iron-zirconium salts	19
1.3.3.3 Zinc- and tin-based catalysts.....	22
1.3.4 <i>Metal-free catalysts for esterification</i>	23
2. RESULTS AND DISCUSSION – DIRECT AMIDE FORMATION FROM CARBOXYLIC ACIDS AND AMINES.....	26
2.1 INTRODUCTION	26
2.2 INVESTIGATIONS INTO THERMAL AND BORONIC ACID-CATALYSED DIRECT AMIDE FORMATION.....	26
2.2.1 <i>Thermal contribution to direct amide condensation</i>	27
2.2.2 <i>N,N-Diisopropylbenzylamine-2-boronic acid 80a catalysed reactions</i>	28
2.2.2.1 4-Phenylbutyric acid 81	28
2.2.2.2 Trimethylacetic acid 82	30
2.2.2.3 Benzoic acid 83	30
2.2.2.5 Summary of <i>N,N</i> -diisopropylbenzylamine-2-boronic acid 80a screen	31
2.2.3 <i>Comparison of catalysts for direct amide condensation</i>	32
2.2.4 <i>Catalyst stability and proposed mechanism</i>	37
2.2.4.1 Catalyst stability in the presence of carboxylic acid	37
2.2.4.2 Catalyst stability under amide condensation reaction conditions	39
2.2.4.3 Evidence for intermediates and proposed mechanisms	40
2.2.4.3.1 Thermal reaction.....	40
2.2.4.3.2 Catalysed reactions	41
2.2.5 <i>Effect of solvents and dehydration</i>	43
2.2.6 <i>Catalyst optimisation using Design of Experiments (DoE)</i>	45
2.2.6.1 <i>N,N</i> -Diisopropylbenzylamine-2-boronic acid 80a	45
2.2.6.2 Boric acid.....	49



2.2.7 Application of <i>N,N</i> -diisopropylbenzylamine-2-boronic acid 80a for amide formation.....	52
2.2.8 Application to other substrates.....	53
2.2.9 Effect of additives – water and trichloroacetic acid.....	56
2.3 TOWARDS SECOND GENERATION CATALYSTS	57
2.3.1 Fluoro- and methoxy-substituted derivatives	58
2.3.2 Trifluoromethyl-substituted derivative.....	60
2.3.3 Comparison of crystal structures.....	61
2.3.4 Catalyst evaluation	62
2.4 ACTIVITY OF OTHER CATALYSTS	64
2.5 KINETIC RESOLUTION <i>VIA</i> DIRECT AMIDE FORMATION FROM A RACEMIC AMINE AND ACHIRAL CARBOXYLIC ACID	66
2.6 SUMMARY AND CONCLUSIONS.....	70
2.7 FUTURE WORK	71
3. ASYMMETRIC ENAMINE CATALYSIS AND THE DIRECT ALDOL REACTION	73
3.1 INTRODUCTION TO ORGANOCATALYSIS.....	73
3.1.1 THE FIRST EXAMPLES OF ASYMMETRIC ENAMINE CATALYSIS	73
3.1.2 PROPOSED MECHANISM	77
3.2 TOWARDS CARBOHYDRATE SYNTHESIS MEDIATED BY PROLINE.....	78
3.3 CATALYSIS MEDIATED BY OTHER AMINO ACIDS AND PEPTIDES.....	80
3.4 PYRROLIDINE-BASED DERIVATIVES	82
3.5 OTHER CATALYSTS	89
3.6 SYNTHESIS OF ALDOL ADDUCTS CONTAINING QUARternary CENTRES.....	91
3.7 AQUEOUS ALDOL CATALYSIS.....	92
3.8 SUMMARY AND CONCLUSIONS.....	99
4. RESULTS AND DISCUSSION – AMINO-BORONIC ACIDS AS CATALYSTS FOR THE DIRECT ALDOL REACTION	101
4.1 INTRODUCTION	101
4.2 CATALYST SYNTHESIS	102
4.3 BEHAVIOUR IN AQUEOUS SOLUTION.....	106
4.4 CATALYST SCREENING	108
4.4.1 Proof of concept – the aldol reaction.....	108
4.4.2 Solvent effects on the aldol reaction.....	110
4.4.3 Applicability to other substrates	112
4.5 SUMMARY AND CONCLUSIONS.....	115
4.6 FUTURE WORK	115
5. EXPERIMENTAL.....	116
6. REFERENCES	142
APPENDIX.....	153

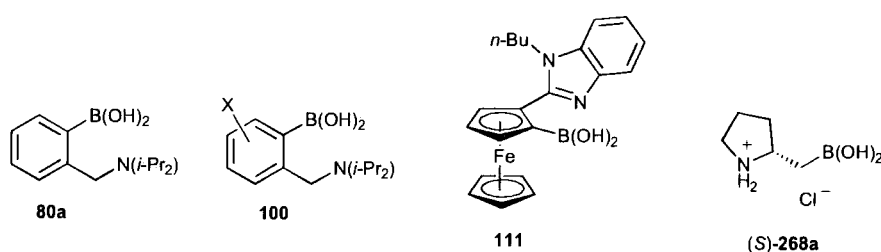
Abbreviations

Ac	acetyl
aq.	aqueous
Ar	aromatic
Bn	benzyl
Boc	<i>tert</i> -butyloxycarbonyl
Bp	boiling point
Bu	butyl
d	doublet
DCM	dichloromethane
DIPEA	<i>diisopropylethylamine</i>
DMF	<i>N,N</i> -dimethylformamide
DMSO	dimethylsulfoxide
DoE	Design of Experiments
d.r.	diastereoisomeric ratio
e.e.	enantiomeric excess
EI	electron ionisation
ES	electrospray (positive ion)
Et	ethyl
Et ₂ O	diethyl ether
EtOAc	ethyl acetate
EtOH	ethanol
GC	gas chromatography
HPLC	high performance liquid chromatography
LDA	lithium <i>diisopropylamide</i>
m	multiplet
M	molar
Mp	melting point
Me	methyl
MeCN	acetonitrile
MeOH	methanol
MS	mass spectrometry
MTBE	methyl <i>tert</i> -butyl ether

NMP	1-methyl-2-pyrrolidinone
NMR	nuclear magnetic resonance
Ph	phenyl
q	quartet
rt	room temperature
s	singlet
t	triplet
TCA	trichloroacetic acid
TFA	trifluoroacetic acid
THF	tetrahydrofuran
TLC	thin layer chromatography
TMS	tetramethylsilyl

Abstract

N,N-Diisopropylbenzylamine-2-boronic acid **80a** has been shown to be an effective catalyst under refluxing fluorobenzene conditions for direct amide formation between equimolar amounts of carboxylic acids and amines, and under these conditions the catalyst **80a** has been shown to be stable. A comparison with other boronic acid catalysts and boric acid has shown **80a** to be more effective for more difficult substrates, and evidence for the cooperative effect of the boronic acid and amine moieties, as well as for reaction intermediates, has been obtained.



The synthesis of novel derivatives of **80a** have allowed the factors affecting direct amide formation to be probed further. The addition of an electron withdrawing group does increase the reactivity of these systems, however, the effect of an electron donating group is more pronounced and results in a substantial decrease in activity. The importance of solvent choice, concentration and water removal has been demonstrated through parallel experiments and Design of Experiments. A non-linear effect for catalyst loading was shown, where a 5 mol% loading of **80a** had a similar effect to 10 mol%.

Furthermore, the application of chiral amino-boronic acid **111** to the kinetic resolution *via* direct amide formation of racemic amines from achiral carboxylic acids, has shown promising levels of enantioselectivity, even in refluxing fluorobenzene (bp 85 °C).

A novel pyrrolidine-based amino-boronic acid (*S*)-**268a** has been synthesised *via* (-)-sparteine-mediated lithiation in high yield and enantioselectivity. The application of (*S*)-**268a** to the direct enantioselective aldol reaction has shown the boronic acid moiety does participate, and the solution behaviour of (*S*)-**268a** has also been investigated.

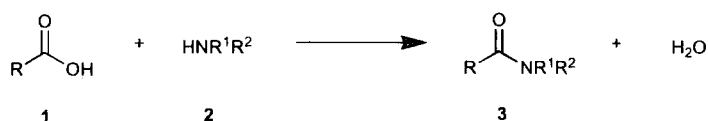
1. Direct catalytic amide and ester formation from unactivated carboxylic acids

1.1 Introduction

The search for catalytic reactions is ongoing and significant benefits can be demonstrated in terms of synthetic efficiency and atom economy, which in turn leads to reduced cost and impact on the environment. The use of chiral catalysts in asymmetric synthesis is highly advantageous since a substoichiometric amount of chiral catalyst can produce a large enantiomeric excess. In addition, there are no extra steps involved in attaching and removing a chiral auxiliary, which can have disadvantageous effects on time, yield and cost.

1.2 Direct amide formation from carboxylic acids and amines

The usual procedure for amide synthesis requires the activation of the acid component to a more reactive intermediate, such as the acid chloride, and is undesirable for a number of reasons, especially in terms of atom economy.¹ The high reactivity of acid chlorides requires the protection of other nucleophilic functional groups in a molecule, as well as a base (*e.g.* triethylamine) to complex the HCl produced. A direct condensation between carboxylic acids and amines, ideally in equimolar amounts, would be advantageous, making the synthesis a one step process and reducing environmental waste (Equation 1). This is especially true if the starting materials are expensive and/or of limited availability.



Equation 1

1.2.1 Thermal methods

Carboxylic acids and amines react together to form salts. Strong heating of these salts can lead to amide formation, as in the case of ammonium acetate to form acetamide.² The reaction is carried out in acetic acid and continuous distillation to remove water ensures the equilibrium is driven to the amide. Similarly, succinimide can be prepared by heating ammonium succinate³ and benzanilide can be prepared by heating

benzoic acid with an excess of aniline.⁴ Water and aniline are removed initially by distillation, followed by addition of more aniline and further heating to complete the reaction.

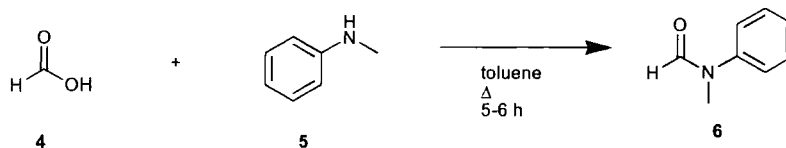
Pyrolysis of these salts under solvent-free conditions can lead to the formation of amides.⁵ Passing ammonia gas through various aliphatic acids, with the acid being kept at a temperature between 125-190 °C to facilitate the removal of water, and subjecting the resulting ammonium salt to these conditions for 3-15 hours, furnished the corresponding amides in greater than 70% yield. Applying the same conditions, but replacing ammonia with dimethylamine, forms the corresponding dimethylamides with yields in excess of 70% and with shorter reaction times (less than 3.5 hours).

The use of higher boiling amines simplifies the procedure further.⁶ Optimum conditions involve heating the acid-amine mixture for 10-30 minutes at 160-180 °C. Undoubtedly, the pyrolysis of ammonium salts is a simple route to amides, requiring no solvent or catalyst and only short reaction times. However, despite the advantages, certain prerequisites for the reactants have prevented wider, more general use of this route. The acids and amines must be thermally stable, melt below 200 °C, and be non-volatile and high boiling. In addition, excessive heating can lead to tar formation, whereas insufficient heating leads to poor conversion.

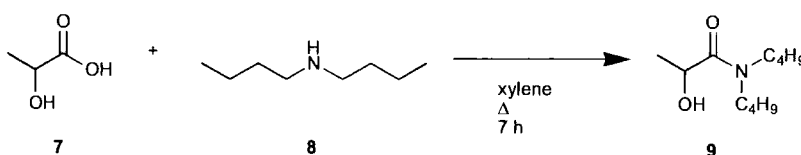
Subjecting an acid-amine mixture to heating at 150 °C using microwave radiation also leads to amide formation, in the majority of cases with increased yield *versus* conventional heating at 150 °C.⁷ Benzylamine reacted to give good conversion (80%) with phenylacetic and decanoic acid in 30 minutes, but it required an excess of the acid or amine component (1.5 equivalents) with benzoic acid for good yields. Lower yields were also encountered with the benzoic acid and *n*-octylamine (10%), aniline (12%) and 4-methoxyaniline (33%) reactions, with the electron-donating methoxy group having the expected beneficial effect.

Azeotropic removal of water using hydrocarbon solvents is another method for driving the reaction of acid-amine mixtures to completion. Representative examples

are the preparation of *N*-methylformanilide **6** in refluxing toluene,⁸ isolated in 93-97% yield, and *N,N*-dibutylactamide **9** (83%) in refluxing xylene.⁹

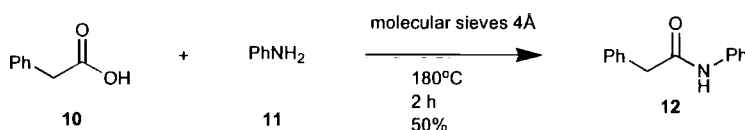


Equation 2

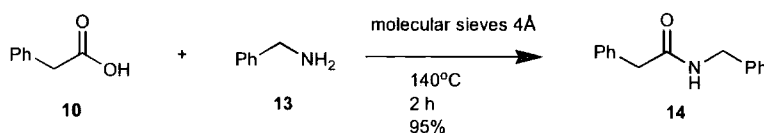


Equation 3

Molecular sieves can also be used to effect the removal of water. The heating of an acid-amine mixture in the presence of 4 Å molecular sieves facilitated amide condensation, but only in the case of primary amines.¹⁰ The reaction of phenylacetic acid **10** with morpholine and *N*-methylcyclohexylamine failed to yield any product, even though the mixture was subjected to a temperature of 180 °C for 2 hours, with only the formation of the ammonium salt being observed. Under these conditions, however, aniline **11** formed the desired amide **12** in 50% yield (Equation 4), and the more reactive amines (*e.g.* benzylamine **13**) reacted with phenylacetic acid at 140 °C for 2 hours to afford the corresponding amides in at least 95% yield (Equation 5).



Equation 4



Equation 5

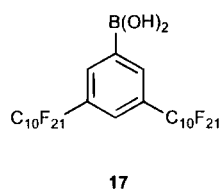
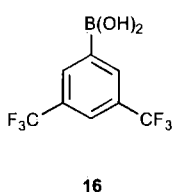
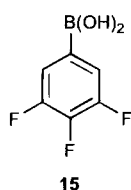
1.2.2 Catalytic amide condensation

In theory, the development of a universally applicable catalytic route to carboxamides should allow for the direct amide condensation between equimolar amounts of carboxylic acids and amines under mild conditions, and therefore the use of more sensitive substrates. In order to make possible the use of lower temperatures and faster reaction times, high activity catalysts are required. In addition, catalysts should be of low cost, low toxicity and easy to handle.

There are relatively few examples in the literature of direct catalytic amide condensations. The most notable examples are those mediated by arylboronic acids bearing electron-withdrawing substituents and boric acid. These will now be covered in detail.

1.2.2.1 Arylboronic acid catalysts

Yamamoto has demonstrated that arylboronic acids bearing electron-withdrawing substituents are effective catalysts for amide condensation. In particular, 3,4,5-trifluorophenylboronic acid¹¹ **15**, 3,5-bis(trifluoromethyl)phenylboronic acid **16** and 3,5-bis(perfluorodecyl)phenylboronic acid¹² **17**.

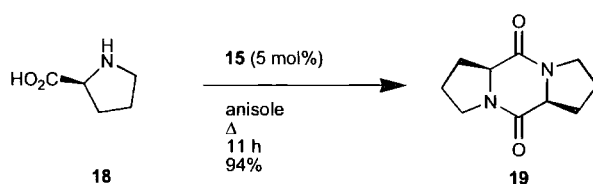


Amide condensations carried out in the presence of 1 mol% of **15** generally proceeded well, with azeotropic removal of water afforded by 4 Å molecular sieves in a soxhlet thimble, for example, 4-phenylbutyric acid and benzylamine were refluxed in toluene for 18 hours to furnish the corresponding amide in 96% yield. Less active substrates required more forcing conditions, however. The condensation of aniline with 4-phenylbutyric acid required refluxing mesitylene (bp 163-166 °C) for 4 hours to afford the anilide in 99% yield. Benzoic acid and 3,5-dimethylpiperidine were subjected to refluxing mesitylene for 20 hours, with the desired amide being isolated in 95% yield.

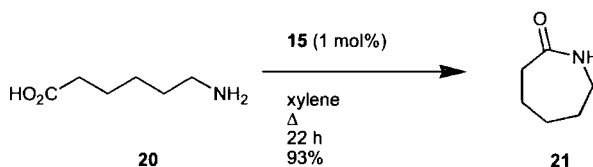
Boronic acid **17** had lower activity *versus* **15** and **16**. However, it could be recycled easily due to its insolubility in toluene and xylene at room temperature by simply decanting the reaction mixture.¹¹ The recovered catalyst showed no loss of activity in 10 cycles. The utility of boronic acid **15** in the direct polycondensation of carboxylic acids and amines has also been demonstrated.¹³

1.2.2.1.1 Amidation with chiral substrates

Catalyst **15** was also used to mediate lactam formation from amino acids. L-Proline **18** dimerised with less than 2% loss of enantiomeric purity, although a higher catalyst loading (5 mol%) and refluxing anisole (bp 154 °C) were required (Equation 6). Lactamisation of 6-aminocaproic acid **20** was more facile, proceeding under milder conditions in xylene (bp 136-140 °C) with 1 mol% **15** to afford caprolactam **21** in 93% yield (Equation 7).

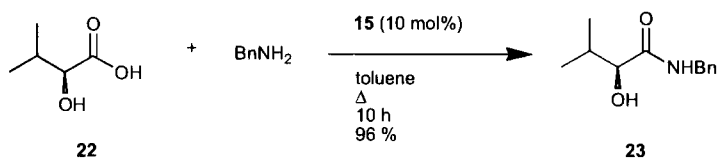


Equation 6



Equation 7

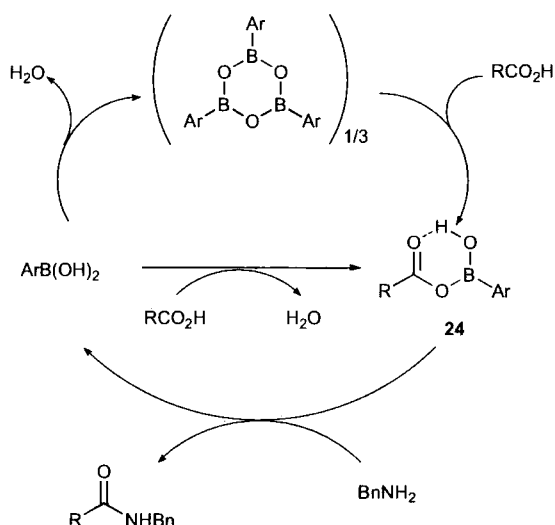
In addition, amide condensation with chiral α -hydroxycarboxylic acids was carried out in refluxing toluene with a 10 mol% loading of **15** (Equation 8). Minimal racemisation occurred, and complete selectivity for amide formation was observed.



Equation 8

1.2.2.1.2 Mechanistic considerations

The proposed mechanism for boronate-catalysed amide formation involves an acyloxyboronic acid intermediate **24** with formation of this from the boroxine being the rate-determining step (Scheme 1).^{11a}

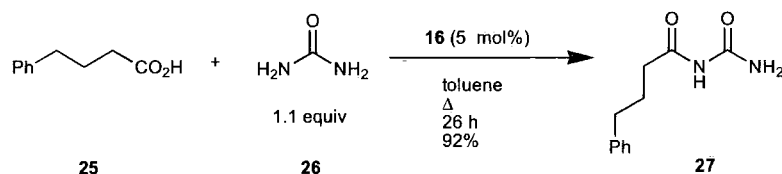


Scheme 1. Proposed mechanism for arylboronic acid catalysed direct amide formation.

Intermediate **24** was claimed to have been isolated after heating a 2:1 mixture of 4-phenylbutyric acid and boronic acid **16** in d_8 -toluene with removal of water. However, it is noteworthy that analytical and spectroscopic evidence was not definitive, and that no bis-acyloxyboronic acid was detected, with claimed exclusive formation of **24**. Subsequent addition of benzylamine certainly led to amidation at ambient temperature, though the acylation species remains unproved, being based upon an IR stretch at 1586 cm^{-1} , which does not relate to a known acylboron species. In fact, Brown and coworkers have reported the IR stretches to be around 1725 cm^{-1} for a variety of acyloxyboranes.¹⁴

1.2.2.1.3 Carboxylic acid condensation with ureas

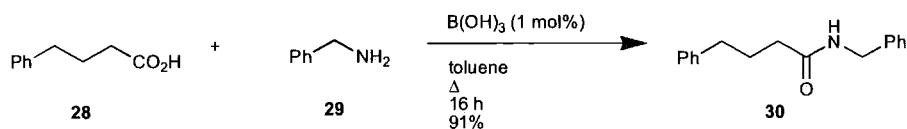
In an extension to this work, boronic acid **16** was shown to effectively mediate the condensation of carboxylic acids with ureas to afford the *N*-monoacylurea exclusively.¹⁵ Due to the lower nucleophilicity of ureas, a higher catalyst loading (5 or 10 mol%) was required (Equation 9), and as in the condensation with amines, less active substrates required a higher temperature for reaction. The same mixed anhydride type acyloxyboronic acid **24** was proposed as the intermediate.



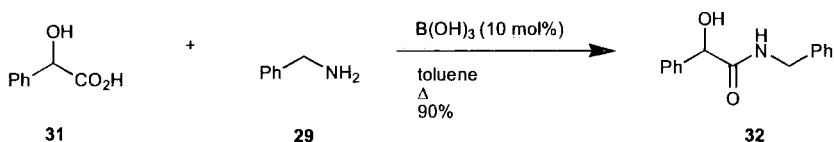
Equation 9

1.2.2.2 Boric acid and boric acid ester mediated amide condensation

Recently, Tang has shown that cheap and readily available boric acid catalyses the direct condensation of carboxylic acids and amines.¹⁶ 4-Phenylbutyric acid **28** and benzylamine **29** react in the presence of 1 mol% $B(OH)_3$ to afford amide **30** in 91% yield (Equation 10). Azeotropic removal of water is again required and generally, 5 mol% catalyst was adequate for most substrates. Anilines, however, needed a 25 mol% $B(OH)_3$ loading, and it was noted that side reactions from hydroxyl groups present on the acid or amine were absent (Equation 11). As for arylboronic acid mediated amidation, an acyloxyborate intermediate **24** (Ar = OH) is the proposed acylating agent, although no independent evidence for this is presented.

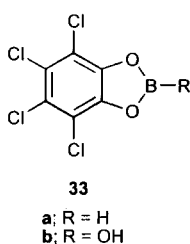


Equation 10



Equation 11

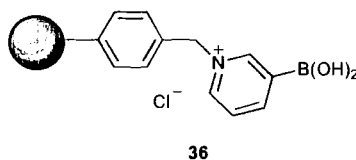
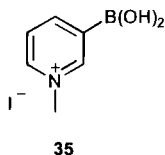
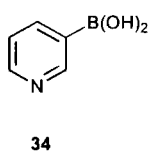
In 2006, Yamamoto compared the activity of 4,5,6,7-tetrachlorobenzo-[1,3,2]dioxaborole **33a** and 4,5,6,7-tetrachlorobenzo-[1,3,2]dioxaborol-2-ol **33b** with 3,5-bis(trifluoromethyl)phenylboronic acid **16** and found them to be more active in the amide condensation of sterically demanding carboxylic acids.^{17,18} At a 5 mol% loading and azeotropic reflux in toluene or *o*-xylene for up to 24 h, the desired amides were formed in over 90% yield. However, the thermal contributions (*i.e.* the background, uncatalysed reactions) were not assessed and only two amines were screened (benzylamine and *N*-benzyl-*N*-methylamine).



1.2.2.3 Other catalytic amide condensations

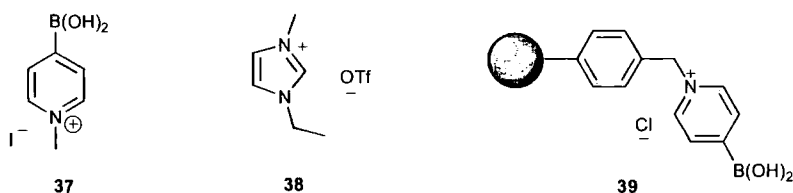
1.2.2.3.1 Pyridine boronic acids

Wang and co-workers have shown that pyridine-3-boronic acid **34** and *N*-methylpyridine-3-boronic acid **35** were efficient catalysts for direct amide condensation at a loading of 1 mol% under azeotropic reflux conditions in toluene.¹⁹ Attachment to a polystyrene support provided solid-phase amidation catalyst **36**, which was air stable, easily isolated and recycled 3 times with no loss of activity.



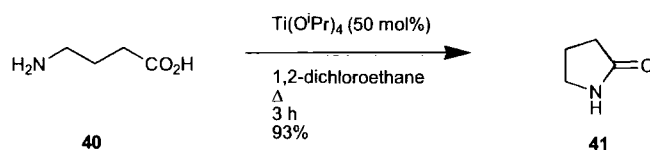
Yamamoto has also screened *N*-alkyl-4-boronopyridinium salts (5 mol%) for the direct amide condensation and observed **37** to be more thermally stable to protodeboronation when compared with 3-substituted derivative **35**, although it was not significantly more active.^{18,20} In addition, this group developed more efficient reaction conditions, employing a biphasic mixture of toluene and [emim⁺][⁻OTf] **38**

(5:1), which facilitated reuse of the catalyst since it remained in the [emim⁺][OTf] layer. Attachment to a polystyrene support to afford **39** provided a heterogeneous catalyst which allowed the ionic liquid to be omitted (reaction carried out in toluene or *o*-xylene), with the catalyst recovered by filtration.



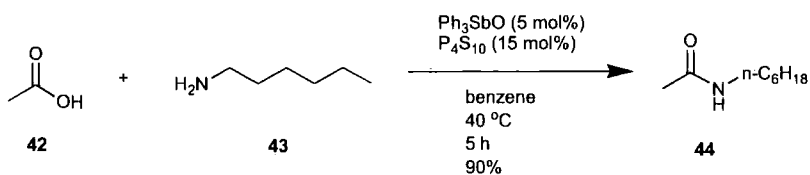
1.2.2.3.2 Titanium and antimony mediated amidation

The formation of 5- and 6-membered lactams from ω -amino acids is promoted by Ti(O^{*i*}Pr)₄ in 75-93% yield (Equation 12).²¹ For good yields, 50 mol% Ti(O^{*i*}Pr)₄ is required and the route is not applicable to intermolecular amidation, leading to isolation of the ammonium salts. The use of boronic acid derivatives is, therefore, significantly more widely applicable in terms of substrates, as well as catalyst loading.



Equation 12

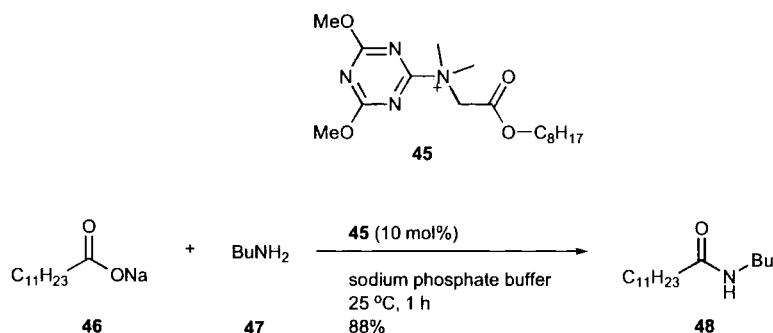
A more effective catalyst for direct amide condensation is a mixture of triphenylstibene oxide and phosphorus decasulfide in a 1:3 ratio (Equation 13).²² The reaction is suggested to proceed *via* the thiocarboxylic acid, which is generated *in situ*. The coupling of *N*-protected amino acids also proceeded well in DCM at 30 °C, with no racemisation. Antimony(III) ethoxide (Sb(OEt)₃) has also been demonstrated as an amidation catalyst at a loading of 5-10 mol% in refluxing toluene.²³



Equation 13

1.2.2.3.3 Amide formation at the interface of micelles of fatty acid salts

In 2005, Kunishima and co-workers elegantly demonstrated that the amide formation between sodium salts of several fatty acids and butylamine, in the presence of a triazine condensing agent **45** (10 mol%), proceeded in phosphate buffer (pH 8).²⁴ For example, sodium laurate **46** and butylamine **47** when stirred at 25 °C for 1 h, produced amide **48** in 88% yield (Equation 14). The efficiency of the reaction depends strongly on the length of the alkyl chains on both the condensing agent **45** and sodium carboxylate **46**, and their subsequent ability to form micelles. Shortening the alkyl chain on **46** to a propyl decreases the reaction rate (>1200 fold), whilst increasing the length to C₁₆H₃₃ on **45** assists the formation of mixed micelles, and hence, increases the reaction rate.



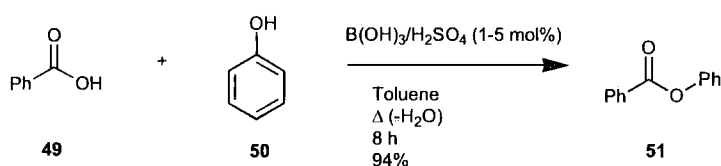
1.3 Direct synthesis of esters from carboxylic acids and alcohols

1.3.1 Introduction

The esterification of carboxylic acids with alcohols is an equilibrium reaction and is usually driven towards the product ester by the addition of the alcohol in excess, or by removal of the water produced. A catalytic protocol should ideally use equimolar amounts of carboxylic acid and alcohol without the need for dehydration, a neutral catalyst to increase substrate scope, and proceed to 100% conversion.²⁵ The development of high activity, low toxicity and low cost, as well as recyclable catalysts, is a challenging task.

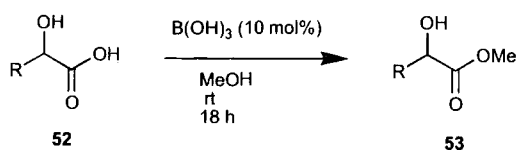
1.3.2 Boronic acid catalysed esterification

Along with the direct amide condensation, boric acid has been shown to catalyse esterification of acids and alcohols, although so far, with limited substrate applicability. The relatively difficult esterification of phenol **50** *versus* aliphatic alcohols proceeds in high yield, in the presence of 1-5 mol% mixture of boric and sulfuric acids.²⁶ The reaction is carried out in refluxing toluene with azeotropic removal of water to afford phenyl benzoate **51** in 94% yield (Equation 15). Interestingly, both boric acid and sulfuric acid are necessary for the reaction to proceed.



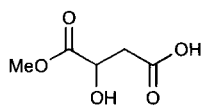
Equation 15

The room temperature esterification of α -hydroxycarboxylic acids is catalysed by boric acid alone.²⁷ Methyl esters were formed in the presence of 10 mol% boric acid using methanol as solvent over 18 hours, in 65-99% yield (Equation 16).

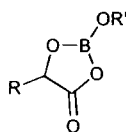


Equation 16

α -Hydroxycarboxylic acids reacted selectively with methanol in the presence of a β -hydroxycarboxylate as demonstrated by formation of the monoester of DL-malic acid **54**. Dimer and diester formation were suppressed by higher dilution. Where no α -hydroxy group was present, negligible reaction was observed, as in the case of benzoic acid, which gave no reaction.



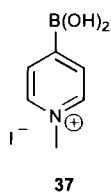
54



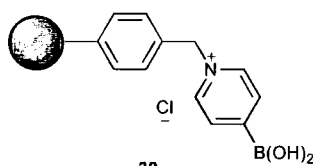
55

Borate **55** ($R' = \text{Me}$) is the proposed intermediate, rather than mixed anhydride **24** because of selective ester formation at the α -hydroxycarboxylic acid moiety, but this has not been confirmed. The use of ethanol and *isopropanol* required refluxing or a higher catalyst loading (20 mol%). However, the reaction of DL-malic acid with *isopropanol* showed low selectivity for the α -acid ($\alpha/\beta = 3:1$), and no reaction was seen with *t*-butanol with any of the substrates tested.

In 2005, Yamamoto compared *N*-alkyl-4-boronopyridinium iodide **37** with boric acid for the esterification of α -hydroxycarboxylic acids and found that boric acid (5-10 mol%, up to 21 h) at azeotropic reflux in toluene or xylene was highly active for the reaction between an equimolar mixture of acid and alcohol.^{18,28} However, with an excess of alcohol (*i.e.* as solvent), **37** (5-10 mol%, rt or reflux, up to 22 h) was demonstrated to be more efficient. Polystyrene-bound derivative **39** was also found to be an active and recoverable catalyst in the presence of excess alcohol.



37



39

The active amidation catalyst 3,4,5-trifluorophenylboronic acid **15** was also shown to catalyse the esterification of 4-phenylbutyric acid in *n*-butanol (bp 117.7 °C), with a 1 mol% loading furnishing the *n*-butyl ester in 88% yield.¹¹ However, the methyl ester was isolated in only 14% yield.

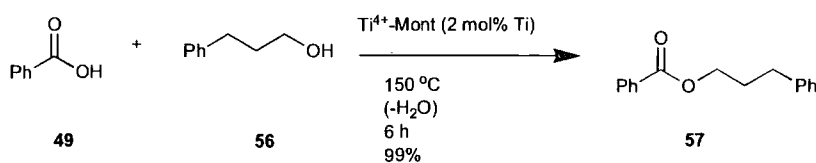
1.3.3 Metal-based catalysts for esterification

1.3.3.1 Nickel, iron and titanium

The use of $\text{NiCl}_2 \cdot 6\text{H}_2\text{O}$ at a 10 mol% loading has been shown to catalyse the formation of methyl and ethyl esters from aliphatic carboxylic acids in an excess of refluxing alcohol over 3-13 hours.²⁹ However, the catalyst is ineffective with *t*-butanol as the alcohol component and shows limited or no activity in reactions involving aromatic or conjugated acids. Similarly, $\text{Fe}_2(\text{SO})_4 \cdot x\text{H}_2\text{O}$ catalyses the esterification of aliphatic acids with unbranched aliphatic alcohols.³⁰

Under comparable conditions to the $\text{NiCl}_2 \cdot 6\text{H}_2\text{O}$ catalysed esterification, Fe^{3+} -K-10 montmorillonite clay also mediates the esterification of acids and alcohols, but again is not active for aromatic acids, and excess alcohol is used as the solvent.³¹ This can be useful if the selective esterification of a molecule containing an aromatic and aliphatic acid is required. The catalyst can also be isolated and reused. On the other hand, the substrate scope of the method is limited, and the use of excess alcohol would be problematic if the esterification is required between an alcohol of limited availability or high cost.

Of significant interest from a 'green' standpoint is the heterogeneous catalytic esterification mediated by montmorillonite-enwrapped titanium (Ti^{4+} -mont) between equimolar amounts of carboxylic acid and alcohols under solvent-free conditions.³² Benzoic acid **49** and 3-phenyl-1-propanol **56** were heated at 150 °C for 6 hours, with removal of water by 4Å molecular sieves in a soxhlet thimble, to afford the ester **57** in 99% yield (Equation 17).

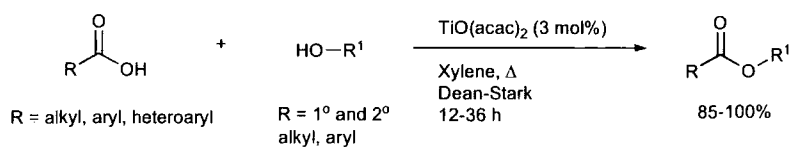


Equation 17

Trimethylacetic acid was found to react under the same conditions with alcohol **56** to produce the corresponding ester in 99% yield after 3 hours. The recyclability of the catalyst (isolated by filtration) was demonstrated in the esterification of lauric acid

(CH₃(CH₂)₁₀CO₂H) with alcohol **56** (120 °C, 3 hours) to afford the condensation product in 96% yield even after 4 cycles.

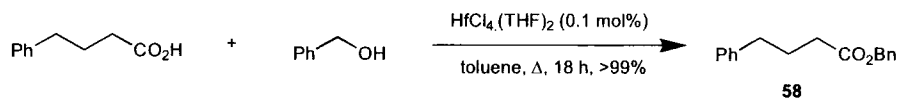
More recently, Chen and co-workers have employed TiO(acac)₂ (3 mol%) as a general catalyst for esterification between a wide variety of carboxylic acids and alcohols (1:1) in refluxing xylene with excellent yields (Equation 18).³³



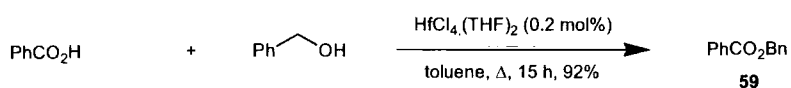
Equation 18

1.3.3.2 Hafnium, zirconium and iron-zirconium salts

Yamamoto has shown that the direct esterification of equimolar amounts of carboxylic acids and alcohols is catalysed efficiently by hafnium(IV) and zirconium(IV) salts.³⁴ In particular, the tetrahydrofuran complex HfCl₄.(THF)₂ was found to be particularly active.

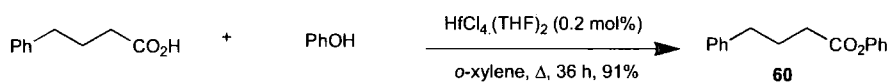


Equation 19

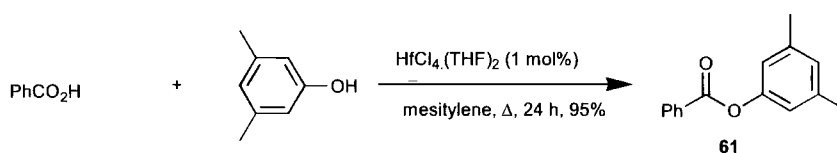


Equation 20

For most acid and alcohol combinations, a loading of 0.2 mol% in refluxing toluene (under argon) was sufficient to furnish the esters in >90% yield (e.g. esters **58** and **59**). Removal of water was found to be very important, affording better results than a solvent free system at the same temperature. Aromatic substrates required a higher catalyst loading (1 mol%) and/or a higher boiling solvent such as *o*-xylene or 1,3,5-mesitylene (e.g. esters **60** and **61**).

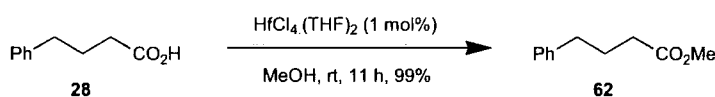


Equation 21



Equation 22

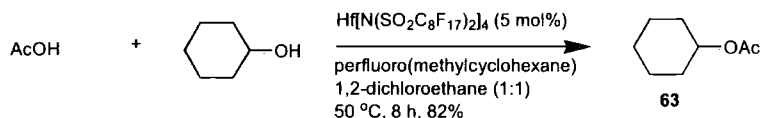
Although the reaction failed to proceed with tertiary alcohols, esterification with low boiling methanol at room temperature afforded the methyl ester **62** in 99% yield, without removal of water (Equation 23). The selective catalytic esterification of primary alcohols in the presence of secondary or aromatic alcohols was also demonstrated.³⁵



Equation 23

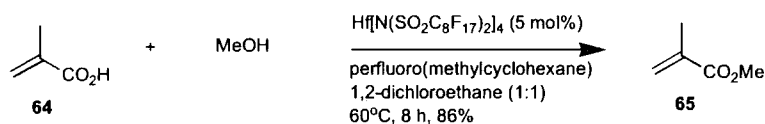
In an extension to this work, $\text{ZrOCl}_2 \cdot 8\text{H}_2\text{O}$ was shown to be an air stable, water-tolerant and recyclable catalyst for direct esterification.³⁵ The reaction of 4-phenylbutyric acid **28** and benzyl alcohol at azeotropic reflux in heptane, over 8 hours in the presence of 1 mol% $\text{ZrOCl}_2 \cdot 8\text{H}_2\text{O}$ afforded ester **58** in 95% yield. The remarkably simple recycling procedure involves addition of 1M HCl to the reaction, decantation, addition of another portion of acid and alcohol in heptane to the aqueous solution and subsequent reflux. The yield of ester **58** only decreases to 93% over 3 cycles.

Hafnium(IV) bis(perfluorooctanesulfonyl)amide complex ($\text{Hf}[\text{NSO}_2\text{C}_8\text{F}_{17}]_2$)₄) was used in a fluorous biphasic system for the direct esterification of carboxylic acids and alcohols under mild conditions (Equation 24).³⁶ The removal of water is not required and the reactants are used in equimolar amounts. Under these conditions, $\text{HfCl}_4 \cdot (\text{THF})_2$ furnished cyclohexyl acetate **63** in only 29% yield.



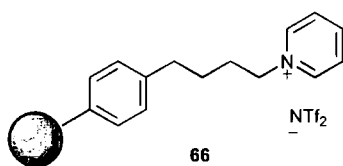
Equation 24

Recycling of the fluorous phase 5 times and subsequent esterification afforded ester **63** with negligible decrease in catalytic activity, although extension of the system to other substrates failed to produce consistently high yields, *e.g.* benzoic acid and benzyl alcohol formed the corresponding ester **59** in only 21% yield. However, the conversion of methacrylic acid **64** to methyl methacrylate **65** proceeded in 86% yield at 60 °C (Equation 25). Further investigation of methyl methacrylate formation, using a different solvent system, 5 equivalents of methanol and in the presence of 1.6 equivalents of water, showed the initial rate of esterification with $\text{Hf}[\text{N}(\text{SO}_2\text{C}_8\text{F}_{17})_2]_4$ was 9 times that of H_2SO_4 at identical loading.³⁷



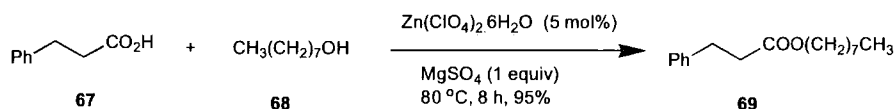
Equation 25

An iron(III)-zirconium (IV) combined salt, prepared from $\text{Zr}(\text{OiPr})_4$ and $\text{Fe}(\text{OiPr})_3$ *in situ* has also been shown to be an active ester condensation catalyst for equimolar amounts of carboxylic acids and alcohols.³⁸ In order to facilitate catalyst recovery and product isolation, the combined salt has been immobilised on *N*-(polystyrylbutyl)pyridinium triflylimide **66** *in situ*.³⁹ Interestingly, the combined salt is immobilised on **66** only after the esterification is complete (which leads to the reaction mixture turning colourless) and is therefore a homogenous catalysis. A catalyst loading of 2 mol%, refluxing heptane and 24 h was sufficient for excellent yields of the substrates screened, even after four runs.



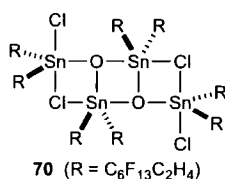
1.3.3.3 Zinc- and tin-based catalysts

Zinc perchlorate hexahydrate ($\text{Zn}(\text{ClO}_4)_4 \cdot 6\text{H}_2\text{O}$) has been shown to catalyse the direct condensation between carboxylic acids and alcohols under solvent-free conditions.⁴⁰ 3-Phenylpropionic acid **67** and 1-octanol **68** react to produce the corresponding ester **69** in 95% yield, in the presence of 5 mol% of catalyst and a stoichiometric amount of MgSO_4 as dehydrating agent (Equation 26). The catalyst has wide substrate scope, but fails to esterify tertiary alcohols. More sterically hindered substrates require a higher catalyst loading (10 mol%) or higher temperature (100 °C), but the catalyst is of low cost, non-toxic, air stable and easily recyclable. The recycling procedure simply requires the dilution of the reaction mixture with DCM, subsequent filtration and heating in an oven (60 °C) overnight to reactivate the catalyst.

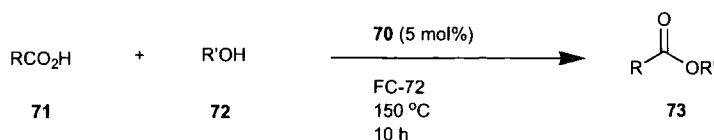


Equation 26

Otera and co-workers have also developed a recyclable esterification catalyst – fluoros distannoxane catalyst **70** catalyses the esterification of equimolar amounts of carboxylic acids and alcohols.⁴¹ The fluoroalkyl groups render **70** virtually insoluble in most organic solvents, and extremely fluorophilic.



Reactions were carried out in FC-72 (perfluorohexanes, 3M company, St. Paul, MN) in the presence of 5 mol% of **70** with heating at 150 °C (Equation 27).



Equation 27

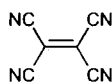
Reaction of **71** (R=Ph(CH₂)₂) with benzyl alcohol **72** (R'=PhCH₂) afforded the corresponding ester **73** in quantitative yield. The catalyst **70** could be recovered from the fluorous phase after addition of toluene, although on scale up, product ester could be removed with a pipette and subsequent reuse of the fluorous phase over 10 cycles still afforded quantitative yields of ester. The reaction shows limited substrate scope, however, with the esterification of secondary alcohols failing to proceed in adequate yield. In addition, only electron-deficient aromatic acids **71** (R = C₆F₅, *p*-NO₂C₆H₄, *p*-CF₃C₆H₄) reacted satisfactorily, with benzoic acid affording only 22% conversion.

1.3.4 Metal-free catalysts for esterification

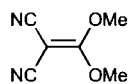
A remarkably simple metal-free procedure for ester formation involves heating a 1:1 mixture of acid and amine under microwave irradiation for 3-10 minutes, in the presence of *p*-toluenesulfonic acid (0.5 equivalents).⁴² Benzoic acid and *n*-octanol produced the corresponding ester in 97% yield after 3 minutes under these conditions.

Iodine has also been shown to catalyze esterification.⁴³ Refluxing the carboxylic acid in an excess of the alcohol for 4-20 hours in the presence of 1 mol% iodine afforded yields in the 90% region for most substrates. The reaction proceeds with primary and secondary alcohols, but *t*-butanol required a higher catalyst loading, longer reaction time and afforded only moderate yield. The reaction of aromatic acids failed to proceed but the reaction system was found to be water tolerant and did not require dehydration.

Tetracyanoethylene **74** and dicyanoketene dimethyl acetal **75** catalyzed esterification is another system which uses excess alcohol as solvent and does not require dehydration.⁴⁴



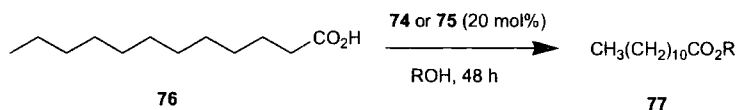
74



75

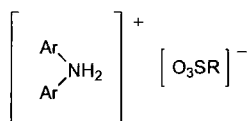
Reaction of lauric acid **76** with primary aliphatic alcohols proceeded well at room temperature (Equation 28). More difficult substrates required heating at 60 °C, but

secondary alcohols were nevertheless esterified in lower yield and *t*-butanol failed to react.



Equation 28

The use of equimolar amounts of carboxylic acid and alcohol is beneficial in terms of atom economy. Diaryl ammonium arenesulfonates **78** have been shown to catalyse esterification with a 1:1 ratio of acid and alcohol.

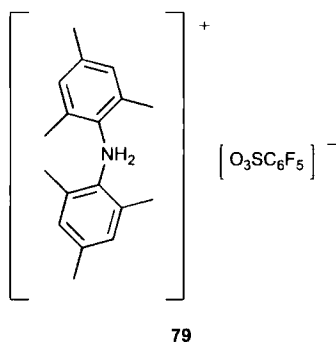


78

Diphenylammonium triflate (DPAT) **78** (Ar = Ph, R = CF₃) was demonstrated as an active esterification catalyst, with 1 mol% loading furnishing the esters from primary alcohols in the 90% region within 4-8 hours at 80 °C in toluene.⁴⁵ Secondary alcohols required 5-10 mol% catalyst and 24 hours, and benzoic acid with octanol required 48 hours in the presence of 5 mol% DPAT (94% yield). The removal of water from the reaction mixture was not required. The use of fluorous solvents, in particular perfluorohexane (C₆F₁₄), in place of toluene was shown to have a beneficial effect on the esterification of hindered substrates, but the esterification of tertiary alcohols still failed.⁴⁶ Modification of DPAT to incorporate a *p*-nitro group on one of the phenyl rings had no beneficial effect on catalytic activity.⁴⁷

Ishihara has shown that bulky diarylammonium arenesulfonates, particularly dimesitylammonium pentafluorobenzenesulfonate **79**, are efficient esterification catalysts, without the strong acidity of DPAT.⁴⁸ In fact, substituting the pentafluorobenzenesulfonate counter ion for tosylate had little effect on catalytic activity and [Ph₂NH₂]⁺[OTs]⁻ was found to be more active than DPAT. This was proposed to be due to the effect of surrounding the ammonium group with hydrophobic *N*-aryl and *S*-aryl groups. The catalyst **79** showed wide substrate scope

with heating in heptane at 80 °C in the presence of 1 mol% catalyst generally being sufficient. In addition, methyl and octyl esters could be formed at room temperature under solvent free conditions.



An interesting concept is the facilitation of esterification reactions in water. In terms of ‘green’ chemistry, the use of water as a solvent is ideal. The use of surfactant-type acid catalyst *p*-dodecylbenzenesulfonic acid (DBSA) leads to the formation of emulsion droplets in water, with the hydrophobic interior containing the reactants.⁴⁹ Generated water is expelled from the droplets, driving the equilibrium to ester formation. Although, the system works well only with lipophilic reactants, *e.g.* lauric acid **76** in the presence of 2 equivalents of long chain aliphatic alcohols (89-99% yield), the conditions are very mild – 10 mol% catalyst, 40 °C, 48 hours. Increasing the temperature or catalyst loading resulted in decreased yields of ester.⁵⁰ The detrimental effect of increased catalyst loading was attributed to the formation of smaller emulsion droplets and thus, a smaller hydrophobic area available for the reaction to take place.

2. Results and Discussion – Direct amide formation from carboxylic acids and amines

2.1 Introduction

As discussed in the introduction, there are limited examples of direct catalytic amide formation from carboxylic acids and amines. The existing examples suffer from a range of drawbacks to include inadequate substrate scope, a general lack of reactivity requiring forcing reaction conditions and, consequently, issues regarding catalyst stability. In addition, the thermal contributions to the reactions have only been assessed in a very limited number of cases.

The design, synthesis and screening of amino-boronic acids as catalysts for direct amide formation offers the opportunity to address some of these concerns. Amino-boronic acids utilise the cooperative effect of a Lewis acidic boronic acid and basic amine moiety attached to a rigid backbone, providing the potential to function as bifunctional organic catalysts (Figure 1). Important considerations include the distance between the boronic acid and amine, their relative strengths and the structure of the amine.

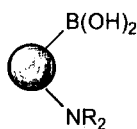
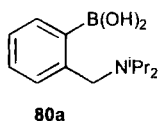


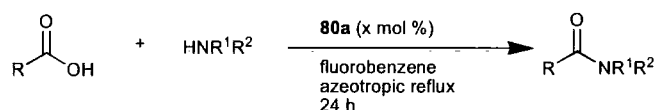
Figure 1. General structure for an amino-boronic acid.

2.2 Investigations into thermal and boronic acid-catalysed direct amide formation

The direct catalytic amide condensation between equimolar amounts of carboxylic acids and amines was first examined with *N,N*-diisopropylbenzylamine-2-boronic acid **80a**.⁵¹



Previous work in the group has identified **80a** as an efficient catalyst for the direct amide condensation in toluene. The use of lower temperature conditions would be advantageous allowing the use of more sensitive substrates and reducing the thermal contribution to the reaction. Fluorobenzene (bp 85 °C) was selected as a suitable solvent, allowing azeotropic removal of water, yet avoiding the hazards of using benzene (Equation 29).



Equation 29

2.2.1 Thermal contribution to direct amide condensation

First of all, the thermal contributions to the amide condensation were assessed between various carboxylic acids and amines, selected to provide a diverse range of steric and electronic properties (Figure 2).

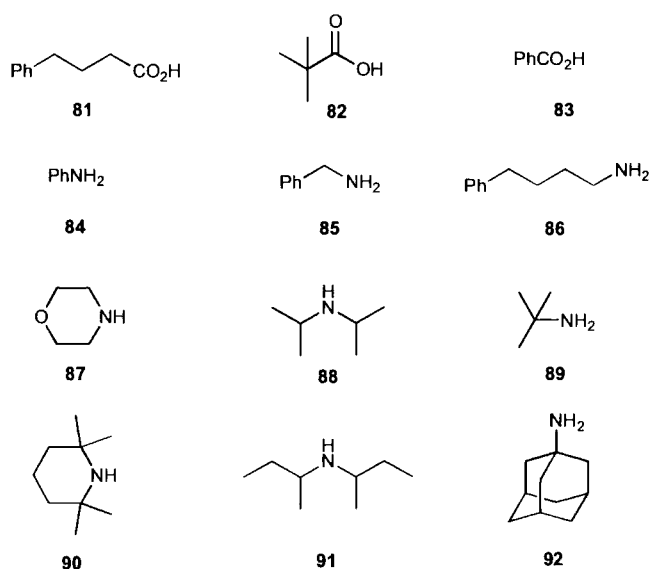


Figure 2. Substrates screened in the amide condensation.

A mixture of the acid and amine in equimolar amounts were stirred at reflux in fluorobenzene (no inert atmosphere) for 24 hours, with water removal afforded by a soxhlet thimble containing calcium hydride (Equation 29). Isolated yields of amide for the various acid and amine combinations are shown in Table 1.

Table 1. Isolated yields for the thermal contribution to the amide condensation in fluorobenzene.

Amine	Acid	4-Phenylbutyric acid 81	Trimethylacetic acid 82	Benzoic acid 83
Aniline 84		-	-	-
Benzylamine 85		16%	0.5%	1%
4-Phenylbutylamine 86		2%	0.5%	-
Morpholine 87		4%	-	-
Diisopropylamine 88		-	-	-
<i>t</i> -Butylamine 89		-	-	-
2,2,6,6-Tetramethylpiperidine 90		-	-	-

^aConditions: acid (5 mmol), amine (5 mmol), fluorobenzene (50 mL), 85°C, 24 h; isolated yields.

4-Phenylbutyric acid **81** and benzylamine **85** is the only combination that produces a significant amount of amide under thermal conditions. Increasing steric hindrance at the acid reduces the amide yield substantially and most acid-amine combinations failed to react.

2.2.2 *N,N*-Diisopropylbenzylamine-2-boronic acid **80a** catalysed reactions

2.2.2.1 4-Phenylbutyric acid **81**

Initially, the screening of 4-phenylbutyric acid **81** was carried out in the presence of amino-boronic acid **80a** (1 mol%), under the conditions shown in Equation 29. However at this temperature (85 °C), this catalyst loading proved insufficient to provide a reasonable reaction rate. Therefore, the loading of **80a** was increased to 10 mol% and the reaction with aniline **84** was carried out under argon protection (Table 2). In the absence of an argon atmosphere, aniline oxidation led to the formation of a very dark brown oil and no amide formation was observed.

Table 2. Screening of amide formation using 4-phenylbutyric acid **81** with catalyst **80a**.

Entry	Amine	Yield amide (%) 80a (1 mol%)	Yield amide (%) 80a (10 mol%)	Yield amide (%) 80a (0 mol%)
1 ^a	Aniline 84	1	12	-
2	Benzylamine 85	22	68	16
3	4-Phenylbutylamine 86	12	70	2
4	Morpholine 87	15	67	4
5	Diisopropylamine 88	-	Not run	-
6	<i>t</i> -Butylamine 89	-	Not run	-
7	2,2,6,6-Tetramethylpiperidine 90	Not run	-	-
8	Di- <i>sec</i> -butylamine 91	Not run	-	-
9	1-Adamantylamine 92	Not run	-	-

^aUnder argon. ^bConditions: acid (5 mmol), amine (5 mmol), fluorobenzene (50 mL), 85°C, 24 h; isolated yields.

Runs with benzylamine **85**, 4-phenylbutylamine **86** and morpholine **87** (entries 2-4) afforded the amide in around 70% yield. Less active aniline **84** produced the corresponding anilide in 12% yield (entry 1), which was surprising at this relatively low temperature. A comparison with yields obtained in the absence of catalyst **75**, shows that 4-phenylbutylamine **86** and morpholine **87** give the greatest improvement in yield (entries 3 and 4).

Diisopropylamine **88** (bp 84 °C) and *t*-butylamine **89** (bp 46 °C) failed to react during initial screening with **80a** (1 mol%), and in order to check that this was not only due to their low boiling points, these amines were substituted with di-*sec*-butylamine **91** (bp 135 °C) and 1-adamantylamine **92** (mp 205-208 °C). However, these substrates failed to react under both thermal and catalysed conditions, *i.e.* in the presence of **80a** (entries 8-9), suggesting these hindered amines are considerably more difficult substrates.

2.2.2.2 Trimethylacetic acid **82**

The screening of trimethylacetic acid **82** under identical conditions (Equation 29) afforded substantially reduced yields of amide, presumably due to steric hindrance (Table 3). In addition, the electron-donating *t*-butyl group will also decrease reactivity making this acid a difficult substrate.

Table 3. Screening of amide formation using trimethylacetic acid **82** with catalyst **80a**.

Entry	Amine	Yield amide (%) 80a (10 mol %)	Yield amide (%) 80a (0 mol%)
1 ^a	Aniline 84	-	-
2	Benzylamine 85	15	0.5
3	4-Phenylbutylamine 86	6	0.5
4	Morpholine 87	-	-
5	2,2,6,6-Tetramethylpiperidine 90	-	-
6	Di- <i>sec</i> -butylamine 91	-	-
7	1-Adamantylamine 92	-	-

^aUnder argon. ^bConditions: acid (5 mmol), amine (5 mmol), fluorobenzene (50 mL), 85°C, 24 h; isolated yields.

Amide was only produced in the case of the more active primary amines benzylamine **85** and the non-hindered 4-phenylbutylamine **86** (entries 2-3), however, catalyst turnover is extremely slow. No reaction was observed with secondary amines (entries 4-6), and deactivated aniline **84**, as well as hindered 1-adamantylamine **92**, also failed to react (entries 1 and 7).

2.2.2.3 Benzoic acid **83**

The results obtained with benzoic acid **83** under the same conditions (Equation 29) were more promising (Table 4), suggesting that the increase in steric hindrance afforded by the phenyl group is less detrimental to amide yields than that of the *t*-butyl group of trimethylacetic acid **82**.

Table 4. Screening of amide formation using benzoic acid **83** with catalyst **80a**.

Entry	Amine	Yield amide (%) 80a (10 mol%)	Yield amide (%) 80a (0 mol%)
1	Aniline 84	-	-
2	Benzylamine 85	50	1
3	4-Phenylbutylamine 86	10	-
4	Morpholine 87	11	-
5	2,2,6,6-Tetramethyl-piperidine 90	-	-
6	Di- <i>sec</i> -butylamine 91	-	-
7	1-Adamantylamine 92	-	-

^aUnder argon. ^bConditions: acid (5 mmol), amine (5 mmol), fluorobenzene (50 mL), 85°C, 24 h; isolated yields.

Benzylamine **85** formed the corresponding amide in 50% yield (entry 2). The reaction with 4-phenylbutylamine **86** produced the benzamide in 10% yield, with no contribution from the thermal reaction (entry 3). This was also the case with secondary amine morpholine **87** (entry 4), but turnover is very slow or non-existent in both these cases. Hindered substrates again failed to react.

2.2.2.5 Summary of *N,N*-diisopropylbenzylamine-2-boronic acid **80a** screen

A summary of the results of the screen of *N,N*-diisopropylbenzylamine-2-boronic acid **80a** (10 mol%) is shown in Table 5. Unhindered, 4-phenylbutyric acid **81** is the most reactive acid and benzylamine **85** the most reactive amine. 4-Phenylbutylamine **86** reacted to form amide in all cases, but the yield was only satisfactory with 4-phenylbutyric acid **81** (70%). Morpholine **87** (an unhindered secondary amine) reacted well with 4-phenylbutyric acid **81**, and deactivated aniline **84** also reacted with this acid. The amide condensation mediated by catalyst **80a** is significantly affected by steric and electronic factors and as a result is highly substrate dependent.

Table 5. Results of screen of catalyst **80a** (10 mol%) in direct amide condensation.

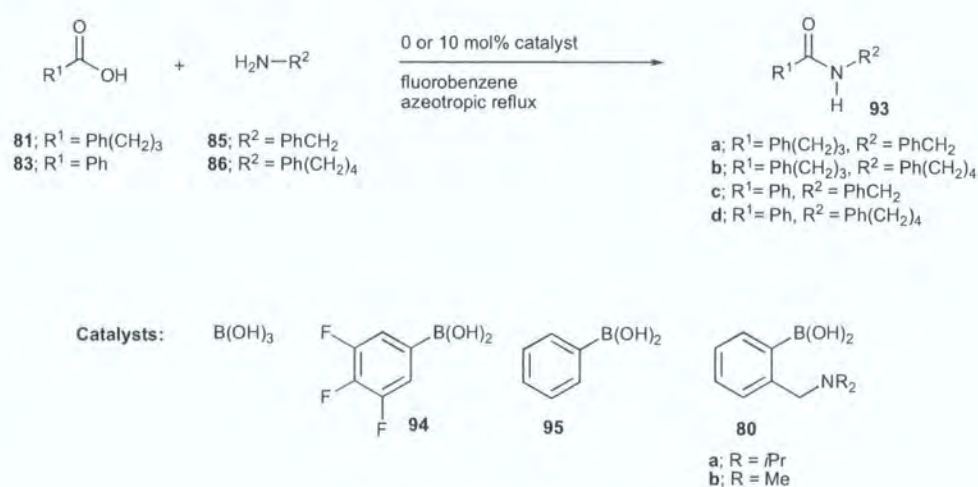
Amine	Acid	4-Phenylbutyric acid 81	Trimethylacetic acid 82	Benzoic acid 83
Aniline 84 ^a		12%	-	-
Benzylamine 85		68%	15%	50%
4-Phenylbutylamine 86		70%	6%	10%
Morpholine 87		67%	-	11%
2,2,6,6-Tetramethylpiperidine 90		-	-	-
Di- <i>sec</i> -butylamine 91		-	-	-
Adamantylamine 92		-	-	-

^aUnder argon.

In all these reactions, instantaneous formation of solids on addition of the acid and amine was observed. ¹H NMR confirmed these as the carboxylate-ammonium salts in the cases of 4-phenylbutyric acid **81** with both benzylamine **85** and 1-adamantylamine **92**, in fluorobenzene at room temperature, suggesting the reaction proceeds *via* initial salt formation.

2.2.3 Comparison of catalysts for direct amide condensation⁵²

A comparison of amidation catalysts (**80b**, **94**, **95** and boric acid) was made between 4-phenylbutyric acid **81** and 4-phenylbutylamine **86**, because of the low thermal (2%) and high catalyst contribution to the reaction (Scheme 2). After 24 hours, in the presence of 10 mol% of each catalyst, good yields were obtained in all four cases (Table 6).



Scheme 2. Direct amide formation and catalyst structures.

Table 6. Screen of catalysts for formation of *N*-4-phenylbutyl-4-phenylbutyramide **93b**.

Entry	Catalyst (10 mol%)	Yield 93b (%)
1	80b	86%
2	B(OH) ₃	82%
3	95	78%
4	94	88%

Since there is no significant difference between the obtained yields of amide over 24 hours in the presence of these catalysts, conversion vs. time data was obtained for four reaction combinations, as outlined in Scheme 2. A Gilson 215 liquid handler with ReactArray setup was employed to monitor amide formation by direct sampling and online HPLC analysis. This consists of a needle attached to a robotic arm and syringe pump, programmed to carry out sampling directly from the reaction vessels as required. Acetonitrile is aspirated initially as a quench and then a sample is taken. The sample and quench are transferred to an HPLC vial and mixed by blowing air through at a rate set by the user. Once the mix cycle is complete, more acetonitrile is aspirated for use as diluent and a sample is subsequently aspirated from the first HPLC vial. This is dispensed into a second HPLC vial and mixed. Further dilutions can be carried out until the required HPLC concentration is reached, and the sample is then analysed using the integrated HPLC system.

The parallel reactions were carried out in a heating block capable of running 10 reactions at a single temperature simultaneously, under argon with dehydration afforded by azeotropic reflux *via* 3 Å molecular sieves.

During initial experiments, crossover between the reaction vessels was observed, and the reaction volume was reduced from 15 mL to 10 mL. In order to quantify the data, an internal standard was used and naphthalene was found to be ideal, being both non-volatile and allowing easy separation from the other reaction components by reverse phase HPLC.

Further problems with respect to the sampling consistency of the ReactArray workstation were rectified following consultation with ReactArray and the method was subjected to several modifications. The injection concentration was increased from 1 to 2.5 $\mu\text{L}/\text{mL}$, as well as that of the internal standard from 5 to 15 mol%. In addition, one dilution step was removed in order to reduce the sampling error. Hence the sampling procedure was modified from sample 100 μL , quench 900 μL , two 10-fold dilutions to sample 50 μL , quench 950 μL , one 20-fold dilution and the mixing protocol was made more thorough (air mix 75%, 5 times, aspirate/dispense 2 mL/min to air mix 100%, 10 times, aspirate 10 mL/min, dispense 20 mL/min).

Reactions were carried out in the presence of no catalyst, boric acid¹⁶ and catalysts **94**,^{11a} **95**, **80a**⁵¹ and **80b** for each of the four substrate combinations. The data was fitted to first order kinetics⁵³ where possible and initial rate constants⁵⁴ are given where the reaction was too slow (Figure 3).

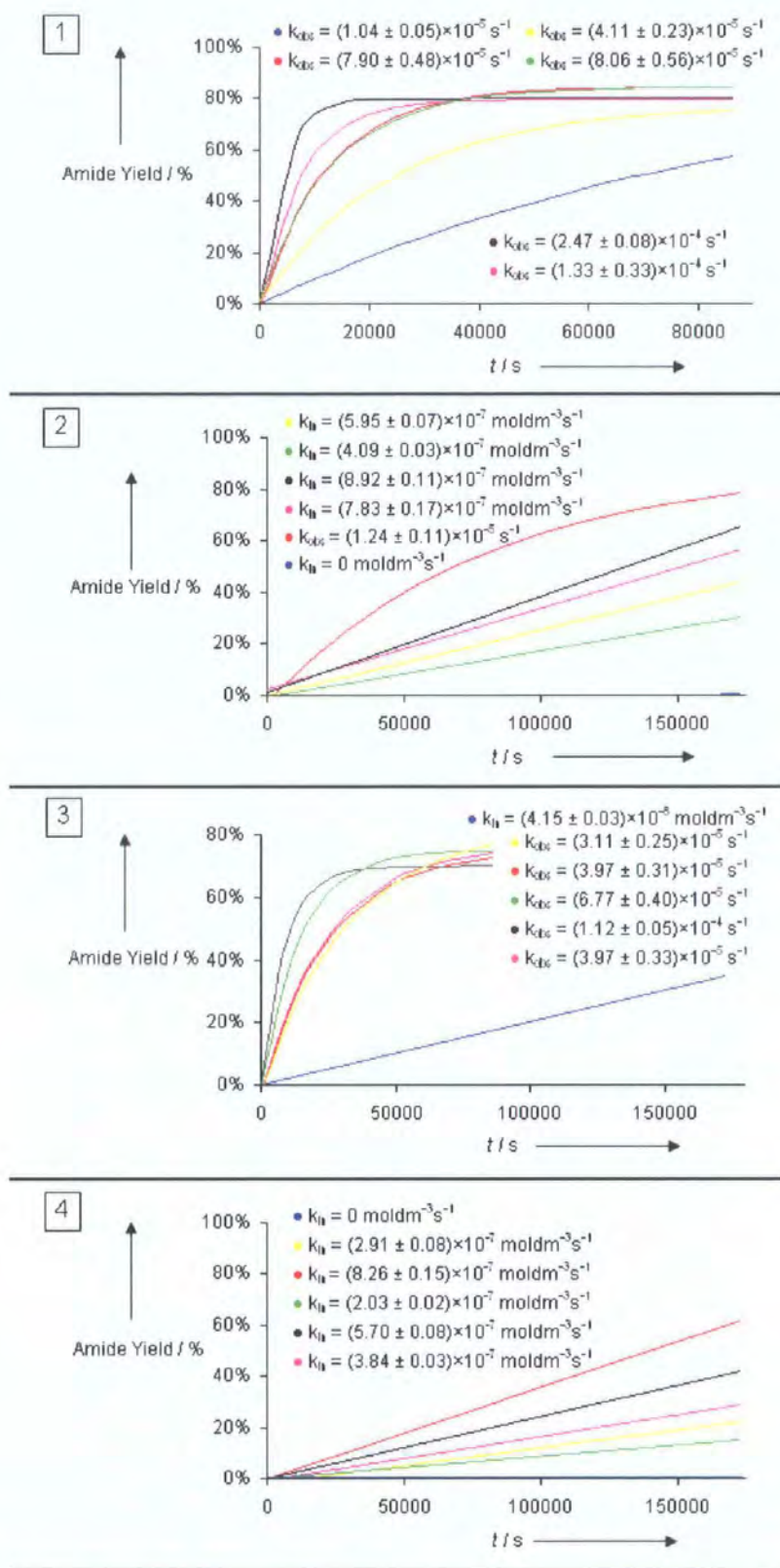


Figure 3. Yield vs. time data and rate constants for the catalytic amide condensation.

Reaction key (Figure 3):

1. 4-Phenylbutyric acid **81** + Benzylamine **85**
2. Benzoic acid **83** + Benzylamine **85**
3. 4-Phenylbutyric acid **81** + 4-Phenylbutylamine **86**
4. Benzoic acid **83** + 4-Phenylbutylamine **86**

Catalyst key:

-----Thermal reaction

-----Boric acid

-----*N,N*-Diisopropylbenzylamine-2-boronic acid **80a**

-----*N,N*-Dimethylbenzylamine-2-boronic acid **80b**

-----3,4,5-Trifluorophenylboronic acid **94**

-----Phenylboronic acid **95**

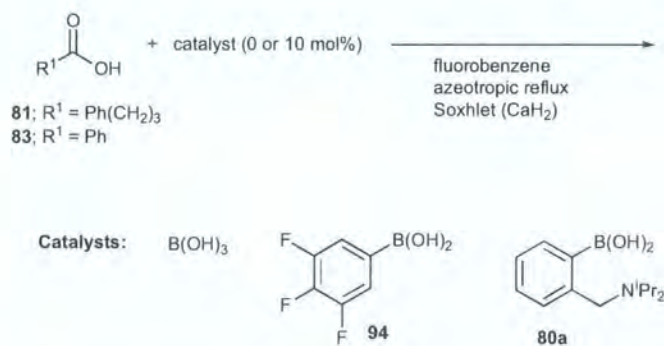
The thermal reaction between 4-phenylbutyric acid **81** and benzylamine **85** (Reaction 1) accounts for *ca.* 60% conversion in 24 h. 3,4,5-Trifluorophenylboronic acid **94** was the best catalyst for this combination, whilst boric acid was the least effective. With 4-phenylbutylamine **86** (Reaction 3), there was a significantly reduced thermal contribution to the formation of amide **93b** (*ca.* 40% in 48 h). Catalyst **94** was again the most effective, followed by phenylboronic acid **6**, with the others being virtually identical.

Benzoic acid **83** led to the observation of enhanced differences between catalysts (Reactions 2 and 4). The thermal reaction was non-existent in the case of either amine and catalyst **80a** stood out clearly as the most active catalyst. Since the reaction between benzoic acid **83** and 4-phenylbutylamine **86** (Reaction 4) showed no enhanced reactivity ($k_i = (2.32 \pm 0.04) \times 10^{-7}$) upon addition of diisopropylethylamine (10 mol%) to the phenylboronic acid-catalysed reaction, and diisopropylethylamine alone did not catalyse the reaction, the advantage of an intramolecular base (*i.e.* bifunctional catalysis) was clearly demonstrated. Structurally related **80b** was less effective, presumably because of B-N chelation in both solid and solution states, which is disfavoured in **25a** because of the hindered diisopropylamine moiety.⁵¹

2.2.4 Catalyst stability and proposed mechanism

2.2.4.1 Catalyst stability in the presence of carboxylic acid

In order to determine the stability of the catalysts used in the catalytic amide condensation, the catalysts were heated with carboxylic acid under reaction conditions with sampling and analysis by ^1H and ^{11}B NMR (Scheme 3). In particular, decomposition of the boronic acid catalysts **94** and **80a** to boric acid, along with any difference in interaction between the aliphatic acid **81** and aromatic acid **83** towards the catalysts was investigated. Boric acid is cheap and readily available, and therefore, if catalyst decomposition is facile, work needed to be focused upon improving catalyst stability through the design of new catalysts or modification of reaction conditions.



Scheme 3. Testing catalyst stability in the presence of carboxylic acid.

Samples were taken after stirring at ambient temperature for 1 h, and then after heating for 1, 2, 4, and 24 hours. Since boric acid is insoluble in CDCl_3 , a D_2O shake was employed to allow detection by ^{11}B NMR. ^1H NMR was taken before the D_2O shake in order to detect the presence of anhydride, however, it proved difficult to determine whether anhydride (symmetric or mixed) had been formed because of the broad carboxylic acid proton signal. In addition, ^{13}C NMR and IR analysis of the stability testing experiments in the presence of 4-phenylbutyric acid **81** showed no characteristic differences. The boric acid reaction mixture was not homogenous after 4 h reflux, whereas the catalyst **94** reaction mixture was homogeneous after stirring for 1 h at ambient temperature. In comparison, catalyst **80a** was seen to dissolve in 15 minutes at room temperature, presumably due to formation of the carboxylate-ammonium salt.

Table 7. ^{11}B NMR data for $\text{RCO}_2\text{H} + \text{boric acid}$.

Temperature $T/^\circ\text{C}$	Time @ $T/^\circ\text{C}$	δ_{B} (CDCl_3) ^a	
		4-Phenylbutyric acid 81	Benzoic acid 83
Ambient	1 h	19.4	19.5
85	1 h	19.6	19.5
85	2 h	19.4	19.6
85	4 h	19.6	19.5
85	24 h	19.6	19.4

^aAfter D_2O shake.

Boric acid showed negligible change in the ^{11}B NMR, displaying the expected signal for boric acid at $\delta_{\text{B}} = 19.5$ (

Table 7). In comparison, 3,4,5-trifluorophenylboronic acid **94** showed some decomposition to boric acid ($\delta_{\text{B}} = 19.5$) with 4-phenylbutyric acid **81** over 24 hours, but the main species remained the boronic acid ($\delta_{\text{B}} = 28$). Less deboration was seen in the case of benzoic acid **83**, with deboration appearing to have reached a maximum after 4 h at reflux. However, the poor solubility of boric acid makes this difficult to quantify (Table 8).

Table 8. ^{11}B NMR data for $\text{RCO}_2\text{H} + 3,4,5\text{-trifluorophenylboronic acid } \mathbf{94}$.

Temperature $T/^\circ\text{C}$	Time @ $T/^\circ\text{C}$	δ_{B} (CDCl_3) ^a	
		4-Phenylbutyric acid 81	Benzoic acid 83
Ambient	1 h	28.2	28.1
85	1 h	28.3	28.3
85	2 h	28.2 and 19.6 (6:1)	28.3
85	4 h	28.3 and 19.5 (5:1)	28.2 and 19.5 (6:1)
85	24 h	28.2 and 19.6 (3:1)	28.3 and 19.5 (6:1)

^aAfter D_2O shake. Peak height ratio is given in parentheses.

On the other hand, *N,N*-diisopropylbenzylamine-2-boronic acid **80a** showed no decomposition to boric acid in the ^{11}B NMR (Table 9). A white precipitate was seen in the flask after 4 h at reflux, and after 24 h, the reaction mixture was a turbid

suspension. The ^{11}B NMR showed signals that were not anticipated, with the shift to lower frequency suggesting an increasing negative charge on boron and formation of a tetrahedral ‘ate’-complex. Due to the broad peaks observed with ^{11}B NMR, the signals at δ_{B} 6.6 and 3.2 are presumably indicative of the formation of the same type of species. These observations coupled with the evidence from mass spectrometry analysis (*vide infra*), suggests formation of a triacylboron ‘ate’ complex **I**.

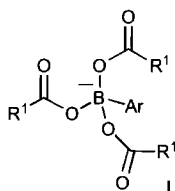


Table 9. ^{11}B NMR data for $\text{RCO}_2\text{H} + N,N$ -diisopropylbenzylamine-2-boronic acid **80a**.

Temperature T/°C	Time @ T/°C	δ_{B} (CDCl_3) ^a	
		4-Phenylbutyric acid 81	Benzoic acid 83
Ambient	1 h	27.6	26.5
85	1 h	27.6	27.4
85	2 h	28.3	26.8
85	4 h	27.3	27.1
85	24 h	3.2	6.6

^a After D_2O shake.

2.2.4.2 Catalyst stability under amide condensation reaction conditions

In order to determine whether proto-deboronation of trifluorophenylboronic acid **94** (10 mol%) occurred in the presence of amine, the catalyst was heated under reaction conditions with 4-phenylbutyric acid **81** and 4-phenylbutylamine **86**. The more electron rich acid **81** was selected since proto-deboronation of catalyst **94** is faster compared with benzoic acid **83** in the absence of amine. The amine **86** was selected because of its lower reactivity towards direct amide formation compared with benzylamine **85**.

The reaction was carried out in toluene- d_8 (at 85 and 110 °C) in NMR tubes over 22 h. ^{19}F NMR showed clearly that **94** was stable at the lower temperature of 85°C. However, trifluorobenzene formation could not be detected by HPLC in the higher

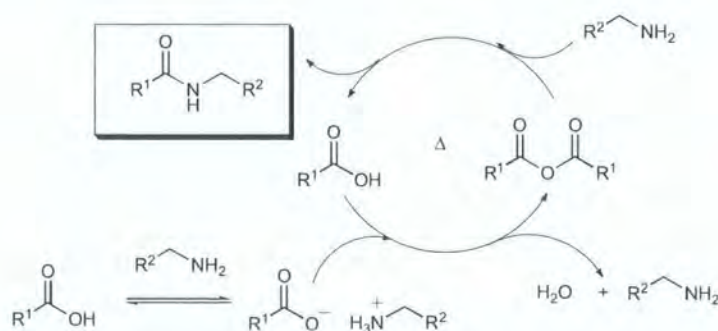
temperature reaction. Since trifluorobenzene (bp 94-95 °C) may have been lost from the NMR tube, the reaction was repeated in refluxing toluene over 24 h. Naphthalene (5 mol%) was used as an internal standard, a condenser was fitted, and samples were taken after 30 minutes cooling at 0, 2, 17 and 24 hours. HPLC analysis (Phenomenex Gemini C18 5 μm , 150 mm x 4.60 mm; gradient MeCN (0.05% TFA) / water (0.05% TFA) 0:100 to 100:0 over 29 minutes; 1 mL min⁻¹) showed no trifluorobenzene (t_r = 15.97 min) had been formed and that the amount of trifluorophenylboronic acid remained constant at each sample point.

It may be the case that proto-deboronation is not observed because of the fast amidation reaction, which is virtually complete in 2 h when an increased loading of catalyst **94** (10 mol%) is used. For more difficult amide condensations, where the carboxylate-ammonium salt is present for a longer period, proto-deboronation may still take place.

2.2.4.3 Evidence for intermediates and proposed mechanisms

2.2.4.3.1 Thermal reaction

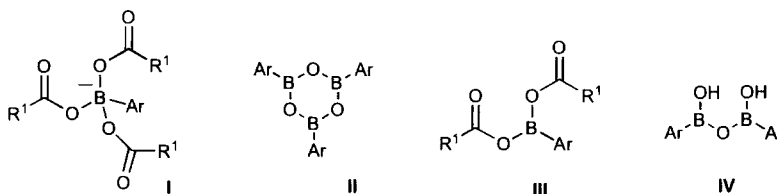
The reaction of benzoic anhydride with benzylamine **85** showed 100% conversion to *N*-benzylbenzamide **93c** in less than 2 minutes, suggesting that anhydride formation is the most likely rate determining step in the thermal reaction. Hence, the proposed mechanism is shown in Scheme 4. Unfortunately, heating 4-phenylbutyric acid **81** in toluene for 8 h, both in the presence and absence of diisopropylethylamine (1 equivalent) with monitoring by ReactIR, failed to lead to detection of any symmetric anhydride.



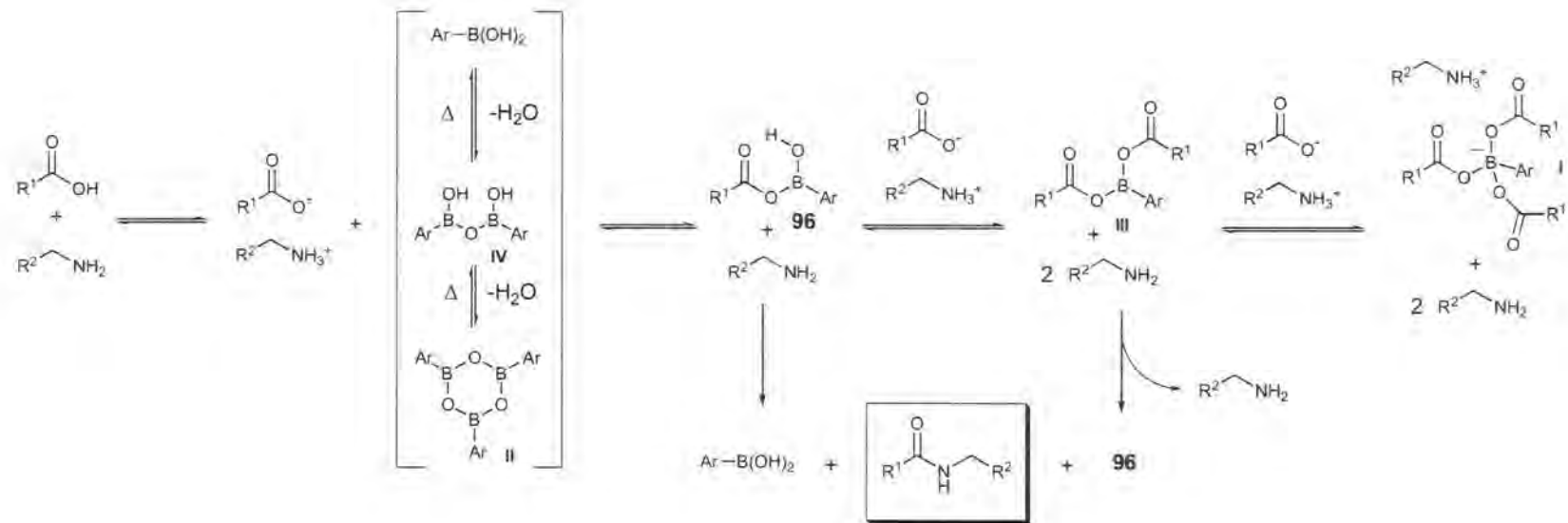
Scheme 4. Proposed mechanism for thermal amide formation.

2.2.4.3.2 Catalysed reactions

On heating a mixture of 4-phenylbutyric acid **81** and catalyst **80a** (2:1) in C₆D₆ for 6 hours, under identical conditions to those of the direct amide formation (*i.e.* azeotropic reflux *via* 3Å molecular sieves), and analysis by electrospray mass spectrometry led to evidence for several intermediates. ‘Ate’-complex **I**, boroxine **II**, diacyloxyboronate **III** and dimer **IV** corresponded to the following ESI-MS signals: m/z 714.1 [**I**+Na]⁺, 652.5 [**II**+H]⁺, 550.3 [**III**+Na]⁺, 528.3 [**III**+H]⁺ and 453.3 [**IV**+H]⁺. ¹H NMR showed broad signals indicating exchange and ¹³C NMR showed no significant difference *versus* 4-phenylbutyric acid **81**, whilst ¹¹B NMR showed two signals at $\delta_B = 29.9$ and 3.7. The signal at $\delta_B = 29.9$, corresponds to sp²-hybridised boron, *i.e.* free boronic acid **80a**, boroxine **II** and diacyloxyboronate **III**, and $\delta_B = 3.7$ corresponds to ‘ate’-complex **I**. Infrared showed no significant difference compared to 4-phenylbutyric acid **81**. In addition, ReactIR showed no change on heating a mixture of 4-phenylbutyric acid **81** and phenylboronic acid **95** (1:1) in toluene, after 8 h.

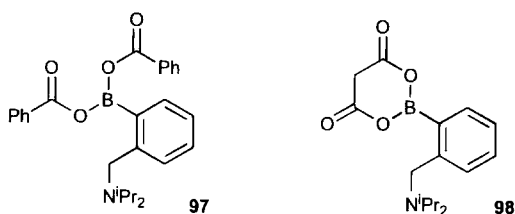


On the basis of this evidence, the proposed mechanism shown in Scheme 5 was formulated. By analogy with the thermal reaction, the rate determining step is likely to be the formation of monoacyloxyboronate **96** and diacyloxyboronate **III**.



Scheme 5. Proposed mechanism for amide formation catalysed by boric or boronic acids.

In an attempt to isolate diacyloxyboronate **97**, a mixture of benzoic acid **83** and catalyst **80a** (2:1) were heated in toluene for 22 h. Subsequent addition of amine (2 equiv) should lead to amide in either 50% or 100% yield, depending on the acylating ability of the monoacyloxyboronate **96**. However, ^{11}B NMR suggested that the obtained white sticky solid ($\delta_{\text{B}} = 4.0$) was most likely to be ‘ate’ complex **I** (R^1 , Ar = Ph), and addition of amine to the NMR sample led to regeneration of the boronic acid **80a** ($\delta_{\text{B}} = 28$) and no amide formation, suggesting that **I** had already been hydrolysed. In fact, the sensitivity of **I** was observed when a sample on the end of a spatula was seen to transform from a sticky solid to a white powder, presumably due to hydrolysis. The ^{11}B NMR of this sample showed only one signal corresponding to the boronic acid **80a** ($\delta_{\text{B}} = 28.1$).



Diaclyoxyboronate **98** (formed from **80a** and malonic acid) should allow isolation of the monoacyloxyboronate on addition of 1 equivalent of amine and thus a mixture of **80a** and malonic acid were heated in refluxing toluene for 18 h. However, attempted isolation of **98** was unsuccessful, resulting in a sample containing several unidentifiable species and starting material.

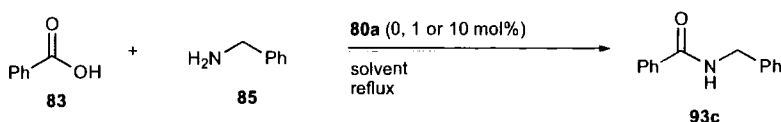
2.2.5 Effect of solvents and dehydration

A variety of solvents (fluorobenzene, toluene, propionitrile and water) were examined for the amide condensation between benzoic acid **83** and benzylamine **85** (Figure 4). The reactions were monitored over 48 h using the ReactArray system, and in the absence of a soxhlet containing molecular sieves. All were carried out with catalyst **80a** (0 or 10 mol%), except in the case of toluene, which was run with a reduced loading of **80a** (0 or 1 mol%) because of its higher boiling point.

Surprisingly, the use of a soxhlet containing 3Å mol. sieves had a negligible effect on the final conversion to amide **93c**. On this scale, there is some water removal from the reaction on cooling of the azeotrope in the condenser in which droplets of water are deposited and not returned to the reaction mixture. Although the hydrolysis of amides is not catalysed by **80a** (as evidenced by the fact that product yields do not decrease once a reaction has reached equilibrium), the putative mixed anhydride intermediate (a mono- or diacyloxy-boronate **96** and **III** respectively) would react readily with water, and therefore the reaction not reaching 100% conversion is highly likely to be limited by the efficiency of reaction dehydration.

Another possible reason for the conversion levelling off at around 75% is due to the use of an internal standard (naphthalene) to calculate amounts from the HPLC traces, and subsequently generate conversion *vs.* time data. However, as the concentration of product increases, the corresponding HPLC peak will get broader and peak integration becomes less accurate. Sample concentrations are determined beforehand in a reference chromatogram to provide a compromise between detecting amide at both low and high concentrations. A simple way to avoid this issue in the future would be to carry out additional dilution steps on samples containing higher product concentrations before HPLC analysis.

As expected, no conversion to amide was observed in water and the best solvents are non-polar toluene and fluorobenzene, as used in previous experiments. In toluene, **80a** (1 mol%) is sufficient for good reactivity, and the thermal reaction accounts for approximately 10 % conversion. Significantly more polar propionitrile proved detrimental to the reaction, affording only 20% conversion to **93c** in 48 hours.



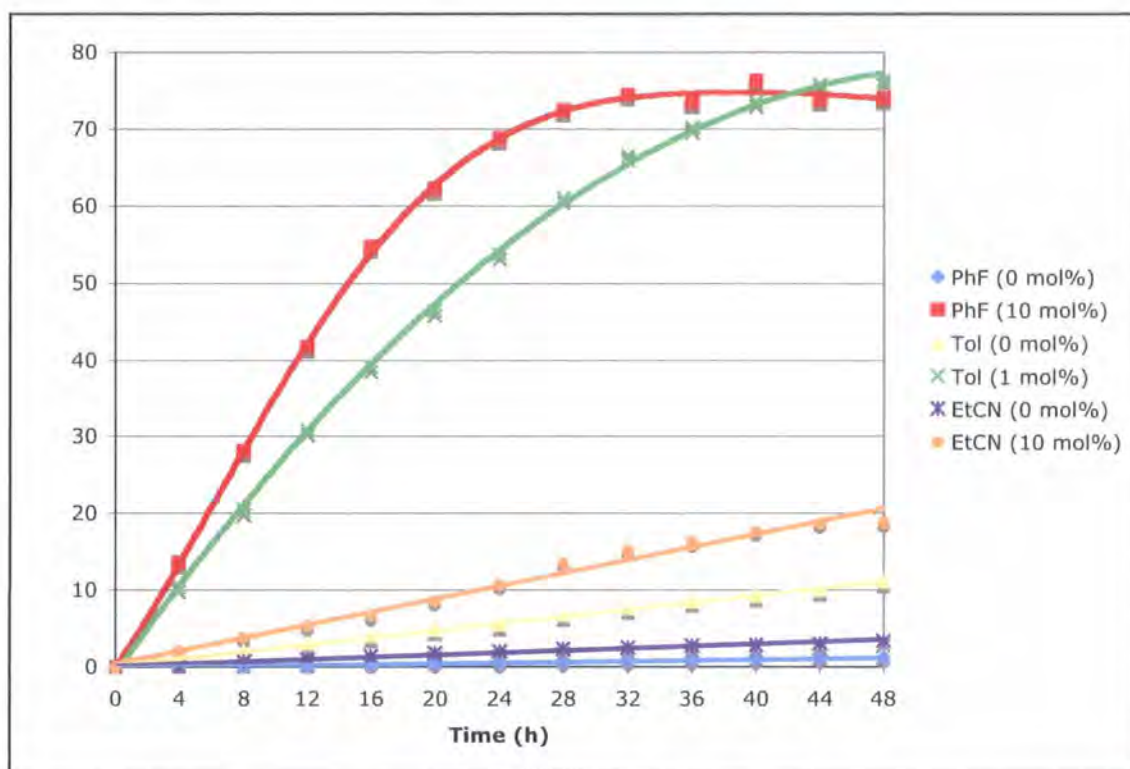
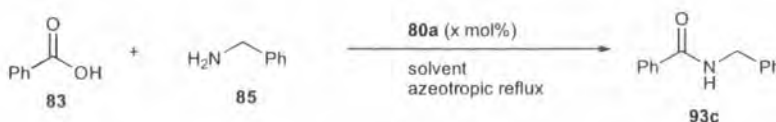


Figure 4. Solvent effects on the formation of *N*-benzylbenzamide **93c** in the absence of molecular sieves (the loading of **80a** is shown in parentheses).

2.2.6 Catalyst optimisation using Design of Experiments (DoE)

2.2.6.1 *N,N*-Diisopropylbenzylamine-2-boronic acid **80a**

To gain an insight into the key reaction parameters that influence the direct amide condensation a DoE study was carried out on the formation of amide **93c** catalysed by **80a** (Equation 30).⁵⁵ Four factors were examined (Table 10) and to simplify subsequent analysis of the results, separate designs were carried out for fluorobenzene and toluene. Temperature could not be included as a factor in these individual studies, because azeotropic reflux is necessary to enable the reaction to proceed efficiently (*vide supra*). A fractional factorial design of 8 experiments was selected⁵⁶ and 4 centre points were included to provide a measure of variation and indicate curvature.



Equation 30

Table 10. Factors and ranges chosen for the factorial design.

Factor	Low	Centre	High
80a / mol%	1	5.5	10
Acid / equiv	0.8	1.1	1.4
Conc / M	0.1	0.3	0.5
Time / h	4	12	20

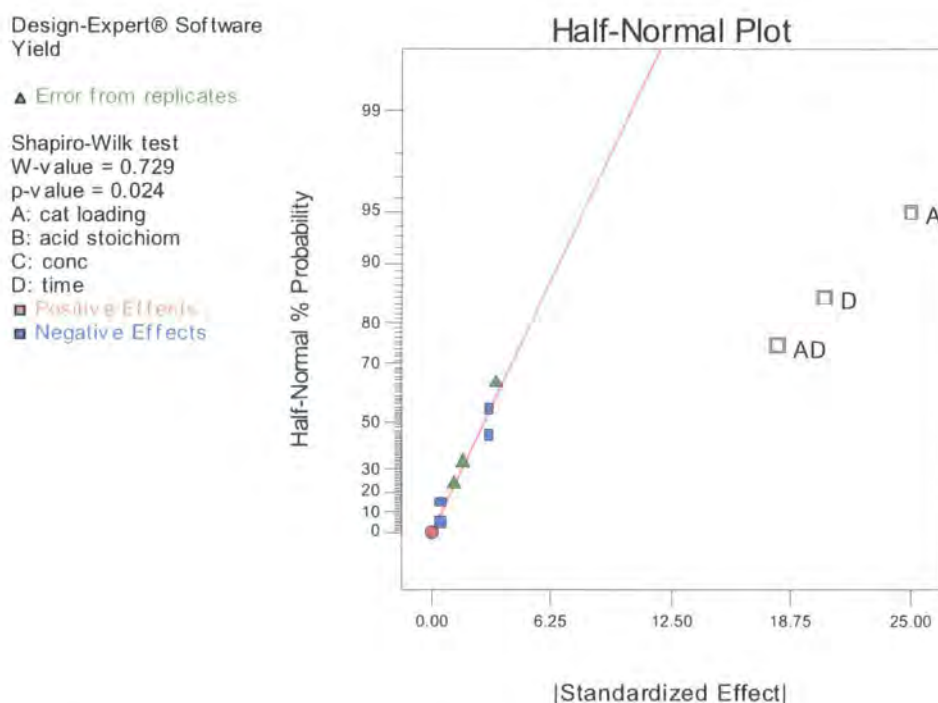


Figure 5. Half normal plot visualising the most important factors determining yield in the direct amide condensation in fluorobenzene.

Once the experiments are completed, a half normal plot is generated using Design-Expert software (Stat-Ease Inc.) and this shows the most significant factors affecting the outputs that are being monitored. In this case, there is only one output (amide yield) and the further a factor lies to the right of the trendline, the larger its effect on the output. Hence, the half normal plot from the DoE in fluorobenzene (Figure 5) shows the most important effects are catalyst loading followed by time and then their interaction, whilst acid stoichiometry and concentration have no significant effect. An interaction graph can now be generated for catalyst loading and time (Figure 6) and

this shows that at the high value of time (20 h), increasing the catalyst loading to 10 mol% results in a larger increase in amide yield *versus* increasing the catalyst loading when the reaction time is only 4 h. In a case where there is no interaction between the factors, the lines plotted at high and low values of time would be parallel with increasing catalyst loading. The centre points, shown as green circles in the interaction graph, show no significant deviation from the linear relationship plotted since they fall between the trendlines plotted at high and low values of time, *i.e.* there is no significant curvature, and the linear relationship plotted is a good representative model. Thus, the DoE suggests in order to increase yield of amide **93c**, catalyst loading and time should be increased. Although increasing reaction time is a possibility, increasing the loading of **80a** beyond 10 mol% would be undesirable.

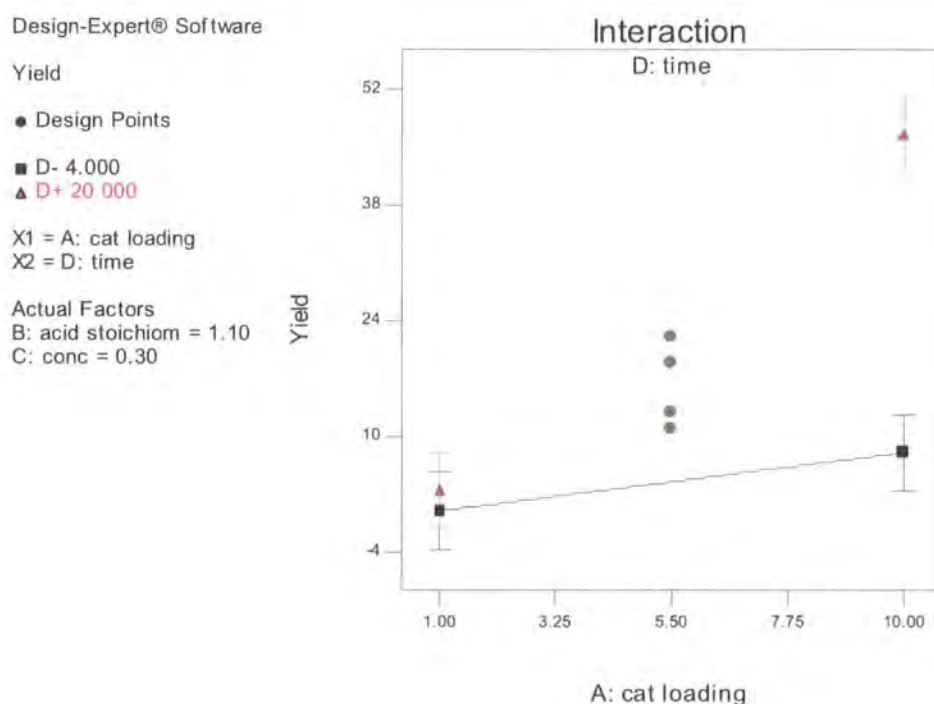


Figure 6. Interaction graph for the direct amide condensation in fluorobenzene.

The same design run in toluene shows catalyst loading is again the most important effect, followed by time; acid stoichiometry still has no significant effect (Figure 7). However, concentration and catalyst loading are now involved in an interaction, with the model suggesting that in order to increase yields of amide **13**, both low concentration and higher catalyst loading are required (Figure 8). The interaction

graph shows significant curvature indicating that the design space is over an optimum. Since catalyst loading is the most important effect, this appears to indicate that similar yields of amide **93c** could be obtained if the loading of **80a** is decreased below 10 mol%. In fact, the centre points indicate that a catalyst loading of 5.5 mol% gives a similar effect, whilst the concentration effect suggests that reaction rate is limited by azeotropic removal of water, and therefore, low concentration is beneficial (*vide supra*).

Design-Expert® Software
Yield

▲ Error from replicates

Shapiro-Wilk test

W-value = 0.998

p-value = 0.915

A: cat loading

B: acid stoichiometry

C: conc

D: time

■ Positive Effects

■ Negative Effects

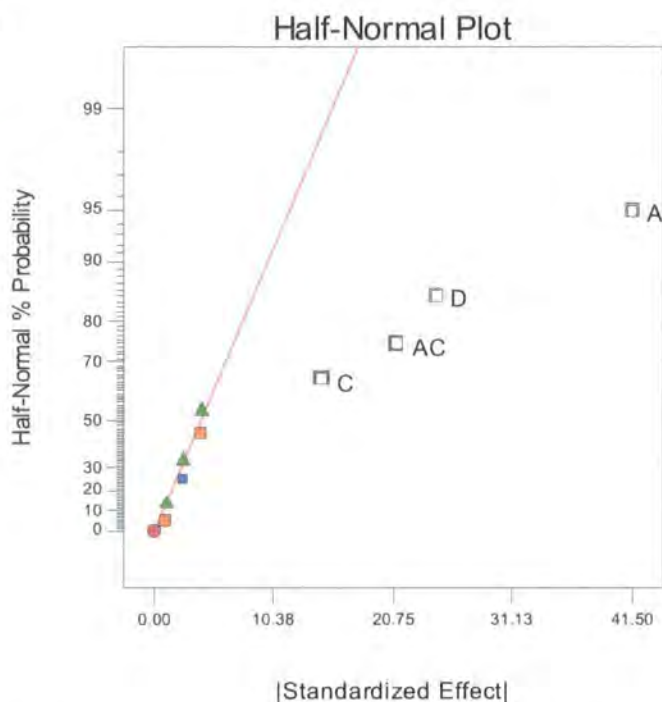


Figure 7. Most important factors determining yield in the direct amide condensation in toluene.

(Figure 10 and Figure 11). The interaction graphs show significant curvature indicating that the design space is over an optimum. Again, this indicates that similar yields of amide could be obtained with reduced amounts of catalyst. However, higher conversions to amide **93c** were observed when **80a** is used as a catalyst compared to boric acid.

Design-Expert® Software
Yield

▲ Error from replicates

A: cat loading

B: acid stoichiom

C: conc

D: time

■ Positive Effects

■ Negative Effects

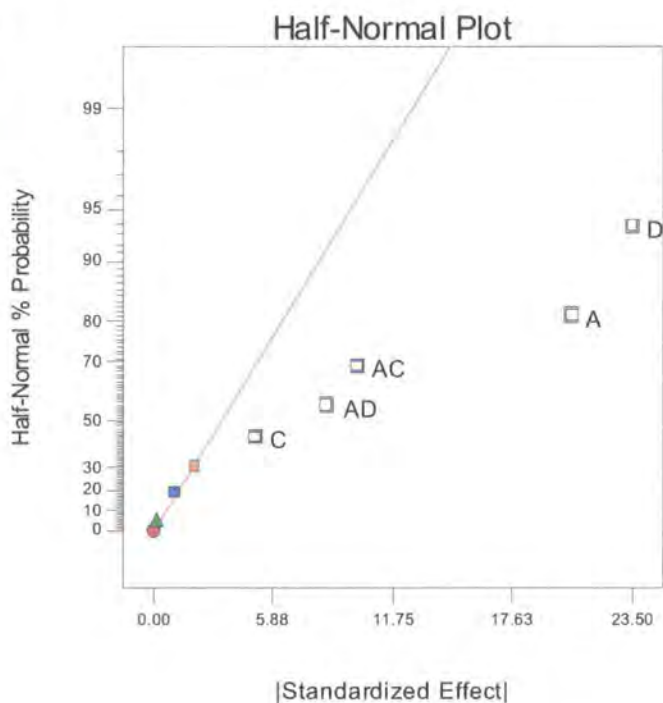


Figure 9. Most important factors determining yield in the boric acid catalysed direct amide condensation in toluene.

Design-Expert® Software

Yield

● Design Points

■ C- 0.100

▲ C+ 0.500

X1 = A: cat loading

X2 = C: conc

Actual Factors

B: acid stoichiom = 1.10

D: time = 12.00

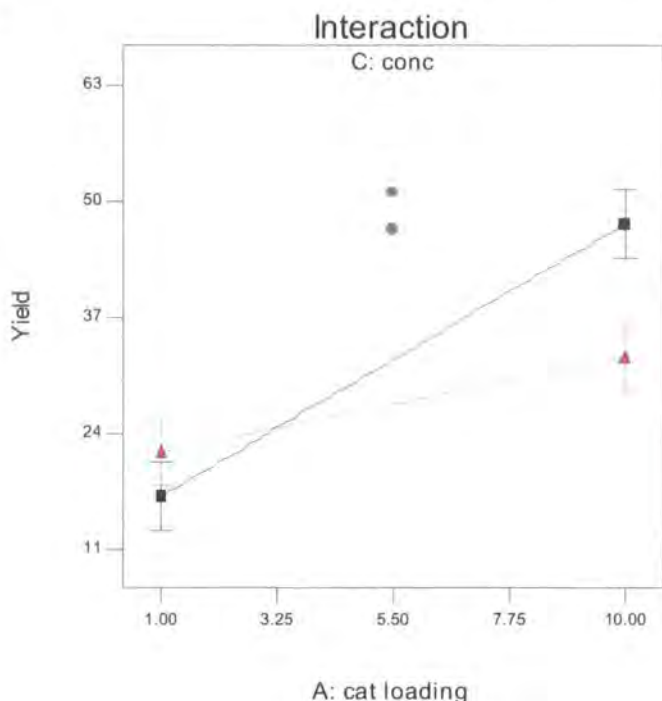


Figure 10. Catalyst loading/concentration interaction graph for the boric acid catalysed direct amide condensation in toluene.

Design-Expert® Software

Yield

● Design Points

■ D- 4.000

▲ D+ 20.000

X1 = A: cat loading

X2 = D: time

Actual Factors

B: acid stoichiom = 1.10

C: conc = 0.30

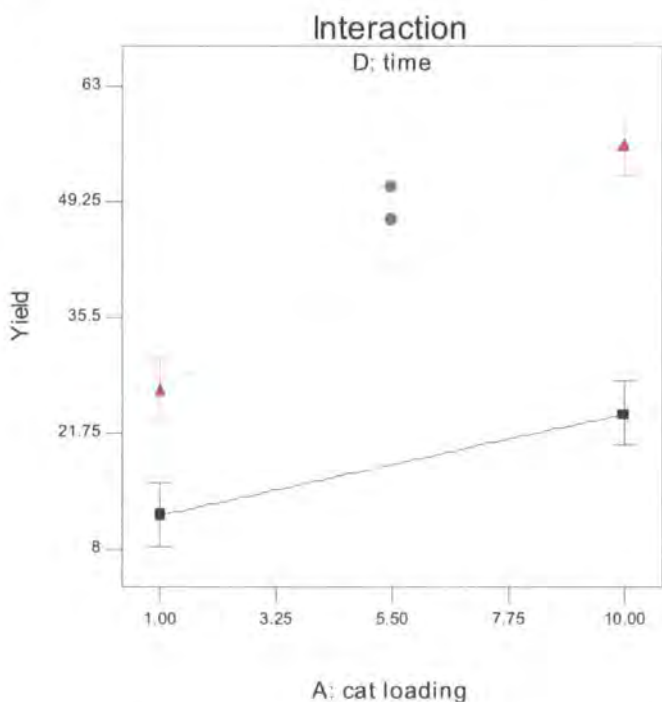
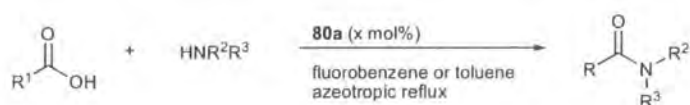


Figure 11. Catalyst loading/time interaction graph for the boric acid catalysed direct amide condensation in toluene.

2.2.7 Application of *N,N*-diisopropylbenzylamine-2-boronic acid **80a** for amide formation

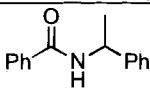
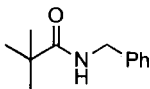
With the DoE optimised reaction conditions in hand, the scope of the direct amide condensation catalysed by **80a** was evaluated. Initially, the reactions were run in fluorobenzene with **80a** (10 mol%), and then in toluene if necessary where the reactions were slow with reaction times of up to 48 h (Equation 32). In the reactions run in toluene, the catalyst loading was adjusted accordingly to provide a reasonable reaction rate and the thermal reactions were assessed in all cases (Table 11).



Equation 32

Table 11. Isolated yields for the direct amide condensation catalysed by **80a**.

Entry	Solvent	80a (mol %)	Time (h)	Product	Yield (%)
1	PhF	0	24		16 ^c
		10			68 ^c
2	PhF	0	24		2 ^c
		10			70 ^c
3	Toluene	0	22		0 ^{a,c}
		1			46 ^{a,c}
4	PhF	0	24		4 ^c
		10			67 ^c
5	PhF	0	22		10 ^{b,c}
		10			53 ^c
6	PhF	0	24		1 ^c
		10			50 ^c
7	PhF	0	48		0 ^c
		10			55 ^{b,c}
	Toluene	5	24		71 ^d
		10			75 ^d
8	PhF	0	24		0 ^c
		10			11 ^c
	Toluene	0	24		0 ^d
		5			16 ^d
		10	30		21 ^d

9	PhF	0	48		0 ^{b,d}
		10			52 ^{b,d}
	Toluene	0	24		0 ^d
10	PhF	5	24		49 ^d
		10			71 ^d
		0			0 ^c
	Toluene	10	15 ^c		
	5	7 ^d			
		10		42 ^d	
				59 ^d	

^aUnder argon. ^bDetermined by HPLC. ^cConditions: acid (5 mmol), amine (5 mmol), 0.1 M.

^dConditions: acid (1 mmol), amine (1 mmol), 0.1 M.

The results shown in Table 11 show that none of the reactions proceeded to 100% conversion after 48 hours, providing further support for the efficiency of water removal being limiting. Fluorobenzene is suitable for the more reactive amide formation reactions, (entries 1, 2, 4, 5, 6, 7 and 9) using 10 mol% of catalyst **80a**. At this temperature (85 °C), there is a clear advantage to using the catalyst compared to the corresponding thermal conditions. For less reactive substrates, the use of toluene and 5 or 10 mol% catalyst loading was necessary in order to provide an improvement in the isolated yields of each of the amides (entries 8-10). Although increasing the reaction temperature increases reaction rates, the associated thermal reactions also become more significant in certain cases, *e.g.* reaction of 4-phenylbutyric acid and benzylamine (entry 1) shows a significant thermal contribution even in fluorobenzene. Interestingly, aniline reacts relatively well in toluene in the presence of only 1 mol% of catalyst **80a**, however, the reaction must be carried out under an inert atmosphere to prevent amine oxidation (entry 3). The case of benzoic acid and 4-phenylbutylamine (entry 7) demonstrates the non-linear relationship between catalyst loading and yield, as observed in the DoE, with no significant difference between a 5 and 10 mol% loading of catalyst **80a**. In the case of morpholine benzoylamide (entry 8), the isolated yield could not be increased to a reasonable level by changing either catalyst loading or reaction temperature.

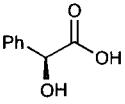
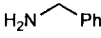
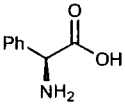
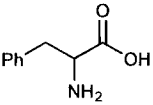
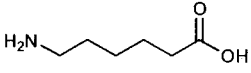
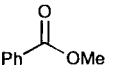
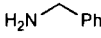
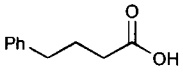
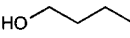
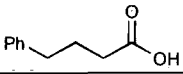
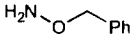
2.2.8 Application to other substrates

Further screening focussed on the condensation of a variety of substrates, with reactions carried out in fluorobenzene. For more difficult substrates, the reactions were carried out at higher temperature, *i.e.* in refluxing toluene, but with lower

catalyst loading (1 mol %). Substrates, reaction conditions and isolated yields are shown in Table 12.

Attempts to form diketopiperazines were unsuccessful under thermal and catalysed conditions (entries 2 and 3), and the catalytic contribution to the formation of (*S*)-*N*-benzylmandelamide was disappointing (entry 1). In addition, 6-aminohexanoic acid failed to condense to caprolactam under these reaction conditions (entry 4). No amide was detected under thermal or catalysed conditions with methyl benzoate and benzylamine (entry 5), presumably because formation of an active acyloxyboron species cannot occur (*vide supra*). Esterification of 4-phenylbutyric acid with 1-butanol (bp 117.6 °C) proceeds well under neat conditions, in the presence of excess alcohol and **80a** (1 mol%), to afford 72% of the desired ester in 22 h (entry 6). However, the thermal contribution to the reaction is significant (50%). In contrast, reaction in fluorobenzene led to no ester formation in the thermal reaction, and only 5% in the presence of **80a** (1 mol%). The lower nucleophilicity of alcohols *versus* amines appears to make esterification considerably more difficult.

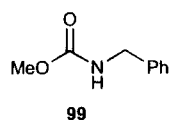
Table 12. Isolated yields for extending the use of catalyst **80a** to other substrates.

Entry	Substrate 1	Substrate 2	Solvent	80a (mol%)	Time (h)	Yield (%)
1			PhF	0	22	0
				10		0
			Toluene	0		7.5
				1		11
2		-	PhF	0	24	0
				10		0
			Toluene	0		0
3		-	PhF	0	24	0
				10		0
4		-	Toluene	0	22	0
				1		0
5			Toluene	0	22	0
				1		0
6			PhF	0	22	0 ^b
				10		5 ^b
			None	0		50 ^c
7			Toluene	0	22	0
				1		72 ^c
				1		0

8			PhF	0	24	0 ^d
		1 or 2 equiv		10		0 ^d
9			None	0	21	25 ^e
		1 or 2 equiv		10		25 ^e
10			Toluene	0	22	0
				1		0

^aUnder argon. ^bAzeotropic removal of water by soxhlet (CaH₂). ^cIn the presence of 1-butanol (2.5 mL). ^dAzeotropic removal of water by soxhlet (4Å mol. sieves). ^e*N*-Benzylmethylcarbamate was produced irrespective of benzylamine stoichiometry.

In addition, the synthesis of urethanes and ureas was attempted from dimethyl carbonate and either 1 or 2 equivalents of benzylamine. Initially, the reaction was carried out in refluxing fluorobenzene over 24 h. However, no urea or urethane was detected with 1 or 2 equivalents of benzylamine, either thermally or in the presence of **80a** (entry 8). The reaction was then attempted under neat conditions, again with and without **80a**, and with benzylamine (1 or 2 equivalents). *N*-Benzylmethylcarbamate **99** was produced in 25% yield over 21 h in all four cases (entry 9). As expected, formation of the urea is more difficult as the reactivity of **99** is reduced *versus* dimethyl carbonate and there is no catalyst contribution to formation of **99**, again because formation of an acyloxyboronate is not possible (*vide supra*).



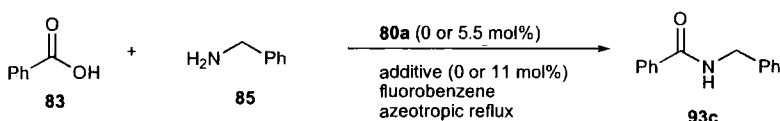
Attempted formation of a sulfonamide from *p*-toluenesulfonic acid and benzylamine (reflux toluene, 22 h), under both thermal conditions and in the presence of **80a** (1 mol%), led to no product formation in either case (entry 10).

In summary, catalyst **80a** is effective for a wide scope of intermolecular direct amide condensations between various carboxylic acid and amine combinations. However, amino acids have proven to be unreactive under these conditions, presumably due to a lack of solubility. The immediately formed carboxylate-ammonium salts are usually soluble in fluorobenzene or toluene at elevated temperature, precipitating on cooling to room temperature. This is not observed in the case of amino acids and the reaction mixture never becomes homogeneous. Condensations involving esters as a coupling partner, ester formation itself, as well as sulfonamide formation are more difficult.

This can be rationalised by either the inability to form an activated acyloxyboron species, or the slow attack on this activated intermediate by the relevant nucleophile (*i.e.* alcohol).

2.2.9 Effect of additives – water and trichloroacetic acid

The effect of water and trichloroacetic acid (TCA) on the formation of *N*-benzylbenzamide **93c** was investigated and the conversion *versus* time data is plotted in Figure 12.



Equation 33

The addition of water (1.6 mL in 9 mL PhF) proved detrimental to the reaction, providing further evidence for an activated acyloxyboron species (Figure 12, entry 1 *vs.* 3), suggesting that the efficiency of water removal affects the final equilibrium and hence the final observed conversion to amide. This is also supported by the final equilibrium conversions seen under the same reaction conditions in toluene *vs.* fluorobenzene (90% *vs.* 65%), with the higher temperature providing more efficient water removal.

The addition of trichloroacetic acid (TCA) was examined in an attempt to make carboxylic acid activation by the formation of either mixed or symmetrical anhydrides more facile. Since trimethylacetic acid is relatively unreactive towards amide formation, TCA would be expected to behave similarly, but because of the electron-withdrawing trichloromethyl moiety, its ability as a good leaving group should be enhanced. TCA was added in a 2:1 ratio to catalyst **80a** (*i.e.* 11 mol%) in fluorobenzene and provides a slight increase in the rate of amide formation (entry 4 *vs.* 3). TCA alone has no effect (entry 2). In toluene, TCA does not have a significant effect both under thermal conditions (entries 5 and 6) and in the presence of catalyst **80a** (entries 7 and 8).

Table 13. Key for Figure 12.

Entry	Solvent	80a (mol%)	TCA (mol%)
1	PhF + water	5.5	0
2	PhF	0	11
3	PhF	5.5	0
4	PhF	5.5	11
5	Tol	0	0
6	Tol	0	11
7	Tol	5.5	0
8	Tol	5.5	11

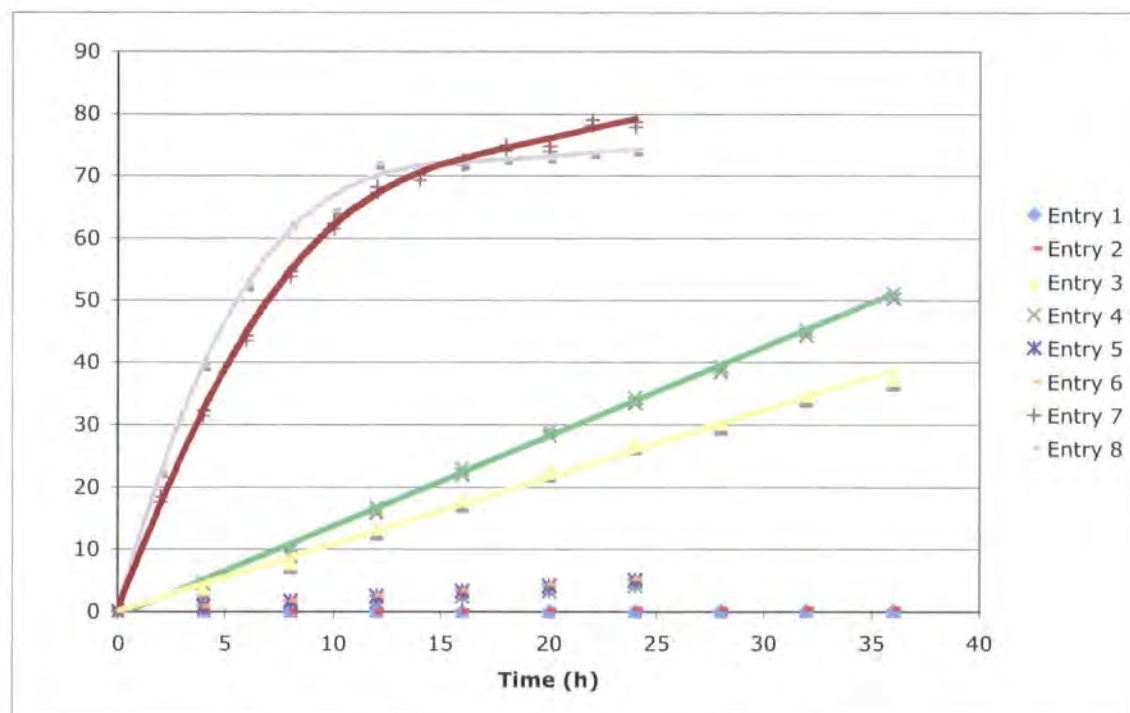
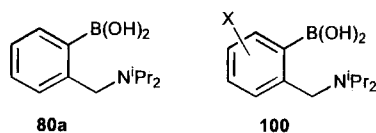


Figure 12. Effect of water, catalyst **80a** and trichloroacetic acid on the direct amide formation of *N*-benzylbenzamide.

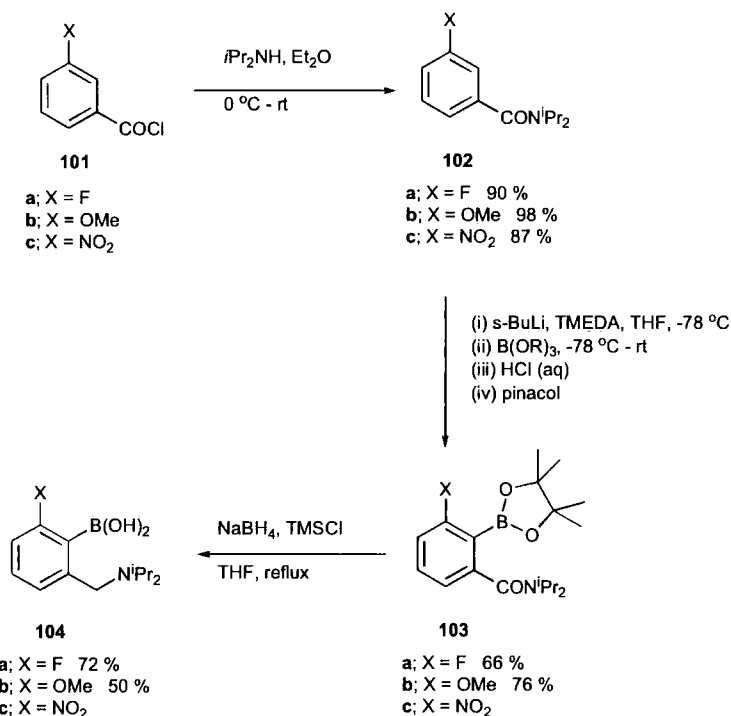
2.3 Towards second generation catalysts

Novel derivatives based on system **80a** were synthesised, in which the hindered *N,N*-diisopropylbenzylamine function was retained. This was due to the clear benefit over the less hindered *N,N*-dimethyl system **80b** as demonstrated previously.⁵² In addition, the new systems **100** were chosen with the aim of testing the effect of changing the Lewis acidity of the boronic acid function by suitable choice of the functional group X.



2.3.1 Fluoro- and methoxy-substituted derivatives

The synthesis of new catalysts based on system **100**, started with the fluoro- and methoxybenzylamineboronic acids **104a** and **b** respectively (Scheme 6). Hence, *N,N*-diisopropyl-3-fluorobenzylamine-2-boronic acid **104a** was prepared starting with 3-fluorobenzoyl chloride **101a** resulting in the formation of amide **102a** upon reaction with diisopropylamine, which was then subjected to directed metallation. Following several attempts to achieve directed *ortho*-metallation of **102a**, direct isolation of the corresponding boronic acid proved unsuccessful, and it was decided to access the pinacol ester **103a** in order to simplify isolation and purification. Hence, reaction of amide **102a** with *sec*-butyllithium followed by addition of trimethylborate, followed by hydrolysis and esterification with pinacol derived the boronate ester **103a**.



Scheme 6. Synthesis of fluoro- and methoxy-substituted amino boronic acids **104**.

The reduction method chosen to convert the pinacol ester **103a** was selected in order to achieve both amide reduction and deprotection of the boronate ester in one step.⁵¹

Although the reduction proceeded well using sodium borohydride-trimethylsilyl chloride, isolation of the amino-boronic acid **104a** proved troublesome due to its high water solubility. However, use of an acidification-neutralisation sequence during the work up allowed direct extraction of the amino-boronic acid **104a**, which could then be efficiently precipitated to give pure product in 72% yield.

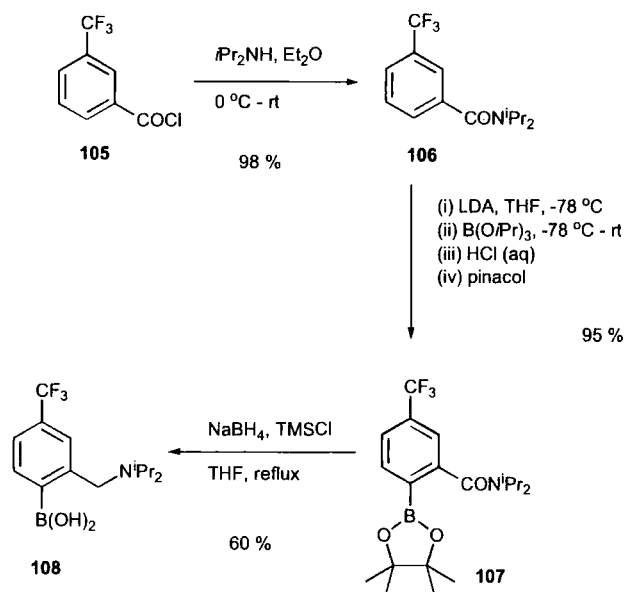
The same strategy was employed in order to synthesise *N,N*-diisopropyl-3-methoxybenzylamine-2-boronic acid **104b**. As before, the amidation of acid chloride **101b** efficiently provided diisopropylamide **102b** (Scheme 6). However, the directed metallation of **102b** proved problematic at first, and resulted in low conversion to the pinacol ester **103b**, *i.e.* *sec*-butyllithium-TMEDA, -78 °C. This was solved by allowing much longer reaction times for the intermediate aryllithium to react with the borate electrophiles (*ca.* 12 hours), resulting in the isolation of pinacol ester **103b** in good yield. It is worth noting that metallation-borylation of amide **102b** fails to proceed at all with *n*-butyllithium, whereas the alkyllithium source has no significant effect upon the metallation of **102a**. In addition, attempted metallation of methoxy-substituted system **102b** with lithium diisopropylamide, followed by triisopropyl borate resulted in the formation of ester **103b**, but in only 11% yield.

Having obtained boronate ester **103b**, reduction was attempted as for **103a**, resulting in only low yields of amino-boronic acid **104b** (10%). The methoxy system **104b** appears to have increased water solubility compared to **104a**, and therefore, suitable changes to the workup procedure (THF evaporation and minimisation of aqueous solution and solvent volumes) resulted in a reasonably efficient isolation of **104b**, which after subsequent recrystallisation was isolated in a reasonable 50% yield.

In order to compare catalysts of type **100**, systems with different electronic properties were required. Several attempts were made to access the system **104c**, *via* formation of the corresponding amide **102c** (Scheme 6). However, all attempts (*s*-BuLi-TMEDA, *n*-BuLi-TMEDA, *n*-BuLi alone and LDA were tried in THF at -78 °C; *t*-BuLi was also tried in THF at 0 °C) to achieve deprotonation of **102c** to access boronate **103c** led to the formation of intractable complex products, which is consistent with other unsuccessful attempts to achieve lithiation of nitroaryl systems.⁵⁷

2.3.2 Trifluoromethyl-substituted derivative

As an alternative to the nitro-substituted system, the final catalyst prepared was the trifluoromethyl-substituted system **108**, which proved reasonably straightforward to access (Scheme 7). Thus, amidation of acid chloride **105** provided amide **106** in 98% yield. Directed *ortho*-metallation under the same conditions as used for systems **103** (*n*- or *s*-BuLi-TMEDA) led to a mixture of *ortho*- and *para*-CF₃ boronates, with low total conversion (*ca.* 10%). A number of attempts at improvement (increasing reaction temperature, metallation time, *etc.*) failed to improve matters and alternative metallating agents were examined. A mixture of potassium *tert*-butoxide and *n*-BuLi⁵⁸ gave no reaction, however, use of lithium diisopropylamide led to metallation at the less hindered *para*-CF₃ position to afford boronate **107** selectively and in high yield (95%). Initial attempts at reduction of the amide **106** using borane-dimethyl sulfide in THF at reflux failed to give an observable reaction, however, using the TMSCl-borohydride conditions resulted in formation of boronic acid **107** after work up, albeit *via* a slow reaction which resulted in only 40% conversion in 40 hours. The solution to this problem was to decrease the reaction concentration used for the reduction conditions, which resulted in complete conversion in 24 hours (Scheme 6), and after modification of the workup conditions used for amino-boronic acid **104b**, the trifluoromethyl-boronic acid **108** was obtained in 60% yield after recrystallisation.



Scheme 7. Synthesis of trifluoromethyl-substituted boronic acid **108**.

2.3.3 Comparison of crystal structures

Crystals of both **104a** and **108** suitable for single crystal X-ray analysis were readily prepared, however, attempts to derive good quality crystals of the methoxy derivative **104b** were unsuccessful. However, fluoro and trifluoro derivatives **104a** and **108** respectively are essentially isostructural with one another and also with the analogue **80a**.⁵¹ Molecular conformations are also similar (Figure 13). The C(1)BO(1)O(2) moiety is planar and inclined to the benzene ring plane by 25.8° (**104a**) or 21.8° (**108**). Larger twist in **104a** obviously is caused by steric repulsion between the F and O(2) atoms. One hydroxyl group, O(1)H, forms an intramolecular hydrogen bond with the amino N atom which is slightly pyramidalised, with the mean C-N-C angle of 113°. Molecules are linked into centrosymmetric dimers by pairs of hydrogen bonds O(2)-H...O(1)[1-x, 1-y, 1-z]. There are only marginal differences in bond distances between **80a**, **104a** and **108** (Table 14). It is interesting to note that the trifluoromethyl system **108** exhibits a shorter C-B bond length compared with the fluoro system **104a**, however, it is little different to the non-substituted system **80a**. This probably suggests that there is not a major difference in Lewis acidity between systems **80a** and **108**, though **104a** might be slightly less Lewis acidic. Unfortunately, these solid state structures cannot be compared with the methoxy derivative **104b**, and ¹¹B NMR also does not seem to suggest significant differences in the properties of the boronic acid function which show resonances at δ 28.8,⁵¹ 28.4, 29.3 and 28.5 for **80a**, **104a**, **104b** and **108** respectively.

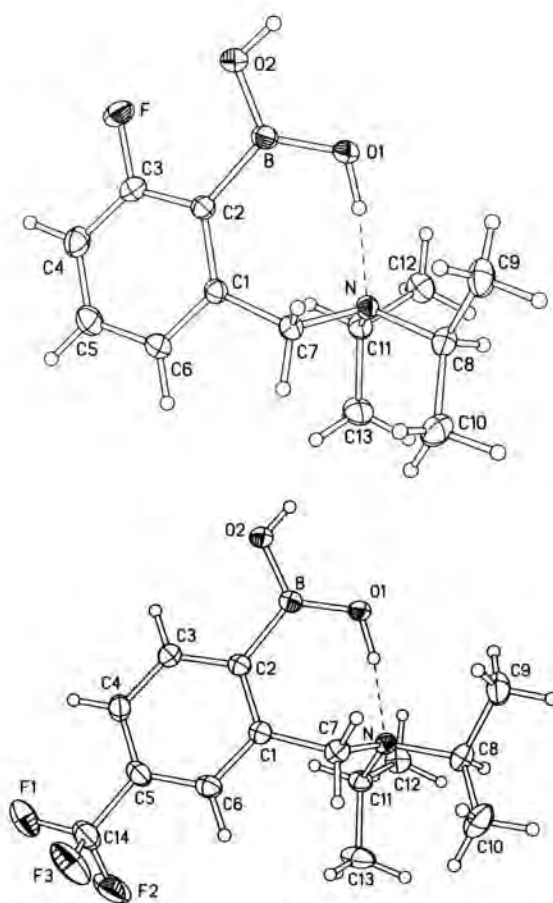


Figure 13. X-ray molecular structures of **104a** (top) and **108**. Thermal ellipsoids are drawn at 50 % probability level.

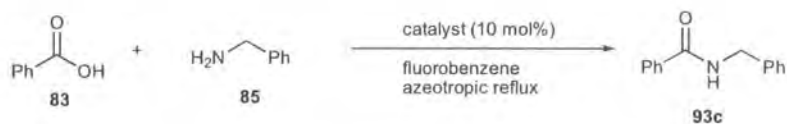
Table 14. Selected bond distances (Å).

	80a	104a	108
C(2)-B	1.588(2)	1.5965(14)	1.5876(17)
B-O(1)	1.356(2)	1.3547(13)	1.3575(15)
B(1)-O(2)	1.366(2)	1.3581(13)	1.3609(16)
O(1)...N	2.637(1)	2.607(1)	2.623(1)
C(1)-C(2)	1.412(2)	1.4204(12)	1.4169(16)
C(1)-C(7)	1.522(2)	1.5171(13)	1.5187(16)
C(7)-N	1.480(1)	1.4837(12)	1.4795(15)

2.3.4 Catalyst evaluation

Having previously shown⁵² that the boronic acid **80a**, and related systems, promote amidation reactions, which are highly substrate dependent and that the use of more difficult substrates under lower temperature conditions (refluxing fluorobenzene) exposes differences in catalyst activity, the new catalysts were evaluated and compared using the reaction between benzoic acid and benzylamine (Equation 34).

The direct (uncatalysed) thermal formation of amide **93c** under these conditions is non-existent and the results of this comparison are shown in Figure 14.



Equation 34

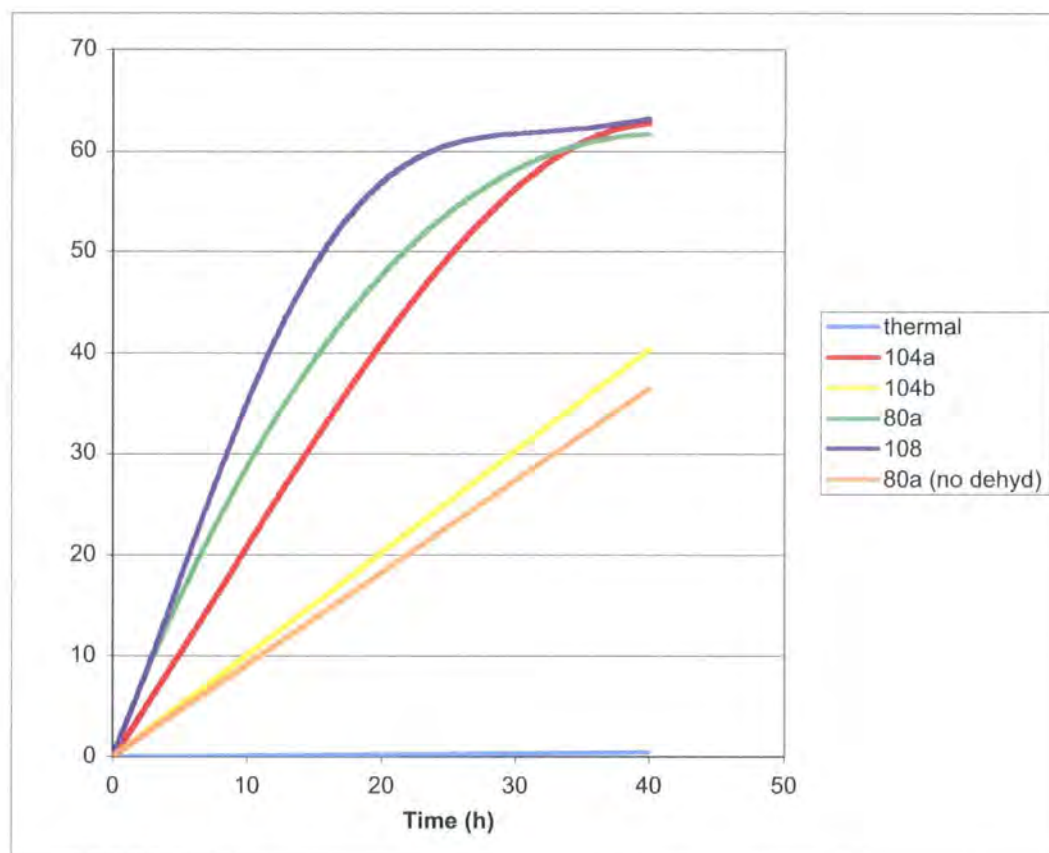


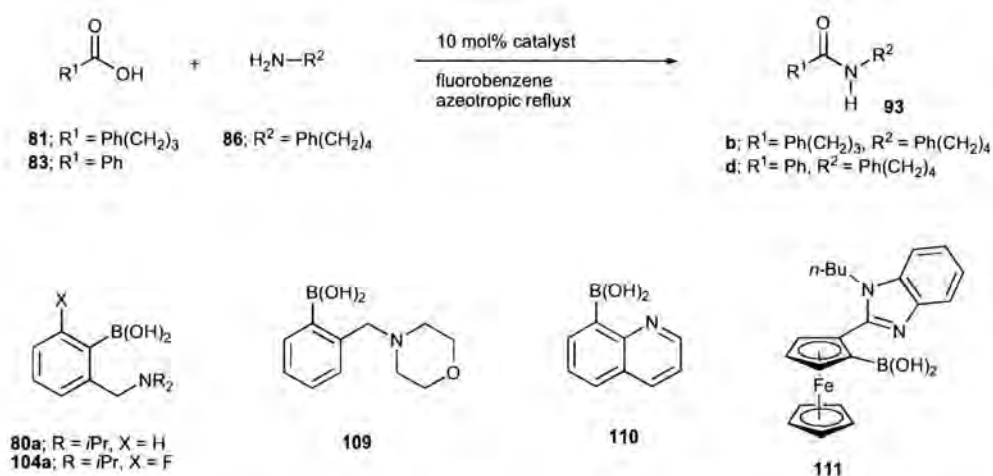
Figure 14. Yield vs. time data for the formation of *N*-benzylbenzamide **93c**.

The addition of a *para*-trifluoromethyl group (catalyst **108**) is beneficial to rate of formation of *N*-benzylbenzamide **93c** compared to the unsubstituted system **80a**, whereas the addition of the *ortho*-fluorine function, *i.e.* catalyst **104a** decreases reaction rate to a small extent. While the differences between catalysts **80a**, **104a** and **108** are not substantial, increasing the electron density of the phenyl ring by incorporating a methoxy group (electron donation by conjugation of the oxygen lone pair), *i.e.* catalyst **104b**, leads to a significant decrease in reaction rate. This results in only 28% conversion to amide **93c** in 28 hours using **104b** compared to *ca.* 63%

conversion for catalysts **80a**, **108** and **104a**, which have all reached their equilibrium conversions at around this time period. The efficiency of water removal determines the equilibrium position, therefore affecting both final conversion and reaction rate, as demonstrated by the reaction catalysed by **80a** without dehydration, along with the results obtained from the DoE study (*vide supra*).

2.4 Activity of other catalysts

A comparison of the activity of several other amino-boronic acid catalysts on the formation of amides **93b** and **d** was also carried out (Scheme 8).



Scheme 8. Other amino-boronic acids for the direct amide condensation

Fluoro-substituted catalyst **104a** shows essentially equivalent activity to **80a** for the formation of amide **93b** (Figure 15), but **80a** is the most active catalyst for the more difficult formation of benzamide **93d** (Figure 16). This suggests the slight electron deficiency of **104a** is beneficial for the reaction involving 4-phenylbutyric acid **81**, but not with more hindered benzoic acid **83**. This is also supported by trifluorophenylboronic acid **5** being the most active for reactions involving more electron rich 4-phenylbutyric acid **81** (*vide supra*).

In comparison, catalysts **109**, **110** and **111**⁵⁹ are less active when 4-phenylbutyric acid **81** is used as a substrate. However, the differences become more substantial with benzoic acid **83** as the substrate (Figure 16), suggesting the *diisopropylbenzylamine*

moiety is crucial for good activity in this case and assists in formation of a reactive intermediate, possibly by a general acid-catalysed pathway.

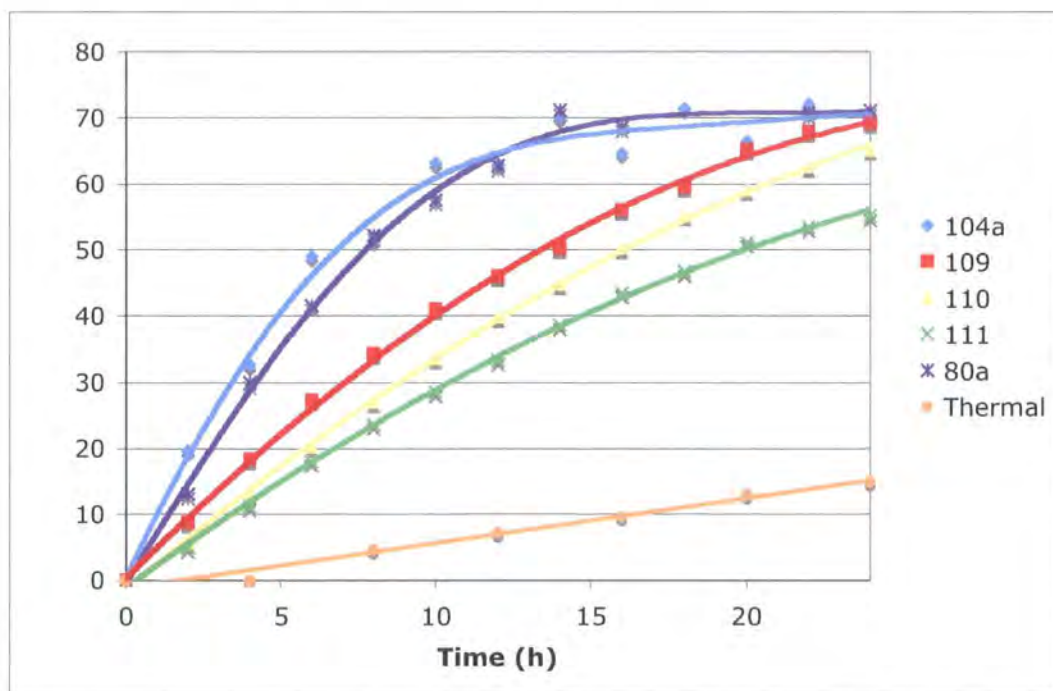


Figure 15. Formation of *N*-4-phenylbutyl-4-phenylbutyramide **93b** over time.

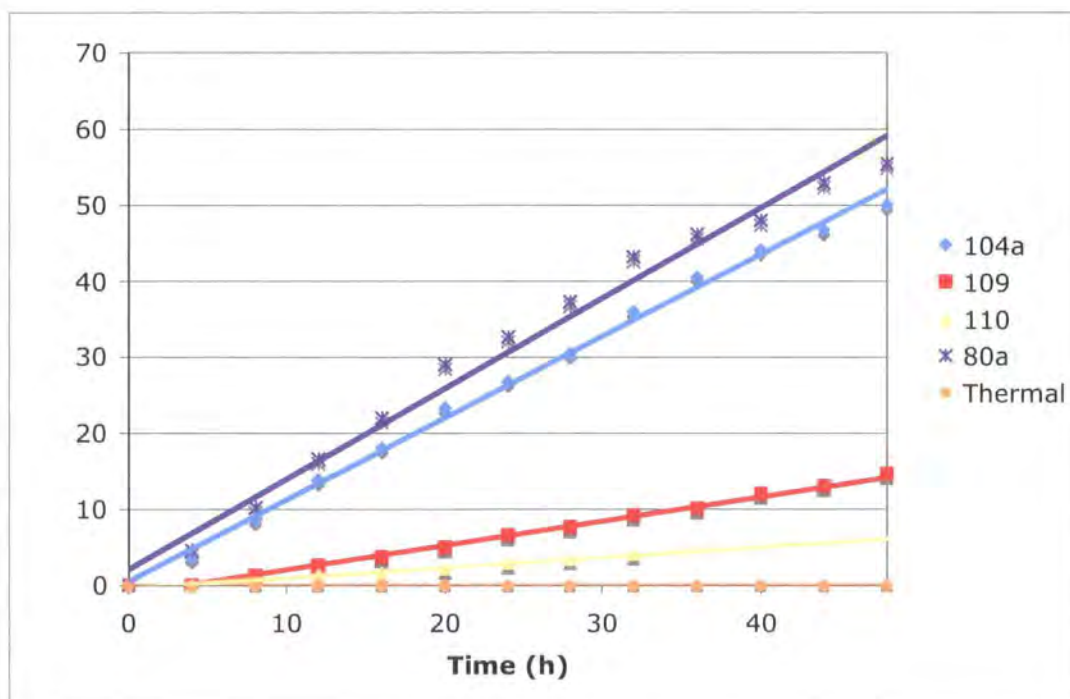
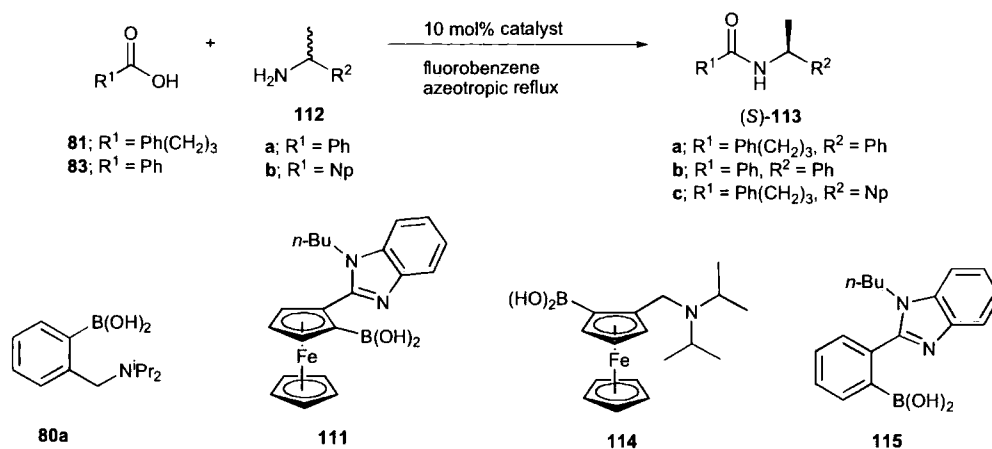


Figure 16. Formation of *N*-4-phenylbutylbenzamide **93d** over time.

2.5 Kinetic resolution *via* direct amide formation from a racemic amine and achiral carboxylic acid

The kinetic resolution of racemic amines *via* direct amide formation is a highly desirable process. However, since direct amide formation is generally a high temperature process and asymmetric induction processes are usually more efficient the lower the temperature, the current reaction conditions that employ refluxing fluorobenzene (85 °C) do not make this goal look promising.

The development of planar chiral ferrocene-based bifunctional amino-boronic acids within the group allowed this idea to be explored.⁵⁹⁻⁶⁰ Ferrocene catalysts containing both a benzimidazole moiety **111** and the familiar *diisopropylamine* function, **114**, were screened initially on the reaction between benzoic acid **83** and (\pm)- α -methylbenzylamine **112a** to form amide **113b** (Scheme 9). In addition, *diisopropylbenzylamine*-2-boronic acid **80a** and phenylbenzimidazole boronic acid^{59,61} **115** were screened for comparison (Figure 17). All the catalysed reactions were carried out in refluxing fluorobenzene with a 10 mol% catalyst loading and the thermal contributions were also assessed.



Scheme 9. Kinetic resolution *via* amide formation.

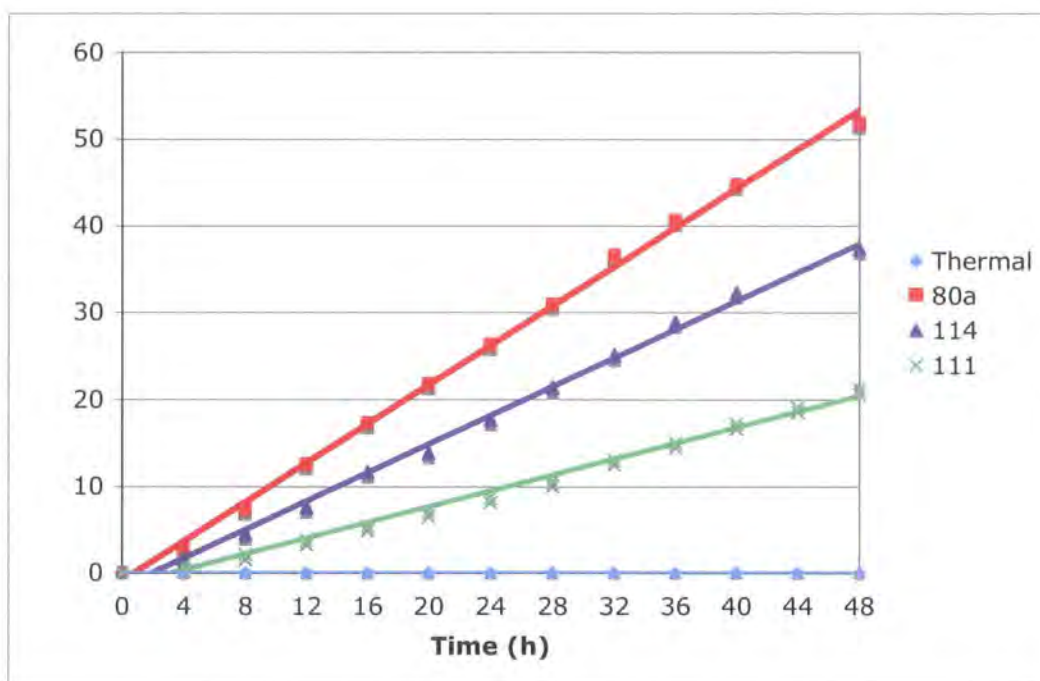


Figure 17. Formation of *N*-(1-phenylethyl)benzamide **113b**.

Amino-boronic acid **80a** is the superior catalyst for formation of **113b** and this appears to be a consistent observation with amide condensations employing benzoic acid **83** (Table 15, entry 2) (*vide supra*). Ferrocene catalyst **114** shows 38% conversion in 48 h, which is approximately 10% less than phenyl derivative **80a**, but unfortunately, no evidence of kinetic resolution was observed (entry 3). The thermal contribution to the reaction, which must be racemic, is zero for this acid/amine combination and the reaction was repeated with *R*-(+)- α -methylbenzylamine. Subsequent chiral HPLC analysis of the product amide (*R*)-**113b**, confirmed that no racemisation had occurred. Employing a larger substituent *ortho* to the boronic acid, as in the case of benzimidazole-based ferrocene catalyst **111**, results in lower activity compared to the other catalysts screened, but kinetic resolution was observed and the product amide (*S*)-**113b** was formed with 21% conversion and 41% e.e. (entry 4).

Table 15. Conversion and e.e.s for amino-boronic acid catalysed kinetic resolution.

Entry	Catalyst	Conversion ^a (%)	e.e. ^b (%)	Product 113
1	Thermal	0 (48 h)	-	b
2	80a	52 (48 h)	-	b
3	114	38 (48 h)	0	b
4	111	21 (48 h)	41	b
5	115	0 (48 h)	-	b
6	Thermal	11 (48 h)	-	a
7	111	34 (12 h)	29	a
		73 (48 h)	19	
8	Thermal	13 (48 h)	-	c
9	111	- ^c (12 h)	20	c
		85 ^d (48 h)	9	

^aDetermined by HPLC. ^bDetermined by chiral HPLC. ^cNot determined. ^dIsolated yield.

Since *N,N*-diisopropylbenzylamine-2-boronic acid **80a** is more active than the ferrocene analogue **114**, phenylbenzimidazole boronic acid **115** was also screened to see if the same would hold true in the benzimidazole series. However, phenylbenzimidazole **115** failed to show any activity, giving 0% conversion to amide **113b** (entry 5). This could be due in part to B-N chelation, since the diisopropylamine-based catalysts **80a** and **114**, along with ferrocene-benzimidazole **111** show no B-N chelation. On the other hand, phenylbenzimidazole **115** is a mixture of B-N chelate, free boronic acid and boroxine in solution, as evidenced by ¹¹B NMR, with the boroxine showing partial B-N interactions in the solid state, as shown by single crystal X-ray analysis where two of the three boron atoms are four-coordinate.⁶¹ In addition, the benzimidazole moiety is closer to the boronic acid in the phenyl system **115** versus **111**, suggesting the benzimidazole is acting as more than just a steric block, and that the distance between the boron and nitrogen functions is crucial for efficient proton transfer and, therefore, catalysis.

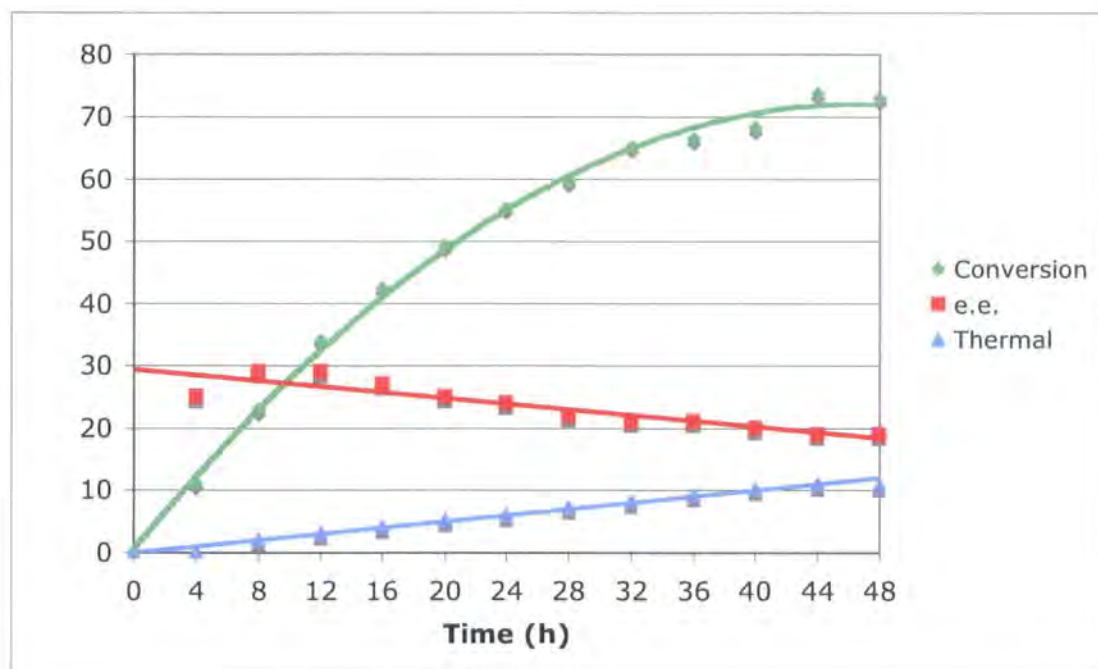


Figure 18. Formation and e.e. of (*S*)-*N*-(1-phenylethyl)-4-phenylbutyramide **113a** in the presence of catalyst **111**.

In an attempt to increase amide conversion levels, ferrocene-benzimidazole **111** was screened on the formation of amide (*S*)-**111a**, employing more reactive 4-phenylbutyric acid **81** as a substrate (Scheme 9 and Figure 18). The racemic thermal reaction in this case accounts for 11% conversion in 48 h, whereas the catalysed reaction has reached its final equilibrium conversion of 73% in 44 h (entries 6 and 7, Table 15). The e.e. of (*S*)-**113a** decreases from 29% to 19% over 48 h and this is due to the reaction being run in the presence of 1 equivalent of racemic amine (and hence the maximum yield of resolved amide is 50%).

The amine was subsequently changed for (\pm)-1-(1-naphthyl)ethylamine **112b** with the hope that the larger naphthyl substituent would increase the efficiency of kinetic resolution *versus* (\pm)- α -methylbenzylamine **112a**. Unfortunately, formation of (*S*)-**113c** led to disappointing results, with 20% e.e. after 12 h and only 9% e.e. (85% conversion) after 48 h (entry 9, Table 15).

In a further attempt to try and improve the levels of asymmetric induction, other azeotroping solvents with lower boiling points were tested. Cyclohexane (bp 81 °C) and diisopropyl ether (bp 68 °C) were selected and the thermal reactions were

screened. In cyclohexane, formation of amide **113a** in the absence of catalyst led to 4% conversion in 44 h, whereas in diisopropyl ether, the thermal reaction is non-existent. The results of the solvent screen in the presence of catalyst **111** are shown in Table 16 and interestingly, the use of lower boiling solvents failed to improve matter with the e.e.s suggesting there are other significant solvent effects involved. Cyclohexane provided (*S*)-**113a** in 20% e.e. after 12 h compared with 29% e.e. in fluorobenzene (entries 1 and 2). Diisopropylether afforded (*S*)-**113a** in only 16% e.e. after 48 h, with only 21% conversion (entry 3) and since the thermal reaction does not proceed at this temperature, product formation must proceed *via* the catalysed pathway. As expected, lowering the reaction temperature also led to a significant decrease in reaction rate.

Table 16. Solvent screen for formation of (*S*)-*N*-(1-phenylethyl)-4-phenylbutyramide **113a** in the presence of catalyst **111**.

Entry	Solvent	Conversion ^a (%)	e.e. ^b (%)
1	Fluorobenzene	34 (12h)	29
		73 (48h)	19
2	Cyclohexane	23 (12h)	20
		50 (48h)	12
3	Diisopropyl-ether	21 ^c (48h)	16

^aDetermined by HPLC. ^bDetermined by chiral HPLC. ^cIsolated yield.

2.6 Summary and conclusions

N,N-Diisopropylbenzylamine-2-boronic acid **80a** has been shown to be effective under refluxing fluorobenzene conditions for direct amide formation between equimolar amounts of carboxylic acids and amines. Under these lower temperature conditions (compared with toluene), the catalyst **80a** is stable, thermal contributions are minimised, and proto-deboronation does not compete. A comparison of the rates of amide formation between various boron-based catalysts clearly showed the enhanced activity of catalyst **80a** for the more difficult substrates under the developed reaction conditions and the cooperative effect of the amine and boronic acid moiety was subsequently demonstrated for direct amide formation reactions involving benzoic acid.

The synthesis of novel substituted analogues of the bifunctional catalyst **80a** has allowed the subtleties of direct amide formation involving arylboronic acid-mediated catalysis to be further investigated. The addition of electron withdrawing functions to the aryl ring of **80a**, for example trifluoromethyl derivative **108**, does lead to increased catalytic activity for amide formation, reinforcing the view that such catalysts act by forming a mixed anhydride-type analogue,⁵² with the electron withdrawing group increasing the leaving group ability during the amide formation step. However, there is not a substantial difference in overall activity between **80a** and **108**, and hence, in terms of practical applications either catalyst is suitable, whereas less hindered amine systems⁵² (e.g. **80b**) or more electron rich aryl systems (e.g. **104b**) are less efficient. DoE studies on the use of catalyst **80a** show a non-linear relationship between catalyst loading and amide conversion, with a 5 mol% loading producing a similar effect to 10 mol% in toluene. Interestingly, variation of carboxylic acid stoichiometry had no significant effect on amide conversion. In addition, the water-removing capacity of the solvent has been shown to be an important consideration during routine use of these types of catalysts, and therefore, higher dilutions are preferred in order to minimise reaction times. These optimised conditions have been demonstrated to be applicable to a wide range of substrates.

The development of chiral ferrocene-benzimidazole catalyst **111** within the group has allowed the kinetic resolution of racemic amines and achiral carboxylic acids to be investigated. Initial results in refluxing fluorobenzene have provided encouraging results, with amides produced in up to 41% e.e. The inactivity of the phenyl-benzimidazole system **115** suggests the importance of the distance between the boronic acid and amine functions.

2.7 Future work

Despite the progress that has been made with respect to direct amide bond formation, the need to produce generally more active catalysts is still an unsolved problem. Specifically, this includes the development of catalysts that are active at lower temperatures, applicable to a wide range of substrates as well as related reactions (e.g. ester formation), and show generally higher levels of activity as catalysts. To address these issues, further variation of catalyst structure could be investigated to include variation of the amine function beyond *diisopropyl*- and *dimethylbenzyl*amine, as

well as varying the substitution pattern to examine *meta*- and *para*-substituted amino-boronic acids.

There is also a requirement to develop a library of chiral catalysts for screening, particularly for the kinetic resolution of amines. The synthesis of catalysts bearing a chiral amine function *via* reductive amination of commercially available 2-formylphenylboronic acid, would quickly allow the potential of this strategy to be investigated. Chiral substituents could also be added to the phenyl ring. The identification of factors that are beneficial to catalyst activity could provide lower temperature reaction conditions, which could then be applied to ferrocene-benzimidazole **111** mediated kinetic resolution. The development of new catalysts coupled with lower temperature reaction conditions through further solvent screens, could lead to higher levels of both amide conversion and asymmetric induction, as well as providing further information on the factors that control catalyst activity.

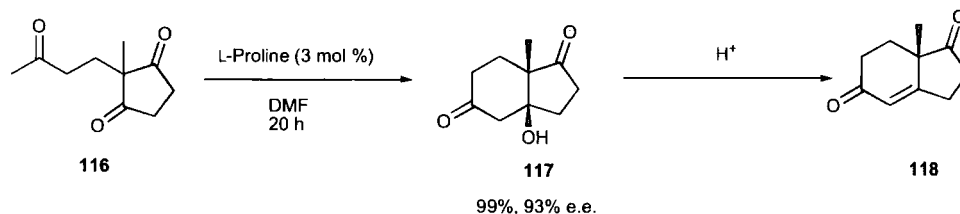
3. Asymmetric enamine catalysis and the direct aldol reaction

3.1 Introduction to organocatalysis

Organocatalysis is defined as the rate increase imparted by the addition of an organic compound to a reaction and has received much attention in recent years. In particular, the use of proline and related derivatives for many transformations has been noteworthy since the beginning of the century.⁶² Some of the disadvantages of metal-based catalysts *versus* organocatalysis include cost, environmental impact, toxicity and product contamination. The scope and utility of organocatalysis has been demonstrated by its use in natural product synthesis.⁶³

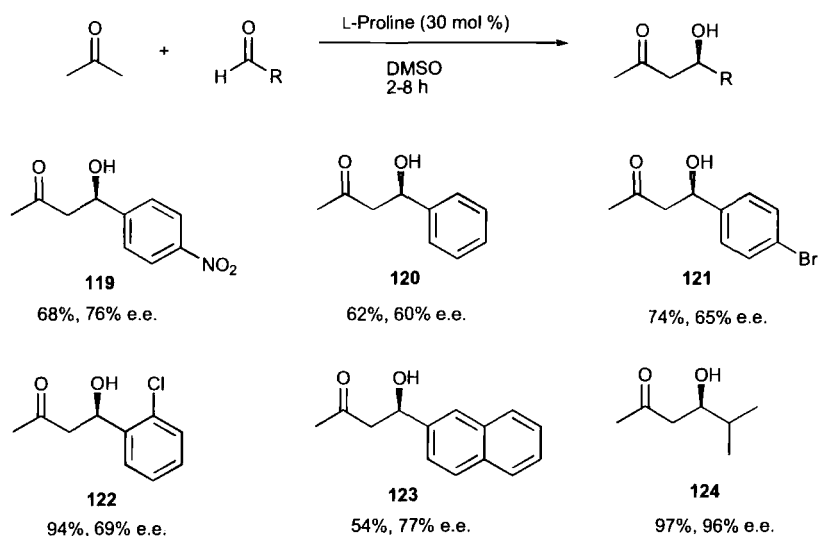
3.1.1 The first examples of asymmetric enamine catalysis

In the 1970s, the development of the intramolecular aldol reaction of ketone **116** catalysed by (*S*)-proline was the first example of using a small molecule catalyst for an asymmetric aldol reaction (Scheme 10).⁶⁴ Aldol adduct **117** was obtained after reaction in DMF for 20 h in 99% yield and 93% e.e., in the presence of proline (3 mol%).



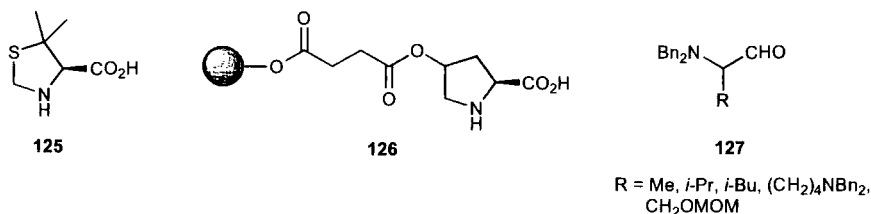
Scheme 10. Hajos-Parrish-Eder-Sauer-Wiechert reaction.

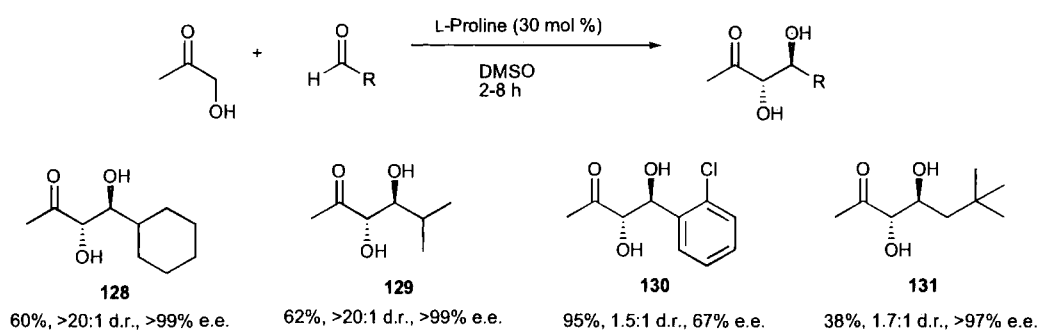
In 2000, List and Barbas described the first intermolecular direct asymmetric aldol reactions catalysed by proline between various aldehydes and acetone (Equation 35).⁶⁵ The reaction between *p*-nitrobenzaldehyde and acetone proceeded in 68% yield and 76% e.e. after 4 h with proline (30 mol%), and the other aromatic aldehydes screened furnished generally good yields and good to excellent e.e. The reaction time could be significantly reduced under microwave activation, as demonstrated by Alexakis in 2006 where **119** was produced in 68% yield and 74% e.e.⁶⁶ At 25°C with microwave irradiation at 10 W, the reaction time was reduced to only 15 minutes.



Equation 35

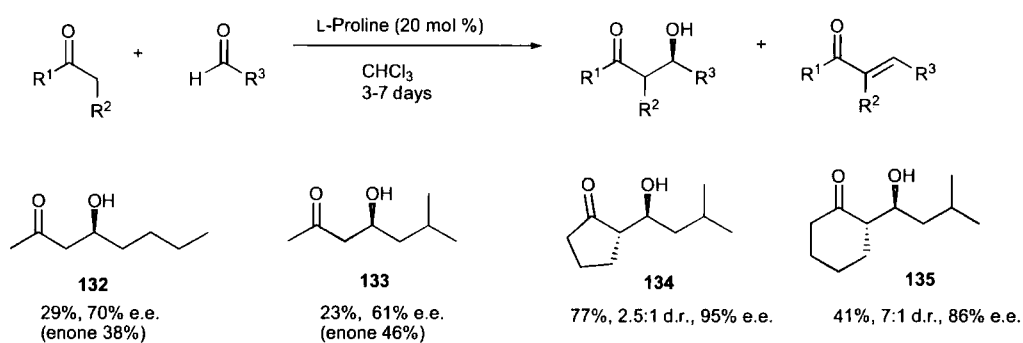
This methodology was extended to the use of hydroxyacetone as a donor, affording *anti*-1,2-diols in generally good yield, along with excellent diastereoselectivity ratio and e.e. (Equation 36).⁶⁷ The product from using 3,3-dimethylbutyraldehyde as acceptor **131** was obtained with poor diastereoselectivity, as was 2-chlorobenzaldehyde adduct **130** which also displayed moderate e.e. In comparison, the use of 5,5-dimethyl thiazolium-4-carboxylate **125** as an aldol catalyst generally provided improved e.e. values with aromatic aldehydes as substrates *versus* L-proline, but lower yields.⁶⁸ The immobilisation of (2*S*,4*R*)-4-hydroxyproline on PEG₅₀₀₀ monomethyl ether (MeOPEG) **126**, with a succinate spacer, provided similar yields and e.e.s to unsupported proline, allowing simple catalyst recovery and reuse.⁶⁹ Later it was demonstrated that *N,N*-dibenzyl- α -amino aldehydes **127** were also suitable acceptors, the proline-catalysed reaction proceeding with moderate to good yield and diastereoselectivity.⁷⁰





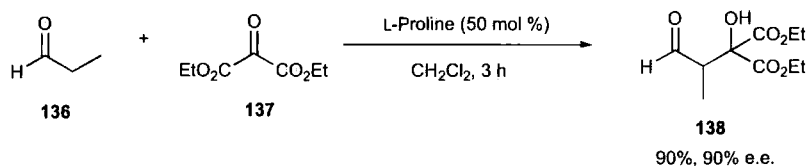
Equation 36

The challenging use of α -unsubstituted aldehydes as acceptors in the cross-aldol reaction has been demonstrated.⁷¹ Deprotonation of the aldehyde component was successfully suppressed therefore preventing self-coupling, but substantial amounts of the undesired aldol condensation products were observed in many cases (Equation 37).



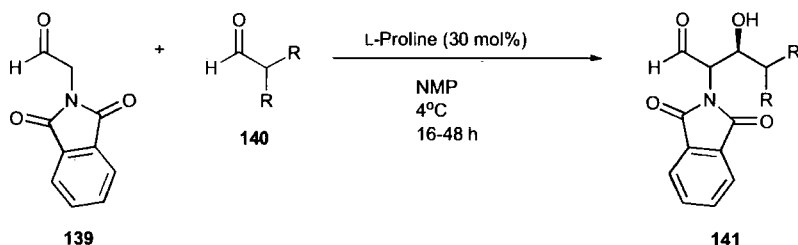
Equation 37

Aldehydes can also be used as donors with activated carbonyl compounds (e.g. diethyl ketomalonate **137**), but high catalyst loadings (50 mol%) are required to prevent the decrease in e.e. observed with extended reaction times (Equation 38).⁷²



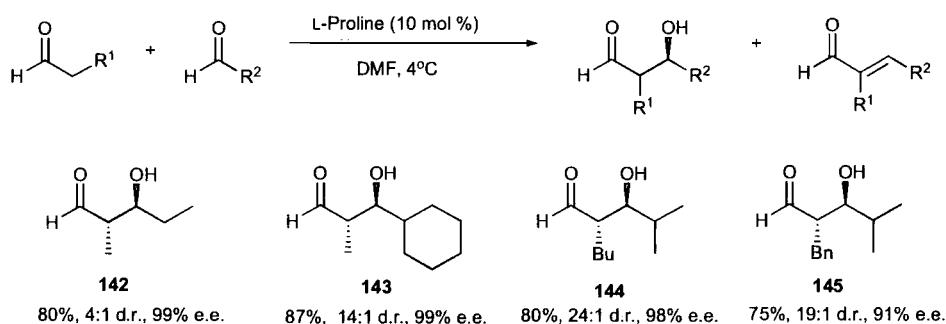
Equation 38

On the other hand, the use of a protected α -amino aldehyde (phthalimidoacetaldehyde **139**) as donor with $\alpha,\tilde{\alpha}$ -disubstituted aldehydes (5-10 equivalents) afforded the desired aldol adducts in good yield, high diastereoselectivity (up to >100:1 d.r.) and enantioselectivity (up to >99.5% e.e.).⁷³ Optimised conditions involved reaction in NMP at 4 °C, in the presence of L-proline (30 mol%), as shown in Equation 39.



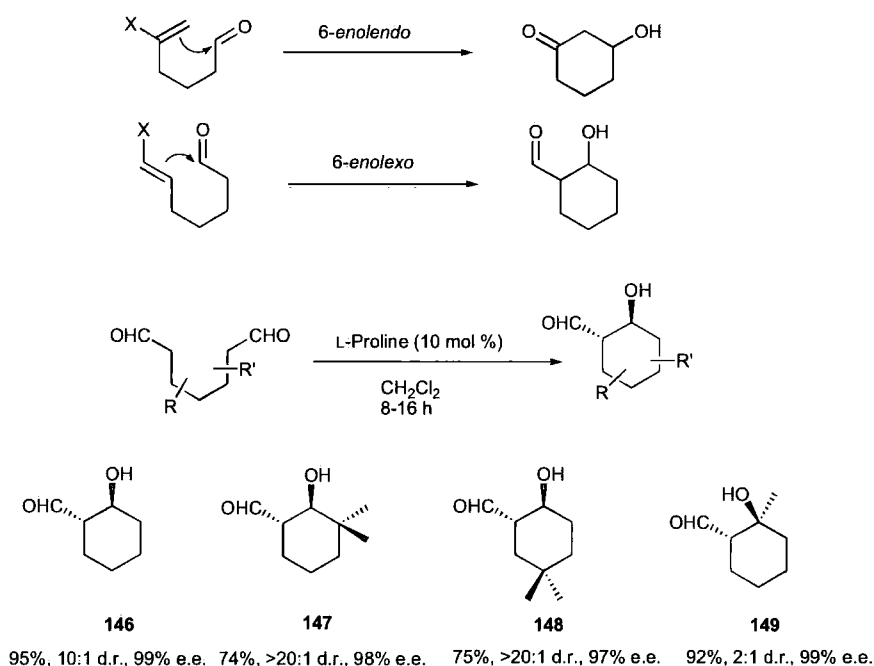
Equation 39

In 2002, MacMillan introduced the first direct enantioselective cross-aldol reaction of aldehydes. Proline (10 mol%) in DMF at 4 °C, with syringe pump addition of the donor aldehyde (this forms the enolate equivalent, in this case an enamine), afforded high yields and stereoselectivity of the desired cross-aldol products (Equation 40).⁷⁴



Equation 40

The Hajos-Parrish-Eder-Sauer-Wiechert reaction (Scheme 10) is a *6-enolendo* aldolisation and proline was shown by List and coworkers to also catalyse *6-enolexo* aldolisation of heptanedials and keto aldehydes with excellent enantioselectivity (Scheme 11).⁷⁵



Scheme 11. Proline-catalysed 6-enolexo aldolisation.

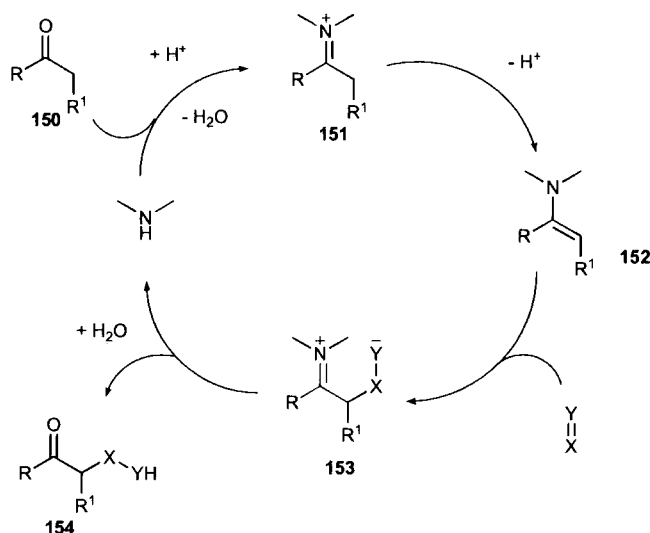
The extension of the proline-catalysed aldol reaction to more expensive and less volatile ketones can be facilitated by the addition of water (1-5 equivalents) to the reaction in DMF, allowing stoichiometric use of the ketone donor.⁷⁶ Although purification is simplified, reaction rates were slow (5-30 days with non-activated aldehyde acceptors).

3.1.2 Proposed mechanism

The proposed mechanism for enamine catalysis involves the initial formation of an iminium ion **151**. Tautomerisation to the enamine **152** and reaction with an electrophile generates iminium ion **153** which, after subsequent hydrolysis, generates product **154** (Scheme 12).⁷⁷ Additional evidence is provided by ESI-MS detection of the proposed intermediates.⁷⁸

The enantioselectivity (equation 1, Figure 19) and diastereoselectivity (equation 2, Figure 19) in the proline-catalysed aldol reaction is explained by the transition states computed from the B3LYP/6-31G(d) density functional theory method. The enamine and carbonyl acceptor are in a partial Zimmerman-Traxler-like arrangement with the *anti*-enamine preferred.⁷⁹

The one-proline enamine mechanism is consistent with experimental data showing no non-linear effects in the proline-catalysed aldol reaction,⁸⁰ and high O-18 incorporation into the aldol products when O-18 enriched water is used.⁸¹



Scheme 12. Proposed mechanism for enamine catalysis.

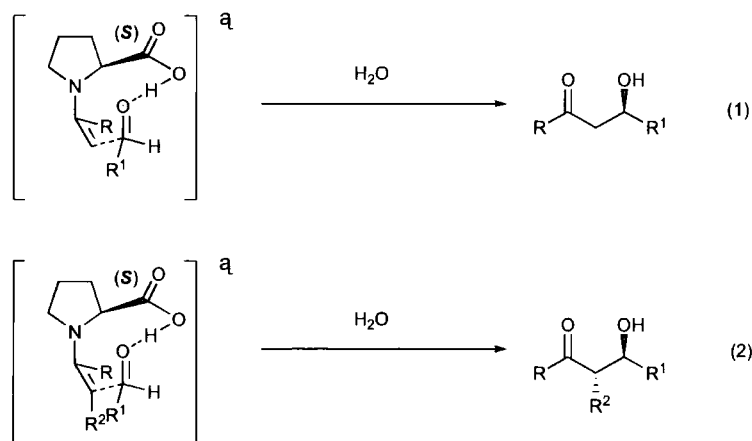
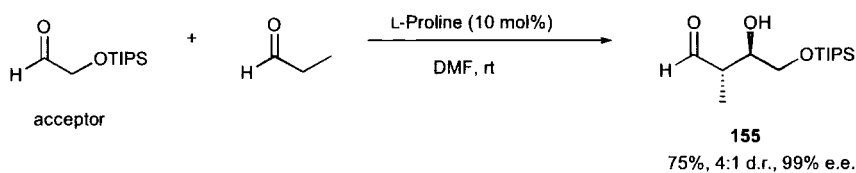


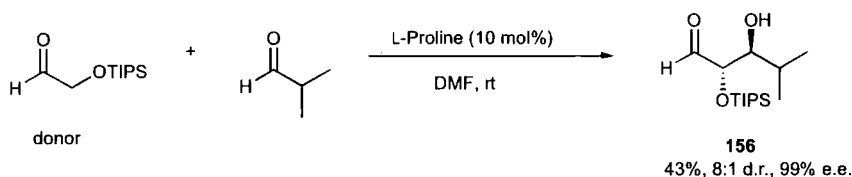
Figure 19. Computed transition states for the proline-catalysed aldol reaction.

3.2 Towards carbohydrate synthesis mediated by proline⁸²

The direct enantioselective aldol reaction of α -oxygenated aldehydes as both donors and acceptors, provides access to protected polyols *via* self-reaction, as well as *anti*-1,2-diols *via* cross aldolisation (Equation 41 and Equation 42).⁸³

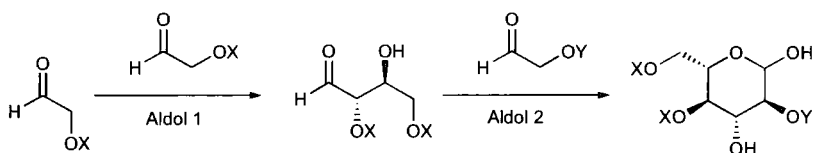


Equation 41



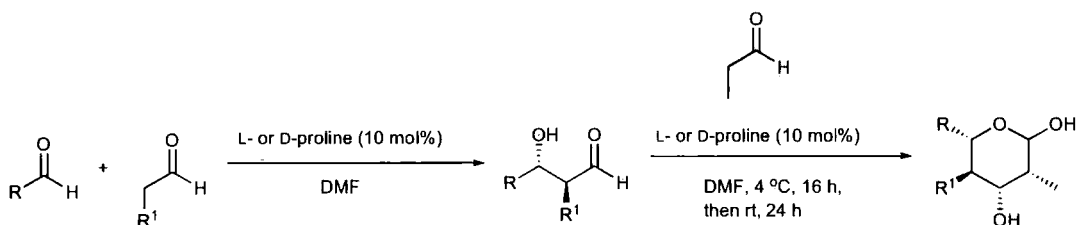
Equation 42

The self-aldolisation is the first of a two-step carbohydrate synthesis (Scheme 13), with the second step reported soon after, *via* a Lewis acid-mediated tandem Mukaiyama aldol addition-cyclisation.⁸⁴



Scheme 13. Two-step carbohydrate synthesis *via* self-aldolisation.

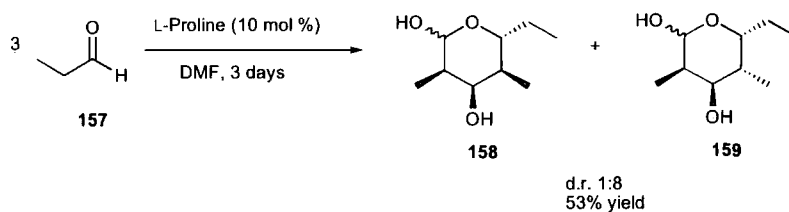
Around the same time, Córdova reported a similar two-step approach to carbohydrates in which both steps are proline-catalysed.⁸⁵ A wide-range of alkyl substituents are tolerated and yields ranged from 15-42% with excellent enantioselectivity ($\geq 99\%$ e.e.) in all the examples presented (Scheme 14).



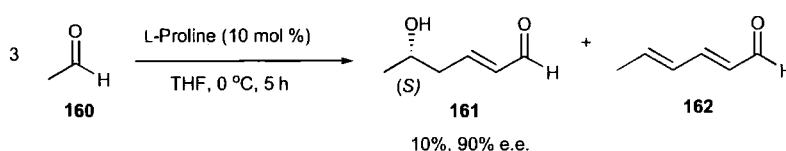
Scheme 14. Proline-catalysed carbohydrate synthesis.

The proline-catalysed one-step trimerisation of propionaldehyde **157** afforded polyketide **159** containing four chiral centres with good diastereoselectivity but modest enantioselectivity (47% e.e. after 10 h, 33% e.e. after 3 days).⁸⁶ Reducing the

temperature to 4 °C saw the enantioselectivity improve to 85% e.e. Similarly, self-aldolisation of acetaldehyde afforded hexenal **161** in 90% e.e. at 0 °C in THF, whilst minimising formation of side product **162**.⁸⁷

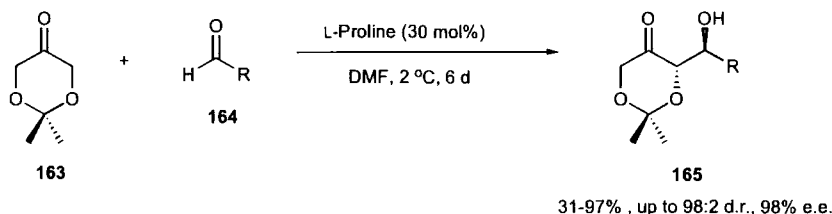


Equation 43



Equation 44

Another approach by the Enders group employed 2,2-dimethyl-1,3-dioxan-5-one **163** as a protected dihydroxyacetone equivalent.⁸⁸ Proline (30 mol%) in DMF at 2 °C for 6 days afforded good diastereoselectivity, enantioselectivity and generally good yields (Equation 6). Barbas also demonstrated the use of **163** under similar conditions.⁸⁹

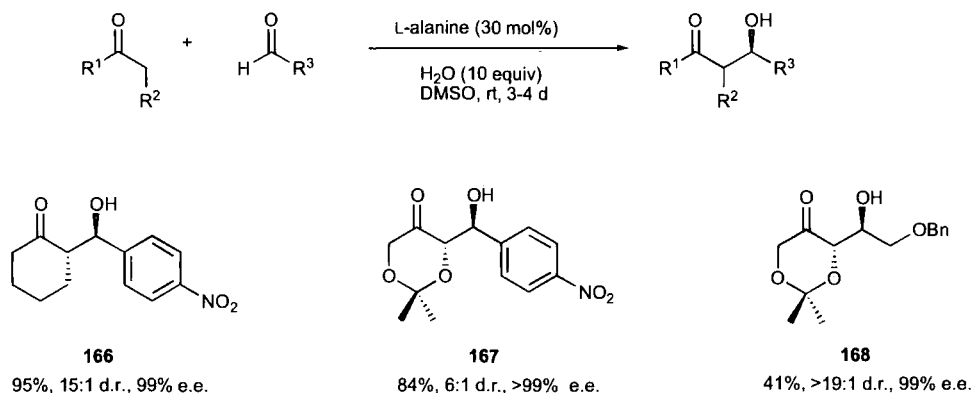


Equation 45

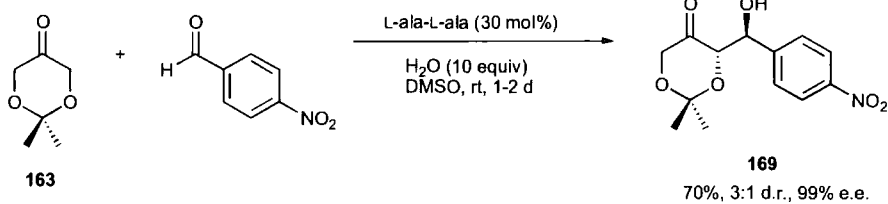
3.3 Catalysis mediated by other amino acids and peptides

In 2005, Córdova showed that the intermolecular aldol reaction could be catalysed by linear amino acids in wet DMSO, and hence, a pyrrolidine moiety was not essential for catalysis (Equation 46).⁹⁰ Alanine, valine, *isoleucine* and aspartate were all active in the aldol reaction between 4-nitrobenzaldehyde and cyclohexanone, providing good stereoselectivity and yields. Alanine was screened further and it was found that donor

163 afforded better yields than cyclohexanone, although enantioselectivity was consistently high. This was later extended to various di- and tripeptides possessing a primary amino group, with e.e.s of up to 99% obtained (for example, see Equation 47).⁹¹

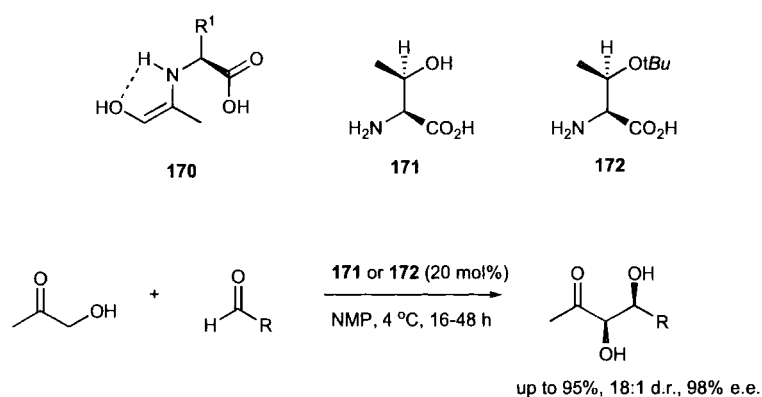


Equation 46



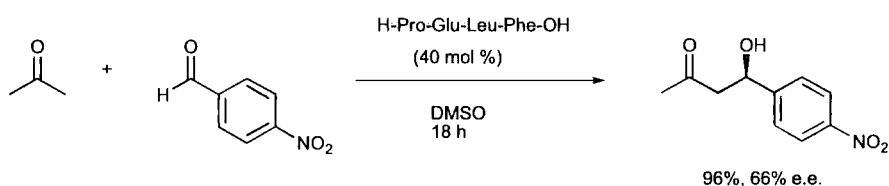
Equation 47

Barbas elegantly demonstrated that the use of primary amino acids could mediate the *syn*-aldol reaction with hydroxyacetone as donor.⁹² It was proposed that the reaction would proceed through *Z*-enamine **170**, stabilised by a hydrogen bond between the hydroxyl and amino groups. L-Threonine **171** and L-O-*t*-butyl-threonine **172** were screened with a range of electron-deficient aromatic aldehydes and hydroxyacetone, affording high yields of *syn*-1,2-diols with good enantioselectivity (Equation 48). This has very recently been expanded to the use of TBS, benzyl-protected and unprotected dihydroxyacetone as a donor in the *syn*-aldol reaction, again catalysed by **172**.⁹³



Equation 48

Oligopeptides with *N*-terminal proline residues have been shown by Reymond to also catalyse the aldol reaction between 4-nitrobenzaldehyde and acetone in 96% yield and 66% e.e. (Equation 49).⁹⁴ Combinatorial peptide synthesis could allow the development of a large library of potential catalysts for screening.

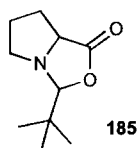


Equation 49

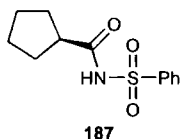
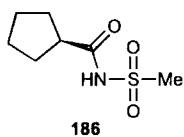
3.4 Pyrrolidine-based derivatives

Unsurprisingly, most derivatives are based on the modification of chiral pyrrolidines and usually involve replacing the carboxylic acid function of proline. Yamamoto and coworkers have developed diamine-protonic acid derivatives for the aldol reaction, and the best compromise between reaction rate, e.e. and suppressing formation of the condensation product was found to be a 1:1 ratio of **173** and **174**, where **173** acts as a convenient source of triflic acid (Equation 50).⁹⁵ Low catalyst loadings provided high e.e.s and generally good yields with the ketone donor as solvent.

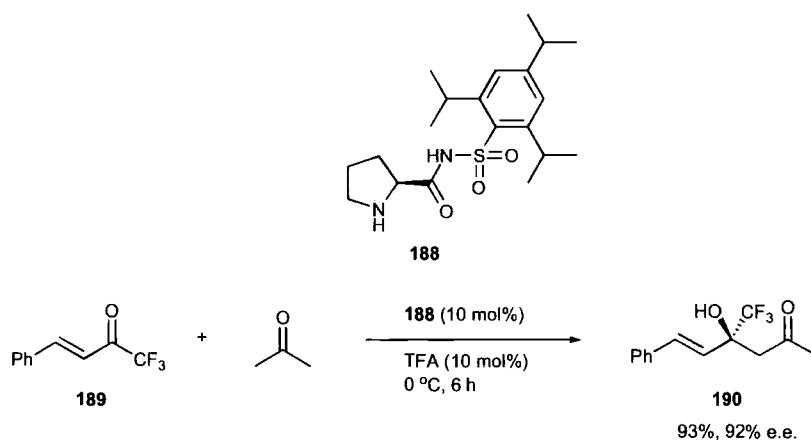
Tetrazole **179** has also been screened in the reaction of 4-nitrobenzaldehyde and acetone, where optimised conditions (20 mol%, DMF, -50 °C, 4 h) afforded the product in 77% yield and 86% e.e.⁹⁷ The rate of reaction of acetone with 4-methoxybenzaldehyde and pivaldehyde, was significantly increased with catalysis by **179** versus L-proline. This was explained by the improved solubility of **179** and the quantitative formation of a bicyclic oxazolidinone **185**, detected on mixing L-proline with pivaldehyde by ¹H NMR .



The Ley group has screened the acyl sulfonamides **186** and **187** (20 mol%) in the direct asymmetric aldol reaction of various ketones and 4-nitrobenzaldehyde leading to good yields and e.e.s in the majority of examples presented.⁹⁸ Dichloromethane was found to offer the best compromise between reaction rate and enantioselectivity. However, the use of cyclopentanone as a donor led to low e.e.s, and the diastereoselectivity was poor with cyclic ketones. The higher enantioselectivity observed with catalyst **187** was attributed to the electron withdrawing phenyl group lowering the pK_a of the sulfonamide.

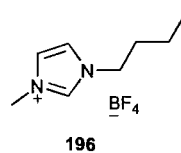
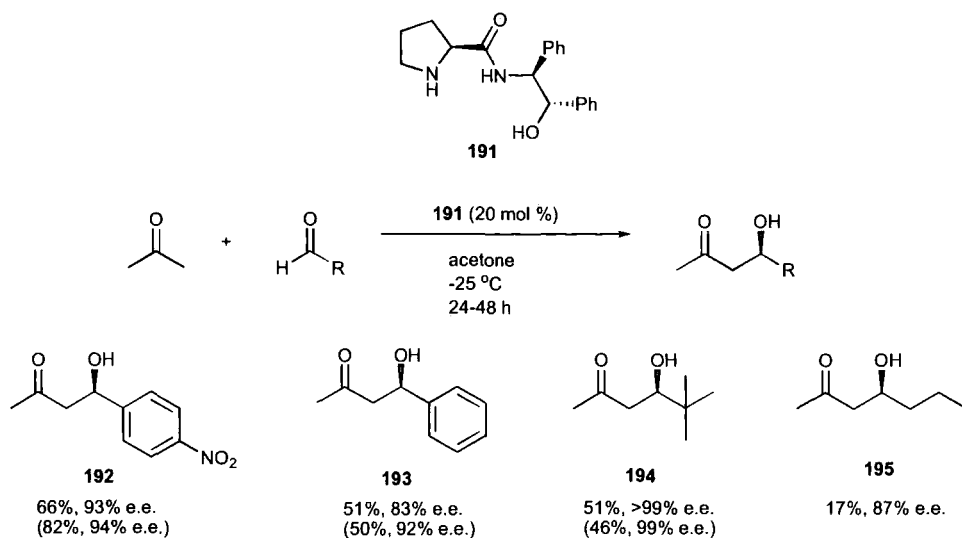


Sulfonamide **188**, bearing a bulkier aromatic substituent, has been used in the aldol reaction of methyl ketones with α,β -unsaturated trifluoromethyl ketones, e.g. **189**.⁹⁹ Good yields and high enantioselectivities were obtained with the ketone donor as solvent and a wide variety of phenyl substituents were tolerated, but cyclic ketones failed to react (Equation 53).

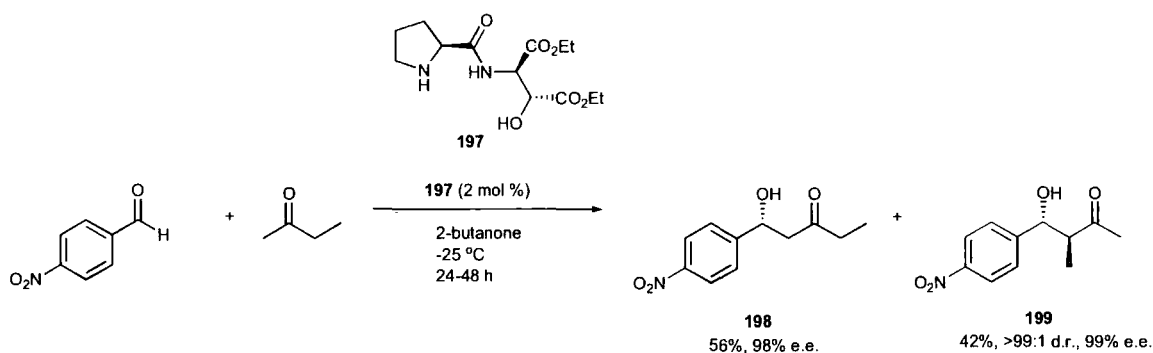


Equation 53

The use of L-prolinamide derivative **191** provided aldol adducts using acetone as donor in generally moderate yields with very good e.e.s (Equation 54).¹⁰⁰ However, the use of α -unbranched aldehydes saw low yields, and low temperature was necessary in order to obtain high e.e.s. The terminal hydroxy group of **191** was deemed to be essential for catalysis. The use of the ionic liquid [bmim][BF₄] **196** at 0 °C for 24 h afforded generally improved yields for aromatic aldehydes with higher enantioselectivity observed in all cases (yields and e.e.s for the reaction in [bmim][BF₄] shown in parentheses in Equation 54).¹⁰¹ Replacement of the phenyl substituents in **191** with ester groups leads to a more active catalyst **197**, which is used under identical conditions but at a loading of 2 mol%.¹⁰² Again, the increase in activity is explained by the increased acidity of the amide. However, the use of 2-butanone as a donor leads to poor regioselectivity, although the overall yield, enantioselectivity and diastereoselectivity are very high (Equation 55).

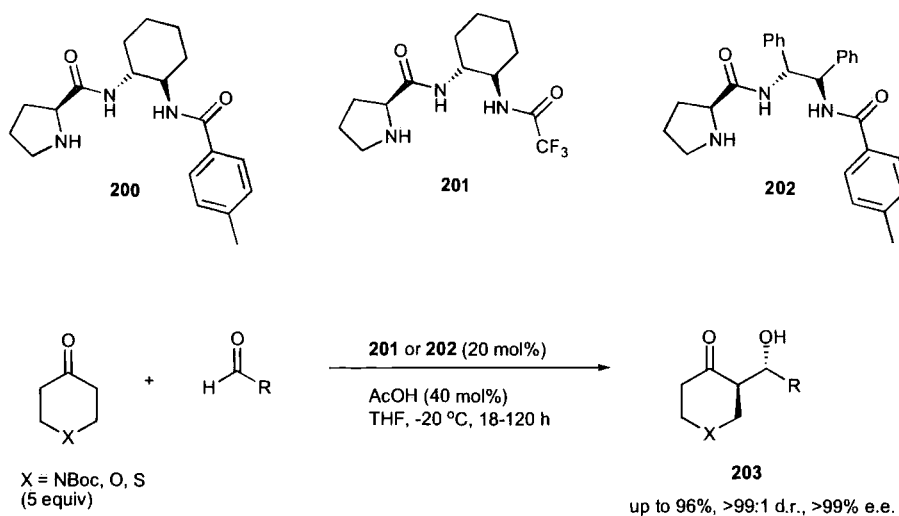


Equation 54



Equation 55

Another prolinamide derivative **200** was shown to be active in the direct aldol reaction with cyclohexanone and various aromatic aldehydes in the presence of acetic acid (**200**:AcOH, 1:1), providing good selectivity for the *anti*-diastereomer and high enantioselectivities.¹⁰³ Chloroform was used as the solvent and the reaction of 4-nitrobenzaldehyde with 2-butanone, in the presence of **200** (2 mol%) led to improved regioselectivity compared to **197**, affording **199** in 63% yield, 95:5 d.r. and 99% e.e. (**198** was formed in 9% yield). Modification of the catalyst structure led to **201** and **202**, which were efficient catalysts for the aldol reaction of heterocyclic ketones (Equation 56).¹⁰⁴

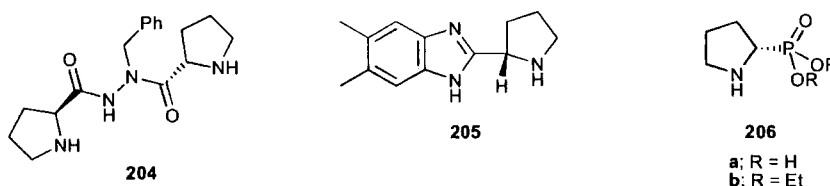


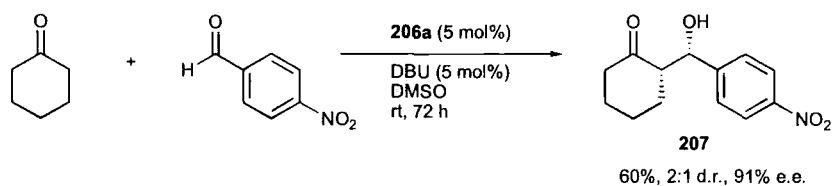
Equation 56

Proline hydrazide derivative **204** and TFA (20 mol%, 1:1) were found to provide high yields and enantioselectivities in toluene at 0 °C, but only with electron-deficient aldehydes.¹⁰⁵ Slow reaction was observed with electron-rich aromatic aldehydes and aliphatic aldehydes failed to react.

Benzimidazole-pyrrolidine **205** also required the use of a TFA additive for efficient reactivity, where excellent enantioselectivity in THF was observed, especially with cyclic ketones (although diastereoselectivity was modest).¹⁰⁶ Catalyst loadings could be reduced to as little as 2 mol% with only 1.1 equivalents of ketone donor.

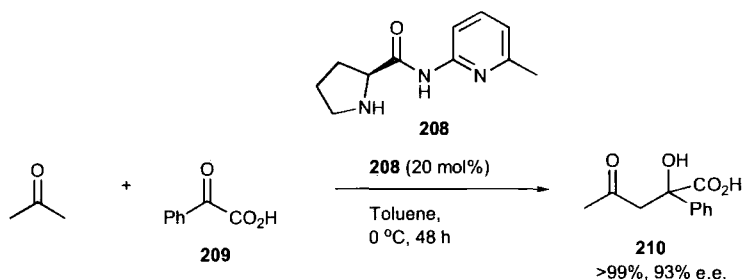
In the reaction between 4-nitrobenzaldehyde in acetone, aminophosphonate **206b** (20 mol%) afforded the aldol product in 69% yield and 82% e.e. in 24 h and proved more active than **206a**, presumably due to its better solubility.¹⁰⁷ Interestingly, the *anti*-preference with cyclohexanone as donor could be reversed by addition of DBU (5 mol%) to the reaction catalysed by **206a** in DMSO (Equation 57).





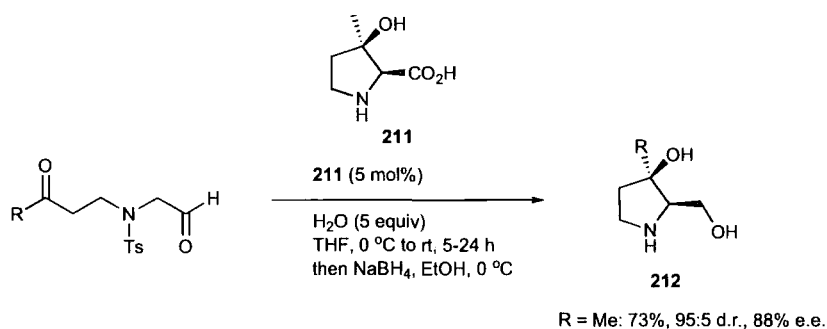
Equation 57

The first use of α -keto acids as acceptors (e.g. **209**) was catalysed by aminopyridine amide **208**, providing β -hydroxy carboxylic acids with a tertiary stereogenic centre (e.g. **210**) in high yields and excellent enantioselectivities (Equation 58).¹⁰⁸ Toluene proved to be the best solvent and a range of aryl and alkyl α -keto acids were screened.



Equation 58

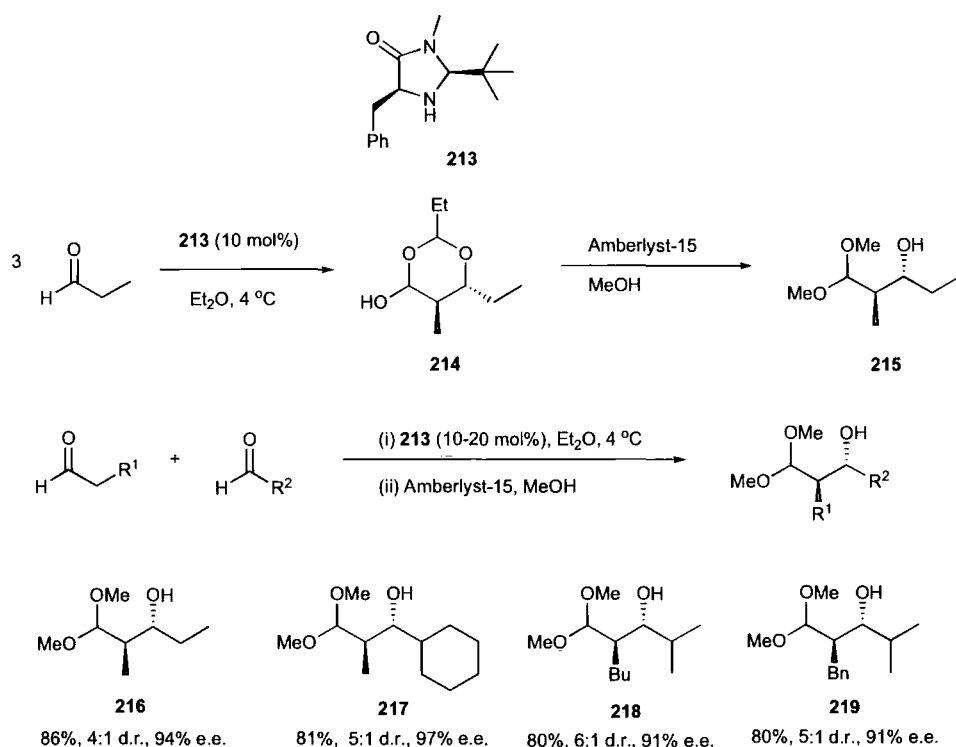
The first cyclisation to 3-alkyl substituted pyrrolidine derivatives **212**, via a *syn*-selective intramolecular aldol reaction catalysed by (2*S*,3*R*)-3-hydroxy-3-methylproline **211** (Equation 59), has also been reported recently.¹⁰⁹



Equation 59

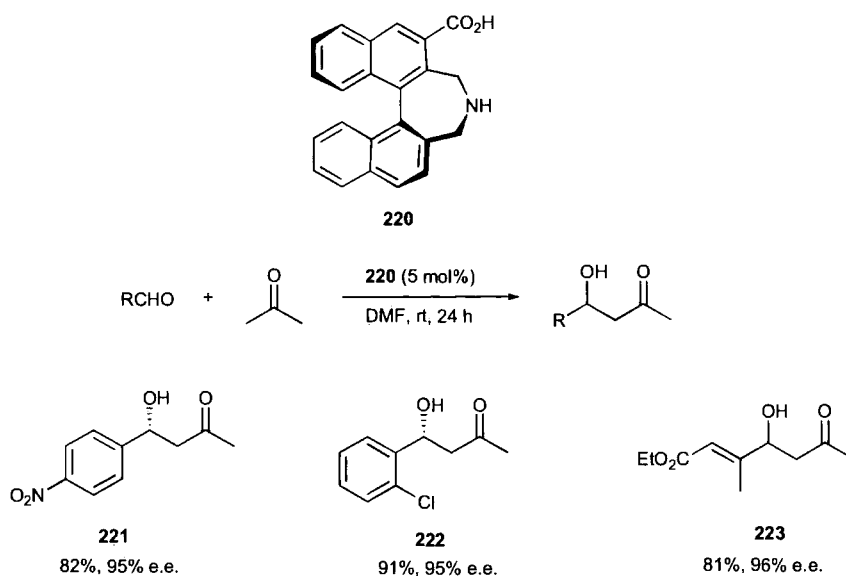
3.5 Other catalysts

The enantioselectivity of the trimerisation of propionaldehyde to **214** can be increased to 94% e.e. by using one of MacMillan's imidazolidinone derivatives **213** and this is accompanied by an increased yield of 86%.¹¹⁰ Methanolysis of **214** leads directly to β -hydroxy dimethoxyacetal derivatives **215**, and the syringe pump addition of the donor aldehyde leads to good yields and high enantioselectivities in the cross-aldol reaction of various aldehydes (Scheme 15).



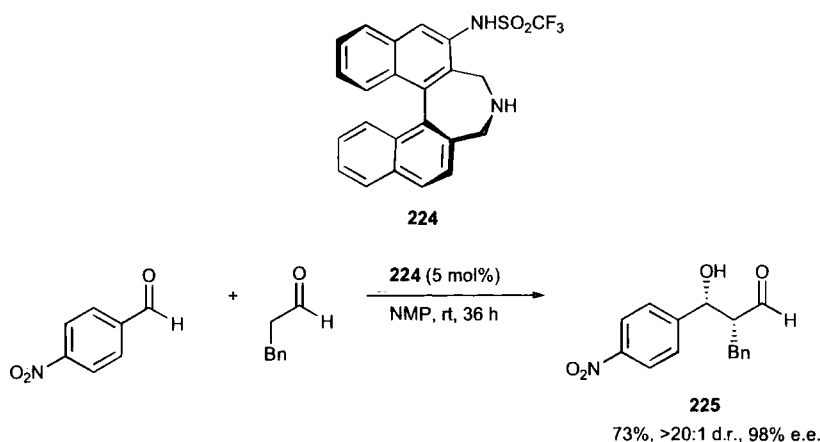
Scheme 15. Cross-aldol reaction of aldehydes catalysed by imidazolidinone **213**.

Maruoka and coworkers developed a binaphthyl-based catalyst **220** for the direct asymmetric aldol reaction of electron-deficient aldehydes with acetone, showing improved reactivity and enantioselectivity *versus* proline (Equation 60).¹¹¹ Excellent e.e.s were seen with the aldehydes screened and the binaphthyl structure opens the way to a family of potentially improved catalysts based on this moiety.



Equation 60

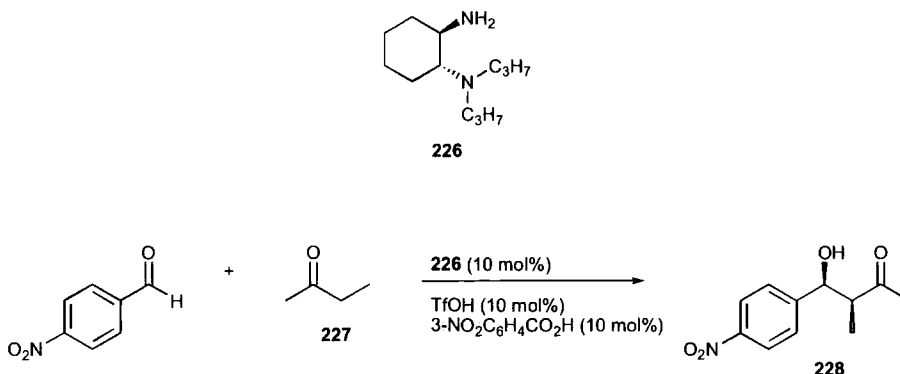
Amino sulfonamide derivative **224** has recently been demonstrated as a catalyst for the *syn*-selective cross-aldol reaction of aldehydes, where slow addition of the donor aldehyde was not required.¹¹² Electron-deficient aldehydes reacted with a variety of aliphatic aldehydes in moderate to good yields with excellent diastereo- and enantioselectivity (Equation 61).



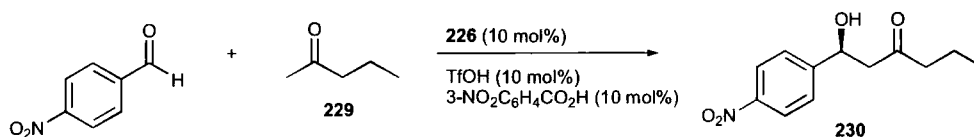
Equation 61

The use of linear aliphatic ketones as donors has been addressed by the group of Cheng with the use of primary-tertiary diamine **226**, in the presence of triflic acid and 3-nitrobenzoic acid (10 mol%, 1:1:1).¹¹³ Aliphatic aldehydes were unsuitable substrates probably due to their self-condensation, but ethyl ketones (*e.g.* 2-butanone **227**) reacted preferentially at the methylene carbon affording the branched products

with *syn*-selectivity (e.g. **228**). However, longer chain aliphatic ketones, e.g. methylpropyl ketone **229**, afforded linear products, e.g. **230**.

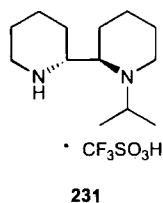


Equation 62



Equation 63

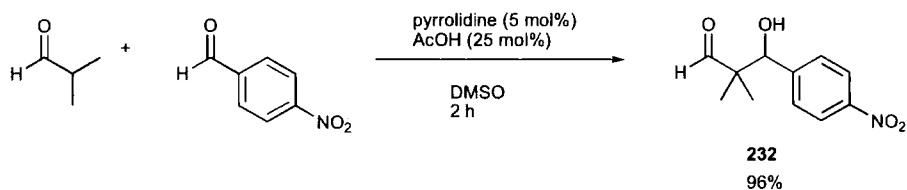
A range of bismorpholine derivatives have also been screened in the aldol reaction, of which **231** was found to be the most active.¹¹⁴ Enantioselectivities were good in the reaction of aromatic aldehydes with acetone, but high catalyst loadings (30 mol%), long reaction times (6 days) and poor yields with non-activated aldehydes were observed.



3.6 Synthesis of aldol adducts containing quarternary centres

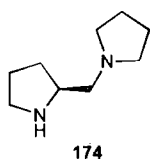
Barbas and coworkers identified that a pyrrolidine-acetic acid combination facilitates the reaction of α,α -dialkylaldehyde donors and activated arylaldehyde acceptors.¹¹⁵ A novel fluorescent screening method was employed, which allowed rapid identification of active pyrrolidine-acid combinations. For example, the reaction of *isobutyraldehyde* and 4-nitrobenzaldehyde afforded product **232** in 96% yield after 2

h (Equation 64). In comparison, proline (30 mol%) was a poor catalyst for this reaction providing **232** in 34% yield after 3 days, although the reaction proceeded with good enantioselectivity (80% e.e.).



Equation 64

The asymmetric version of the reaction employed chiral diamine **174** and TFA, both at a loading of 30 mol%, providing **232** in excellent yield (95%) and enantioselectivity (94%) in only 2 h.¹¹⁶ Reducing the catalyst loading to 5 mol% still afforded aldol product **232** in 92% yield and 96% e.e., after 24 h.

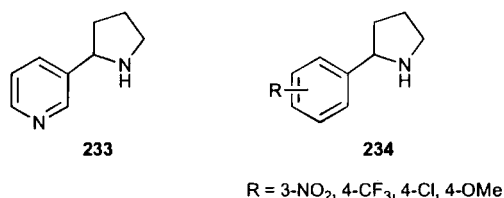


3.7 Aqueous aldol catalysis¹¹⁷

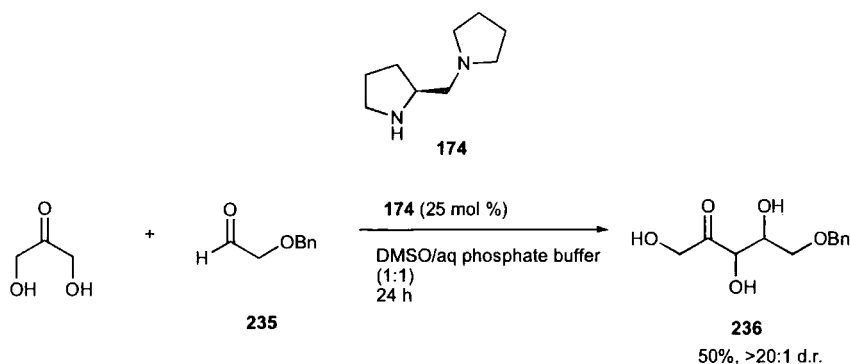
The use of water as a solvent is highly desirable because of the environmental, cost and safety benefits it offers. These are complementary to the advantages of organocatalysis and as a result, there has been a substantial drive to develop organocatalysts that are active in water.

To this end, in 2002, Janda showed nornicotine **233** could catalyse the aldol reaction between activated aldehydes with sufficient water solubility (e.g. 4-nitrobenzaldehyde, 2-chlorobenzaldehyde) in aqueous phosphate buffer (pH 7.4), however, the reaction failed to proceed in organic solvents.¹¹⁸ Although the yield for reaction between 4-nitrobenzaldehyde and acetone was 81%, the e.e. was disappointingly low (~20%). Evidence for an enamine intermediate between nornicotine **233** and acetone was successfully obtained by trapping with NaCNBH₃. In addition, the results from testing a range of 2-arylpyrrolidines **234** indicated that

electron-withdrawing substituents were beneficial due to the reduced pK_a of the pyrrolidine nitrogen.¹¹⁹

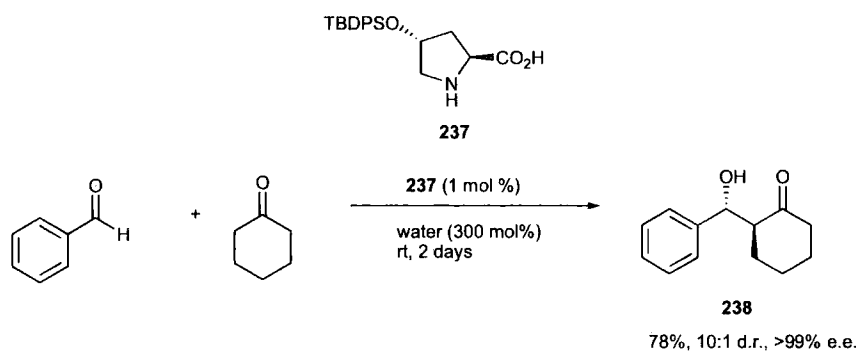


Diamine **174** (25 mol%), also in aqueous phosphate buffer but also containing DMSO (1:1), catalysed the reaction of dihydroxyacetone with various aldehydes, providing a direct route to monosaccharides.¹²⁰ For example, benzyl-protected pentulose **236** was obtained with high selectivity for the *anti*-diastereomer (Equation 65). When the reaction was carried out with L-proline, no diastereoselectivity was observed and neither L-proline nor **174** afforded any significant diastereoselectivity in a screen of a number of ketone donors with 4-nitrobenzaldehyde.



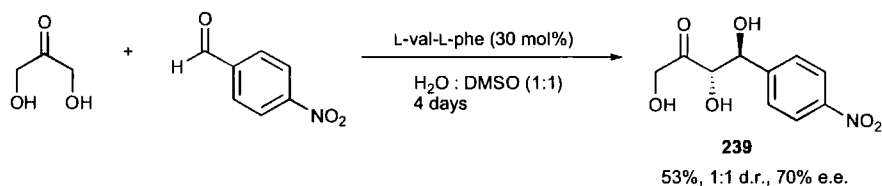
Equation 65

In 2006, Hayashi and coworkers used 4-*tert*-butyldiphenylsiloxy proline **237** as the first asymmetric organocatalyst for the direct aldol reaction in the presence of water.¹²¹ Although cyclohexanone reacted in good yields and with high stereoselectivity, acetone and hydroxyacetone provided only moderate enantioselectivity. Catalyst loadings as low as 1 mol% could be employed, although the use of **237** in organic solvents led to reduced diastereo- and enantio-selectivities (Equation 66).



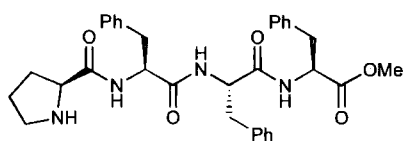
Equation 66

Shortly after, di- and tri-peptides with a primary amine at the *N*-terminus (e.g. L-val-L-val, L-val-L-phe) were shown to catalyse the direct aldol reaction.¹²² In comparison to **237**, diastereoselectivity was generally poor, a 30 mol% peptide loading was required and the majority of reactions were carried out in a 1:1 mixture of water-methanol or water-DMSO. However, the first enantioselective reaction of unprotected dihydroxyacetone as an aldol donor was demonstrated providing the aldol product **239** in 53% yield, 1:1 d.r. and 70% e.e. (Equation 67), whereas proline produced **239** in only trace amounts and less than 10% e.e.

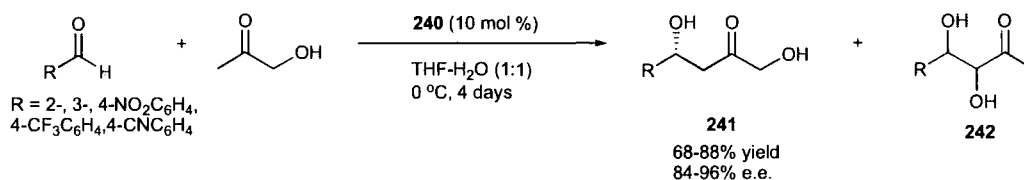


Equation 67

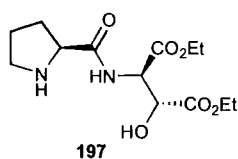
A noteworthy variation of the reaction between hydroxyacetone and electron-deficient aldehydes is that catalysed by peptide **240**.¹²³ In a water-THF mixture, the 1,4-diol **241** is formed as the major product in good yields and high enantioselectivities (Equation 68). This is in contrast to the favoured 1,2-diol **242** observed in L-proline catalysed reactions (*vide supra*). The use of less activated benzaldehyde and aliphatic cyclohexylformaldehyde as acceptors was solved by the use of prolinamide **197**, with the presence of water crucial for the observed regioselectivity (Equation 69, yields for the reaction in THF are shown in parentheses).¹²⁴



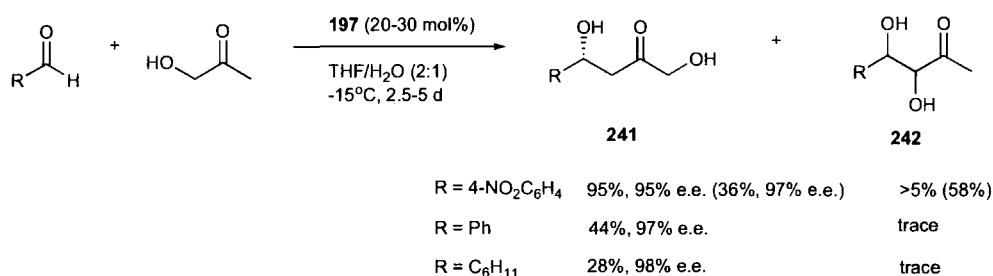
Pro-Phe-Phe-Phe-OMe **240**



Equation 68

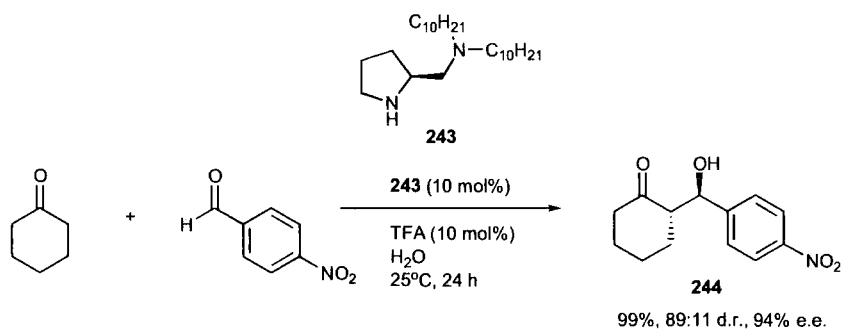


197

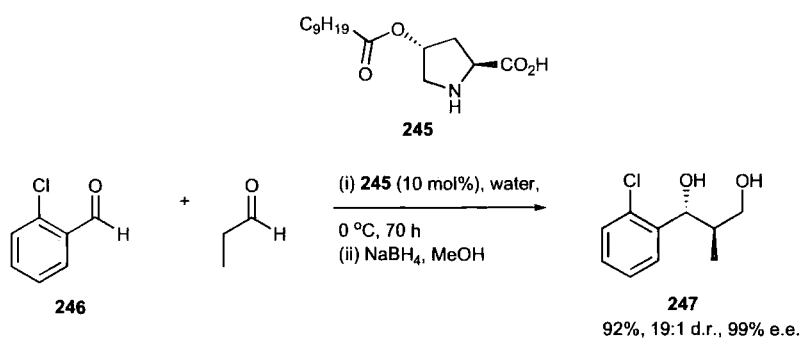


Equation 69

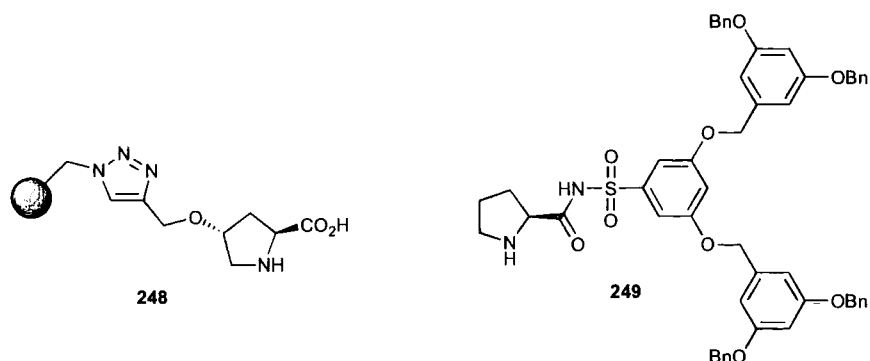
In early 2006, Barbas established the utility of diamine **243** with TFA (1:1) for the aldol reaction in the presence of water, affording aldol product **244** in 99% yield, 89:11 d.r. and 94% e.e (Equation 70).¹²⁵ It was found that the presence of hydrophobic *n*-decyl groups was essential for activity, allowing the reaction to proceed in a concentrated organic phase. In addition, the amount of donor could be reduced to only 1 equivalent without detrimental effect. Electron-deficient aldehydes reacted well as acceptors, but when aliphatic ketones (acetone, 2-butanone) were employed as donors, only moderate enantioselectivity was observed.



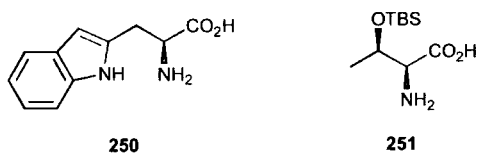
Catalyst **245**, bearing a decanoate moiety, was shown by Hayashi to catalyze the direct cross-aldol reaction of aldehydes in water (Equation 71), where slow addition of the donor and an acid derivative were not required (*vide supra*).¹²⁶ High diastereo- and enantio-selectivities were observed in all cases, but yields were low in the case of aliphatic aldehydes. This was explained by their insufficient hydrophobicity and the necessary reaction emulsion was not formed.



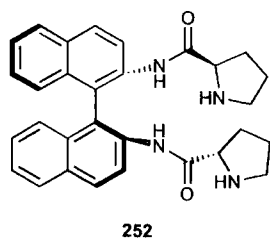
Some recoverable catalysts have also been developed for the aldol reaction in water. Polystyrene-supported hydroxyproline **248** was effective particularly with electron-deficient aromatic aldehydes, and recovered by simple filtration.¹²⁷ Dendritic *N*-propyl sulfonamide **249** also provided high yields, diastereo- and enantioselectivities with electron-deficient aldehydes and could be recovered by precipitation on addition of hexane-ethyl acetate.¹²⁸ Successful reaction with acetone was accomplished in both cases by increasing the number of equivalents to between 20-25. However, in neither case were aliphatic aldehydes screened as acceptors.



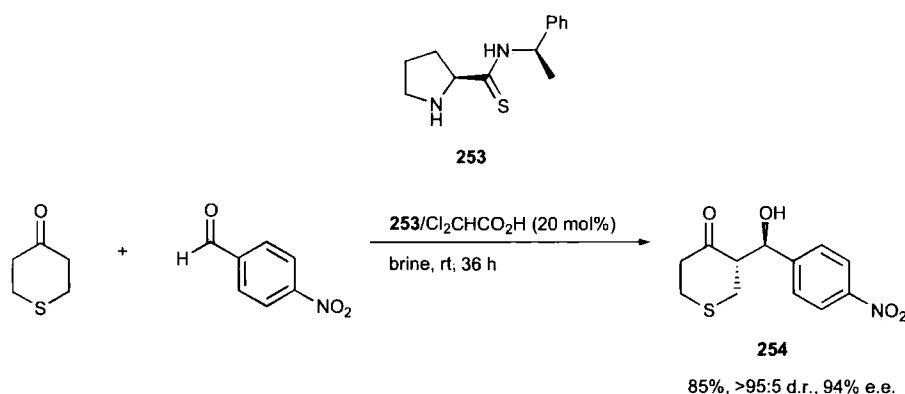
Tryptophan **250** has also been demonstrated by Lu to catalyze the direct aldol reaction between cyclic ketones and aromatic aldehydes in water, with high diastereo- and enantio-selectivity.¹²⁹ Electron-deficient aromatic aldehydes provided good yields within 24 hours, but less reactive substrates required longer reaction times (*e.g.* benzaldehyde and cyclohexanone required 92 h to afford 47% yield, 78:1 d.r. (*anti:syn*) and 89% e.e). In addition, acyclic ketones and aliphatic aldehydes failed to react, presumably again due to insufficient hydrophobicity (reaction mixture was heterogeneous with suspended tryptophan visible). The same group have also demonstrated the use of TBS-protected threonine **251** (2-10 mol%) as a catalyst for the direct aldol reaction in the presence of water.¹³⁰ Cyclohexanone and TBS-protected hydroxyacetone were reacted with a variety of aromatic aldehydes providing moderate to good yields and diastereoselectivity, with excellent enantioselectivity.



Chiral binaphthyl derivative **252** (10 mol%) with stearic acid ($C_{17}H_{35}COOH$, 20 mol%) has also been shown to be a good general catalyst for the aldol reaction in water.¹³¹ Even deactivated 4-methoxybenzaldehyde reacted in 57% yield and 87% e.e in 12 h, and acetone could be employed as a donor when the reaction was run in acetone-water (1:1).

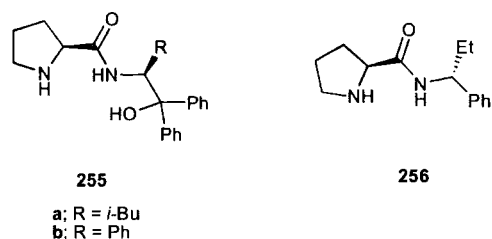


L-Prolinethioamide **253** was shown to catalyse the direct aldol reaction in various organic solvents (DMF, THF, NMP), with the addition of TFA providing the most remarkable increases in yield and enantioselectivity of the large selection of additives screened (up to 99% yield and 98% e.e).¹³² This was recently extended to reaction in brine (promoting the formation of a concentrated organic phase) with dichloroacetic acid used in place of TFA, and a 5 mol% catalyst loading sufficient for the majority of substrates screened.¹³³ It was found that as little as 1.2 equivalents of cyclic ketone could be employed, but the reaction of non-activated aldehydes resulted in low yields. The use of heterocyclic ketones was also demonstrated with the products isolated in good yields with high diastereo- and enantioselectivities (Equation 72).

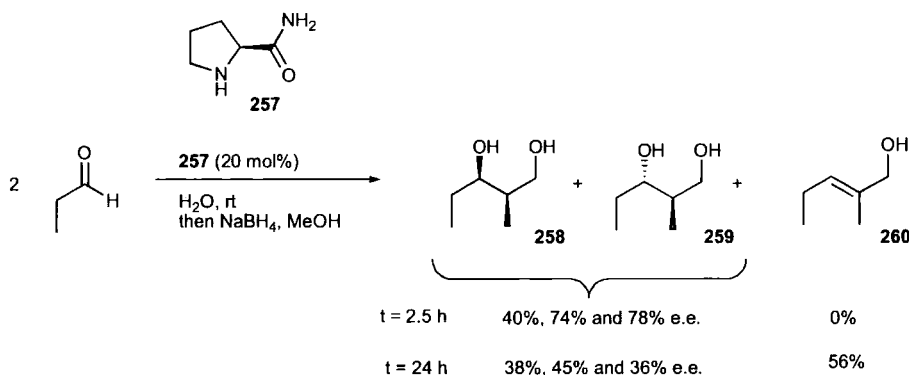


Equation 72

Recently, Singh has demonstrated the use of L-prolinamide **255** for the reaction of cyclic and acyclic ketones with a range of aldehydes, again employing brine as a reaction medium.¹³⁴ Good yields and excellent diastereo- and enantioselectivities were obtained, even with deactivated aldehydes, no acid additive was required, and a very low catalyst loading (0.5 mol%) was used in comparison to other aldol organocatalysts. On the other hand, prolinamide **256** proved to be relatively poor, providing good yields but with only up to 62% e.e, suggesting the importance of the terminal hydroxy group.¹³⁵



The dimerisation of propanal, catalysed by proline amide **257** is the first and only example of a direct aldol reaction that takes place in the aqueous phase (a homogeneous reaction in water, rather than proceeding in a concentrated organic phase).¹³⁶ The reaction afforded the aldol product in moderate yield, with virtually no diastereoselectivity (1.1:1), but good enantioselectivity (78%) after 2.5 h. After 24 h, the amount of aldol product remained almost the same due to dehydration providing **260** in 56% yield (Equation 73).



Equation 73

3.8 Summary and conclusions

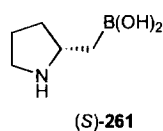
In summary, organocatalysis of the aldol reaction has been thoroughly investigated with proline and various derivatives. In general, high enantioselectivities can be obtained at room temperature with reasonable reaction rates. It is particularly interesting to note that linear amino acids are active aldol catalysts and that the development of water-tolerant catalysts has recently experienced good progress. However, a catalyst that displays good general activity with all substrates remains elusive. The use of a large excess of ketone donor, ketones as acceptors, and aliphatic aldehydes as acceptors with ketone donors, remain unsolved problems in the majority of cases. The use of additives, such as highly corrosive TFA, is also both fairly

widespread and undesirable. Surprisingly, the use of a Lewis acid attached to the pyrrolidine ring for acceptor activation has yet to be examined.

4. Results and Discussion – Amino-boronic acids as catalysts for the direct aldol reaction

4.1 Introduction

In recent years, the field of asymmetric enamine catalysis has experienced explosive growth, with the screening of proline providing a benchmark against which to compare modified derivatives with. Proline is both cheap and readily available, can provide high yields and excellent e.e.s, and therefore is a suitable choice for comparison. However, there are a number of problems with proline, not all of which have been addressed with the many derivatives that have been synthesised. Notably, proline requires high catalyst loadings, usually around 20-30 mol% and this is mainly due to its limited solubility in organic solvents. Therefore, typical solvents for proline-catalysed reactions tend to be highly polar, *e.g.* DMSO, DMF, NMP, which in turn leads to difficulties with product isolation and purification, as well as environmental concerns. In addition to this, the substrate scope of proline is limited. For example, the use of linear aliphatic ketones as donors, and ketones generally as acceptors is difficult. In most cases, there is also the need for a large excess of the ketone donor in order to ensure reasonable reaction rates. In order to try and address some of these issues, the synthesis of amino-boronic acid **261** incorporating a pyrrolidine moiety, was undertaken.



By replacing the carboxylic acid function of proline with a boronic acid, it was envisaged that enamine formation and Lewis acid activation by boron would lead to asymmetric induction in an analogous fashion to the carboxylic acid's role in proline catalysis (Figure 20).⁷⁹



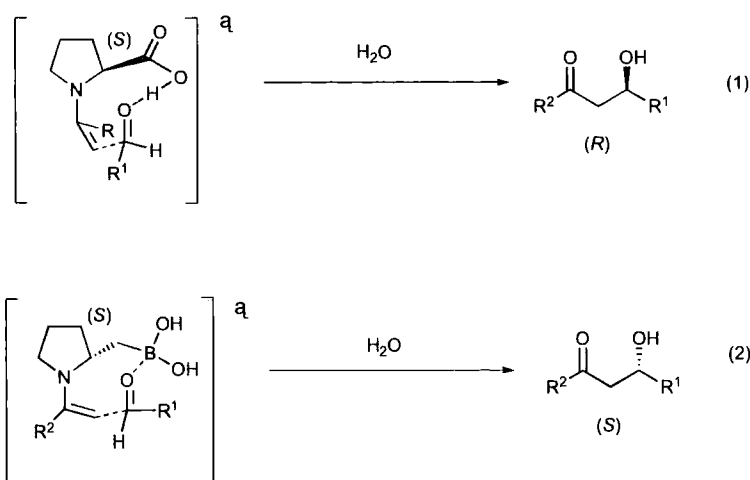
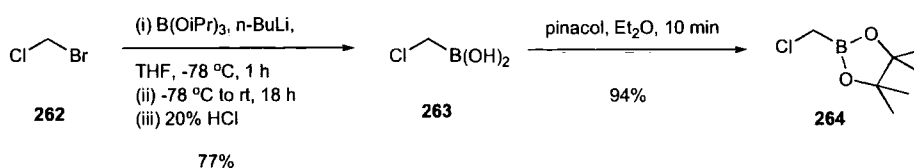


Figure 20. Transition state for the proline-catalysed aldol reaction (1) and proposed transition state for **261**-catalysed aldol reaction (2).

4.2 Catalyst synthesis

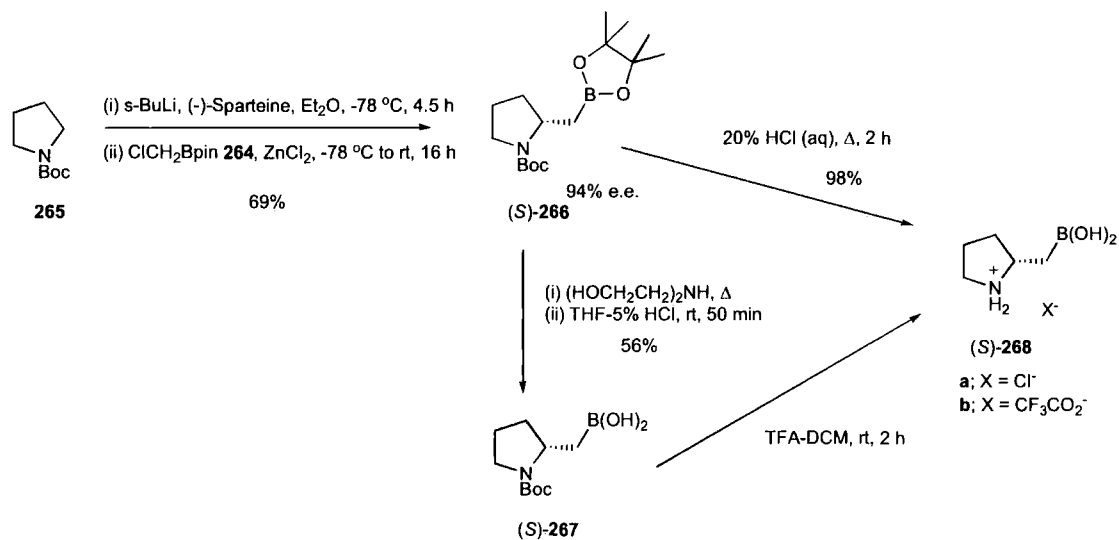
The synthesis of amino-boronic acid **261** was initiated with preparation of the chloromethylboronate electrophile **264** (Scheme 16). Initially, lithium-halogen exchange of bromochloromethane **262** with triisopropylborate *in situ*, warming to room temperature and addition of a 0.7 equivalents of pinacol, allowed isolation of crude boronate **264** containing excess pinacol. Attempts to purify this using Kugelrohr distillation proved problematic due to co-distillation of pinacol. Therefore, pinacol was not added after lithium-halogen exchange, allowing the boronic acid **263** to be isolated in a good 77% yield. Subsequent recrystallisation from hexane-ether and esterification with pinacol (1 equivalent) afforded the desired boronate **264** in 94% yield.



Scheme 16. Synthesis of chloromethylboronate **264**.

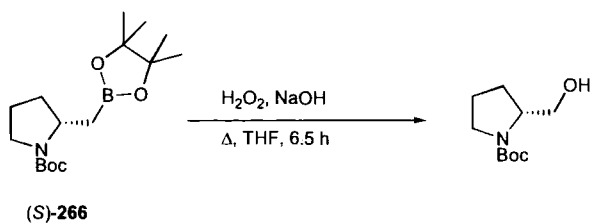
The first attempts at (-)-sparteine-mediated lithiation of *N*-Boc-pyrrolidine **265**, in the absence of zinc chloride, afforded (*S*)-**266** in only 12% yield. The yield of (*S*)-**266** was improved moderately to 25% on heating the reaction mixture to reflux for 2 h, after warming to room temperature. Collapse of the intermediate 'ate'-complex was assisted by addition of zinc chloride,¹³⁷ allowing isolation of protected boronate (*S*)-

266 in a good 69% yield. Similar results (71% yield) were obtained when replacing sparteine with TMEDA. The resulting racemic mixture **266** was used to develop the resolution method on chiral GC, revealing (*S*)-**266** had been produced in 94% e.e. (Scheme 17).



Scheme 17. Synthesis of amino-boronic acid (*S*)-**268**.

In order to confirm the expected absolute stereochemistry of (*S*)-**268**, (*S*)-**266** was oxidised in the presence of hydrogen peroxide and sodium hydroxide to afford *N*-Boc prolinol (Equation 74). Comparison of the sign of the optical rotation ($[\alpha]_D^{22} +50.8$) with the available literature data¹³⁸ confirmed the assignment of (*S*)-**268**.



Equation 74

Initially, pinacol deprotection was attempted by transesterification with phenylboronic acid in hexane-water, but this was unsuccessful leading to recovery of starting material from the organic phase.¹³⁹ Pinacol deprotection by transesterification with diethanolamine was more effective, and subsequent hydrolysis afforded boronic acid (*S*)-**267** in 56% yield.¹⁴⁰ However, since the diethanolamine ester did not crystallise

out from the reaction mixture, the pinacol had to be removed by distillation at reduced pressure and this proved difficult to completely achieve. Nevertheless, slow crystallisation from THF provided crystals suitable for X-ray analysis (Figure 21).

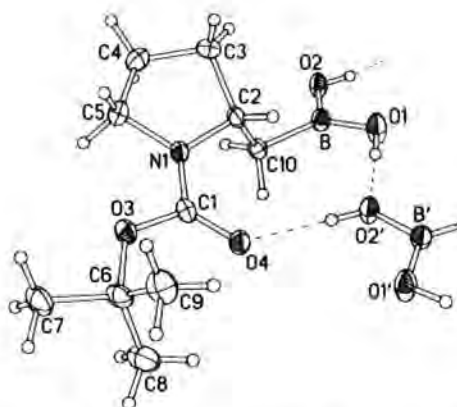


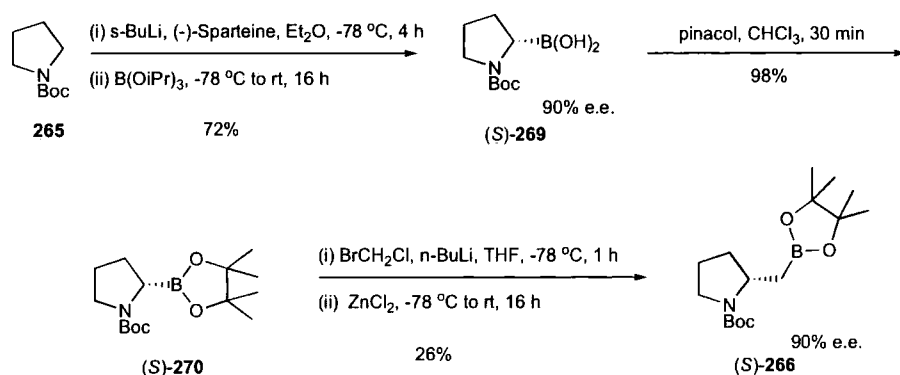
Figure 21. X-ray molecular structure of (*S*)-**267**. Thermal ellipsoids are drawn at 50% probability level.

Boc deprotection was attempted using TFA-DCM (1:1), but this led to isolation of an impure brown oil which could not be purified despite extensive efforts to induce crystallisation (Scheme 17).¹⁴¹ Boc deprotection using methanolic HCl-MeOH led to isolation of a pale yellow oil.¹⁴¹ In both cases, ¹H and ¹¹B NMR in D₂O showed the deprotection had been successful, but final purification could not be achieved.

Simultaneous Boc and pinacol deprotection was achieved by heating (*S*)-**266** with 20% (w/v) aqueous HCl for 2 h. The resultant brown oil was subjected to ion exchange chromatography using Dowex 50WX8-200, and the product (*S*)-**261**, was eluted using 3.5% ammonium hydroxide. However, this failed to purify the crude product and afforded a mixture of boron species to include the boronic acid, dimer and ammonium 'ate'-complex. Omitting the ion exchange chromatography and simply washing the crude with several portions of ether, allowed the product to be isolated as the HCl salt (*S*)-**268a** in an excellent 98% yield. The ¹¹B NMR showed one signal at δ_B 31, confirming the presence of free boronic acid, *i.e.* with no boron-nitrogen chelation.

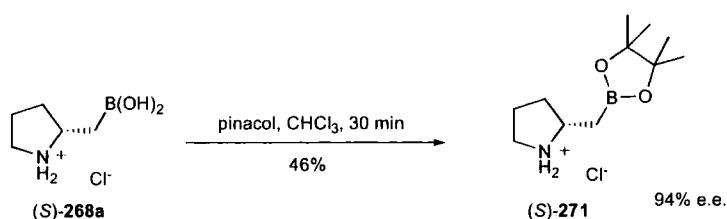
Another route to boronate (*S*)-**266** was achieved by homologation of protected boroproline (*S*)-**270** by treatment with chloromethyl lithium, generated *in situ* by

treating bromochloromethane with *n*-BuLi (Scheme 18).^{137,142} Again, the addition of zinc(II) chloride proved necessary, and (*S*)-**266** was produced in 26% yield with retention of configuration. The e.e. and absolute configuration of (*S*)-**269** were determined by chiral HPLC of the (–)-pinanediol ester and X-ray analysis of the (1*S*,2*S*)-hydrobenzoin ester respectively,¹⁴² and although there was no change in the e.e. of (*S*)-**266** by chiral GC, the previously described route was selected because of the lower yield in this case.



Scheme 18. Synthesis of (*S*)-**266** by homologation of protected boroproline (*S*)-**270**.

The pinacol ester of amino-boronic acid (*S*)-**268a** was also synthesised for subsequent screening. Due to the high water solubility of (*S*)-**268a**, the use of THF in the presence of 1 equivalent of triethylamine led to a biphasic reaction mixture and no product conversion. The same result was observed when aqueous sodium hydroxide was used as the base, with the starting material (*S*)-**268a** remaining in the aqueous phase. Fortunately, vigorously stirring a mixture of (*S*)-**268a** and pinacol in chloroform afforded the desired product (*S*)-**271** in reasonable 46% yield (Equation 75). Recrystallisation from acetone provided crystals suitable for X-ray analysis (Figure 22). It is worth noting that the recrystallisation step could have increased the e.e. of (*S*)-**271**, which is based on the e.e. of (*S*)-**266** (as determined by chiral GC).



Equation 75

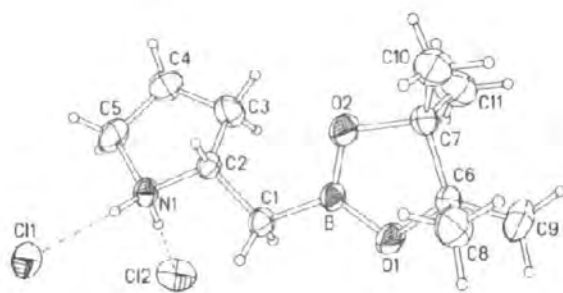


Figure 22. X-ray molecular structure (*S*)-**271**. Thermal ellipsoids are drawn at 50% probability level.

4.3 Behaviour in aqueous solution

The titration curve for HCl salt (*S*)-**268a** allowed the pK_a values to be determined as 7.8 and 10.9 and provides information on the effect of pH on solution behaviour (Figure 23).¹⁴³

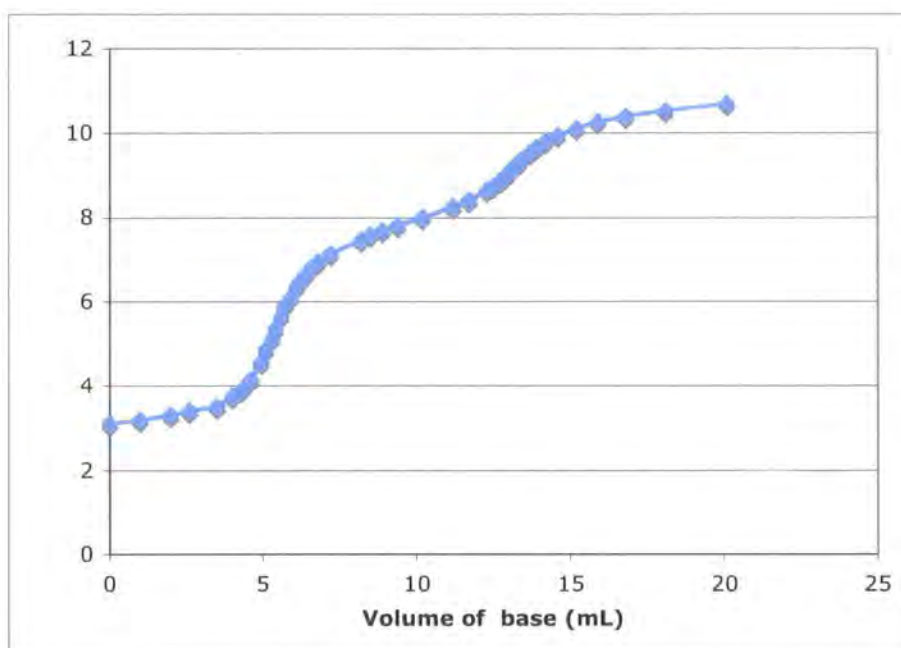


Figure 23. Titration curve for (*S*)-pyrrolidin-2-yl-methylboronic acid **268a** with sodium hydroxide in H_2O .

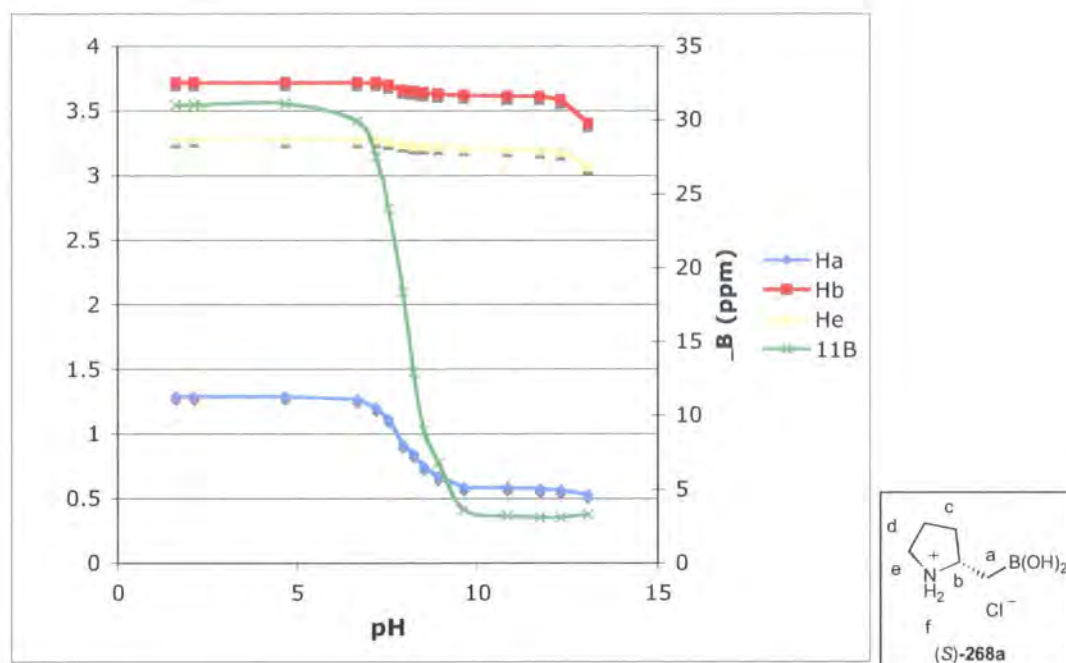
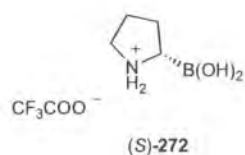
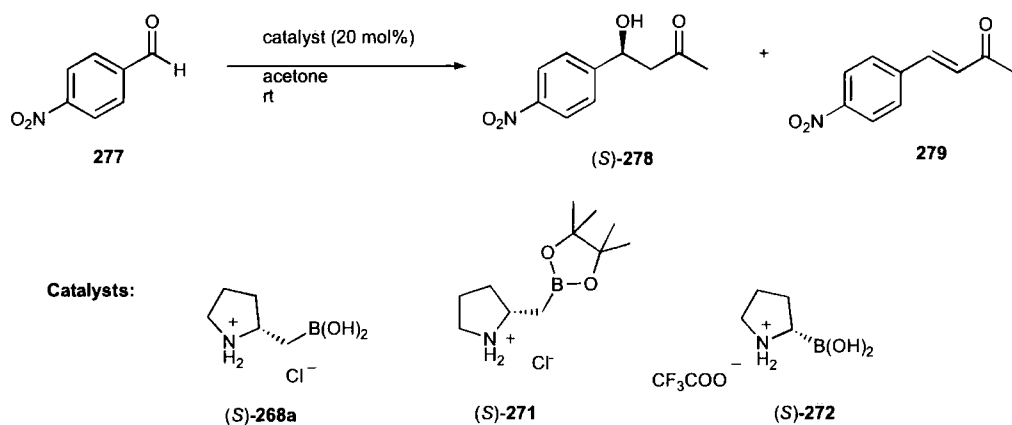


Figure 24. Variation of ^1H and ^{11}B NMR shifts of (*S*)-pyrrolidin-2-yl-methylboronic acid **268a** with pH.

The first pK_a corresponds to quarternerisation of boron and the second to neutralisation of the ammonium ion, and this is further evidenced by ^1H and ^{11}B NMR titration data (Figure 24).^{142,144} The ^{11}B NMR shifts start to decrease around pH 7 from $\delta_{\text{B}} = 31$ to $\delta_{\text{B}} = 3$, along with the ^1H NMR shifts for H_a , confirming quarternerisation of boron. The NMR shifts for H_b and H_e start to fall at approximately pH 10, confirming neutralisation of the ammonium salt. The observation of averaged ^{11}B NMR shifts between $\delta_{\text{B}} = 31$ to $\delta_{\text{B}} = 3$ suggests that interconversion between sp^2 and sp^3 boron is fast on the NMR timescale.



In comparison, boroproline (*S*)-272 has pK_a values of 5.2 and 11.2, and therefore the boron is more acidic and the amine about the same basicity *versus* (*S*)-268a.¹⁴² This can be rationalised by the closer proximity of boron and nitrogen in (*S*)-272, as well as the inductive effect of the additional methylene group. Boroproline (*S*)-272 is also



Scheme 20. Amino-boronic acid catalysed aldol reaction between 4-nitrobenzaldehyde **277** and acetone.

Table 17. Isolated yields and e.e.s for the catalyst screen on the aldol reaction between 4-nitrobenzaldehyde **277** and acetone.

Entry	Conditions	Time (h)	Yield (S)-278 (%)	e.e. ^a (%)	Yield 279 (%)
1	(S)-268a	24	0	-	0
2	KO ^t Bu	24	43	0	11
3	(S)-268a + KO ^t Bu	24	62	8	11
4	Et ₃ N	24	0	-	0
5	(S)-268a + Et ₃ N	24	90	38	10
6	(S)-272 + Et ₃ N	24	14	0	0
7	(S)-271	6	0	-	-
8	(S)-271 + Et ₃ N	6	46	30	36

^aDetermined by chiral HPLC.

In the presence of potassium *tert*-butoxide alone, aldol product **278** was formed in 43% yield, along with 11% of chalcone **279** (entry 2). When (S)-268a was screened in conjunction with KO^tBu, the yield of (S)-278 was improved to 62% but the e.e. was very low at 8% because of the general base catalysed reaction (entry 3). The base catalysed reaction was suppressed on switching the base to triethylamine, and hence in the presence of (S)-268a the aldol product (S)-278 was produced in 90% yield and

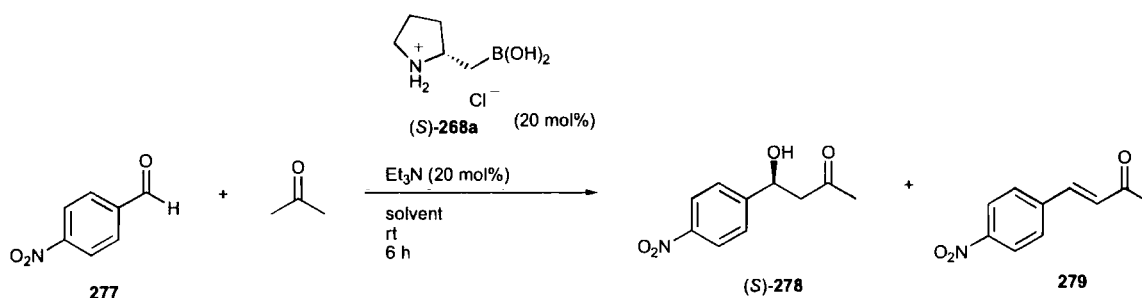
38% e.e. with a similar amount of chalcone **279** formed to the reactions in the presence of KO^tBu (entries 4 and 5). The expected absolute stereochemistry of **278** was confirmed by chiral HPLC of the corresponding product from the L-proline catalysed reaction.⁶⁵

The fact that boroproline (*S*)-**272** and triethylamine leads to **278** in only 14% yield (entry 6) and with no asymmetric induction suggests that catalyst (*S*)-**268a** could be operating in a bifunctional manner with participation of the boronic acid moiety. This is expected based on the boron-nitrogen distance in (*S*)-**272** and the proposed proline transition state (see Figure 20).

The pinacol ester (*S*)-**271** was also examined in the hope the pinacol ester would act as a steric shield. Again, in the absence of base, no conversion was observed (entry 7, Table 17). In the presence of triethylamine, total conversion was a good 82% in 6 h, but only 46% of the aldol product (*S*)-**278** was formed, the rest being chalcone **279** (36%). Asymmetric induction was observed, however, but since the chalcone **279** must be formed from dehydration of the aldol adduct (*S*)-**278**, increasing the reaction time would likely lead to quantitative formation of **279** (entry 8).

4.4.2 Solvent effects on the aldol reaction

Next, a variety of solvents were examined for their effect on conversion and e.e. with catalyst (*S*)-**268a** and triethylamine (20 mol%), on the reaction between 4-nitrobenzaldehyde **277** and acetone (Equation 76). Whilst the use of a large excess of the ketone donor is acceptable in the case of acetone, this would be undesirable with more expensive substrates.



Equation 76

Conversion to the aldol adduct (*S*)-**278** vs. time data was obtained using the Gilson 215 liquid handler, with conversion monitored by direct sampling and online HPLC analysis (Figure 25). The reaction mediated by L-proline in acetone was also run for comparison.

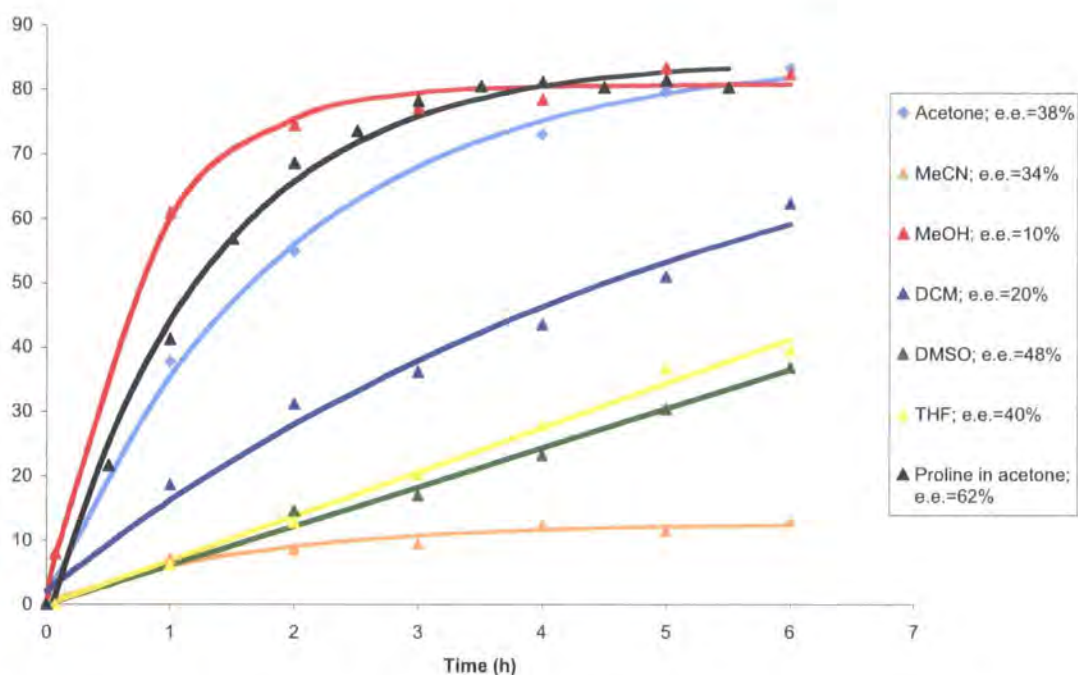


Figure 25. Solvent effects on conversion to aldol adduct (*S*)-**278** vs. time for the reaction between 4-nitrobenzaldehyde and acetone catalysed by (*S*)-**268a**

The influence of the reaction solvent on both reaction rates and e.e. is substantial. The use of neat acetone leads to fast reaction, with that mediated by (*S*)-**268a** being comparable to the L-proline catalysed reaction, but the e.e. is higher in the latter case (62% vs. 38%). The use of a polar aprotic solvent DMSO produces the highest e.e. (48%) observed in the presence of (*S*)-**268a**, suggesting this favours boronic acid activation of the aldehyde (Figure 20). The use of THF provides a similar rate but a lower e.e. of 40%; DCM shows a faster rate but the e.e. drops off significantly to 20%. Acetonitrile, another polar aprotic solvent, has a negative effect on reaction conversion and appears to stop the reaction proceeding beyond 10% conversion.

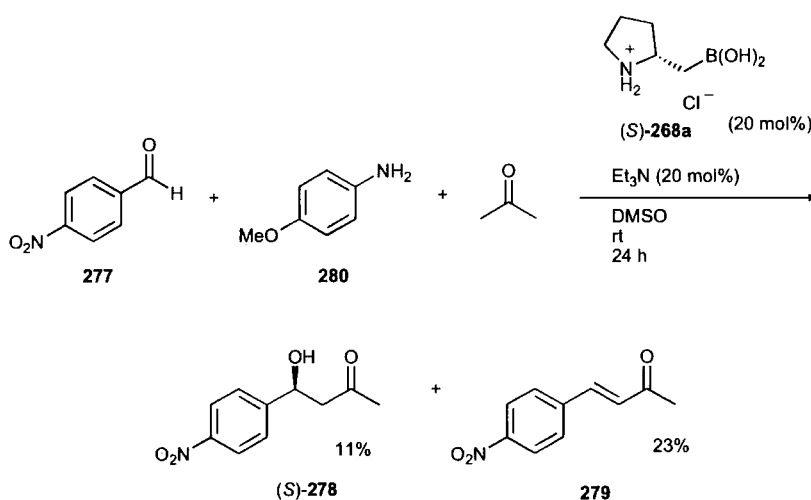
Surprisingly, the use of methanol as the reaction medium leads to the fastest reactions, but also the lowest e.e. of 10% suggesting a detrimental interaction with the boronic acid moiety of (*S*)-**268a**. Methanol readily esterifies boronic acids to produce the

corresponding methyl esters, but this would not be expected to be that significant and disruption of the transition state required for high asymmetric induction *via* solvent insertion is more likely.¹⁴⁴

4.4.3 Applicability to other substrates

The scope of catalyst (*S*)-**268a** was examined initially on the 3-component Mannich reaction¹⁴⁵ between 4-nitrobenzaldehyde **277**, *p*-anisidine **280** and acetone in DMSO over 24 h (Equation 77). Interestingly, the Mannich reaction failed to proceed at all, with aldol adduct (*S*)-**278** and chalcone **279** isolated in 11% and 23% yield respectively. Analysis of the crude reaction mixture revealed all the aldehyde had been converted to the corresponding imine and suggests that (*S*)-**268a** does not mediate the Mannich reaction.

It has already been established that amide bond formation catalyst *N,N*-dimethylbenzylamine-2-boronic acid **80b** exists only in its B-N chelated form (*vide supra*), and since boronic acid activation of the imine would require a B-N interaction, this would not be expected to be unfavourable. Therefore, it is likely that the formation of a stable B-N complex is preventing the reaction from proceeding.

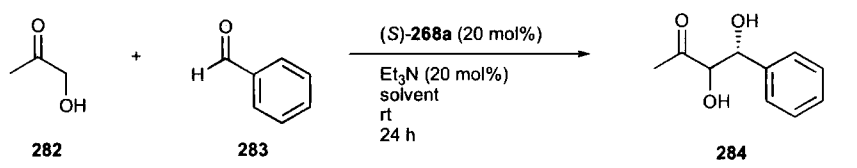


Equation 77

Therefore, attention was returned to the aldol reaction, in particular that of benzaldehyde **283** and hydroxyacetone **282** for which several solvents were examined

for their effect on conversion, diastereo- and enantioselectivity of the aldol adduct **284** (Table 18). The reaction was completely regioselective for product **284**, with relative and absolute stereochemistries determined by comparison of the ^1H NMR and chiral HPLC for the product obtained from the L-proline catalysed reaction.¹⁵² Solvent choice was based on the enantioselectivities and reaction rates observed previously (see Figure 25), hence, two polar aprotic solvents NMP and DMSO were selected, along with THF.

Table 18. (*S*)-**268a** catalysed aldol reaction between benzaldehyde and hydroxyacetone.



Entry	Solvent	Conversion ^a 284 (%)	<i>anti</i> : <i>syn</i> ^a	e.e. ^b (%)
1	NMP	39	41:59	42 (<i>anti</i>) 46 (<i>syn</i>)
2	DMSO ^c	55	43:57	46 (<i>anti</i>) 52 (<i>syn</i>)
3	THF	51	49:51	26 (<i>anti</i>) 42 (<i>syn</i>)

^aDetermined by ^1H NMR. ^bDetermined by chiral HPLC. ^cThe background reaction was checked in DMSO and does not proceed.

The use of DMSO afforded the highest e.e.s for both *syn*- and *anti*-**284** (entry 2, Table 18) and this confirms it as the solvent of choice for the highest enantioselectivities of those screened. DMSO also shows the highest conversion to product **284** (55%) and THF provides the lowest e.e.s (entry 3), and this is again consistent with the earlier solvent screen. In all cases, formation of the dehydrated enone was not detected and diastereoselectivities were poor. This is comparable to the results obtained with L-proline catalysis for this reaction.^{68a}

Further substrates for the (*S*)-**268a**-catalysed aldol reaction were examined using DMSO as a solvent, and the results after 48 h are shown in Table 19. Unfortunately, these proved to be disappointing. The use of 2-butanone as a donor led to no reaction even with the activated acceptor 4-nitrobenzaldehyde, and cyclohexanecarboxaldehyde failed to react with acetone. Fortunately, 2-

naphthaldehyde did react with acetone to afford the aldol adduct but with only 7% conversion – the corresponding enone was formed in 17% yield (entry 1, Table 19). However, the enantioselectivity of 38% is at the expected level for this catalyst, and the absolute stereochemistry was confirmed by comparison of the chiral HPLC of the product obtained from the L-proline catalysed reaction.^{68a} The use of *isobutyraldehyde* as an acceptor did proceed, albeit slowly affording 6% of the aldol product (entry 2) and the combination of 2-octanone and 4-nitrobenzaldehyde afforded a similarly low level of conversion (entry 3). In the latter two cases, the enantioselectivity could not be determined due to problematic product purification, and therefore, chiral HPLC resolution.

Table 19. Conversions and e.e.s for the (*S*)-**268a** catalysed aldol reaction in DMSO.

Entry	Product	Conversion ^a (%)	e.e. ^b (%)	Conversion enone ^a (%)
1		7	38	17
2		6	- ^c	0
3		5	- ^c	0

^aDetermined by ¹H NMR. ^bDetermined by chiral HPLC. ^cNot determined.

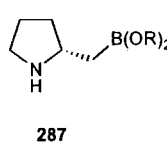
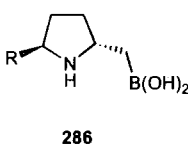
Although catalysis of the aldol reaction between 4-nitrobenzaldehyde and acetone proceeds well, amino-boronic acid (*S*)-**268a** shows limited substrate scope. The use of small 3-carbon donors (acetone or hydroxyacetone) leads to comparable reaction rates to L-proline even with less activated acceptors than 4-nitrobenzaldehyde, and this suggests enamine activation does occur. However, the lower enantioselectivities obtained with (*S*)-**268a** indicates that some product formation is occurring *via* enamine activation only, with no boronic acid participation. The use of larger donors appears to switch off enamine activation as well, leading to no product formation.

4.5 Summary and conclusions

In summary, (*S*)-**268a** has been synthesised in good yield and high enantioselectivity. It has been demonstrated as a catalyst for the direct aldol reaction, although with limited substrate scope at present. In the reaction between 4-nitrobenzaldehyde and acetone, (*S*)-**268a** catalyses the reaction at a comparable rate to L-proline and DMSO is preferred for higher enantioselectivities. The fact that asymmetric induction is observed confirms a bifunctional mode of action with both enamine activation and Lewis acid activation by boron. The solution behaviour of (*S*)-**268a** at different pH's has also been examined, allowing the pK_a's for boron quarternerisation and ammonium deprotonation to be determined and assigned.

4.6 Future work

Although the use of amino-boronic acid (*S*)-**268a** has demonstrated that a boronic acid moiety can participate in the aldol reaction, which in conjunction with enamine activation can lead to asymmetric induction, the enantioselectivities obtained range from moderate to poor. In addition, (*S*)-**268a** does not solve the problems associated with proline catalysis. This includes the use of high catalyst loadings and highly polar solvents. In order to address these issues, further amino-boronic acids need to be synthesised and screened on reactions proceeding *via* enamine/iminium ion catalysis, with the structures **285-287** providing a good starting point. For example, the addition of a phenyl ring and in particular, an aryl boronic acid as in **285**, would serve to both adjust the B-N distance and increase the Lewis acidity of the boronic acid. The addition of another group to the pyrrolidine ring, as in **286**, could help to improve levels of enantioselectivity, as could the screening of boronate esters **287**. Boronate esters have the advantage of being easier to handle *versus* the free boronic acids. They also display increased Lewis acidity along with steric hindrance, and chiral esters can be employed if desired.



5. Experimental

General experimental information

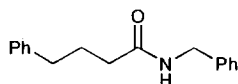
Glassware was oven dried (130 °C) as required and cooled under a positive pressure of argon. Dry solvents were prepared using the Innovative Technology Inc. solvent purification system and analysed with Metrohm 831 KF coulometer. All other materials were purchased directly from standard chemical suppliers (Aldrich, Acros, Fluka, Frontier) and used without further purification, unless stated otherwise. TLC was performed on plastic backed silica gel plates with visualisation achieved using a UV lamp, or by staining with KMnO₄ or PMA. Drying was carried out over anhydrous MgSO₄, followed by filtration. Evaporations were carried out at 20 mmHg using a rotary evaporator and water bath, followed by evaporation to dryness under vacuum (<2 mmHg). Purification by medium pressure column chromatography was performed using silica gel 35-70 μm. Melting points were determined using an electrothermal melting point apparatus and are reported uncorrected. All ¹H and ¹³C NMR were recorded with either a Varian Mercury-400, Bruker Avance-400 or Varian Inova-500 spectrometers. ¹¹B NMR were recorded with Bruker Avance-400 or Varian Inova-500 spectrometers. ¹⁹F NMR were recorded with Varian Mercury-400 or Inova-500 spectrometers. Chemical shifts are expressed as parts per million (ppm) downfield from the internal standard TMS for proton and carbon, external BF₃.Et₂O for ¹¹B and CFCl₃ for ¹⁹F. Elemental analysis was performed using an Exeter Analytical E-440 Elemental Analyser. EI mass spectrometry was performed on a Micromass Autospec, Finnigan MAT 900XLT or Finnigan MAT 95XP with electrospray methods, both +ve and -ve, conducted on a VG platform. IR spectra were recorded with a Perkin-Elmer 1615 FTIR or 298 FTIR spectrometer. Molecular sieves were activated by heating to 450°C. Optical rotations, [α]_D values, are given in deg cm⁻² g⁻¹ and recorded at the D line of Sodium (589 nm). Chiral HPLC analyses were performed on a Gilson HPLC system equipped with a Gilson 321 pump, a Gilson 234 autoinjector, two Gilson valvemates, a Metachem Technologies Degassit degasser, a Gilson UV-Vis detector 118 using the appropriate chiral column. Conversion vs. time data for catalyst screenings was obtained using a Gilson 215 Synthesis Workstation equipped with ReactArray racks and heating block, carried out using ReactArray Control Software (version 3,0,0,3048) and HPLC data analysed either directly using Gilson Unipoint (version 5.11) or using ReactArray

DataManager (version 1,1,33,0). HPLC conditions were under Gilson Unipoint (version 5.11) control and injections carried out in conjunction with ReactArray DataManager. The HPLC system consisted of Gilson 322 Pump, Gilson 402 Syringe Pump, Agilent 1100 Series UV Diode Array Detector and Phenomenex Gemini C18 5 μm , 150 mm x 4.60 mm column. Design of Experiments was carried out on a Gilson SK233 with Reactivate heating block, using ReactArray software (version 2.00). The HPLC system (Agilent 1100 series) consisted of a G1322A degasser, G1312A binary pump, G1316A column compartment, variable wavelength detector (254 nm) and Phenomenex Gemini C18 5 μm , 150 mm x 4.60 mm column with HPLC injections controlled by Waters Empower (Build 1154). Design of Experiments setup and analysis was carried out using Design-Expert (Version 7.0.0), Stat-Ease Inc.

General procedure for isolation of amides (fluorobenzene)

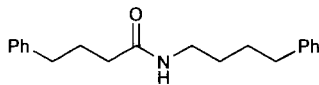
A 2-necked round-bottomed flask was equipped with stirrer bar, pressure equalising dropping funnel (in vertical neck) with a soxhlet thimble containing CaH_2 (~1 g) inside, followed by a condenser. The appropriate carboxylic acid (5 mmol), followed by fluorobenzene (50 mL), and amine (5 mmol) were added, followed by catalyst **80a** (117.6 mg, 0.5 mmol, 10 mol%). The mixture was allowed to stir at reflux for 24 h, before being concentrated *in vacuo*. The residue was then redissolved in DCM (25 mL), washed with brine (25 mL), 5% (w/v) HCl (25 mL), brine (25 mL), 5% (w/v) NaOH (25 mL), brine (25 mL), dried over MgSO_4 , and the solvent evaporated *in vacuo*.

N-Benzyl-4-phenylbutyramide **93a**:¹⁷



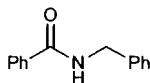
Yield: (0.86 g, 68%) as a white solid; HPLC (gradient MeCN (0.05% TFA) / water (0.05% TFA) 0:100 to 100:0 over 15 minutes; 1 mL min^{-1} , t_r = 10.28 min); mp 83-84 $^{\circ}\text{C}$; ν_{max} (film)/ cm^{-1} 3288, 2921, 1643s, 1547s, 1215, 696s, 494; δ_{H} (400 MHz; CDCl_3) 1.92-2.02 (2H, m, CH_2), 2.19 (2H, t, J 6.9, CH_2), 2.64 (2H, t, J 7.5, CH_2), 4.40 (2H, d, J 5.7, CH_2), 5.87 (1H, br s, CONH), 7.13–7.35 (m, 10 H, ArH).

N-4-Phenylbutyl-4-phenylbutyramide **93b**:



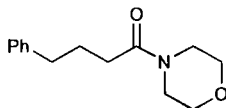
Yield: (1.03 g, 70%) as a white solid; HPLC (gradient MeCN (0.05% TFA) / water (0.05% TFA) 0:100 to 100:0 over 19 minutes; 1 mL min⁻¹, t_r = 14.21 min); mp 59-60 °C; (Found: C, 81.24; H, 8.57; N, 4.69. C₂₀H₂₅NO requires C, 81.31; H, 8.53; N, 4.74%); ν_{max} (film)/cm⁻¹ 3304, 2925, 2861, 1635s, 1535s, 741s and 693vs; δ_H (400 MHz; CDCl₃) 1.47-1.56 (2H, m, CH₂), 1.60-1.69 (2H, m, CH₂), 1.92-2.01 (2H, m, CH₂), 2.15 (2H, t, *J* 7.4, CH₂), 2.64 (4H, m, 2 x ArCH₂), 3.26 (2H, m, CH₂N), 5.44 (1H, br s, CONH), 7.15-7.22 (6H, m, ArH) and 7.25-7.31 (4H, m, ArH); δ_C (100.6 MHz; CDCl₃) 27.3 (CH₂), 28.8 (CH₂), 29.3 (CH₂), 35.3 (CH₂), 35.6 (CH₂), 36.0 (CH₂), 39.4 (CH₂), 125.9 (ArC), 126.1 (ArC), 128.45 (ArC), 128.49 (ArC), 128.51 (ArC), 128.6 (ArC), 141.6 (ArC-CH₂), 142.2 (ArC-CH₂) and 172.7 (CONH); *m/z* (ES) 318.3 (100%, [M+Na]⁺), 296.3 (60, [M+H]⁺).

N-Benzylbenzamide **93c**:¹⁴⁶



Yield: (0.53 g, 50%) as a white solid; HPLC (gradient MeCN (0.05% TFA) / water (0.05% TFA) 0:100 to 100:0 over 15 minutes; 1 mL min⁻¹, t_r = 9.12 min); mp 104-105°C; δ_H (400 MHz; CDCl₃) 4.63 (2H, d, *J* 4.8, CH₂), 6.58 (1H, br s, CONH), 7.20-7.52 (8H, m, ArH), 7.78 (2H, d, *J* 7.6, ArH).

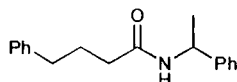
N-4-phenylbutan-1-one morpholine **93d**:



Yield: 0.78 g (67%) as a white solid. Mp 110-111°C; (Found: C, 71.91; H, 8.24; N, 6.12. C₁₄H₁₉NO₂ requires C, 72.07; H, 8.21; N, 6.00%); ν_{max} (film)/cm⁻¹ (inter alia) 2856, 1647vs, 1433s and 1116s; δ_H (400 MHz; CDCl₃) 1.98 (2H, quintet, *J* 7.6, CH₂), 2.31 (2H, t, *J* 7.6, CH₂), 2.68 (2H, t, *J* 7.6, CH₂), 3.35-3.39 (2H, m, morpholino), 3.58-3.68 (4H, m, morpholino), 7.16-7.22 (3H, m, ArH) and 7.25-7.31 (2H, m, ArH); δ_C (100.6 MHz; CDCl₃) 26.7 (CH₂), 32.2 (CH₂), 35.4 (CH₂), 42.0 (CH₂N), 46.1

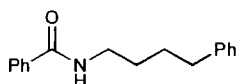
(CH₂N), 66.8 (CH₂O), 67.1 (CH₂O), 126.1 (ArC), 128.5 (ArC), 128.6 (ArC), 141.7 (ArC) and 171.6 (CON); *m/z* (ES) 234.2 (100%, [M+H]⁺).

N-(1-Phenylethyl)-4-phenylbutyramide **113a**:¹⁷



Yield: (0.71 g, 53%) as a white solid; HPLC (gradient MeCN (0.05% TFA) / water (0.05% TFA) 0:100 to 100:0 over 15 min; 1 mL min⁻¹; *t_r* = 13.10 min); chiral HPLC: Daicel Chiralcel OD. Hexane-EtOH, 97.5:2.5, 1 mL min⁻¹, 210 nm: *t_r* (*R*) = 34.3 min; *t_r* (*S*) = 41.5 min; δ_H (400 MHz; CDCl₃) 1.56 (3H, *J* 7.2, CH₃), 2.03 (2H, m, CH₂), 2.38 (2H, t, *J* 7.8, CH₂), 2.68 (2H, t, *J* 7.8, CH₂), 3.60 (1H, q, *J* 7.2, CH(CH₃)), 5.65 (1H, br s, CONH), 7.10–7.28 (10H, m, ArH).

N-4-Phenylbutylbenzamide **93d**



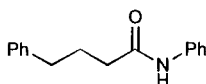
To a stirred solution of benzoyl chloride (0.12 mL, 1 mmol) in dry Et₂O (6 mL) under argon at 0°C, was added triethylamine (0.21 mL, 1.5 mmol) and 4-phenylbutylamine (0.16 mL, 1 mmol). The reaction was allowed to warm to rt, stirred for 2 hours and then quenched with 5% (w/v) HCl (5 mL). The organic layer was separated and washed again with 5% (w/v) HCl (5 mL), then brine (5 mL), 5% (w/v) NaOH (2 x 5 mL), brine (5 mL), dried over MgSO₄, and concentrated *in vacuo* to afford *N*-4-phenylbutylbenzamide **93d** (0.25 g, 99%) as a white solid. HPLC (gradient MeCN (0.05% TFA) / water (0.05% TFA) 0:100 to 100:0 over 15 minutes; 1 mL min⁻¹, *t_r* = 10.83 min); mp 76-77 °C; (Found: C, 80.50; H, 7.59; N, 5.44. C₁₇H₁₉NO requires C, 80.60; H, 7.56; N, 5.53%); ν_{max} (film)/cm⁻¹ 3328, 2936, 2859, 1633s, 1521s and 691vs; δ_H (400 MHz; CDCl₃) 1.60-1.78 (4H, m, 2 x CH₂), 2.66 (2H, t, *J* 7.4, 2 x ArCH₂), 3.47 (2H, m, CH₂N), 6.21 (1H, br s, CONH), 7.19 (3H, t, *J* 7.4, ArH), 7.28 (2H, t, *J* 7.6, ArH), 7.41 (2H, t, *J* 7.2, ArH), 7.49 (1H, t, *J* 7.4, ArH) and 7.75 (2H, dt, *J* 7.4 and 1.2, ArH); δ_C (100.6 MHz; CDCl₃) 28.8 (CH₂), 29.4 (CH₂), 35.6 (CH₂), 40.0 (CH₂N), 126.0 (ArC), 126.9 (ArC), 128.47 (ArC), 128.54 (ArC), 128.7 (ArC), 131.5

(ArC), 134.8 (ArC-CH₂), 142.2 (ArC-CONH) and 167.7 (CONH); *m/z* (ES) 276.5 (100%, [M+H]⁺).

General procedure for isolation of amides (toluene)

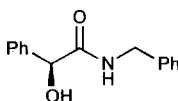
The appropriate carboxylic acid (5 mmol), followed by toluene (50 mL), and amine (5 mmol) were added, followed by catalyst **80a** (11.8 mg, 0.05 mmol). The mixture was allowed to stir at reflux for 22 h, before being concentrated *in vacuo*. The residue was then redissolved in Et₂O (25 mL), washed with brine (25 mL), 5% (w/v) HCl (25 mL), brine (25 mL), 5% (w/v) NaOH (25 mL), brine (25 mL), dried over MgSO₄, and the solvent evaporated *in vacuo*.

4-Phenylbutyranilide:^{11a}



Yield: (0.55 g, 46%) as an off-white solid; δ_{H} (400 MHz; CDCl₃) 1.98-2.08 (2H, m, CH₂), 2.38 (2H, t, *J* 7.7, CH₂), 2.75 (2H, t, *J* 7.4, CH₂), 5.87 (1H, br s, CONH), 7.12–7.35 (8H, m, ArH), 7.50 (2H, d, *J* 8.0, ArH).

(*S*)-*N*-Benzylmandelamide:^{11a}



Yield: (0.13 g, 11%) obtained as a white solid. In the absence of catalyst **80a**, (*S*)-*N*-benzylmandelamide (0.11 g, 7.5%) was obtained as a white solid; δ_{H} (400 MHz; CDCl₃) 3.50 (1H, d *J* 3.3, CHOH), 4.43 (1H, dd, *J* 6.2 and 14.2, PhCHH), 4.49 (1H, dd, *J* 6.2 and 14.2, PhCHH), 6.32 (1H, br s, CONH), 7.12–7.48 (10H, m, ArH).

General procedure for monitoring direct amide formation over time using Gilson 215 Synthesis Workstation

The appropriate catalyst (0.233 mmol, 10 mol %) was manually weighed into each reaction vessel, followed by assembly of a micro-soxhlet apparatus loaded with activated 3 Å molecular sieves under argon. Solid reagents were added using the ReactArray as standard solutions (0.5 M in fluorobenzene). Naphthalene (0.35 mmol,

15 mol %) and amine (2.33 mmol) were added to the reaction vessels at ambient temperature. The appropriate amount of fluorobenzene was then added to each reaction vessel in order to give a final reaction volume of 10 mL. After heating to reflux, carboxylic acid (2.33 mmol) was added to the stirred solution. Reactions were sampled (50 μ L) at 2 or 4 h intervals (24 or 48 h reaction time respectively). Samples were quenched with MeCN (950 μ L), diluted once (50 μ L in 950 μ L MeCN) mixed and analysed by HPLC (gradient MeCN (0.05% TFA) / water (0.05% TFA) 0:100 to 100:0 over 15 or 19 minutes; 1 mL min⁻¹). Naphthalene was used as an internal standard, with response factors calculated automatically by ReactArray DataManager.

General procedure for catalyst stability testing in the presence of carboxylic acid

A 2-necked round-bottomed flask was equipped with stirrer bar, pressure equalising dropping funnel (in vertical neck) containing a soxhlet thimble loaded with CaH₂ (~1 g), surmounted by a condenser. The appropriate carboxylic acid (5 mmol), fluorobenzene (50 mL) and catalyst (0.5 mmol, 10 mol %) were added. The mixture was allowed to stir for 1 h at ambient temperature and a sample (1 mL) was taken *via* syringe. The mixture was then allowed to reflux for 24 h, with further samples (1 mL) taken at 1, 2, 4, and 24 h intervals. Samples were concentrated *in vacuo*, redissolved in CDCl₃ and submitted for ¹H and ¹¹B NMR. Following a D₂O shake, samples were resubmitted for ¹H and ¹¹B NMR.

Procedure for detection of reaction intermediates

4-Phenylbutyric acid (164 mg, 1 mmol) and catalyst **80a** (118 mg, 0.5 mmol) were weighed into a ReactArray reaction vessel, followed by assembly of a micro-soxhlet apparatus loaded with activated 3Å molecular sieves under argon. C₆D₆ (10 mL) was added and the mixture was stirred at reflux for 6 h before two samples (1 mL) were taken. Sample 1 was analysed by NMR. Sample 2 was concentrated *in vacuo* and the residue analysed by IR and MS.

General procedure for use of ReactArray workstation – effects of solvent and dehydration on formation of *N*-benzylbenzamide 93c using Gilson 215 Synthesis Workstation

Catalyst **80a** (54.9 mg, 0.233 mmol or 5.5 mg, 0.0233 mmol) was manually weighed into each reaction vessel, followed by benzoic acid (0.285 g, 2.33 mmol). A micro-soxhlet apparatus loaded with activated 3Å molecular sieves under argon was assembled, in cases where dehydration was required. Naphthalene (700 µL, 0.5M in PhF, 0.35 mmol, 15 mol %) and benzylamine (255 µL, 2.33 mmol) were added to the reaction vessels at ambient temperature. The appropriate amount of solvent (fluorobenzene, toluene, propionitrile or water) was then added to each reaction vessel in order to give a final reaction volume of 10 mL. Reactions were sampled (50 µL) at 4 h intervals over 48 h. Samples were quenched with MeCN (950 µL), diluted once (50 µL in 950 µL MeCN) mixed and analysed by HPLC (gradient MeCN (0.05% TFA) / water (0.05% TFA) 0:100 to 100:0 over 15 minutes; 1 mL min⁻¹; t_r = 9.12 min). Naphthalene was used as an internal standard, with response factors calculated automatically by ReactArray DataManager.

General procedure for Design of Experiments on formation of *N*-benzylbenzamide 93c using Gilson SK233

Benzoic acid (1, 3 or 5 mmol) was weighed into ReactArray tubes to give the appropriate reaction concentration (0.1, 0.3 or 0.5 M) followed by catalyst **80a** (1, 5.5 or 10 mol%). A ReactArray azeotropic condenser set was assembled, naphthalene (25 mol%) was added as a 0.5 M standard solution, followed by fluorobenzene or toluene to give a final reaction volume of 10.6 mL. The mixture was heated to reflux under nitrogen and benzylamine (1, 3 or 5 mmol) was added. The reaction was stirred at reflux with sampling at 4 h intervals. Samples were subjected to the following quench/dilution protocols:

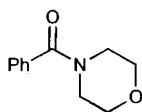
- 0.1M: 90 µL into 910 µL MeCN
- 0.3 M: 50 µL into 1650 µL MeCN
- 0.5 M: 100 µL into 900 µL MeCN, 176 µL into 824 µL MeCN

Samples were mixed and analysed by HPLC (gradient MeCN (0.05% TFA) / water (0.05% TFA) 0:100 to 100:0 over 15 min; 1 mL min⁻¹; t_r = 9.12 min). Naphthalene was used as an internal standard.

General procedure for isolation of amides following Design of Experiments using Gilson SK233

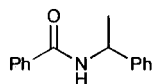
The appropriate carboxylic acid (1 mmol) and catalyst **80a** (23.5 mg, 0.1 mmol or 11.8 mg, 0.05 mmol) were weighed into ReactArray tubes followed by attachment of a ReactArray azeotroping condenser set. The appropriate amount of toluene was added to give a final reaction volume of 10 mL and the mixture heated to reflux under nitrogen. The appropriate amine (1 mmol) was added and the mixture stirred at reflux for 24 or 30 h, before being concentrated under vacuum. The residue was then redissolved in MTBE (10 mL), washed with 5% (w/v) HCl (10 mL), brine (10 mL), 5% (w/v) NaOH (10 mL), brine (10 mL), dried over MgSO₄, and the solvent evaporated under vacuum.

Morpholin-4-yl-phenylmethanone:¹⁴⁷



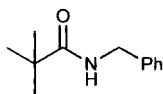
Yield: 0.04 g (21%), as a pale yellow solid; δ_{H} (400 MHz; CDCl₃) 3.35-3.39 (2H, br m, morpholino), 3.58-3.68 (6H, br m, morpholino), 7.32-7.50 (5H, m, ArH).

N-(1-Phenylethyl)benzamide **113b**:¹⁴⁸



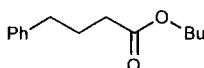
Yield: 0.16 g (71%), as a white solid. HPLC (MeCN (0.05% TFA) / water (0.05% TFA) 65:35 for 8 min; 1 mL min⁻¹; t_r = 2.94 min); chiral HPLC: Daicel Chiralcel OD. Hexane-EtOH, 90:10, 0.75 mL min⁻¹, 210 nm: t_r (R) = 11.9 min; t_r (S) = 14.2 min; mp 120-121°C; δ_{H} (400 MHz; CDCl₃) 1.60 (3H, d, *J* 7.1, CH(CH₃)), 5.33 (1H, q, *J* 7.2, 1H, CH(CH₃)), 6.40 (1H, br s, CONH), 7.19-7.50 (8H, m, ArH), 7.75 (2H, d, *J* 7.2, ArH).

N-Benzylpivalamide:¹⁷



Yield: 0.11 g (59%), as a white solid; mp 85-86°C; δ_{H} (400 MHz; CDCl₃) 1.23 (9H, s, *t*-Bu), 4.44 (2H, d, *J* 5.4, PhCH₂), 5.93 (1H, br s, CONH), 7.25–7.37 (5H, m, ArH).

Butyl 4-phenylbutyrate^{11a}



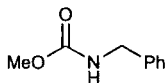
In fluorobenzene:

A 2-necked round-bottomed flask was equipped with stirrer bar, pressure equalising dropping funnel (in vertical neck) with a soxhlet thimble containing CaH₂ (~1 g) inside, followed by a condenser. 4-Phenylbutyric acid (0.821 g, 5 mmol), fluorobenzene (50 mL), and 1-butanol (0.46 mL, 5 mmol) were added, followed by catalyst **80a** (117.6 mg, 0.5 mmol). The mixture was allowed to stir at reflux for 24 h, before being concentrated *in vacuo*. The residue was then redissolved in Et₂O (10 mL), washed with 5% (w/v) HCl (10 mL), brine (10 mL), 5% (w/v) NaOH (10 mL), brine (10 mL), dried over MgSO₄, and the solvent evaporated *in vacuo* to afford butyl 4-phenylbutyrate (0.06 g, 5%) as a colourless oil; δ_{H} (400 MHz; CDCl₃) 0.88 (3H, t, *J* 7.3, CH₃), 1.28-1.35 (2H, m, CH₂), 1.48-1.58 (2H, m, CH₂), 1.84-1.92 (2H, m, CH₂), 1.96-2.06 (2H, m, CH₂), 2.25 (2H, t, *J* 7.4, CH₂), 2.58 (2H, t, *J* 7.4, CH₂), 7.10-7.26 (5H, m, ArH).

In the absence of solvent:

4-Phenylbutyric acid (0.821g, 5 mmol), 1-butanol (2.5 mL, 27.3 mmol) and catalyst **80a** (11.8 mg, 0.05 mmol) were heated at reflux for 24 h. Et₂O (20 mL) was added and the organic layer washed with 5% (w/v) NaOH (25 mL), brine (25 mL), 5% (w/v) HCl (25 mL), brine (25 mL), dried over MgSO₄, and concentrated *in vacuo* to afford butyl 4-phenylbutyrate (0.79 g, 72%) as a colourless oil. In the absence of **80a**, butyl 4-phenylbutyrate (0.55 g, 50%) was obtained as a colourless oil.

***N*-Benzylmethylcarbamate**¹⁴⁹

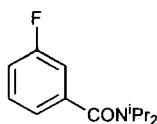


A stirred mixture of dimethyl carbonate (0.42 mL, 5 mmol) and benzylamine (0.55 mL, 5 mmol or 1.10 mL, 10 mmol) was heated at reflux for 21 h. The mixture was cooled to rt, Et₂O (10 mL) added, washed 5% (w/v) HCl (10 mL), then brine (10 mL), dried over MgSO₄, and concentrated *in vacuo* to afford *N*-benzylmethylcarbamate (0.21 g, 25%) as a pale yellow solid; δ_{H} (400 MHz; CDCl₃) 3.63 (3H, s, OCH₃), 4.31 (2H, d, *J* 6.0, PhCH₂), 5.44 (1H, br s, CONH), 7.24-7.31 (5H, m, ArH).

General procedure for effect of additives on formation of *N*-benzylbenzamide 93c using Gilson SK233

Benzoic acid (0.37 g, 3 mmol) was weighed into ReactArray tubes followed by catalyst **80a** (1, 5.5 or 10 mol%). A ReactArray azeotroping condenser set was assembled and naphthalene (96.1 mg, 0.75 mmol, 25 mol%) was added as a 0.5 M standard solution. Either water (1.6 mL) or trichloroacetic acid (53.9 mg, 0.33 mmol, 11 mol%) was then added, followed by fluorobenzene or toluene to give a final reaction volume of 10.6 mL. The mixture was heated to reflux under nitrogen and benzylamine (328 μ L, 3 mmol) was added. Reactions were sampled (50 μ L) at 2 or 4 h intervals (24 or 48 h reaction time respectively). Samples were quenched with MeCN (1650 μ L), mixed and analysed by HPLC (gradient MeCN (0.05% TFA) / water (0.05% TFA) 0:100 to 100:0 over 15 min; 1 mL min⁻¹; t_{r} = 9.12 min). Naphthalene was used as an internal standard.

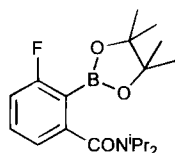
***N,N*-Diisopropyl-3-fluorobenzamide 102a**



To a stirred solution of 3-fluorobenzoyl chloride (2.68 g, 16.9 mmol) in dry Et₂O (40 mL) under argon at 0°C, was added dry diisopropylamine (6.0 mL, 42 mmol) dropwise. The reaction was allowed to warm to rt, stirred for 18 hours and then quenched with 5% (w/v) HCl (25 mL). The organic layer was separated and washed again with 5% (w/v) HCl (2 x 25 mL), then brine (25 mL), 5% (w/v) NaOH (2 x 25 mL), brine (25 mL), dried over MgSO₄, and concentrated *in vacuo* to afford amide

102a (3.40 g, 90%) as a white solid. Mp 74-76 °C; (Found: C, 69.73; H, 8.07; N, 6.10. C₁₃H₁₈NOF requires C, 69.93; H, 8.13; N, 6.27%); $\lambda_{\max}(\text{MeCN})/\text{nm}$ 200 ($\epsilon/\text{dm}^3 \text{ mol}^{-1} \text{ cm}^{-1}$ 12400) and 267 (1400); $\nu_{\max}(\text{film})/\text{cm}^{-1}$ (inter alia) 3072, 2971, 1629s, 1583, 1437, 1344s and 1140; δ_{H} (500 MHz; CDCl₃) 1.17 (6H, br s, (CH₃)₂CH), 1.54 (6H, br s, (CH₃)₂CH), 3.55 (1H, br s, (CH₃)₂CH), 3.81 (1H, br s, (CH₃)₂CH), 7.01-7.11 (3H, m, ArH) and 7.37 (1H, td, J_{HH} 8.0 and J_{FH} 5.5, ArH); δ_{C} (100.6 MHz; CDCl₃) 20.9 (br s, (CH₃)₂CH), 46.2 (br s, (CH₃)₂CH), 51.1 (br s, (CH₃)₂CH), 113.2 (d, $^2J_{\text{FC}}$ 22, ArC), 115.9 (d, $^2J_{\text{FC}}$ 21, ArC), 121.5 (d, $^4J_{\text{FC}}$ 3, ArC), 130.5 (d, $^3J_{\text{FC}}$ 8, ArC), 141.1 (d, $^3J_{\text{FC}}$ 7, ArC-CONⁱPr₂), 162.9 (d, $^1J_{\text{FC}}$ 247, ArC-F) and 169.7 (d, $^4J_{\text{FC}}$ 2, CONⁱPr₂); δ_{F} (376.3 MHz; CDCl₃) -112.5 (m); m/z (ES) 246.1260 (100%, [M+Na]⁺. [C₁₉H₁₃NOFNa]⁺ requires 246.1265).

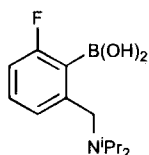
***N,N*-Diisopropyl-3-fluoro-2-(4,4,5,5-tetramethyl-[1,3,2]dioxaborolan-2-yl)-benzamide 103a**



To a stirred solution of *N,N*-diisopropyl-3-fluorobenzamide **102a** (5.0 g, 22.4 mmol) and TMEDA (4.0 mL, 26.9 mmol) in dry THF (50 mL) under argon at -78°C, was added *n*-BuLi (16.8 mL, 1.6 M, 26.9 mmol) dropwise over 10 min. The mixture was left to stir for 1 h and then trimethyl borate (3.0 mL, 26.9 mmol) was added rapidly. The mixture was allowed to reach rt (2 h) and then quenched with 20% (w/v) HCl (10 mL), followed by addition of pinacol (3.2 g, 26.9 mmol). The mixture was extracted into ether (3 x 20 mL) and the combined organic extracts washed with sat. aq. NaHCO₃ (3 x 20 mL) and brine (2 x 20 mL). The extracts were dried over MgSO₄ and concentrated *in vacuo*. Column chromatography on silica gel (hexane:EtOAc, 2:1) afforded pinacol boronate **103a** (5.16 g, 66%) as a white crystalline solid. Mp 104-106 °C; (Found: C, 65.41; H, 8.46; N, 3.99. C₁₉H₂₉BFNO₃ requires C, 65.34; H, 8.37; N, 4.01%); $\lambda_{\max}(\text{MeCN})/\text{nm}$ 197 ($\epsilon/\text{dm}^3 \text{ mol}^{-1} \text{ cm}^{-1}$ 28100), 242 (3320) and 271 (1220); $\nu_{\max}(\text{film})/\text{cm}^{-1}$ (inter alia) 2973, 2930, 2361, 1617s, 1439, 1335vs and 1144s; δ_{H} (500 MHz; CDCl₃) 1.19 (6H, br s, (CH₃)₂CH), 1.33 (12H, s, 4 x Me), 1.54 (6H, br s, (CH₃)₂CH), 3.54 (1H, br s, (CH₃)₂CH), 3.98 (1H, br s, (CH₃)₂CH), 6.98-7.04 (2H, m, ArH) and 7.32 (1H, td, J_{HH} 8.0 and J_{FH} 5.5, ArH); δ_{C} (125.7 MHz; CDCl₃) 20.6 (br

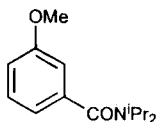
s, (CH₃)₂CH), 25.0 (pinacol CH₃), 46.6 (br s, (CH₃)₂CH), 51.2 (br s, (CH₃)₂CH), 83.6 (pinacol C-O), 116.0 (d, ²J_{FC} 25, ArC), 120.8 (d, ⁴J_{FC} 4, ArC), 131.5 (d, ³J_{FC} 9, ArC), 144.9 (d, ³J_{FC} 9, ArC-CONⁱPr₂), 166.3 (d, ¹J_{FC} 249, ArC-F) and 170.3 (d, ⁴J_{FC} 3, CONⁱPr₂); δ_B (128.4 MHz; CDCl₃) 26.9; δ_F (376.3 MHz; CDCl₃) -103.2 (s); *m/z* (ES) 721.4 (60%), 699.5 (25), 372.2 (100, [M+Na]⁺), 350.2295 (48, [M+H]⁺. [C₁₉H₃₀BFNO₃]⁺ requires 350.2297).

N,N-Diisopropyl-3-fluorobenzylamine-2-boronic acid **104a**



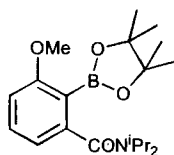
To a stirred solution of pinacol boronate **103a** (5.16 g, 14.8 mmol) and NaBH₄ (5.6 g, 148 mmol) in dry THF (70 mL) under argon was added TMSCl (37.6 mL, 296 mmol) and the mixture stirred at reflux for 20 h. The reaction was quenched by slow addition of 5% (w/v) HCl then 20% (w/v) HCl taking the aqueous layer to pH 1, and washed with Et₂O (1 x 50 mL, 3 x 100 mL). Sat. aq. NaHCO₃ was added to the aqueous phase, until it reached pH 7 and the mixture was extracted into Et₂O (3 x 100 mL). Organic extracts were combined and washed with brine (2 x 100 mL), dried over MgSO₄ and concentrated *in vacuo*. Recrystallisation from DCM-hexane afforded boronic acid **104a** (2.71 g, 72%) as a white solid. Slow crystallisation from MeCN provided crystals suitable for single crystal X-ray analysis (see Appendix). Mp 110-111 °C; (Found: C, 61.53; H, 8.41; N, 5.30. C₁₃H₂₉BFNO₂ requires C, 61.69; H, 8.36; N, 5.53%); λ_{max}(MeCN)/nm 194 (ε/dm³ mol⁻¹ cm⁻¹ 10000), 216 (6970) and 272 (1280); ν_{max} (film)/cm⁻¹ (inter alia) 3307, 2971, 2539, 1604, 1565, 1450s, 1385vs and 1144s; δ_H (500 MHz; CDCl₃) 1.10 (12H, d, *J* 7.0, (CH₃)₂CH), 3.08 (2H, septet, *J* 7.0, (CH₃)₂CH), 3.82 (2H, s, ArCH₂), 6.97-7.03 (1H, m, ArH), 7.07 (1H, d, *J* 7.5, ArH), 7.30 (1H, td, *J*_{HH} 7.5 and *J*_{FH} 6.5, ArH) and 9.27 (2H, br s, B(OH)₂); δ_C (125.7 MHz; CDCl₃) 19.9 ((CH₃)₂CH), 47.7 ((CH₃)₂CH), 52.0 (d, ⁴J_{FC} 2, ArCH₂), 115.4 (d, ²J_{FC} 28, ArC), 127.7 (d, ⁴J_{FC} 2, ArC), 131.7 (d, ³J_{FC} 11, ArC), 144.7 (d, ³J_{FC} 8, ArCCH₂NⁱPr₂) and 168.0 (d, ³J_{FC} 244, ArC-F); δ_B (128.4 MHz; CDCl₃) 28.4; δ_F (376.3 MHz; CDCl₃) -104.5 (m); *m/z* (ES) 254.1722 (100%, [M+H]⁺. [C₁₃H₂₂BFNO₂]⁺ requires 254.1728).

N,N-Diisopropyl-3-methoxybenzamide **102b**



To a stirred solution of *m*-anisoyl chloride (0.82 mL, 6 mmol) in dry Et₂O (25 mL) under argon at 0°C, was added dry diisopropylamine (2.1 mL, 15 mmol) dropwise. The reaction was allowed to warm to rt, stirred for 3 h and then quenched with 5% (w/v) HCl (25 mL). The organic layer was separated and washed again with 5% (w/v) HCl (2 x 25 mL), brine (25 mL), 5% (w/v) NaOH (2 x 25 mL), brine (25 mL), dried over MgSO₄, and concentrated *in vacuo* to afford amide **102b** (1.38 g, 98%) as a white solid. Mp 92-93 °C; (Found: C, 71.45; H, 9.07; N, 5.81. C₁₄H₂₁NO₂ requires C, 71.46; H, 8.99; N, 5.95%); λ_{max}(MeCN)/nm 200 (ε/dm³ mol⁻¹ cm⁻¹ 21300) and 280 (2290); ν_{max}(film)/cm⁻¹ (inter alia) 3090, 2974, 1621vs, 1578, 1340vs, 1293 and 1032; δ_H (500 MHz; CDCl₃) 1.16 (6H, br s, (CH₃)₂CH), 1.54 (6H, br s, (CH₃)₂CH), 3.53 (1H, br s, (CH₃)₂CH), 3.83 (3H, s, OCH₃), 3.86 (1H, br s, (CH₃)₂CH), 6.86 (1H, s, ArH), 6.89 (1H, d, *J* 8.0, ArH), 6.91 (1H, d, *J* 8.0, ArH) and 7.61 (1H, t, *J* 8.0, ArH); δ_C (125.7 MHz; CDCl₃) 20.8 ((CH₃)₂CH), 46.0 (br s (CH₃)₂CH), 51.0 (br s, (CH₃)₂CH), 55.4 (OCH₃), 111.1 (ArC), 114.7 (ArC), 117.8 (ArC), 129.7 (ArC), 140.3 (ArC-OMe), 159.7 (ArC-CONⁱPr₂) and 170.9 (CONⁱPr₂); *m/z* (ES) 236.1646 (100%, [M+H]⁺. [C₁₄H₂₂NO₂]⁺ requires 236.1645).

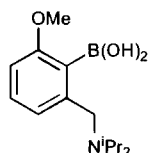
N,N-Diisopropyl-3-methoxy-2-(4,4,5,5-tetramethyl-[1,3,2]dioxaborolan-2-yl)-benzamide **103b**



To a stirred solution of *N,N*-diisopropyl-3-methoxybenzamide **103a** (1.75 g, 7.44 mmol) and TMEDA (1.56 mL, 10.4 mmol) in dry THF (25 mL) under argon at -78°C, was added *s*-BuLi (7.44 mL, 1.4 M, 10.4 mmol) dropwise over 10 minutes. The mixture was left to stir for 90 min and then triisopropyl borate (1.89 mL, 8.18 mmol) was added rapidly. The mixture was allowed to reach rt overnight (19 h) and then quenched with 20% (w/v) HCl (6 mL), followed by addition of pinacol (0.97 g, 8.18 mmol). The mixture was allowed to stir for 10 min before being extracted into ether

(3 x 20 mL) and the organic extracts washed with sat. aq. NaHCO₃ (3 x 10 mL), and brine (20 mL). The combined organic extracts were dried over MgSO₄ and concentrated *in vacuo*. Column chromatography on silica gel (hexane:EtOAc, 1:1) afforded pinacol boronate **103b** (2.05 g, 76%) as a white solid. Mp 90-91 °C; (Found: C, 66.22; H, 8.98; N, 3.82. C₂₀H₃₂BNO₄ requires C, 66.49; H, 8.93; N, 3.88%); ν_{\max} (film)/cm⁻¹ (inter alia) 2973, 1615s, 1431, 1335vs and 1146; δ_{H} (500 MHz; CDCl₃) 1.19 (6H, br s, (CH₃)₂CH), 1.35 (12H, s, 4 x Me), 1.54 (6H, br s, (CH₃)₂CH), 3.50 (1H, br s, (CH₃)₂CH), 3.81 (3H, s, OMe), 4.00 (1H, br s, (CH₃)₂CH), 6.82 (2H, d, *J* 8.0, ArH) and 7.28 (1H, t, *J* 8.0, ArH); δ_{C} (125.7 MHz; CDCl₃) 20.7 (br s, (CH₃)₂CH), 25.0 (pinacol CH₃), 46.3 (br s, (CH₃)₂CH), 51.0 (br s, (CH₃)₂CH), 55.8 (OMe), 83.5 (pinacol C-O), 110.7 (ArC), 117.3 (ArC), 130.3 (ArC), 144.0 (ArC-CONⁱPr₂), 163.4 (ArC-OMe) and 171.4 (CONⁱPr₂); δ_{B} (128.4 MHz; CDCl₃) 29.0; *m/z* (ES) 362.2497 (100%, [M+H]⁺. [C₂₀H₃₃BNO₄]⁺ requires 362.2497).

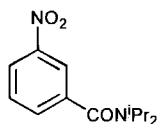
N,N*-Diisopropyl-3-methoxybenzylamine-2-boronic acid **104b*



To a stirred solution of pinacol boronate **103b** (0.99 g, 2.74 mmol) and NaBH₄ (1.04 g, 27.4 mmol) in dry THF (50 mL) under argon was added TMSCl (6.95 mL, 54.8 mmol) and the mixture stirred at reflux for 21 h. The reaction was quenched by slow addition of 5% (w/v) HCl (7 mL) and the THF was removed *in vacuo*. A further portion of 5% (w/v) HCl (15 mL) was added (aqueous layer to pH 1) and the mixture washed with Et₂O (1 x 25 mL, 2 x 15 mL). The Et₂O extracts were extracted into 5% (w/v) HCl (5 mL) and the combined aqueous phase washed with Et₂O (2 x 10 mL). The combined aqueous phase was neutralised with NaOH (s) then 20% (w/v) NaOH until no further precipitation of white solid was observed (pH 9). The mixture was extracted into DCM (3 x 15 mL), organic extracts were combined, washed with brine (15 mL), dried over MgSO₄ and concentrated *in vacuo*. Recrystallisation from hexane afforded boronic acid **104b** (0.36 g, 50%) as a white solid. Mp 164-165 °C; (Found: C, 63.82; H, 9.04; N, 5.16. C₁₄H₂₄BNO₃ requires C, 63.42; H, 9.12; N, 5.28%); ν_{\max} (KBr)/cm⁻¹ (inter alia) 3414, 2965, 1597s, 1466s, 1249s and 1084; δ_{H} (400 MHz; CDCl₃) 1.11 (12H, d, *J* 6.8, (CH₃)₂CH), 3.10 (2H, septet, *J* 6.8, (CH₃)₂CH), 3.80 (2H,

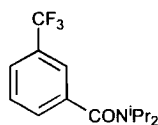
s, ArCH₂), 3.89 (3H, s, OMe), 6.90 (1H, d, *J* 8.0, ArH), 6.93 (1H, d, *J* 7.6, ArH), 7.31 (1H, dd, *J* 8.4 and 7.6, ArH) and 9.75 (2H, br s, B(OH)₂); δ_C (100.6 MHz; CDCl₃) 19.9 ((CH₃)₂CH), 47.5 ((CH₃)₂CH), 52.4 (ArCH₂), 56.0 (OMe), 110.5 (ArC), 125.6 (ArC), 131.2 (ArC), 144.8 (ArC) and 164.8 (ArC-OMe); δ_B (128.4 MHz; CDCl₃) 29.3; *m/z* (ES) 266.1923 (100%, [M+H]⁺). [C₁₄H₂₅BNO₃]⁺ requires 266.1922).

N,N-Diisopropyl-3-nitrobenzamide **102c**



To a stirred solution of 3-nitrobenzoyl chloride (1.41 g, 6.71 mmol) in dry Et₂O (25 mL) under argon at 0°C, was added dry diisopropylamine (2.7 mL, 19 mmol). The reaction was allowed to warm to rt, stirred for 18 h and then quenched with 5% (w/v) HCl (25 mL). The organic layer was separated and washed again with 5% (w/v) HCl (2 x 25 mL), then brine (25 mL), 5% (w/v) NaOH (2 x 25 mL), brine (25 mL), dried over MgSO₄, and concentrated *in vacuo* to afford amide **102c** (1.66 g, 87%) as a white solid. Mp 78-79 °C; (Found: C, 62.34; H, 7.27; N, 11.18. C₁₃H₁₈N₂O₃ requires C, 62.38; H, 7.25; N, 11.19%); λ_{max}(MeCN)/nm 194 (ε/dm³ mol⁻¹ cm⁻¹ 24000) and 252 (6960); ν_{max} (film)/cm⁻¹ 2930, 1625, 1527, 1438, 1334 and 1153; δ_H (500 MHz; CDCl₃) 1.21 (6H, br s, (CH₃)₂CH), 1.56 (6H, br s, (CH₃)₂CH), 3.52 (1H, br s, (CH₃)₂CH), 3.55 (1H, br s, (CH₃)₂CH), 7.60 (1H, t, *J* 8.1, ArH), 7.67 (1H, d, *J* 8.1, ArH), 8.20 (1H, s, ArH) and 8.25 (1H, d, *J* 8.1, ArH); δ_C (125.7 MHz; CDCl₃) 20.9 (br s, (CH₃)₂CH), 46.5 (br s, (CH₃)₂CH), 51.5 (br s, (CH₃)₂CH), 121.2 (ArC), 123.8 (ArC), 130.0 (ArC), 132.0 (ArC), 140.5 (ArC-CONⁱPr₂), 148.3 (ArC-NO₂) and 168.4 (CONⁱPr₂); *m/z* (ES) 273.1203 (100%, [M+Na]⁺). [C₁₃H₁₈N₂O₃Na]⁺ requires 273.1210).

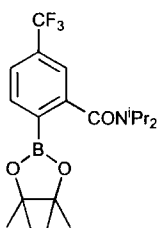
N,N-Diisopropyl-3-trifluoromethylbenzamide **106**



To a stirred solution of 3-(trifluoromethyl)benzoyl chloride (1.78 mL, 12 mmol) in dry Et₂O (30 mL) under argon at 0°C, was added dry diisopropylamine (4.24 mL, 30 mmol) dropwise. The reaction was allowed to warm to rt, stirred for 2 h and then

quenched with 5% (w/v) HCl (25 mL). The organic layer was separated and washed again with 5% (w/v) HCl (25 mL), then brine (25 mL), 5% (w/v) NaOH (2 x 25 mL), brine (25 mL), dried over MgSO₄, and concentrated *in vacuo* to afford amide **106** (3.23 g, 98%) as a white solid. Mp 58-59 °C; (Found: C, 61.24; H, 6.59; N, 4.96. C₁₄H₁₈F₃NO requires C, 61.53; H, 6.64; N, 5.13%); $\lambda_{\max}(\text{MeCN})/\text{nm}$ 200 ($\epsilon/\text{dm}^3 \text{ mol}^{-1} \text{ cm}^{-1}$ 22300) and 252 (7150); $\nu_{\max}(\text{film})/\text{cm}^{-1}$ 2970, 1621s, 1373, 1311s, 1162 and 1123; δ_{H} (500 MHz; CDCl₃) 1.17 (6H, br s, (CH₃)₂CH), 1.53 (6H, br s, (CH₃)₂CH), 3.57 (1H, br s, (CH₃)₂CH), 3.72(1H, br s, (CH₃)₂CH), 7.47-7.54 (2H, m, ArH), 7.57 (1H, s ArH) and 7.63 (1H, d, *J* 8.5, ArH); δ_{C} (100.6 MHz; CDCl₃) 20.8 ((CH₃)₂CH), 46.3 (br s, (CH₃)₂CH), 51.3 (br s, (CH₃)₂CH), 122.8 (q, ³*J*_{FC} 4, ArC), 123.9 (q, ¹*J*_{FC} 273, CF₃), 125.6 (q, ³*J*_{FC} 4, ArC), 129.1 (ArC), 129.2 (ArC), 131.1 (q, ²*J*_{FC} 33, ArC-CF₃), 139.6 (ArC-CONⁱPr₂), 169.5 (CONⁱPr₂); δ_{F} (376.3 MHz; CDCl₃) -63.2 (s); *m/z* (ES) 274.1413 (100%, [M+H]⁺. [C₁₄H₁₉F₃NO]⁺ requires 274.1413).

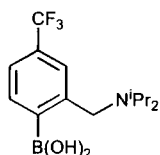
N,N*-Diisopropyl-2-(4,4,5,5-tetramethyl-[1,3,2]dioxaborolan-2-yl)-5-trifluoromethyl-benzamide **107*



To a stirred solution of *N,N*-diisopropyl-3-trifluoromethylbenzamide **106** (1.01 g, 3.70 mmol) in dry THF (20 mL) under argon at -78°C, was added LDA (2.47 mL, 1.8 M, 4.44 mmol) dropwise over 15 min. The mixture was left to stir for 70 min and then triisopropyl borate (0.94 mL, 4.07 mmol) was added rapidly. The mixture was allowed to reach rt overnight (17 h) and then quenched with 20% (w/v) HCl (6 mL), followed by addition of pinacol (0.48 g, 4.07 mmol). The mixture was allowed to stir for 15 min before being extracted into ether (2 x 20 mL, 1 x 10 mL) and the organic extracts washed with sat. aq. NaHCO₃ (3 x 10 mL), and brine (20 mL). The combined organic extracts were dried over MgSO₄ and concentrated *in vacuo*. Column chromatography on silica gel (hexane:EtOAc, 4:1) afforded pinacol boronate **107** (1.40 g, 95%) as a white solid. Mp 130-131 °C; (Found: C, 60.37; H, 7.34; N, 3.38. C₂₀H₂₉BF₃NO₃ requires C, 60.17; H, 7.32; N, 3.51%); $\nu_{\max}(\text{film})/\text{cm}^{-1}$ 2978, 1627s,

1312vs, and 1132vs; δ_{H} (500 MHz; CDCl_3) 1.13 (6H, d, J 6.5, $(\text{CH}_3)_2\text{CH}$), 1.32 (12H, s, 4 x Me), 1.58 (6H, d, J 6.5, $(\text{CH}_3)_2\text{CH}$), 3.53 (1H, m, $(\text{CH}_3)_2\text{CH}$), 3.63 (1H, m, $(\text{CH}_3)_2\text{CH}$), 7.39 (1H, s, ArH), 7.56 (1H, d, J 8.5, ArH) and 7.91 (1H, d, J 7.5, ArH); δ_{C} (125.7 MHz; CDCl_3) 20.3 ($(\text{CH}_3)_2\text{CH}$), 20.5 ($(\text{CH}_3)_2\text{CH}$), 25.0 (pinacol CH_3), 46.1 ($(\text{CH}_3)_2\text{CH}$), 51.2 ($(\text{CH}_3)_2\text{CH}$), 84.4 (pinacol C-O), 121.4 (q, $^3J_{\text{FC}}$ 4, ArC), 123.9 (q, $^1J_{\text{FC}}$ 273, CF_3), 124.1 (q, $^3J_{\text{FC}}$ 4, ArC), 132.5 (q, $^2J_{\text{FC}}$ 33, ArC- CF_3), 136.2 (ArC), 145.6 (ArC- CON^iPr_2) and 169.9 (CON^iPr_2); δ_{B} (160.3 MHz; CDCl_3) 29.8; δ_{F} (470.3 MHz; CDCl_3) -63.5 (s); m/z (ES) 400.2265 (100%, $[\text{M}+\text{H}]^+$. $[\text{C}_{20}\text{H}_{30}\text{BF}_3\text{NO}_3]^+$ requires 400.2265).

N,N*-Diisopropyl-5-trifluoromethylbenzylamine-2-boronic acid **108*



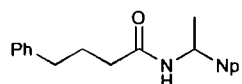
To a stirred solution of pinacol boronate **107** (1.00 g, 2.50 mmol) and NaBH_4 (0.95 g, 25.0 mmol) in dry THF (50 mL) under argon was added TMSCl (6.35 mL, 50.0 mmol) and the mixture stirred at reflux for 21 h. The reaction was quenched by slow addition of 5% (w/v) HCl (7 mL) and the THF was removed *in vacuo*. A further portion of 5% (w/v) HCl (5 mL) was added (aqueous layer to pH 1) and washed with Et_2O (3 x 15 mL). The combined Et_2O extracts were extracted into 5% (w/v) HCl (5 mL) and the combined aqueous phase washed with Et_2O (2 x 10 mL). The combined aqueous phase was neutralised to pH 7 with NaOH (s) then 20% (w/v) NaOH , and extracted into DCM (3 x 15 mL). The combined organic extracts were washed with brine (15 mL), dried over MgSO_4 and concentrated *in vacuo*. Recrystallisation from $\text{MeCN-H}_2\text{O}$ afforded boronic acid **108** (0.45 g, 60%) as a white crystalline solid (crystals suitable for single crystal X-ray analysis – see Appendix). Mp 115-116 °C; (Found: C, 55.22; H, 6.85; N, 4.46. $\text{C}_{14}\text{H}_{21}\text{BF}_3\text{NO}_2$ requires C, 55.47; H, 6.98; N, 4.62%); ν_{max} (film)/ cm^{-1} 3324, 2978, 1328s, 1166s, and 1112vs; δ_{H} (400 MHz; CDCl_3) 1.14 (12H, d, J 6.8, $(\text{CH}_3)_2\text{CH}$), 3.13 (2H, septet, J 6.8, $(\text{CH}_3)_2\text{CH}$), 3.90 (2H, s, ArCH_2), 7.47 (1H, s, ArH), 7.55 (1H, d, J 7.6, ArH), 8.10 (1H, d, J 8.0, ArH) and 10.28 (2H, br s, B(OH)_2); δ_{C} (100.6 MHz; CDCl_3) 19.8 ($(\text{CH}_3)_2\text{CH}$), 47.9 ($(\text{CH}_3)_2\text{CH}$), 51.9 (ArCH_2), 123.8 (q, $^3J_{\text{FC}}$ 4, ArC), 124.2 (q, $^1J_{\text{FC}}$ 272, CF_3), 127.0 (q, $^3J_{\text{FC}}$ 4, ArC), 132.0 (q, $^2J_{\text{FC}}$ 32, ArC- CF_3), 137.3 (ArC) and 143.2 (ArC); δ_{B} (128.4

MHz; CDCl₃) 28.5; δ_F (376.3 MHz; CDCl₃) -63.3 (s); m/z (ES) 304.2 (100%, [M+H]⁺).

General procedure for monitoring direct amide formation over time using the Gilson 215 Synthesis Workstation (kinetic resolution)

The appropriate catalyst (0.1 mmol, 10 mol%) was manually weighed into each reaction vessel, followed by assembly of a micro-soxhlet apparatus loaded with activated 3Å molecular sieves under argon. Solid reagents were added using the ReactArray as standard solutions (0.5 M in the desired solvent). Naphthalene (0.15 mmol, 15 mol %) and amine (1 mmol) were added to the reaction vessels at ambient temperature. The appropriate amount of solvent was then added to each reaction vessel in order to give a final reaction volume of 10 mL. After heating to reflux, carboxylic acid (1 mmol) was added to the stirred solution. Reactions were sampled (50 μ L) at 4 h intervals (48 h reaction time respectively). Samples were quenched with MeCN (950 μ L), diluted once (100 μ L in 900 μ L MeCN), mixed and analysed by HPLC. Naphthalene was used as an internal standard, with response factors calculated automatically by ReactArray DataManager. Samples were filtered through 4 cm of silica in a Pasteur pipette, eluted with EtOAc (3 mL) and subjected to chiral HPLC.

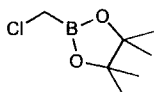
N-(1-Naphthylethyl)-4-phenylbutyramide **113c**



Catalyst **80a** (23.5 mg, 0.1 mmol, 10 mol %) and 4-phenylbutyric acid (164.2 mg, 1 mmol) were weighed into a ReactArray reaction vessel, followed by assembly of a micro-soxhlet apparatus loaded with activated 3Å molecular sieves under argon. Fluorobenzene (10 mL), and 1-(1-naphthyl)ethylamine (161 μ L, 1 mmol) were added and the mixture stirred at reflux for 48 h, allowed to cool and the fluorobenzene removed *in vacuo*. The residue was then redissolved in DCM (25 mL), washed with brine (10 mL), 5% (w/v) HCl (10 mL), brine (10 mL), 5% (w/v) NaOH (10 mL), brine (10 mL), dried over MgSO₄, and concentrated *in vacuo* to afford (1-naphthylethyl)-4-phenylbutyramide **113c** (0.273 g, 86%) as a white solid. Mp 107-108 °C; (Found: C, 82.93; H, 7.31; N, 4.33. C₂₂H₂₃NO requires C, 83.24; H, 7.30; N, 4.41%); ν_{\max} (film)/cm⁻¹ 3297, 2931, 1633s, 1532s and 777vs; δ_H (500 MHz; CDCl₃)

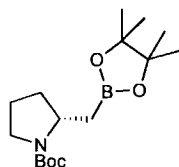
1.67 (3H, d, J 6.5, CH₃), 1.93-2.01 (2H, m, CH₂), 2.09-2.20 (2H, m, CH₂CO), 2.56-2.67 (2H, m, ArCH₂), 5.62 (1H, br d, J 8.5, CONH), 5.96 (1H, quintet, J 7.0, NCHCH₃), 7.10 (2H, d, J 7.5, ArH), 7.16 (1H, t, J 7.5, ArH), 7.23 (2H, t, J 7.5, ArH), 7.45 (1H, t, J 7.5, ArH), 7.50 (2H, t, J 7.0, ArH), 7.54 (1H, t, J 7.5, ArH), 7.81 (1H, d, J 8.0, ArH), 7.87 (1H, d, J 8.5, ArH) and 8.11 (1H, d, J 8.5, ArH); δ_c (125.7 MHz; CDCl₃) 20.7 (CH₂), 27.2 (CH₂), 35.2 (CH₃), 36.1 (CH₂), 44.5 (CHN), 122.7 (ArC), 123.6 (ArC), 125.3 (ArC), 126.1 (ArC), 126.7 (ArC), 128.48 (ArC), 128.56 (ArC), 128.61 (ArC), 128.9 (ArC), 131.3 (ArC), 134.1 (ArC), 138.3 (ArC), 141.6 (ArC) and 171.6 (CONH); m/z (ES) 340.2 (100%, [M+Na]⁺). Chiral HPLC: Daicel Chiralcel OD. Hexane-EtOH, 85:15, 1 mL min⁻¹, 210 nm: t_r (R) = 7.60 min; t_r (S) = 13.9 min.

2-Chloromethyl-4,4,5,5-tetramethyl-[1,3,2]dioxaborolane¹⁵⁰ **264**



To a stirred solution of bromochloromethane (2.14 mL, 33 mmol) and triisopropyl borate (6.92 mL, 30 mmol), in dry THF (30 mL) under argon at -78 °C was added *n*-BuLi (14.4 mL, 2.5 M, 36 mmol) dropwise. The mixture was allowed to stir at -78 °C for 1 h, warmed to rt overnight (18 h) and then quenched with 20% (w/v) HCl (6 mL). The mixture was extracted into ether (3 x 10 mL) and the organic extracts washed with brine (10 mL). The extracts were dried over MgSO₄ and concentrated *in vacuo*. The obtained white solid was recrystallised from hexane-Et₂O, redissolved in Et₂O (10 mL) followed by addition of pinacol (2.72 g, 23 mmol) and the mixture stirred for 10 mins. After drying (MgSO₄) and solvent removal, boronate **264** (3.81 g, 72%) was obtained as a pale yellow oil.

(S)-2-(4,4,5,5-Tetramethyl-[1,3,2]dioxaborolan-2-ylmethyl)pyrrolidine-1-carboxylic acid *tert*-butyl ester **266**



Via (-)-sparteine-mediated lithiation:

To a stirred solution of (-)-sparteine (1.79 mL, 7.8 mmol) in dry Et₂O (30 mL) under argon at -78 °C, was added *s*-BuLi (5.6 mL, 1.4 M, 7.8 mmol) dropwise and the

solution stirred for 10 min. To this was added *N*-Boc-pyrrolidine (1.05 mL, 6 mmol) in Et₂O (5 mL) dropwise and reaction mixture stirred at -78°C for 4.5 h. 2-Chloromethyl-4,4,5,5-tetramethyl-[1,3,2]dioxaborolane **264** (1.27 g, 7.2 mmol) was added dropwise followed by ZnCl₂ (11.4 mL, 1.0 M in Et₂O, 11.4 mmol), the mixture warmed to room temperature and stirred overnight (16 h). The reaction was quenched with 5 % (w/v) HCl (20 mL) and filtered through Celite. The phases were separated and the aqueous extracted into Et₂O (2 x 10 mL). The combined organic extracts were washed with brine (15 mL), dried over MgSO₄ and concentrated *in vacuo*. Silica gel chromatography (pet ether:EtOAc, 9:1) afforded boronate **266** (1.28 g, 69 %) as a colourless oil. $[\alpha]_{\text{D}}^{22} +20.0$ (*c* 1.00 in CH₂Cl₂); ν_{max} (film)/cm⁻¹ 2976, 1694s, 1397 and 1144; δ_{H} (400 MHz; CDCl₃) 0.80-1.00 (2H, br m, CH₂Bpin), 1.20 (6H, s, pinacol CH₃), 1.21 (6H, s, pinacol CH₃), 1.43 (9H, s, (CH₃)₃C), 1.50-1.60 (1H, br m), 1.65-1.75 (1H, m), 1.77-1.88 (1H, m), 1.96-2.04 (1H, m), 3.20-3.40 (2H, br m, CH₂N) and 3.92 (1H, br s, CHN); δ_{C} (125.7 MHz; CDCl₃) 18.3 (CH₂Bpin), 23.5 (CH₂), 24.7 (pinacol CH₃), 28.6 ((CH₃)₃C), 33.2(CH₂), 46.2 (CH₂N), 54.2 (CHN), 78.8 ((CH₃)₃C), 83.1 (pinacol C-O) and 154.5 (C=O); δ_{B} (128.4 MHz; CDCl₃) 32.7; *m/z* (ES) 334.2160 (100%, [M+Na]⁺. [C₁₆H₃₀BNO₄Na]⁺ requires 334.2166); chiral GC: CP-Chiralsil-Dex-CB (25 m x 0.25 mm, 0.25 μm), 128°C, FID: *t_r* (*S*) = 124.4 min; *t_r* (*R*) = 126.9 min; 94 % e.e.

By homology of (S)-2-(4,4,5,5-tetramethyl-[1,3,2]dioxaborolan-2-yl)pyrrolidine-1-carboxylic acid tert-butyl ester 270:

To a stirred solution of bromochloromethane (0.12 mL, 1.90 mmol) and (*S*)-2-(4,4,5,5-tetramethyl-[1,3,2]dioxaborolan-2-yl)pyrrolidine-1-carboxylic acid *tert*-butyl ester **270** (0.47 g, 1.58 mmol) in dry THF (20 mL) under argon at -78 °C was added *n*-BuLi (0.88 mL, 2.5 M, 2.21 mmol) dropwise. The mixture was stirred for 1 h at -78 °C, ZnCl₂ (0.95 mL, 1.0 M in Et₂O, 0.95 mmol) was added, the mixture warmed to room temperature and stirred overnight (16 h). The reaction was quenched with 5 % (w/v) HCl (10 mL) and extracted into Et₂O (3 x 10 mL). The combined organic extracts were washed with brine (15 mL), dried over MgSO₄ and concentrated *in vacuo*. Silica gel chromatography (pet ether:EtOAc, 9:1) afforded boronate **266** (0.13 g, 26 %) as a colourless oil.

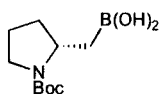
Preparation of racemate for GC method development:

To a stirred solution of *N*-Boc-pyrrolidine (0.35 mL, 2 mmol) and TMEDA in dry Et₂O (15 mL) under argon at -78 °C, *s*-BuLi (1.9 mL, 1.4 M, 2.6 mmol) was added dropwise and the reaction mixture stirred at -78 °C for 4 h. 2-Chloromethyl-4,4,5,5-tetramethyl-[1,3,2]dioxaborolane **264** (0.42 g, 2.4 mmol) was added dropwise followed by ZnCl₂ (3.8 mL, 1.0 M in Et₂O, 3.8 mmol), the mixture warmed to room temperature and stirred overnight (18 h). The reaction was quenched with 5 % (w/v) HCl (10 mL) and filtered through Celite. The phases were separated and the aqueous extracted into Et₂O (2 x 10 mL). The combined organic extracts were washed with brine (10 mL), dried over MgSO₄ and concentrated *in vacuo*. Silica gel chromatography (pet ether:EtOAc, 9:1) afforded boronate **266** (0.44 g, 71 %) as a colourless oil.

Confirmation of the absolute stereochemistry of (S)-266:

(*S*)-**266** (0.52 g, 1.67 mmol) was dissolved in THF (5 mL), cooled to 0°C with an ice bath and treated with NaOH (1.8 mL, 3 N solution). Hydrogen peroxide (500 µL, 30% w/v solution) was then added and the mixture heated at reflux for 6.5 h. The solution was then cooled, diluted with brine and extracted with Et₂O (6 × 10 mL). The combined organic phase was then dried over MgSO₄ and concentrated *in vacuo*. Successive silica gel chromatography purifications (DCM:MeOH, 10:1, followed by pet ether:EtOAc, 1:1) afforded (*R*)-*N*-Boc-(2-hydroxymethyl)-pyrrolidine (0.22 g, 66%) as a white solid. [α]_D²² +50.8 (*c* 1.17 in CHCl₃). The other analytical and spectroscopic properties were identical to those reported in the literature.^{138c}

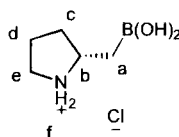
(S)-2-Methylpyrrolidine-1-carboxylic acid *tert*-butyl ester boronic acid 267



To a stirred solution of (*S*)-2-(4,4,5,5-tetramethyl-[1,3,2]dioxaborolan-2-ylmethyl)pyrrolidine-1-carboxylic acid *tert*-butyl ester **266** (1.16 g, 3.73 mmol) in Et₂O (10 mL) was added diethanolamine (4.1 mL, 1.0 M in *isopropanol*, 4.1 mmol). The solvent was removed *in vacuo* and pinacol removed by distillation at reduced pressure (4 mbar). After cooling, the resulting glassy solid was stirred in THF (7 mL) and 5 % (w/v) HCl (7 mL) for 50 min. Another portion of 5 % (w/v) HCl (3 mL) was

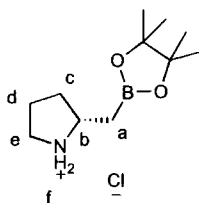
added and the mixture extracted into Et₂O (3 x 10 mL). The combined organic extracts were washed with brine (10 mL), dried over MgSO₄ and concentrated *in vacuo* to afford boronic acid **267** (0.48 g, 56 %) as a white solid. Slow crystallisation from THF afforded crystals suitable for X-ray analysis (see Appendix). Mp 99-100 °C; $[\alpha]_D^{22}$ -60.0 (*c* 1.00 in CH₂Cl₂); (Found: C, 53.02; H, 8.76; N, 5.67. C₁₀H₂₀BNO₄ requires C, 52.43; H, 8.80; N, 6.11%); ν_{\max} (film)/cm⁻¹ 3386, 2974, 1691s, 1400 and 1167; δ_H (400 MHz; CDCl₃) 1.22 (2H, m CH₂B), 1.45 (9H, s, (CH₃)₃C), 1.55-1.65 (1H, br m), 1.68-2.08 (3H, br m), 3.31 (2H, m, CH₂N), 4.11 (1H, br m, CHN) and 6.81 (2H, br s, B(OH)₂); δ_C (125.7 MHz; CDCl₃) 23.3 (CH₂), 28.7 ((CH₃)₃C), 34.6 (CH₂), 46.4 (CH₂N), 54.1 (CHN), 80.6 ((CH₃)₃C) and 157.1 (C=O); δ_B (128.4 MHz; CDCl₃) 32.4; *m/z* (ES) 656.4 (100%, [boroxine+Na]⁺).

(*S*)-(Pyrrolidinium-2-yl)methylboronic acid chloride **268a**



(*S*)-2-(4,4,5,5-Tetramethyl-[1,3,2]dioxaborolan-2-ylmethyl)pyrrolidine-1-carboxylic acid *tert*-butyl ester **266** (1.15 g, 3.70 mmol) was stirred at reflux with 20 % (w/v) HCl (12 mL) for 2 h. The mixture was cooled to room temperature, washed Et₂O (3 x 10 mL) and concentrated *in vacuo*. The residue was redissolved in water (1 mL), toluene (5 mL) was added and the mixture concentrated *in vacuo*. Azeotroping with toluene was repeated a further three times to afford (*S*)-(pyrrolidinium-2-yl)methylboronic acid chloride **268a** (0.60 g, 98 %) as a pale brown oil. $[\alpha]_D^{22}$ +20.0 (*c* 1.00 in H₂O); ν_{\max} (film)/cm⁻¹ 3299, 2975, 1597, 1385vs, 1215 and 1021; δ_H (500 MHz; D₂O) 1.18-1.37 (2H, m, H_a), 1.55-1.65 (1H, m, H_c), 1.93-2.00 (1H, m, H_d), 2.01-2.09 (1H, m, H_d), 2.18-2.26 (1H, m, H_c), 3.22-3.32 (2H, m, H_e) and 3.66-3.73 (1H, m, H_b); δ_C (125.7 MHz; D₂O) 18.2 (br s, CH₂B), 23.2 (CH₂), 31.6 (CH₂), 44.8 (CH₂N) and 58.3 (CHN); δ_B (128.4 MHz; CDCl₃) 31.1; *m/z* (ES) 130.1033 (80%, M⁺. [C₅H₁₃BNO₂]⁺ requires 130.1034).

(S)-2-(4,4,5,5-Tetramethyl-[1,3,2]dioxaborolan-2-ylmethyl)pyrrolidinium chloride 271



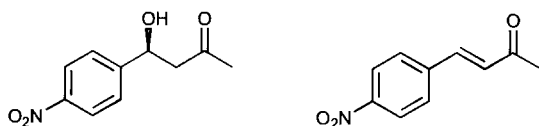
A mixture of (*S*)-(pyrrolidinium-2-yl)methylboronic acid chloride **268a** (0.13 g, 0.79 mmol) and pinacol (92.9 mg, 0.79 mmol) in CHCl₃ (30 mL), was stirred vigorously at rt for 3 h and then concentrated *in vacuo*. Recrystallisation from acetone afforded (*S*)-2-(4,4,5,5-tetramethyl-[1,3,2]dioxaborolan-2-ylmethyl)pyrrolidinium chloride **271** (0.09 g, 46 %) as a white crystalline solid, with crystals suitable for X-ray analysis (see Appendix). Mp 202-203 °C; [α]_D²² +20.0 (*c* 1.00 in CH₂Cl₂); (Found: C, 53.24; H, 9.28; N, 5.43. C₁₁H₂₂BNO₂ requires C, 53.37; H, 9.36; N, 5.66%); ν_{\max} (film)/cm⁻¹ 3392, 2979, 1636, 1380s, and 1145; δ_{H} (400 MHz; CDCl₃) 1.21 (12H, s, pinacol CH₃), 1.35-1.43 (1H, m, H_a), 1.56-1.64 (2H, m, H_a and H_c), 1.89-2.12 (2H, m, H_d), 2.20-2.30 (1H, m, H_c), 3.22-3.44 (2H, m, H_e) and 3.65-3.77 (1H, m, H_b); δ_{C} (100.6 MHz; CDCl₃) 23.5 (CH₂), 24.9 (pinacol CH₃), 25.0 (pinacol CH₃), 31.8 (CH₂), 44.2 (CH₂N), 57.8 (CHN) and 83.9 (pinacol C-O); δ_{B} (128.4 MHz; CDCl₃) 32.1; *m/z* (ES) 212.2 (100%, [M+H]⁺).

Titration of (*S*)-268a

Titration experiments were carried out using a Griffin Model 50 pH meter (PHM-110-134N). (*S*)-**268a** (60 mg, 0.36 mmol) was dissolved in water (20 mL), 5% (w/v) HCl was added till the solution was pH 1.37 and the solution titrated using a 0.039 M aqueous sodium hydroxide solution.

¹H and ¹¹B NMR studies were performed using solutions of (*S*)-**268a** (22.9 mg, 0.138 mmol) in D₂O (4 mL). The pH was adjusted using a 0.8% (w/v) solution of NaOD in D₂O.

(S)-4-Hydroxy-4-(4-nitrophenyl)butan-2-one⁹⁸ **278** and **(E)-4-(4-nitrophenyl)but-3-en-2-one**¹⁵¹ **279**



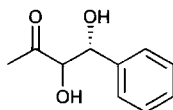
(*S*)-**268a** (0.2 mmol, 20 mol%), 4-nitrobenzaldehyde (151 mg, 1 mmol), potassium *tert*-butoxide (22.4 mg, 0.2 mmol) and acetone (10 mL) were stirred at room temperature for 24 h. The reaction was quenched with sat. aq. NH₄Cl (10 mL) and extracted into EtOAc (2 x 10 mL). The combined organic extracts were dried over MgSO₄ and concentrated *in vacuo*. Silica gel chromatography (pet ether:EtOAc, 7:3) afforded **278** (0.13 g, 62%) as a yellow oil and **279** (0.02 g, 11%) as a yellow solid. Chiral HPLC (**278**): Daicel Chiralcel OJ. Hexane-IPA, 90:10, 1 mL min⁻¹, 254 nm: *t_r* (*R*) = 38.6 min; *t_r* (*S*) = 44.0 min; 8% e.e; δ_H (400 MHz; CDCl₃) 2.23 (3H, s, CH₃), 2.82-2.88 (2H, m, CH₂), 3.61 (1H, s, OH), 5.26 (1H, m, CHOH), 7.55 (2H, d, *J* 8.6, ArH), 8.22 (2H, d, *J* 8.6, ArH).

Procedure for monitoring formation of (S)-4-hydroxy-4-(4-nitrophenyl)butan-2-one 278 over time using the Gilson 215 Synthesis Workstation

Catalyst (*S*)-**268a** (33.1 mg, 0.2 mmol, 20 mol%) was manually weighed into each reaction vessel. The appropriate solvent (7546 μL), toluene (426 μL, 4 mmol), Et₃N (28 μL, 0.2 mmol) and 4-nitrobenzaldehyde (2000 μL, 0.5M in acetone, 1 mmol) were added using the ReactArray. Reactions were sampled (40 μL) at 1 h intervals (6 h reaction time). Samples were quenched with MeCN:H₂O (1:1) (1560 μL), diluted once (40 μL in 1560 μL MeCN:H₂O (1:1)), mixed and analysed by HPLC (gradient MeCN (0.05% TFA) / water (0.05% TFA) 0:100 to 100:0 over 15 minutes; 1 mL min⁻¹; *t_r* = 11.15 min). Toluene was used as an internal standard, with response factors calculated automatically by ReactArray DataManager. Samples were filtered through 4 cm of silica in a Pasteur pipette, eluted with EtOAc (3 mL) and subjected to chiral HPLC: Daicel Chiralcel OJ. Hexane-IPA, 90:10, 1 mL min⁻¹, 254 nm: *t_r* (*R*) = 38.6 min; *t_r* (*S*) = 44.0 min.

General procedure for formation of (4*R*)-3,4-dihydroxy-4-phenylbutan-2-one¹⁵²

284



(*S*)-**268a** (0.1 mmol, 20 mol%), the appropriate solvent (2 mL) benzaldehyde (50.5 μ L, 0.5 mmol), Et₃N (14 μ L, 0.1 mmol) and hydroxyacetone (68.6 μ L, 1 mmol) were stirred at room temperature for 48 h. The reaction was quenched with sat. aq. NH₄Cl (10 mL) and extracted into EtOAc (2 x 7 mL). The combined organic extracts were dried over MgSO₄ and concentrated *in vacuo*. Chiral HPLC: Daicel Chiralcel OJ. Hexane-EtOH-MeOH 90:6.6:3.3, 1.2 mL min⁻¹, 210 nm: t_r (*R*) *anti* = 16.4 min; t_r (*S*) *anti* = 18.2 min; t_r (*R*) *syn* = 20.1 min; t_r (*S*) *syn* = 23.8 min.

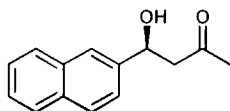
Syn: δ_{H} (400 MHz; CDCl₃) 2.02 (3H, s, CH₃), 4.14 (1H, d, *J* 2.5, CH₃COCHOH), 4.81 (1H, d, *J* 2.5, PhCHOH), 7.17-7.26 (5H, m, ArH).

Anti: δ_{H} (400 MHz; CDCl₃) 1.75 (3H, s, CH₃), 4.26 (1H, d, *J* 4.5, CH₃COCHOH), 4.79 (1H, d, *J* 4.5, PhCHOH), 7.17-7.26 (5H, m, ArH).

General procedure for aldol reactions

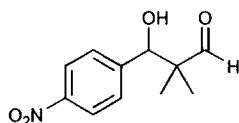
(*S*)-**268a** (0.1 mmol, 20 mol%), the appropriate aldehyde acceptor (0.5 mmol), Et₃N (14 μ L, 0.1 mmol) and donor (2.5 mmol) were stirred at room temperature for 48 h. The reaction was quenched with sat. aq. NH₄Cl (10 mL) and extracted into EtOAc (2 x 7 mL). The combined organic extracts were dried over MgSO₄ and concentrated *in vacuo*.

(*S*)-4-Hydroxy-4-naphthalen-2-ylbutan-2-one:^{68a}



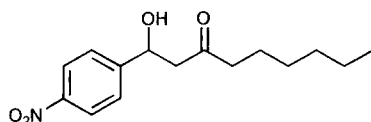
Conversion: 7%, as a yellow oil; chiral HPLC: Daicel Chiralpak AD. Hexane-IPA, 97:3, 1 mL min⁻¹, 254 nm: t_r (*S*) = 10.4 min; t_r (*R*) = 15.3 min; δ_{H} (400 MHz; CDCl₃) 2.21 (3H, s, CH₃), 2.95 (2H, m, CH₂), 3.44 (1H, br s, CHOH), 5.34 (1H, m, CHOH), 7.42-7.47 (3H, m, ArH), 7.78-7.84 (4H, m, ArH). Conversion to enone:¹⁵³ 17%.

3-Hydroxy-2,2-dimethyl-3-(4-nitrophenyl)propionaldehyde:¹²⁵



Conversion: 6%, as an orange solid; δ_{H} (400 MHz; CDCl_3) 0.99 (3H, s, CH_3), 1.08 (3H, s, CH_3), 2.87 (1H, s, CHOH), 5.05 (1H, s, CHOH), 7.50 (2H, d, J 8.0, ArH), 8.20 (2H, d, J 8.0, ArH), 9.63 (1H, s, CHO).

1-Hydroxy-1-(4-nitrophenyl)nonan-3-one:¹²⁵



Conversion: 5%, as an orange solid; δ_{H} (400 MHz; CDCl_3) 0.81-0.89 (3H, m, CH_3), 1.14-1.42 (6H, m, 3 x CH_2), 1.50-1.55 (2H, m, CH_2), 2.84-2.88 (2H, m, $\text{CH(OH)CH}_2\text{CO}$), 3.58 (1H, br s, CHOH), 5.29 (1H, s, CHOH), 7.52 (2H, d, J 8.6, ArH), 8.20 (2H, d, J 8.6, ArH).

6. References

-
- ¹ a) C. A. G. N. Montalbetti, V. Falque, *Tetrahedron*, 2005, **61**, 10827-10852; b) Y. R. Mahajan, S. M. Weinreb, in *Science of Synthesis*, 2005, Vol. 21, Thieme, Stuttgart, New York, p 43-76.
- ² G. H. Coleman, A. M. Alvarado, *Org. Synth.*, 1923, **3**, 3-5.
- ³ H. T. Clarke, L. D. Behr, *Org. Synth.*, 1936, **16**, 75-76.
- ⁴ C. N. Webb, *Org. Synth.*, 1927, **7**, 6-7.
- ⁵ J. A. Mitchell, E. E. Reid, *J. Am. Chem. Soc.*, 1931, **53**, 1879-1883.
- ⁶ B. S. Jursic, Z. Zdravkovski, *Synth. Commun.*, 1993, **23**, 2761-2770.
- ⁷ L. Perreux, A. Loupy, F. Volatron, *Tetrahedron*, 2002, **58**, 2155-2162.
- ⁸ L. F. Fieser, J. E. Jones, *Org. Synth.*, 1940, **20**, 66-67.
- ⁹ M. L. Fein, E. M. Filachione, *J. Am. Chem. Soc.*, 1953, **75**, 2097-2099.
- ¹⁰ J. Cossy, C. Pale-Grosdemange, *Tetrahedron Lett.*, 1989, **30**, 2771-2774.
- ¹¹ (a) K. Ishihara, S. Ohara, H. Yamamoto, *J. Org. Chem.*, 1996, **61**, 4196-4197; (b) K. Ishihara, S. Ohara, H. Yamamoto, *Org. Synth.*, 2004, **79**, 176-185.
- ¹² K. Ishihara, S. Kondo, H. Yamamoto, *Synlett*, 2001, 1371-1374.
- ¹³ K. Ishihara, S. Ohara, H. Yamamoto, *Macromolecules*, 2000, **33**, 3511-3513.
- ¹⁴ H. C. Brown, T. P. Stocky, *J. Am. Chem. Soc.*, 1977, **99**, 8218-8226.
- ¹⁵ T. Maki, K. Ishihara, H. Yamamoto, *Synlett*, 2004, 1355-1358.
- ¹⁶ P. Tang, *Org. Synth.*, 2005, **81**, 262-272.
- ¹⁷ T. Maki, K. Ishihara, H. Yamamoto, *Org. Lett.*, 2006, **8**, 1431-1434. For the stoichiometric use of catecholborane, see: D. B. Collum, S. Chen, B. J. Ganem, *J. Org. Chem.*, 1978, **43**, 4393-4394.
- ¹⁸ T. Maki, K. Ishihara, H. Yamamoto, *Tetrahedron*, 2007, **63**, 8645-8657.
- ¹⁹ R. Latta, G. Springsteen, B. Wang, *Synthesis*, 2001, 1611-1613.
- ²⁰ T. Maki, K. Ishihara, H. Yamamoto, *Org. Lett.*, 2005, **7**, 5043-5046.
- ²¹ M. Mader, P. Helquist, *Tetrahedron Lett.*, 1988, **29**, 3049-3052.
- ²² R. Nomura, T. Nakano, Y. Yamada, H. Matsuda, *J. Org. Chem.*, 1991, **56**, 4076-4078.
- ²³ K. Ishihara, Y. Kuroki, N. Hanaki, S. Ohara, H. Yamamoto, *J. Am. Chem. Soc.*, 1996, **118**, 1569-1570.

-
- ²⁴ M. Kunishima, H. Imada, K. Kikuchi, K. Hioki, J. Nishida, S. Tani, *Angew. Chem. Int. Ed.*, 2005, **44**, 7254-7257.
- ²⁵ J. Otera, *Angew. Chem. Int. Ed.*, 2001, **40**, 2044-2045.
- ²⁶ W. W. Lowrance Jr., *Tetrahedron Lett.*, 1971, 3453-3454.
- ²⁷ T. A. Houston, B. L. Wilkinson, J. T. Blanchfield, *Org. Lett.*, 2004, **6**, 679-681.
- ²⁸ T. Maki, K. Ishihara, H. Yamamoto, *Org. Lett.*, 2005, **7**, 5047-5050.
- ²⁹ R. N. Ram, *Tetrahedron*, 1997, **53**, 7335-7340.
- ³⁰ G.-S. Zhang, *Synth. Commun.*, 1998, **28**, 1159-1162.
- ³¹ K. V. N. S. Srinivas, B. Das, *J. Org. Chem.*, 2003, **68**, 1165-1167.
- ³² T. Kawabata, T. Mizugaki, K. Ebitani, K. Kaneda, *Tetrahedron Lett.*, 2003, **44**, 9205-9208.
- ³³ C.-T. Chen, Y. S. Munot, *J. Org. Chem.*, 2005, **70**, 8625-8627.
- ³⁴ (a) K. Ishihara, S. Ohara, H. Yamamoto, *Science*, 2000, **290**, 1140-1142; (b) K. Ishihara, M. Nakayama, S. Ohara, H. Yamamoto, *Tetrahedron*, 2002, **58**, 8179-8188.
- ³⁵ M. Nakayama, A. Sato, K. Ishihara, H. Yamamoto, *Adv. Synth. Catal.*, 2004, **346**, 1275-1279.
- ³⁶ X. Hao, A. Yoshida, J. Nishikido, *Tetrahedron Lett.*, 2004, **45**, 781-785.
- ³⁷ X. Hao, A. Yoshida, J. Nishikido, *Green Chem.*, 2004, **6**, 566-569.
- ³⁸ A. Sato, Y. Nakamura, T. Maki, K. Ishihara, H. Yamamoto, *Adv. Synth. Catal.*, 2005, **347**, 1337-1340.
- ³⁹ Y. Nakamura, T. Maki, X. Wang, K. Ishihara, H. Yamamoto, *Adv. Synth. Catal.*, 2006, **348**, 1505-1510.
- ⁴⁰ G. Bartoli, J. Boeglin, M. Bosco, M. Locatelli, M. Massaccesi, P. Melchiorre, L. Sambri, *Adv. Synth. Catal.*, 2005, **347**, 33-38.
- ⁴¹ J. Otera, *Acc. Chem. Res.*, 2004, **37**, 288-296.
- ⁴² A. Loupy, A. Petit, M. Ramdani, C. Yvanaeff, *Can. J. Chem.*, 1993, **71**, 90-95.
- ⁴³ K. Ramalinga, P. Vijayalakshmi, T. N. B. Kaimal, *Tetrahedron Lett.*, 2002, **43**, 879-882.
- ⁴⁴ Y. Masaki, N. Tanaka, T. Miura, *Chem. Lett.*, 1997, 55-56.
- ⁴⁵ K. Wakasugi, T. Misaki, K. Yamada, Y. Tanabe, *Tetrahedron Lett.*, 2000, **41**, 5249-5252.
- ⁴⁶ B. Gacem, G. Jenner, *Tetrahedron Lett.*, 2003, **44**, 1391-1393.
- ⁴⁷ X.-G. Liu, W.-X. Hu, *J. Chem. Res.*, 2004, **8**, 564-565.

-
- ⁴⁸ (a) K. Ishihara, S. Nakagawa, A. Sakakura, *J. Am. Chem. Soc.*, 2005, **127**, 4168-4169; (b) A. Sakakura, S. Nakagawa, K. Ishihara, *Tetrahedron*, 2006, **62**, 422-433.
- ⁴⁹ K. Manabe, Xiang-Min Sun, S. Kobayashi, *J. Am. Chem. Soc.*, 2001, **123**, 10101-10102.
- ⁵⁰ K. Manabe, S. Iimura, Xiang-Min Sun, S. Kobayashi, *J. Am. Chem. Soc.*, 2002, **124**, 11971-11978.
- ⁵¹ S. W. Coghlan, R. L. Giles, J. A. K. Howard, M. R. Probert, G. E. Smith, A. Whiting, *J. Organomet. Chem.*, 2005, **690**, 4784-4793.
- ⁵² K. Arnold, B. Davies, R. L. Giles, C. Grosjean, G. E. Smith, A. Whiting, *Adv. Synth. Catal.*, 2006, **348**, 813-820.
- ⁵³ Micromath[®] Scientist[®] for Windows[®], Version 2.02.
- ⁵⁴ Microsoft Excel, 2003.
- ⁵⁵ For example: V. K. Aggarwal, A. C. Staubitz, M. Owen, *Org. Process Res. Dev.*, 2006, **10**, 64-69.
- ⁵⁶ The penalty for reducing the number of experiments is one factor interactions are aliased with three factor interactions, and two factor interactions are aliased with other two factor interactions.
- ⁵⁷ G. Köbrich, P. Buck, *Chem. Ber.*, 1970, **103**, 1412-1419.
- ⁵⁸ (a) M. Schlosser, F. Mongin, J. Porwisiak, W. Dmowski, H. H. Büker, N. M. M. Nibbering, *Chem. Eur. J.*, 1998, **4**, 1281-1286; (b) M. Schlosser, M. Marull, *Eur. J. Org. Chem.*, 2003, 1569-1575.
- ⁵⁹ D. Héroult, K. Aelvoet, A. J. Blatch, A. Al-Majid, C. A. Smethurst, A. Whiting, *J. Org. Chem.*, 2007, **72**, 71-75.
- ⁶⁰ A. S. Batsanov, D. Héroult, J. A. K. Howard, L. G. F. Patrick, M. R. Probert, A. Whiting, *Organometallics*, 2007, **26**, 2414-2419.
- ⁶¹ A. J. Blatch, O. V. Chetina, J. A. K. Howard, L. G. F. Patrick, C. A. Smethurst, A. Whiting, *Org. Biomol. Chem.*, 2006, **17**, 3297-3302.
- ⁶² (a) P. I. Dalko, L. Moissan, *Angew. Chem. Int. Ed.*, 2004, **43**, 5138-5187; (b) P. I. Dalko, L. Moissan, *Angew. Chem. Int. Ed.*, 2001, **40**, 3726-3748; (c) J. Seayad, B. List, *Org. Biomol. Chem.*, 2005, **3**, 719-724.
- ⁶³ R. M. de Figueiredo, M. Christmann, *Eur. J. Org. Chem.*, 2007, 2575-2600.

-
- ⁶⁴ (a) Z. G. Hajos, D. R. Parrish, *J. Org. Chem.*, 1974, **39**, 1615-1621; (b) U. Eder, G. Sauer, R. Wiechert, *Angew. Chem. Int. Ed. Engl.*, 1971, **10**, 496-497.
- ⁶⁵ B. List, R. A. Lerner, C. F. Barbas III, *J. Am. Chem. Soc.*, 2000, **122**, 2395-2396.
- ⁶⁶ S. Mossé, A. Alexakis, *Org. Lett.*, 2006, **8**, 3577-3580.
- ⁶⁷ W. Notz, B. List, *J. Am. Chem. Soc.*, 2000, **122**, 7386-7387.
- ⁶⁸ (a) K. Sakthivel, W. Notz, T. Bui, C. F. Barbas III, *J. Am. Chem. Soc.*, 2001, **123**, 5260-5267; (b) W. Notz, F. Tanaka, C. F. Barbas III, *Acc. Chem. Res.*, 2003, **37**, 580-591.
- ⁶⁹ (a) M. Benaglia, M. Cinquini, F. Cozzi, A. Puglisi, G. Celentano, *Adv. Synth. Catal.*, 2002, **344**, 533-542; (b) M. Benaglia, G. Celentano, F. Cozzi, *Adv. Synth. Catal.*, 2001, **343**, 171-173.
- ⁷⁰ Q. Pan, B. Zou, Y. Wang, D. Ma, *Org. Lett.*, 2004, **6**, 1009-1012.
- ⁷¹ B. List, P. Pojarliev, C. Castello, *Org. Lett.*, 2001, **3**, 573-575.
- ⁷² A. Bøgevig, N. Kumaragurubaran, K. A. Jørgensen, *Chem. Commun.*, 2002, 620-621.
- ⁷³ R. Thayumanavan, F. Tanaka, C. F. Barbas III, *Org. Lett.*, 2004, **6**, 3541-3544.
- ⁷⁴ A. B. Northrup, D. W. C. MacMillan, *J. Am. Chem. Soc.*, 2002, **124**, 6798-6799.
- ⁷⁵ C. Pidathala, L. Hoang, N. Vignola, B. List, *Angew. Chem. Int. Ed.*, 2003, **42**, 2785-2788.
- ⁷⁶ P. M. Pihko, K. M. Laurikainen, A. Usano, A. I. Nyberg, J. A. Kaavi, *Tetrahedron*, 2006, **62**, 317-328; see also: Y. Hayashi, S. Aratake, T. Itoh, T. Okano, T. Sumiya, M. Shoji, *Chem. Commun.*, 2007, 957-959.
- ⁷⁷ B. List, *Chem. Commun.*, 2006, 819-824; B. List, *Acc. Chem. Res.*, 2004, **37**, 548-557.
- ⁷⁸ C. Marquez, J. O. Metzger, *Chem. Commun.*, 2006, 1539-1541.
- ⁷⁹ (a) C. Allemann, R. Gordillo, F. R. Clemente, P. H.-Y. Cheong, K. N. Houk, *Acc. Chem. Res.*, 2004, **37**, 558-569; (b) S. Bahmanyar, K. N. Houk, *Org. Lett.*, 2003, **5**, 1249-1251; (c) S. Bahmanyar, K. N. Houk, H. J. Martin, B. List, *J. Am. Chem. Soc.*, 2003, **125**, 2475-2479; (c) S. Bahmanyar, K. N. Houk, *J. Am. Chem. Soc.*, 2001, **123**, 12911-12912; (d) S. Bahmanyar, K. N. Houk, *J. Am. Chem. Soc.*, 2001, **123**, 11273-11283.
- ⁸⁰ L. Hoang, S. Bahmanyar, K. N. Houk, B. List, *J. Am. Chem. Soc.*, 2003, **125**, 16-17.

-
- ⁸¹ B. List, L. Hoang, H. J. Martin, *Proc. Natl. Acad. Sci.*, 2004, **101**, 5839-5842.
- ⁸² U. Kazmaier, *Angew. Chem. Int. Ed.*, 2005, **44**, 2186-2188.
- ⁸³ A. B. Northrup, Ian K. Mangion, F. Hettche, D. W. C. MacMillan, *Angew. Chem. Int. Ed.*, 2004, **43**, 2152-2153.
- ⁸⁴ A. B. Northrup, D. W. C. MacMillan, *Science*, 2004, **305**, 1752-1755.
- ⁸⁵ J. Casas, M. Engqvist, I. Ibrahim, B. Kaynak, A. Córdova, *Angew. Chem. Int. Ed.*, 2005, **44**, 1343-1345.
- ⁸⁶ N. S. Chowdari, D. B. Ramachary, A. Córdova, C. F. Barbas III, *Tetrahedron Lett.*, 2002, **43**, 9591-9595.
- ⁸⁷ A. Córdova, W. Notz, C. F. Barbas III, *J. Org. Chem.*, 2002, **67**, 301-303.
- ⁸⁸ D. Enders, C. Grondal, *Angew. Chem. Int. Ed.*, 2005, **44**, 1210-1212; see also: (a) I. Ibrahim, W. Zou, Y. Xu, A. Córdova, *Adv. Synth. Catal.*, 2006, **38**, 211-222; (b) C. Grondal, D. Enders, *Tetrahedron*, 2006, **62**, 329-337; (c) D. Enders, J. Palecek, C. Grondal, *Chem. Commun.*, 2006, 655-657; (d) C. Grondal, D. Enders, *Adv. Synth. Catal.*, 2007, **349**, 694-702.; (e) J. T. Suri, S. Mitsumori, K. Albertshofer, F. Tanaka, C. F. Barbas III, *J. Org. Chem.*, 2006, **71**, 3822-3828.
- ⁸⁹ J. T. Suri, D. B. Ramachary, C. F. Barbas III, *Org. Lett.*, 2005, **7**, 1383-1385.
- ⁹⁰ A. Córdova, W. Zou, I. Ibrahim, E. Reyes, M. Engqvist, W.-W. Liao, *Chem. Commun.*, 2005, 3586-3588.
- ⁹¹ W. Zou, I. Ibrahim, P. Dziedzic, H. Sundén, A. Córdova, *Chem. Commun.*, 2005, 4946-4948.
- ⁹² S. S. V. Ramasastry, H. Zhang, F. Tanaka, C. F. Barbas III, *J. Am. Chem. Soc.*, 2007, **129**, 288-289; see also: X.-Y. Xu, Y.-Z. Wang, L.-Z. Gong, *Org. Lett.*, 2007, **9**, 4247-4249.
- ⁹³ (a) S. S. V. Ramasastry, K. Albertshofer, N. Utsumi, F. Tanaka, C. F. Barbas III, *Angew. Chem. Int. Ed.*, 2007, **46**, 5572-5575; (b) N. Utsumi, M. Imai, F. Tanaka, S. S. V. Ramasastry, C. F. Barbas III, *Org. Lett.*, 2007, **9**, 3445-3448.
- ⁹⁴ J. Kofoed, J. Nielsen, J.-L. Reymond, *Tetrahedron Lett.*, 2003, **13**, 2445-2447.
- ⁹⁵ (a) S. Saito, M. Nakadai, H. Yamamoto, *Synlett*, 2001, 1245-1248; (b) M. Nakadai, S. Saito, H. Yamamoto, *Tetrahedron*, 2002, **58**, 8167-8177; (c) S. Saito, H. Yamamoto, *Acc. Chem. Res.*, 2004, **37**, 570-579.
- ⁹⁶ H. Torii, M. Nakadai, K. Ishihara, S. Saito, H. Yamamoto, *Angew. Chem. Int. Ed.*, 2004, **43**, 1983-1986.

- ⁹⁷ (a) A. Hartikka, P. I. Arvidsson, *Tetrahedron: Asymmetry*, 2004, **15**, 1831-1834; (b) A. Hartikka, P. I. Arvidsson, *Eur. J. Org. Chem.*, 2005, 4287-4295.
- ⁹⁸ A. J. A. Cobb, D. M. Shaw, D. A. Longbottom, J. B. Gold, S. V. Ley, *Org. Biomol. Chem.*, 2005, **3**, 84-96.
- ⁹⁹ X.-J. Wang, Y. Zhao, J.-T. Liu, *Org. Lett.*, 2007, **9**, 1343-1345.
- ¹⁰⁰ Z. Tang, F. Jiang, L.-T. Yu, X. Cui, L.-Z. Gong, A.-Q. Mi, Y.-Z. Jiang, Y.-D. Wu, *J. Am. Chem. Soc.*, 2003, **125**, 5262-5263.
- ¹⁰¹ H.-M. Guo, L.-F. Cun, L.-Z. Gong, A.-Q. Mi, Y.-Z. Jiang, *Chem. Commun.*, 2005, 1450-1452.
- ¹⁰² (a) Z. Tang, Z.-H. Yang, X.-H. Chen, L.-F. Cun, A.-Q. Mi, Y.-Z. Jiang, L.-Z. Gong, *J. Am. Chem. Soc.*, 2005, **127**, 9285-9289; (b) Z. Tang, F. Jiang, X. Cui, L.-Z. Gong, A.-Q. Mi, Y.-Z. Jiang, Y.-D. Wu, *Proc. Natl. Acad. Sci.*, 2004, **101**, 5755-5760.
- ¹⁰³ J.-R. Chen, H.-H. Lu, X.-Y. Li, L. Cheng, J. Wan, W.-J. Xiao, *Org. Lett.*, 2005, **7**, 4543-4545.
- ¹⁰⁴ J.-R. Chen, X.-Y. Li, X.-N. Xing, W.-J. Xiao, *J. Org. Chem.*, 2006, **71**, 8198-8202.
- ¹⁰⁵ C. Cheng, J. Sun, C. Wang, Y. Zhang, S. Wei, F. Jiang, Y. Wu, *Chem. Commun.*, 2006, 215-217; see also: C. Cheng, S. Wei, J. Sun, *Synlett*, 2006, 2419-2422.
- ¹⁰⁶ (a) E. Lacoste, E. Vaique, M. Berlande, I. Pianet, J.-M. Vincent, Y. Landais, *Eur. J. Org. Chem.*, 2007, 167-177; (b) E. Lacoste, Y. Landais, K. Schenk, J.-B. Verlhac, J.-M. Vincent, *Tetrahedron Lett.*, 2004, **45**, 8035-8038.
- ¹⁰⁷ P. Dinér, M. Amedjkouh, *Org. Biomol. Chem.*, 2006, **4**, 2091-2096.
- ¹⁰⁸ Z. Tang, L.-F. Cun, X. Cui, A.-Q. Mi, Y.-Z. Jiang, L.-Z. Gong, *Org. Lett.*, 2006, **8**, 1263-1266.
- ¹⁰⁹ Y. Yoshitomi, K. Makino, Y. Hamada, *Org. Lett.*, 2007, **9**, 2457-2460.
- ¹¹⁰ I. K. Mangion, A. B. Northrup, D. W. C. MacMillan, *Angew. Chem. Int. Ed.*, 2004, **43**, 6722-6724.
- ¹¹¹ T. Kano, J. Takai, O. Tokuda, K. Maruoka, *Angew. Chem. Int. Ed.*, 2005, **44**, 3055-3057.
- ¹¹² T. Kano, Y. Yamaguchi, Y. Tanaka, K. Maruoka, *Angew. Chem. Int. Ed.*, 2007, **46**, 1738-1740.
- ¹¹³ S. Luo, H. Xu, J. Li, L. Zhang, J.-P. Cheng, *J. Am. Chem. Soc.*, 2007, **129**, 3074-3075.

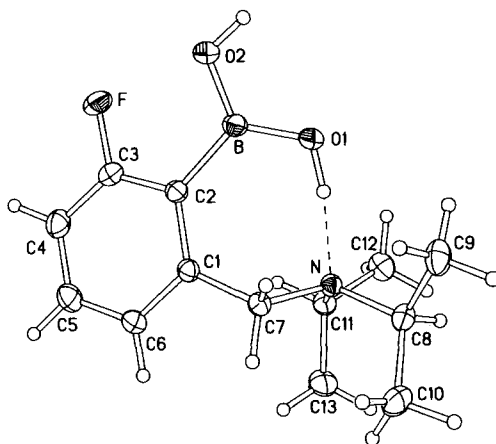
- ¹¹⁴ T. Kanger, K. Kriis, M. Laars, T. Kailas, A.-M. Müürisepp, T. Pehk, M. Lopp, *J. Org. Chem.*, 2007, **72**, 5168-5173.
- ¹¹⁵ N. Mase, F. Tanaka, C. F. Barbas III, *Org. Lett.*, 2003, **5**, 4369-4372.
- ¹¹⁶ N. Mase, F. Tanaka, C. F. Barbas III, *Angew. Chem. Int. Ed.*, 2004, **43**, 2420-2423.
- ¹¹⁷ For discussion of organocatalysis in water, see: (a) A. P. Brogan, T. J. Dickerson, K. D. Janda, *Angew. Chem. Int. Ed.*, 2006, **45**, 8100-8102; (b) Y. Hayashi, *Angew. Chem. Int. Ed.*, 2006, **45**, 8103-8104.
- ¹¹⁸ T. J. Dickerson, K. D. Janda, *J. Am. Chem. Soc.*, 2002, **124**, 3220-3221.
- ¹¹⁹ C. J. Rogers, T. J. Dickerson, A. P. Brogan, K. D. Janda, *J. Org. Chem.*, 2005, **70**, 3705-3708.
- ¹²⁰ A. Córdova, W. Notz, C. F. Barbas III, *Chem. Commun.*, 2002, 3024-3025.
- ¹²¹ Y. Hayashi, T. Sumiya, J. Takahashi, H. Gotoh, T. Urushima, M. Shoji, *Angew. Chem. Int. Ed.*, 2006, **45**, 958-961.
- ¹²² P. Dziejczak, W. Zou, J. Háfren, A. Córdova, *Org. Biomol. Chem.*, 2006, **4**, 38-40; see also: A. Córdova, W. Zou, P. Dziejczak, I. Ibrahim, E. Reyes, Y. Xu, *Chem. Eur. J.*, 2006, **12**, 5383-5397.
- ¹²³ Z. Tang, Z.-H. Yang, L.-F. Cheng, L.-Z. Gong, A.-Q. Mi, Y.-Z. Jiang, *Org. Lett.*, 2004, **6**, 2285-2287.
- ¹²⁴ X.-H. Chen, S.-W. Luo, Z. Tang, L.-F. Cun, A.-Q. Mi, Y.-Z. Jiang, L.-Z. Gong, *Chem. Eur. J.*, 2007, **13**, 689-701.
- ¹²⁵ N. Mase, Y. Nakai, N. Ohara, H. Yoda, K. Takabe, F. Tanaka, C. F. Barbas III, *J. Am. Chem. Soc.*, 2006, **128**, 734-735.
- ¹²⁶ Y. Hayashi, S. Aratake, T. Okano, J. Takahashi, T. Sumiya, M. Shoji, *Angew. Chem. Int. Ed.*, 2006, **45**, 5527-5529.
- ¹²⁷ D. Font, C. Jimeno, M. A. Pericàs, *Org. Lett.*, 2006, **8**, 4653-4655.
- ¹²⁸ Y. Wu, Y. Zhang, M. Yu, G. Zhao, S. Wang, *Org. Lett.*, 2006, **8**, 4417-4420.
- ¹²⁹ Z. Jiang, Z. Liang, X. Wu, Y. Lu, *Chem. Commun.*, 2006, 2801-2803.
- ¹³⁰ X. Wu, Z. Jiang, H.-M. Shen, Y. Lu, *Adv. Synth. Catal.*, 2007, **349**, 812-816.
- ¹³¹ (a) S. Guizetti, M. Benaglia, L. Raimondi, G. Celentano, *Org. Lett.*, 2007, **9**, 1247-1250; (b) S. Guizetti, M. Benaglia, L. Pignataro, A. Puglisi, *Tetrahedron: Asymmetry*, 2006, **17**, 2754-2760; see also: (a) G. Guillena, M. del Carmen Hita, C. Nájera, *Tetrahedron: Asymmetry*, 2006, **17**, 1493-1497; (b) G. Guillena, M. del Carmen Hita,

-
- C. Nájera, *Tetrahedron: Asymmetry*, 2006, **17**, 729-733; (c) G. Guillena, M. del Carmen Hita, C. Nájera, *Tetrahedron: Asymmetry*, 2006, **17**, 1027-1031.
- ¹³² (a) D. Gryko, M. Zimmnicka, R. Lipinski, *J. Org. Chem.*, 2007, **72**, 964-970; (b) D. Gryko, R. Lipinski, *Adv. Synth. Catal.*, 2005, **347**, 1948-1952; (c) D. Gryko, R. Lipinski, *Eur. J. Org. Chem.*, 2006, **17**, 3864-3876.
- ¹³³ D. Gryko, W. J. Saletta, *Org. Biomol. Chem.*, 2007, **5**, 2148-2153.
- ¹³⁴ V. Maya, M. Raj, V. K. Singh, *Org. Lett.*, 2007, **9**, 2593-2595; see also: M. Raj, V. Maya, S. K. Ginotra, V. K. Singh, *Org. Lett.*, 2006, **8**, 4097-4099.
- ¹³⁵ S. Singh Chimni, D. Mahajan, *Tetrahedron: Asymmetry*, 2006, **17**, 2108-2119.
- ¹³⁶ S. Aratake, T. Itoh, T. Okano, T. Usui, M. Shoji, Y. Hayashi, *Chem. Commun.*, 2007, 2524-2526.
- ¹³⁷ (a) D. Matteson, K. M. Sadhu, *J. Am. Chem. Soc.*, 1983, **105**, 2077-2078; (b) H. C. Brown, S. M. Singh, M. V. Rangaishenvi, *J. Org. Chem.*, 1986, **51**, 3150-3155.
- ¹³⁸ (a) D. Braghiroli, R. Avallone, M. Di Bella, *Tetrahedron: Asymmetry*, 1997, **8**, 2209-2213; (b) G. Cardillo, L. Gentilucci, A. Qasem, F. Sgarzi, S. Spampinato, *J. Med. Chem.*, 2002, **45**, 2571-2578; (c) M. Kurokawa, T. Shindo, M. Suzuki, N. Nakajima, K. Ishihara, T. Sugai, *Tetrahedron: Asymmetry*, 2003, **14**, 1323 - 1334.
- ¹³⁹ (a) S. J. Coutts, J. Adams, D. Krolikowski, R. J. Snow, *Tetrahedron Lett.*, 1994, **35**, 5109-5112; (b) A. Belfaitah, M. Isly, B. Carboni, *Tetrahedron Lett.*, 2004, **45**, 1969-1972.
- ¹⁴⁰ M. E. Jung, T. I. Lazarova, *J. Org. Chem.*, 1999, **64**, 2976-2977.
- ¹⁴¹ D. M. Shendage, R. Fröhlich, G. Haufe, *Org. Lett.*, 2004, **6**, 3675-3678.
- ¹⁴² A. S. Batsanov, C. Grosjean, T. Schütz, A. Whiting, *J. Org. Chem.*, 2007, **72**, 6276-6279.
- ¹⁴³ (a) J. C. Norrild, *J. Chem. Soc., Perkin Trans. 2*, 2001, 719-726; (b) J. C. Norrild, I. Søtofte, *J. Chem. Soc., Perkin Trans. 2*, 2001, 727-732.
- ¹⁴⁴ L. Zhu, S. H. Shabbir, M. Gray, V. M. Lynch, S. Sorey, E. V. Anslyn, *J. Am. Chem. Soc.*, 2006, **128**, 1222-1232.
- ¹⁴⁵ B. List, P. Pojarliev, W. T. Biller, H. J. Martin, *J. Am. Chem. Soc.*, 2002, **124**, 827-833.
- ¹⁴⁶ N. Shangguan, S. Katukojvala, R. Greenberg, L. J. Williams, *J. Am. Chem. Soc.*, 2003, **125**, 7754-7755.

-
- ¹⁴⁷ J. D. Moore, R. J. Byrne, P. Vedantham, D. L. Flynn, P. R. Hanson, *Org. Lett.*, **2003**, *5*, 4241-4244.
- ¹⁴⁸ M. Noji, T. Ohno, K. Fuji, N. Futaba, H. Tajima, K. Ishii, *J. Org. Chem.*, 2003, **68**, 9340-9347.
- ¹⁴⁹ M. Aresta, A. Dibenedetto, *Chem. Eur. J.*, 2002, **8**, 685-690.
- ¹⁵⁰ R. J. Mears, A. Whiting, *Tetrahedron*, 1993, **49**, 177-186.
- ¹⁵¹ W. Wang, Y. Mei, H. Li, J. Wang, *Org. Lett.*, 2005, **7**, 601-604.
- ¹⁵² F. Calderón, R. Fernández, F. Sánchez, A. Fernández-Mayoralas, *Adv. Synth. Catal.*, 2005, **347**, 1395-1403.
- ¹⁵³ J.-H. Ho, T.-I. Ho, R. S. H. Lu, *Org. Lett.*, 2001, **3**, 409-411.

Appendix – Crystallographic Data

N,N-Diisopropyl-3-fluorobenzylamine-2-boronic acid 104a



Crystal data

$C_{13}H_{21}BFNO_2$

$M_r = 253.12$

Monoclinic, $P2_1/c$

Hall symbol: ?

$a = 13.748 (2) \text{ \AA}$

$b = 7.701 (1) \text{ \AA}$

$c = 13.781 (2) \text{ \AA}$

$\beta = 110.97 (1)^\circ$

$V = 1362.4 (3) \text{ \AA}^3$

$Z = 4$

$F_{000} = 544$

$D_x = 1.234 \text{ Mg m}^{-3}$

Melting point: 384 K

Mo $K\alpha$ radiation
 $\lambda = 0.71073 \text{ \AA}$

Cell parameters from 9668 reflections

$\theta = 3.0\text{--}29.0^\circ$

$\mu = 0.09 \text{ mm}^{-1}$

$T = 120 (2) \text{ K}$

Cell measurement pressure: ? kPa

Parallelepiped, colourless

$0.4 \times 0.3 \times 0.2 \text{ mm}$

Data collection

Siemens SMART 1K CCD area detector
diffractometer

3616 independent reflections

Radiation source: fine-focus sealed tube

3192 reflections with $I > 2\sigma(I)$

Monochromator: graphite

$R_{\text{int}} = 0.042$

Detector resolution: 8 pixels mm^{-1}

$\theta_{\text{max}} = 29.0^\circ$

$T = 120 (2) \text{ K}$

$\theta_{\text{min}} = 1.6^\circ$

$P = ? \text{ kPa}$

$h = -18 \text{--} 18$

ω scans $k = -10 \ 10$
 Absorption correction: none $l = -18 \ 18$
 15676 measured reflections

Refinement

Refinement on F^2	Secondary atom site location: difference Fourier map
Least-squares matrix: full	Hydrogen site location: inferred from neighbouring sites
$R[F^2 > 2\sigma(F^2)] = 0.037$	All H-atom parameters refined
$wR(F^2) = 0.107$	$w = 1/[\sigma^2(F_o^2) + (0.0591P)^2 + 0.3439P]$ where $P = (F_o^2 + 2F_c^2)/3$
$S = 1.03$	$(\Delta/\sigma)_{\max} < 0.001$
3616 reflections	$\Delta\rho_{\max} = 0.35 \text{ e } \text{\AA}^{-3}$
247 parameters	$\Delta\rho_{\min} = -0.18 \text{ e } \text{\AA}^{-3}$
? constraints	Extinction correction: none
Primary atom site location: structure-invariant direct methods	

Fractional atomic coordinates and isotropic or equivalent isotropic displacement parameters (\AA^2)

	<i>x</i>	<i>y</i>	<i>z</i>	$U_{\text{iso}}^*/U_{\text{eq}}$
F	0.81079 (5)	0.31412 (9)	0.51898 (5)	0.02841 (16)
N	0.69617 (6)	0.63667 (10)	0.81339 (6)	0.01613 (16)
B	0.65058 (8)	0.43779 (14)	0.59035 (8)	0.0189 (2)
O1	0.59332 (5)	0.55515 (9)	0.62006 (5)	0.02116 (16)
H01	0.6296 (14)	0.600 (2)	0.6885 (15)	0.055 (5)*
O2	0.61039 (6)	0.35851 (11)	0.49633 (6)	0.02744 (18)
H02	0.5441 (14)	0.389 (2)	0.4621 (14)	0.049 (5)*
C1	0.80205 (7)	0.39633 (12)	0.77483 (7)	0.01691 (18)
C2	0.76569 (7)	0.38654 (12)	0.66466 (7)	0.01719 (18)
C3	0.83762 (8)	0.32127 (13)	0.62388 (7)	0.0207 (2)
C4	0.93654 (8)	0.26248 (15)	0.68130 (9)	0.0262 (2)
H4	0.9809 (11)	0.2115 (19)	0.6450 (11)	0.031 (4)*
C5	0.96898 (8)	0.27205 (15)	0.78838 (9)	0.0272 (2)
H5	1.0396 (13)	0.231 (2)	0.8319 (12)	0.038 (4)*

C6	0.90243 (8)	0.33999 (13)	0.83429 (8)	0.0217 (2)
H6	0.9252 (11)	0.3459 (18)	0.9094 (11)	0.026 (3)*
C7	0.73473 (7)	0.45559 (12)	0.83498 (7)	0.01801 (19)
H71	0.6734 (10)	0.3810 (17)	0.8193 (10)	0.021 (3)*
H72	0.7760 (10)	0.4395 (17)	0.9098 (10)	0.022 (3)*
C8	0.62479 (8)	0.68238 (13)	0.87061 (8)	0.0209 (2)
H8	0.6262 (10)	0.8092 (18)	0.8751 (10)	0.022 (3)*
C9	0.51343 (8)	0.62887 (15)	0.80617 (10)	0.0279 (2)
H91	0.4891 (12)	0.687 (2)	0.7362 (12)	0.037 (4)*
H92	0.5081 (12)	0.501 (2)	0.7964 (11)	0.035 (4)*
H93	0.4663 (12)	0.665 (2)	0.8430 (12)	0.039 (4)*
C10	0.65453 (10)	0.60695 (17)	0.98019 (9)	0.0314 (3)
H101	0.6463 (12)	0.479 (2)	0.9788 (12)	0.039 (4)*
H102	0.7279 (13)	0.631 (2)	1.0245 (12)	0.038 (4)*
H103	0.6072 (13)	0.661 (2)	1.0138 (12)	0.044 (4)*
C11	0.78144 (7)	0.76416 (13)	0.82605 (8)	0.0193 (2)
H11	0.8234 (10)	0.7123 (17)	0.7869 (10)	0.019 (3)*
C12	0.73779 (9)	0.93673 (14)	0.77469 (9)	0.0257 (2)
H121	0.6848 (12)	0.917 (2)	0.7046 (12)	0.034 (4)*
H122	0.7084 (11)	1.0027 (19)	0.8176 (11)	0.030 (3)*
H123	0.7946 (12)	1.005 (2)	0.7660 (12)	0.037 (4)*
C13	0.85506 (9)	0.79239 (16)	0.93809 (9)	0.0292 (2)
H131	0.8187 (12)	0.849 (2)	0.9821 (12)	0.034 (4)*
H132	0.8861 (12)	0.682 (2)	0.9718 (12)	0.039 (4)*
H133	0.9113 (13)	0.867 (2)	0.9364 (12)	0.041 (4)*

Atomic displacement parameters (\AA^2)

	U^{11}	U^{22}	U^{33}	U^{12}	U^{13}	U^{23}
F	0.0317 (3)	0.0355 (4)	0.0190 (3)	0.0009 (3)	0.0103 (3)	-0.0062 (2)
N	0.0157 (3)	0.0148 (4)	0.0173 (3)	0.0006 (3)	0.0052 (3)	-0.0009 (3)
B	0.0194 (5)	0.0182 (5)	0.0167 (4)	0.0003 (4)	0.0033 (4)	0.0006 (4)
O1	0.0190 (3)	0.0223 (3)	0.0172 (3)	0.0028 (3)	0.0004 (3)	-0.0031 (3)

O2	0.0245 (4)	0.0306 (4)	0.0199 (3)	0.0063 (3)	-0.0010 (3)	-0.0075 (3)
C1	0.0171 (4)	0.0145 (4)	0.0177 (4)	0.0005 (3)	0.0044 (3)	-0.0004 (3)
C2	0.0177 (4)	0.0148 (4)	0.0172 (4)	-0.0007 (3)	0.0040 (3)	-0.0013 (3)
C3	0.0233 (5)	0.0203 (4)	0.0184 (4)	-0.0017 (4)	0.0075 (4)	-0.0032 (3)
C4	0.0212 (5)	0.0289 (5)	0.0299 (5)	0.0021 (4)	0.0110 (4)	-0.0046 (4)
C5	0.0175 (4)	0.0312 (5)	0.0297 (5)	0.0045 (4)	0.0044 (4)	-0.0001 (4)
C6	0.0190 (4)	0.0235 (5)	0.0195 (4)	0.0022 (4)	0.0031 (4)	0.0000 (4)
C7	0.0198 (4)	0.0165 (4)	0.0173 (4)	0.0023 (3)	0.0063 (3)	0.0014 (3)
C8	0.0215 (4)	0.0200 (4)	0.0228 (4)	0.0016 (4)	0.0100 (4)	-0.0026 (4)
C9	0.0199 (5)	0.0273 (5)	0.0387 (6)	-0.0004 (4)	0.0132 (4)	-0.0060 (5)
C10	0.0395 (6)	0.0358 (6)	0.0248 (5)	0.0065 (5)	0.0186 (5)	0.0018 (4)
C11	0.0164 (4)	0.0178 (4)	0.0213 (4)	-0.0017 (3)	0.0038 (3)	-0.0030 (3)
C12	0.0263 (5)	0.0184 (5)	0.0310 (5)	-0.0020 (4)	0.0087 (4)	0.0015 (4)
C13	0.0217 (5)	0.0301 (6)	0.0276 (5)	-0.0017 (4)	-0.0013 (4)	-0.0073 (4)

Geometric parameters (Å, °)

F—C3	1.3591 (11)	C7—H72	0.991 (13)
N—C7	1.4837 (12)	C8—C9	1.5261 (15)
N—C11	1.4907 (12)	C8—C10	1.5307 (15)
N—C8	1.5042 (12)	C8—H8	0.978 (14)
B—O1	1.3547 (13)	C9—H91	1.004 (16)
B—O2	1.3581 (13)	C9—H92	0.996 (16)
B—C2	1.5965 (14)	C9—H93	0.996 (15)
O1—H01	0.960 (19)	C10—H101	0.989 (17)
O2—H02	0.895 (18)	C10—H102	0.991 (16)
C1—C6	1.3981 (13)	C10—H103	1.015 (17)
C1—C2	1.4204 (12)	C11—C12	1.5242 (14)
C1—C7	1.5171 (13)	C11—C13	1.5287 (14)
C2—C3	1.3943 (14)	C11—H11	1.004 (13)
C3—C4	1.3822 (15)	C12—H121	0.991 (15)
C4—C5	1.3824 (16)	C12—H122	0.970 (14)
C4—H4	0.998 (14)	C12—H123	0.983 (16)
C5—C6	1.3875 (15)	C13—H131	1.013 (15)

C5—H5	0.992 (16)	C13—H132	0.993 (16)
C6—H6	0.969 (14)	C13—H133	0.971 (17)
C7—H71	0.978 (13)		
C7—N—C11	112.71 (7)	C9—C8—C10	109.25 (9)
C7—N—C8	111.60 (7)	N—C8—H8	105.4 (8)
C11—N—C8	114.69 (7)	C9—C8—H8	107.4 (8)
O1—B—O2	120.42 (9)	C10—C8—H8	108.9 (8)
O1—B—C2	121.39 (8)	C8—C9—H91	111.0 (9)
O2—B—C2	118.18 (9)	C8—C9—H92	110.9 (9)
B—O1—H01	112.6 (11)	H91—C9—H92	109.1 (12)
B—O2—H02	111.9 (11)	C8—C9—H93	109.1 (9)
C6—C1—C2	120.40 (9)	H91—C9—H93	108.1 (13)
C6—C1—C7	116.13 (8)	H92—C9—H93	108.6 (13)
C2—C1—C7	123.36 (8)	C8—C10—H101	111.7 (9)
C3—C2—C1	114.89 (8)	C8—C10—H102	113.0 (9)
C3—C2—B	120.91 (8)	H101—C10—H102	106.2 (13)
C1—C2—B	124.15 (8)	C8—C10—H103	107.7 (9)
F—C3—C4	115.63 (9)	H101—C10—H103	109.4 (13)
F—C3—C2	118.79 (9)	H102—C10—H103	108.6 (13)
C4—C3—C2	125.57 (9)	N—C11—C12	110.95 (8)
C3—C4—C5	117.98 (10)	N—C11—C13	114.87 (9)
C3—C4—H4	119.6 (8)	C12—C11—C13	110.69 (9)
C5—C4—H4	122.4 (8)	N—C11—H11	104.7 (7)
C4—C5—C6	119.56 (9)	C12—C11—H11	107.7 (7)
C4—C5—H5	120.0 (9)	C13—C11—H11	107.4 (7)
C6—C5—H5	120.4 (9)	C11—C12—H121	110.5 (9)
C5—C6—C1	121.56 (9)	C11—C12—H122	110.7 (8)
C5—C6—H6	119.4 (8)	H121—C12—H122	110.6 (12)
C1—C6—H6	119.0 (8)	C11—C12—H123	108.9 (9)
N—C7—C1	114.66 (8)	H121—C12—H123	107.5 (12)
N—C7—H71	106.9 (8)	H122—C12—H123	108.5 (12)
C1—C7—H71	110.4 (8)	C11—C13—H131	112.1 (9)
N—C7—H72	110.9 (8)	C11—C13—H132	111.7 (9)

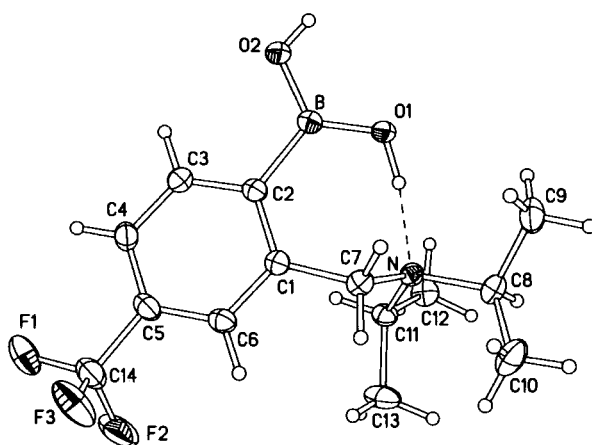
C1—C7—H72	107.3 (8)	H131—C13—H132	108.3 (12)
H71—C7—H72	106.5 (11)	C11—C13—H133	107.7 (10)
N—C8—C9	109.79 (8)	H131—C13—H133	108.9 (13)
N—C8—C10	115.74 (8)	H132—C13—H133	108.0 (13)
C6—C1—C2—C3	-1.12 (13)	C4—C5—C6—C1	1.26 (17)
C7—C1—C2—C3	-177.09 (9)	C2—C1—C6—C5	-0.52 (15)
C6—C1—C2—B	176.54 (9)	C7—C1—C6—C5	175.72 (10)
C7—C1—C2—B	0.58 (14)	C11—N—C7—C1	-52.79 (10)
O1—B—C2—C3	-155.70 (10)	C8—N—C7—C1	176.46 (8)
O2—B—C2—C3	25.22 (14)	C6—C1—C7—N	121.99 (9)
O1—B—C2—C1	26.77 (15)	C2—C1—C7—N	-61.89 (12)
O2—B—C2—C1	-152.31 (10)	C7—N—C8—C9	-86.74 (10)
C1—C2—C3—F	-177.32 (8)	C11—N—C8—C9	143.54 (9)
B—C2—C3—F	4.93 (14)	C7—N—C8—C10	37.50 (12)
C1—C2—C3—C4	2.24 (15)	C11—N—C8—C10	-92.23 (11)
B—C2—C3—C4	-175.51 (10)	C7—N—C11—C12	163.88 (8)
F—C3—C4—C5	177.99 (10)	C8—N—C11—C12	-66.95 (10)
C2—C3—C4—C5	-1.59 (17)	C7—N—C11—C13	-69.64 (11)
C3—C4—C5—C6	-0.26 (17)	C8—N—C11—C13	59.53 (11)

Hydrogen-bond geometry (Å, °)

<i>D</i> —H... <i>A</i>	<i>D</i> —H	H... <i>A</i>	<i>D</i> ... <i>A</i>	<i>D</i> —H... <i>A</i>
O1—H01...N	0.960 (19)	1.659 (19)	2.6069 (11)	168.5 (17)
O2—H02...O1 ⁱ	0.895 (18)	1.872 (19)	2.7646 (11)	174.9 (17)

Symmetry codes: (i) $-x+1, -y+1, -z+1$.

N,N-Diisopropyl-5-trifluoromethylbenzylamine-2-boronic acid 108



Crystal data

$C_{14}H_{21}BF_3NO_2$

$D_x = 1.311 \text{ Mg m}^{-3}$

$M_r = 303.13$

Melting point: 389 K

Monoclinic, $P2_1/c$

Mo $K\alpha$ radiation
 $\lambda = 0.71073 \text{ \AA}$

Hall symbol: ?

Cell parameters from 5776 reflections

$a = 15.4653 (18) \text{ \AA}$

$\theta = 2.7\text{--}29.0^\circ$

$b = 7.7851 (9) \text{ \AA}$

$\mu = 0.11 \text{ mm}^{-1}$

$c = 13.2548 (15) \text{ \AA}$

$T = 120.(2) \text{ K}$

$\beta = 105.71 (1)^\circ$

Cell measurement pressure: ? kPa

$V = 1536.2 (3) \text{ \AA}^3$

Parallelepiped, colourless

$Z = 4$

$0.65 \times 0.27 \times 0.13 \text{ mm}$

$F_{000} = 640$

Data collection

Siemens IK CCD area detector
diffractometer

4059 independent reflections

Radiation source: fine-focus sealed tube 3248 reflections with $I > 2\sigma(I)$

Monochromator: graphite

$R_{\text{int}} = 0.040$

Detector resolution: 8 pixels mm^{-1}

$\theta_{\text{max}} = 29.0^\circ$

$T = 120(2) \text{ K}$

$\theta_{\text{min}} = 1.4^\circ$

$P = ? \text{ kPa}$

$h = -21 \rightarrow 21$

ω scans $k = -10 \rightarrow 8$
 Absorption correction: none $l = -17 \rightarrow 18$
 12199 measured reflections

Refinement

Refinement on F^2	Secondary atom site location: difference Fourier map
Least-squares matrix: full	Hydrogen site location: difference Fourier map
$R[F^2 > 2\sigma(F^2)] = 0.042$	All H-atom parameters refined
$wR(F^2) = 0.112$	$w = 1/[\sigma^2(F_o^2) + (0.0537P)^2 + 0.4413P]$ where $P = (F_o^2 + 2F_c^2)/3$
$S = 1.03$	$(\Delta/\sigma)_{\max} < 0.001$
4059 reflections	$\Delta\rho_{\max} = 0.37 \text{ e } \text{\AA}^{-3}$
274 parameters	$\Delta\rho_{\min} = -0.22 \text{ e } \text{\AA}^{-3}$
? constraints	Extinction correction: none
Primary atom site location: structure-invariant direct methods	

Fractional atomic coordinates and isotropic or equivalent isotropic displacement parameters (\AA^2)

	x	y	z	$U_{\text{iso}}^*/U_{\text{eq}}$
F1	-0.04871 (6)	0.19887 (15)	0.25827 (8)	0.0519 (3)
F2	-0.03995 (6)	0.36853 (14)	0.13451 (9)	0.0590 (3)
F3	-0.00168 (6)	0.10517 (14)	0.13111 (9)	0.0558 (3)
O1	0.42355 (5)	0.54575 (11)	0.38103 (7)	0.02086 (19)
H01	0.3940 (13)	0.592 (3)	0.3138 (16)	0.051 (5)*
O2	0.40227 (6)	0.36640 (12)	0.51644 (7)	0.0239 (2)
H02	0.4535 (13)	0.400 (2)	0.5481 (15)	0.042 (5)*
N	0.33121 (6)	0.62897 (12)	0.19055 (7)	0.0176 (2)
B	0.37216 (8)	0.43470 (17)	0.41867 (10)	0.0185 (3)
C1	0.24101 (8)	0.39282 (14)	0.24273 (9)	0.0183 (2)
C2	0.27388 (7)	0.38147 (14)	0.35321 (9)	0.0182 (2)
C3	0.21545 (8)	0.32020 (16)	0.40924 (10)	0.0226 (2)
H3	0.2368 (10)	0.312 (2)	0.4869 (12)	0.024 (4)*
C4	0.12719 (8)	0.27287 (17)	0.36044 (11)	0.0261 (3)

H4	0.0885 (11)	0.233 (2)	0.4002 (13)	0.031 (4)*
C5	0.09671 (8)	0.28502 (16)	0.25274 (10)	0.0245 (3)
C6	0.15302 (8)	0.34364 (15)	0.19437 (10)	0.0222 (2)
H6	0.1316 (11)	0.355 (2)	0.1182 (13)	0.031 (4)*
C7	0.29767 (8)	0.45064 (15)	0.17162 (9)	0.0201 (2)
H71	0.3515 (10)	0.3769 (19)	0.1829 (11)	0.021 (3)*
H72	0.2614 (9)	0.4353 (18)	0.0989 (11)	0.018 (3)*
C8	0.39251 (9)	0.67397 (16)	0.12391 (10)	0.0232 (3)
H8	0.3939 (9)	0.7999 (19)	0.1202 (11)	0.019 (3)*
C9	0.48805 (9)	0.61623 (19)	0.17775 (12)	0.0310 (3)
H91	0.5109 (12)	0.676 (2)	0.2481 (15)	0.043 (5)*
H92	0.5272 (12)	0.648 (2)	0.1316 (14)	0.042 (5)*
H93	0.4922 (11)	0.491 (2)	0.1858 (13)	0.040 (5)*
C10	0.36478 (12)	0.6045 (2)	0.01183 (11)	0.0357 (3)
H101	0.3712 (12)	0.477 (3)	0.0111 (14)	0.043 (5)*
H102	0.4046 (11)	0.657 (2)	-0.0257 (13)	0.037 (4)*
H103	0.3032 (13)	0.633 (2)	-0.0255 (14)	0.045 (5)*
C11	0.25743 (8)	0.75506 (15)	0.18702 (10)	0.0208 (2)
H11	0.2263 (10)	0.7100 (19)	0.2367 (11)	0.021 (3)*
C12	0.29520 (9)	0.92955 (17)	0.22834 (11)	0.0257 (3)
H121	0.3429 (11)	0.917 (2)	0.2925 (13)	0.031 (4)*
H122	0.3179 (10)	0.995 (2)	0.1756 (12)	0.032 (4)*
H123	0.2466 (12)	0.995 (2)	0.2414 (14)	0.045 (5)*
C13	0.18820 (10)	0.7746 (2)	0.08090 (12)	0.0354 (3)
H131	0.2150 (12)	0.834 (2)	0.0289 (14)	0.043 (5)*
H132	0.1615 (14)	0.663 (3)	0.0544 (16)	0.056 (5)*
H133	0.1401 (14)	0.848 (3)	0.0892 (16)	0.055 (5)*
C14	0.00183 (9)	0.23892 (19)	0.19500 (12)	0.0338 (3)

Atomic displacement parameters (\AA^2)

	U^{11}	U^{22}	U^{33}	U^{12}	U^{13}	U^{23}
F1	0.0209 (4)	0.0701 (7)	0.0635 (6)	-0.0121 (4)	0.0096 (4)	0.0027 (5)
F2	0.0308 (5)	0.0505 (6)	0.0744 (7)	-0.0066 (4)	-0.0222 (5)	0.0180 (5)

F3	0.0350 (5)	0.0556 (6)	0.0703 (7)	-0.0181 (5)	0.0030 (5)	-0.0278 (5)
O1	0.0186 (4)	0.0226 (4)	0.0187 (4)	-0.0025 (3)	0.0004 (3)	0.0029 (3)
O2	0.0211 (4)	0.0283 (5)	0.0191 (4)	-0.0040 (4)	0.0001 (3)	0.0039 (3)
N	0.0193 (5)	0.0162 (5)	0.0171 (4)	0.0002 (4)	0.0047 (4)	0.0006 (4)
B	0.0183 (6)	0.0171 (6)	0.0193 (6)	0.0010 (5)	0.0035 (5)	-0.0012 (5)
C1	0.0199 (5)	0.0136 (5)	0.0205 (5)	0.0002 (4)	0.0042 (4)	-0.0005 (4)
C2	0.0181 (5)	0.0143 (5)	0.0208 (5)	0.0008 (4)	0.0027 (4)	0.0001 (4)
C3	0.0229 (6)	0.0215 (6)	0.0226 (6)	-0.0002 (5)	0.0048 (5)	0.0034 (5)
C4	0.0217 (6)	0.0250 (6)	0.0322 (7)	-0.0026 (5)	0.0083 (5)	0.0052 (5)
C5	0.0175 (5)	0.0196 (6)	0.0325 (7)	-0.0019 (4)	0.0003 (5)	0.0008 (5)
C6	0.0218 (6)	0.0188 (6)	0.0225 (6)	-0.0007 (4)	0.0001 (5)	-0.0006 (5)
C7	0.0246 (6)	0.0170 (5)	0.0185 (6)	-0.0011 (4)	0.0056 (4)	-0.0023 (4)
C8	0.0301 (6)	0.0198 (6)	0.0224 (6)	-0.0011 (5)	0.0114 (5)	0.0024 (5)
C9	0.0273 (6)	0.0302 (7)	0.0409 (8)	0.0017 (5)	0.0182 (6)	0.0062 (6)
C10	0.0516 (9)	0.0364 (8)	0.0237 (7)	-0.0065 (7)	0.0181 (7)	-0.0015 (6)
C11	0.0192 (5)	0.0186 (6)	0.0227 (6)	0.0030 (4)	0.0023 (4)	0.0019 (4)
C12	0.0296 (6)	0.0189 (6)	0.0279 (7)	0.0020 (5)	0.0067 (5)	-0.0012 (5)
C13	0.0307 (7)	0.0315 (8)	0.0337 (8)	0.0042 (6)	-0.0090 (6)	0.0040 (6)
C14	0.0220 (6)	0.0325 (7)	0.0419 (8)	-0.0052 (5)	0.0001 (6)	0.0017 (6)

Geometric parameters (Å, °)

F1—C14	1.3292 (18)	C6—H6	0.977 (16)
F2—C14	1.3408 (18)	C7—H71	0.988 (15)
F3—C14	1.3339 (18)	C7—H72	0.982 (14)
O1—B	1.3575 (15)	C8—C9	1.5242 (19)
O1—H01	0.96 (2)	C8—C10	1.5293 (19)
O2—B	1.3609 (16)	C8—H8	0.982 (15)
O2—H02	0.83 (2)	C9—H91	1.016 (19)
N—C7	1.4795 (15)	C9—H92	1.001 (18)
N—C11	1.4962 (15)	C9—H93	0.982 (19)
N—C8	1.5017 (15)	C10—H101	0.99 (2)
B—C2	1.5876 (17)	C10—H102	0.979 (17)
C1—C6	1.3917 (16)	C10—H103	0.972 (19)

C1—C2	1.4169 (16)	C11—C12	1.5210 (17)
C1—C7	1.5187 (16)	C11—C13	1.5271 (18)
C2—C3	1.3997 (16)	C11—H11	0.979 (15)
C3—C4	1.3925 (17)	C12—H121	0.968 (17)
C3—H3	0.995 (15)	C12—H122	1.003 (16)
C4—C5	1.3801 (19)	C12—H123	0.964 (19)
C4—H4	0.949 (17)	C13—H131	1.007 (19)
C5—C6	1.3892 (18)	C13—H132	0.98 (2)
C5—C14	1.5031 (18)	C13—H133	0.97 (2)
B—O1—H01	113.8 (12)	C10—C8—H8	108.0 (8)
B—O2—H02	113.1 (13)	C8—C9—H91	110.3 (10)
C7—N—C11	112.39 (9)	C8—C9—H92	108.1 (10)
C7—N—C8	111.55 (9)	H91—C9—H92	109.4 (15)
C11—N—C8	115.22 (9)	C8—C9—H93	111.7 (10)
O1—B—O2	121.02 (11)	H91—C9—H93	111.0 (14)
O1—B—C2	122.31 (11)	H92—C9—H93	106.2 (14)
O2—B—C2	116.65 (10)	C8—C10—H101	111.0 (10)
C6—C1—C2	119.43 (11)	C8—C10—H102	107.2 (10)
C6—C1—C7	116.89 (10)	H101—C10—H102	109.4 (14)
C2—C1—C7	123.64 (10)	C8—C10—H103	113.1 (11)
C3—C2—C1	117.84 (10)	H101—C10—H103	107.8 (15)
C3—C2—B	117.33 (10)	H102—C10—H103	108.2 (15)
C1—C2—B	124.82 (10)	N—C11—C12	111.07 (10)
C4—C3—C2	122.43 (12)	N—C11—C13	115.63 (11)
C4—C3—H3	118.3 (9)	C12—C11—C13	110.37 (11)
C2—C3—H3	119.3 (9)	N—C11—H11	104.7 (9)
C5—C4—C3	118.66 (12)	C12—C11—H11	106.8 (9)
C5—C4—H4	120.4 (10)	C13—C11—H11	107.7 (9)
C3—C4—H4	120.9 (10)	C11—C12—H121	110.5 (10)
C4—C5—C6	120.56 (11)	C11—C12—H122	112.1 (9)
C4—C5—C14	121.55 (12)	H121—C12—H122	109.8 (13)
C6—C5—C14	117.88 (12)	C11—C12—H123	107.3 (11)
C5—C6—C1	121.07 (11)	H121—C12—H123	110.0 (14)

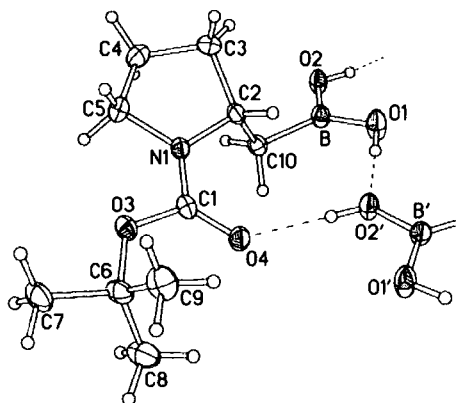
C5—C6—H6	121.0 (9)	H122—C12—H123	106.9 (14)
C1—C6—H6	117.9 (9)	C11—C13—H131	111.1 (10)
N—C7—C1	114.05 (9)	C11—C13—H132	111.3 (12)
N—C7—H71	106.1 (9)	H131—C13—H132	111.7 (16)
C1—C7—H71	109.8 (8)	C11—C13—H133	108.9 (12)
N—C7—H72	111.2 (8)	H131—C13—H133	106.2 (16)
C1—C7—H72	107.5 (8)	H132—C13—H133	107.4 (17)
H71—C7—H72	108.1 (11)	F1—C14—F3	106.71 (12)
N—C8—C9	110.01 (10)	F1—C14—F2	106.45 (12)
N—C8—C10	115.67 (11)	F3—C14—F2	106.12 (13)
C9—C8—C10	109.39 (12)	F1—C14—C5	113.24 (12)
N—C8—H8	106.8 (8)	F3—C14—C5	112.08 (12)
C9—C8—H8	106.6 (8)	F2—C14—C5	111.76 (11)
C6—C1—C2—C3	0.08 (16)	C8—N—C7—C1	175.55 (10)
C7—C1—C2—C3	-177.69 (11)	C6—C1—C7—N	119.91 (11)
C6—C1—C2—B	-179.37 (11)	C2—C1—C7—N	-62.27 (15)
C7—C1—C2—B	2.86 (18)	C7—N—C8—C9	-85.26 (12)
O1—B—C2—C3	-157.36 (11)	C11—N—C8—C9	145.04 (11)
O2—B—C2—C3	21.12 (16)	C7—N—C8—C10	39.27 (15)
O1—B—C2—C1	22.09 (18)	C11—N—C8—C10	-90.43 (13)
O2—B—C2—C1	-159.42 (11)	C7—N—C11—C12	168.36 (10)
C1—C2—C3—C4	-0.76 (18)	C8—N—C11—C12	-62.35 (13)
B—C2—C3—C4	178.73 (11)	C7—N—C11—C13	-64.88 (14)
C2—C3—C4—C5	0.78 (19)	C8—N—C11—C13	64.40 (14)
C3—C4—C5—C6	-0.12 (19)	C4—C5—C14—F1	4.47 (19)
C3—C4—C5—C14	-178.98 (12)	C6—C5—C14—F1	-174.42 (12)
C4—C5—C6—C1	-0.54 (19)	C4—C5—C14—F3	-116.33 (15)
C14—C5—C6—C1	178.36 (12)	C6—C5—C14—F3	64.79 (16)
C2—C1—C6—C5	0.55 (18)	C4—C5—C14—F2	124.69 (15)
C7—C1—C6—C5	178.48 (11)	C6—C5—C14—F2	-54.20 (17)
C11—N—C7—C1	-53.29 (13)		

Hydrogen-bond geometry (Å, °)

<i>D</i> —H... <i>A</i>	<i>D</i> —H	H... <i>A</i>	<i>D</i> ... <i>A</i>	<i>D</i> —H... <i>A</i>
O1—H01...N	0.96 (2)	1.68 (2)	2.6232 (13)	166.8 (19)
O2—H02...O1 ⁱ	0.83 (2)	1.93 (2)	2.7547 (13)	174.3 (19)

Symmetry codes: (i) $-x+1, -y+1, -z+1$.

(*S*)-pyrrolidine-1-carboxylic acid *tert*-butyl-ester-2-methyl boronic acid 267



Crystal data

$C_{10}H_{20}BNO_4$

$M_r = 229.08$

Orthorhombic, $P2_12_12_1$

Hall symbol: ?

$a = 9.3385$ (9) Å

$b = 11.5001$ (11) Å

$c = 12.0643$ (11) Å

$V = 1295.6$ (2) Å³

$Z = 4$

$F_{000} = 496$

$D_x = 1.174$ Mg m⁻³

Melting point: ? K

Mo $K\alpha$ radiation
 $\lambda = 0.71073$ Å

Cell parameters from 7045 reflections

$\theta = 2.5$ – 29.0°

$\mu = 0.09$ mm⁻¹

$T = 120$ (2) K

Cell measurement pressure: ? kPa

Block, colourless

$0.75 \times 0.45 \times 0.20$ mm

Data collection

CCD area detector
diffractometer

13209 measured reflections

Radiation source: fine-focus sealed tube 1968 independent reflections
 Monochromator: graphite 1798 reflections with $I > 2\sigma(I)$
 Detector resolution: ? pixels mm^{-1} $R_{\text{int}} = 0.037$
 $T = 120(2)$ K $\theta_{\text{max}} = 29.0^\circ$
 $P = ?$ kPa $\theta_{\text{min}} = 2.5^\circ$
 phi and ω scans $h = -12 \rightarrow 11$
 Absorption correction: multi-scan SADABS 2.10 (Bruker, 2003) $k = -15 \rightarrow 15$
 $T_{\text{min}} = 0.874, T_{\text{max}} = 1.000$ $l = -16 \rightarrow 16$

Refinement

Refinement on F^2 Secondary atom site location: difference Fourier map
 Least-squares matrix: full Hydrogen site location: difference Fourier map
 $R[F^2 > 2\sigma(F^2)] = 0.031$ All H-atom parameters refined
 $wR(F^2) = 0.077$ $w = 1/[\sigma^2(F_o^2) + (0.0469P)^2 + 0.0994P]$
 where $P = (F_o^2 + 2F_c^2)/3$
 $S = 1.03$ $(\Delta/\sigma)_{\text{max}} = 0.001$
 1968 reflections $\Delta\rho_{\text{max}} = 0.18 \text{ e } \text{\AA}^{-3}$
 225 parameters $\Delta\rho_{\text{min}} = -0.16 \text{ e } \text{\AA}^{-3}$
 ? constraints Extinction correction: none
 Primary atom site location: structure-invariant direct methods

Fractional atomic coordinates and isotropic or equivalent isotropic displacement parameters (\AA^2)

	<i>x</i>	<i>y</i>	<i>z</i>	$U_{\text{iso}}^*/U_{\text{eq}}$
B	0.08781 (17)	0.25166 (14)	0.50012 (14)	0.0200 (3)
O1	0.19867 (12)	0.17739 (9)	0.50937 (10)	0.0298 (3)
H01	0.283 (3)	0.213 (2)	0.503 (2)	0.053 (7)*
O2	-0.04763 (11)	0.20865 (9)	0.50966 (9)	0.0230 (2)
H02	-0.052 (2)	0.141 (2)	0.5283 (18)	0.049 (7)*
O3	0.35581 (11)	0.68124 (8)	0.34303 (8)	0.0234 (2)
O4	0.41529 (11)	0.51781 (8)	0.44002 (8)	0.0238 (2)
N1	0.20960 (12)	0.52995 (10)	0.34006 (9)	0.0184 (2)
C1	0.33376 (15)	0.57160 (11)	0.37901 (11)	0.0191 (3)

C2	0.16457 (15)	0.40863 (11)	0.35915 (11)	0.0180 (3)
H2	0.2489 (19)	0.3578 (15)	0.3452 (13)	0.020 (4)*
C3	0.05019 (19)	0.39207 (13)	0.26907 (13)	0.0287 (3)
H31	0.103 (2)	0.3702 (18)	0.1959 (17)	0.037 (5)*
H32	-0.023 (2)	0.3347 (19)	0.2904 (16)	0.038 (5)*
C4	-0.01351 (18)	0.51336 (14)	0.25333 (14)	0.0300 (3)
H41	-0.082 (2)	0.5296 (18)	0.3166 (16)	0.037 (5)*
H42	-0.061 (2)	0.5224 (18)	0.1819 (17)	0.042 (5)*
C5	0.11606 (17)	0.59301 (13)	0.26250 (12)	0.0240 (3)
H51	0.094 (2)	0.6709 (18)	0.2933 (15)	0.032 (5)*
H52	0.164 (2)	0.6014 (18)	0.1896 (17)	0.039 (5)*
C6	0.49237 (17)	0.74089 (13)	0.36452 (12)	0.0246 (3)
C7	0.4679 (2)	0.85843 (14)	0.31018 (14)	0.0330 (4)
H71	0.559 (2)	0.9055 (19)	0.3206 (17)	0.040 (5)*
H72	0.448 (2)	0.850 (2)	0.2312 (19)	0.049 (6)*
H73	0.387 (2)	0.904 (2)	0.3498 (18)	0.045 (6)*
C8	0.5167 (2)	0.75590 (16)	0.48835 (14)	0.0373 (4)
H81	0.431 (2)	0.7909 (18)	0.5227 (18)	0.043 (6)*
H82	0.542 (2)	0.684 (2)	0.5266 (17)	0.046 (6)*
H83	0.597 (2)	0.8112 (19)	0.4974 (18)	0.043 (5)*
C9	0.6128 (2)	0.67456 (16)	0.30876 (15)	0.0343 (4)
H92	0.601 (2)	0.6668 (19)	0.2314 (18)	0.045 (6)*
H92	0.627 (2)	0.6021 (19)	0.3463 (17)	0.044 (6)*
H93	0.703 (3)	0.718 (2)	0.3216 (17)	0.049 (6)*
C10	0.10697 (15)	0.38742 (11)	0.47650 (11)	0.0189 (3)
H101	0.016 (2)	0.4308 (15)	0.4873 (15)	0.029 (5)*
H102	0.175 (2)	0.4201 (15)	0.5304 (14)	0.025 (4)*

Atomic displacement parameters (\AA^2)

	U^{11}	U^{22}	U^{33}	U^{12}	U^{13}	U^{23}
B	0.0195 (7)	0.0180 (6)	0.0226 (6)	-0.0012 (5)	0.0008 (6)	0.0026 (5)
O1	0.0170 (5)	0.0209 (5)	0.0516 (7)	-0.0001 (4)	0.0019 (5)	0.0093 (5)
O2	0.0163 (5)	0.0177 (4)	0.0351 (5)	-0.0010 (4)	0.0007 (4)	0.0065 (4)

O3	0.0250 (5)	0.0163 (4)	0.0289 (5)	-0.0050 (4)	-0.0017 (4)	0.0045 (4)
O4	0.0210 (5)	0.0192 (4)	0.0312 (5)	-0.0012 (4)	-0.0042 (4)	0.0045 (4)
N1	0.0195 (6)	0.0141 (5)	0.0215 (5)	-0.0001 (4)	-0.0018 (4)	0.0026 (4)
C1	0.0221 (7)	0.0141 (5)	0.0212 (6)	0.0002 (5)	0.0032 (5)	0.0009 (5)
C2	0.0188 (6)	0.0128 (5)	0.0224 (6)	-0.0009 (5)	-0.0008 (5)	-0.0009 (5)
C3	0.0350 (9)	0.0223 (7)	0.0288 (7)	-0.0036 (7)	-0.0115 (6)	-0.0036 (6)
C4	0.0292 (8)	0.0286 (8)	0.0321 (7)	-0.0001 (6)	-0.0121 (6)	0.0037 (6)
C5	0.0276 (8)	0.0216 (6)	0.0229 (6)	0.0028 (6)	-0.0042 (6)	0.0044 (5)
C6	0.0278 (7)	0.0219 (7)	0.0240 (6)	-0.0109 (6)	0.0009 (5)	0.0013 (5)
C7	0.0484 (10)	0.0212 (7)	0.0293 (7)	-0.0115 (7)	0.0035 (7)	0.0032 (6)
C8	0.0536 (12)	0.0332 (8)	0.0251 (7)	-0.0179 (9)	-0.0028 (7)	0.0007 (7)
C9	0.0313 (9)	0.0321 (8)	0.0394 (8)	-0.0065 (7)	0.0078 (7)	0.0050 (7)
C10	0.0176 (6)	0.0162 (5)	0.0228 (6)	-0.0009 (5)	0.0014 (5)	0.0000 (5)

Geometric parameters (Å, °)

B—O1	1.3467 (19)	C4—H41	1.01 (2)
B—O2	1.3629 (18)	C4—H42	0.97 (2)
B—C10	1.597 (2)	C5—H51	0.99 (2)
O1—H01	0.89 (3)	C5—H52	0.99 (2)
O2—H02	0.81 (2)	C6—C9	1.517 (2)
O3—C1	1.3493 (16)	C6—C7	1.520 (2)
O3—C6	1.4711 (17)	C6—C8	1.521 (2)
O4—C1	1.2264 (16)	C7—H71	1.01 (2)
N1—C1	1.3396 (18)	C7—H72	0.97 (2)
N1—C5	1.4712 (17)	C7—H73	1.04 (2)
N1—C2	1.4753 (17)	C8—H81	0.99 (2)
C2—C10	1.5340 (18)	C8—H82	0.98 (2)
C2—C3	1.536 (2)	C8—H83	0.99 (2)
C2—H2	0.995 (17)	C9—H92	0.94 (2)
C3—C4	1.528 (2)	C9—H93	0.96 (2)
C3—H31	1.04 (2)	C9—H93	0.99 (2)
C3—H32	0.98 (2)	C10—H101	0.99 (2)
C4—C5	1.522 (2)	C10—H102	0.986 (18)

O1—B—O2	118.44 (13)	N1—C5—H52	110.1 (12)
O1—B—C10	123.27 (13)	C4—C5—H52	110.7 (12)
O2—B—C10	118.28 (12)	H51—C5—H52	109.7 (16)
B—O1—H01	112.2 (15)	O3—C6—C9	109.30 (12)
B—O2—H02	114.7 (17)	O3—C6—C7	102.02 (12)
C1—O3—C6	120.75 (11)	C9—C6—C7	111.57 (13)
C1—N1—C5	124.11 (12)	O3—C6—C8	110.82 (12)
C1—N1—C2	122.01 (11)	C9—C6—C8	112.47 (15)
C5—N1—C2	113.34 (11)	C7—C6—C8	110.19 (14)
O4—C1—N1	124.58 (12)	C6—C7—H71	107.2 (12)
O4—C1—O3	124.73 (13)	C6—C7—H72	111.3 (13)
N1—C1—O3	110.69 (12)	H71—C7—H72	109.3 (18)
N1—C2—C10	113.23 (10)	C6—C7—H73	111.0 (12)
N1—C2—C3	101.84 (11)	H71—C7—H73	106.6 (15)
C10—C2—C3	112.92 (12)	H72—C7—H73	111.1 (18)
N1—C2—H2	107.7 (10)	C6—C8—H81	109.8 (12)
C10—C2—H2	109.9 (9)	C6—C8—H82	113.8 (12)
C3—C2—H2	110.9 (9)	H81—C8—H82	110.3 (19)
C4—C3—C2	104.21 (12)	C6—C8—H83	107.1 (12)
C4—C3—H31	107.4 (11)	H81—C8—H83	108.0 (16)
C2—C3—H31	107.5 (11)	H82—C8—H83	107.7 (17)
C4—C3—H32	112.1 (12)	C6—C9—H92	113.5 (13)
C2—C3—H32	112.3 (12)	C6—C9—H92	109.1 (13)
H31—C3—H32	112.8 (16)	H92—C9—H92	113.6 (19)
C5—C4—C3	103.35 (13)	C6—C9—H93	107.8 (13)
C5—C4—H41	109.6 (11)	H92—C9—H93	107.6 (19)
C3—C4—H41	108.7 (12)	H92—C9—H93	104.6 (19)
C5—C4—H42	111.1 (12)	C2—C10—B	111.07 (11)
C3—C4—H42	112.5 (12)	C2—C10—H101	109.9 (11)
H41—C4—H42	111.3 (16)	B—C10—H101	111.9 (10)
N1—C5—C4	102.81 (11)	C2—C10—H102	108.8 (10)
N1—C5—H51	109.2 (11)	B—C10—H102	109.1 (10)
C4—C5—H51	114.1 (11)	H101—C10—H102	106.0 (14)

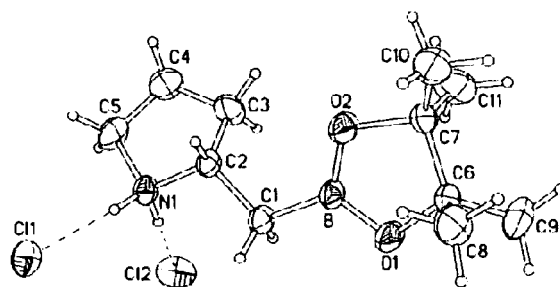
C5—N1—C1—O4	-176.83 (13)	C2—C3—C4—C5	38.72 (16)
C2—N1—C1—O4	-5.8 (2)	C1—N1—C5—C4	-175.32 (12)
C5—N1—C1—O3	3.94 (18)	C2—N1—C5—C4	12.99 (15)
C2—N1—C1—O3	174.94 (11)	C3—C4—C5—N1	-31.25 (15)
C6—O3—C1—O4	7.6 (2)	C1—O3—C6—C9	61.82 (16)
C6—O3—C1—N1	-173.13 (11)	C1—O3—C6—C7	-179.96 (12)
C1—N1—C2—C10	77.22 (16)	C1—O3—C6—C8	-62.67 (18)
C5—N1—C2—C10	-110.90 (13)	N1—C2—C10—B	-169.26 (12)
C1—N1—C2—C3	-161.25 (12)	C3—C2—C10—B	75.66 (15)
C5—N1—C2—C3	10.64 (15)	O1—B—C10—C2	68.22 (19)
N1—C2—C3—C4	-29.97 (15)	O2—B—C10—C2	-110.72 (15)
C10—C2—C3—C4	91.78 (14)		

Hydrogen-bond geometry (Å, °)

<i>D</i> —H \cdots <i>A</i>	<i>D</i> —H	H \cdots <i>A</i>	<i>D</i> \cdots <i>A</i>	<i>D</i> —H \cdots <i>A</i>
O1—H01 \cdots O2 ⁱ	0.89 (3)	1.83 (3)	2.7172 (15)	178 (2)
O2—H02 \cdots O4 ⁱⁱ	0.81 (2)	1.89 (2)	2.6964 (14)	172 (2)

Symmetry codes: (i) $x+1/2, -y+1/2, -z+1$; (ii) $x-1/2, -y+1/2, -z+1$.

(*S*)-2-(4,4,5,5-Tetramethyl-[1,3,2]dioxaborolan-2-ylmethyl)-pyrrolidinium chloride
271



Crystal data

$C_{11}H_{23}BNO_2^{1+} \cdot Cl^{1-}$

$M_r = 247.56$

Monoclinic, *C*2

$D_x = 1.131 \text{ Mg m}^{-3}$

Melting point: ? K

Mo $K\alpha$ radiation
 $\lambda = 0.71073 \text{ \AA}$

Hall symbol: ?	Cell parameters from 6172 reflections
$a = 22.004(4) \text{ \AA}$	$\theta = 2.7\text{--}27.5^\circ$
$b = 6.5982(12) \text{ \AA}$	$\mu = 0.25 \text{ mm}^{-1}$
$c = 10.0393(19) \text{ \AA}$	$T = 200(2) \text{ K}$
$\beta = 93.683(12)^\circ$	Cell measurement pressure: ? kPa
$V = 1454.5(5) \text{ \AA}^3$	Blade, colourless
$Z = 4$	$0.45 \times 0.35 \times 0.13 \text{ mm}$
$F_{000} = 536$	

Data collection

Siemens SMART 1K CCD area detector diffractometer	8899 measured reflections
Radiation source: fine-focus sealed tube	3349 independent reflections
Monochromator: graphite	2990 reflections with $I > 2\sigma(I)$
Detector resolution: 8 pixels mm^{-1}	$R_{\text{int}} = 0.022$
$T = 200(2) \text{ K}$	$\theta_{\text{max}} = 27.5^\circ$
$P = ? \text{ kPa}$	$\theta_{\text{min}} = 1.9^\circ$
ω scans	$h = -28 \rightarrow 28$
Absorption correction: multi-scan SADABS-2006/1	$k = -8 \rightarrow 8$
$T_{\text{min}} = 0.73, T_{\text{max}} = 0.97$	$l = -13 \rightarrow 13$

Refinement

Refinement on F^2	Secondary atom site location: difference Fourier map
Least-squares matrix: full	Hydrogen site location: inferred from neighbouring sites
$R[F^2 > 2\sigma(F^2)] = 0.051$	H atoms treated by a mixture of independent and constrained refinement
$wR(F^2) = 0.132$	$w = 1/[\sigma^2(F_o^2) + (0.0631P)^2 + 0.6355P]$ where $P = (F_o^2 + 2F_c^2)/3$
$S = 1.09$	$(\Delta/\sigma)_{\text{max}} = 0.007$
3349 reflections	$\Delta\rho_{\text{max}} = 0.38 \text{ e \AA}^{-3}$
195 parameters	$\Delta\rho_{\text{min}} = -0.16 \text{ e \AA}^{-3}$
10 restraints	Extinction correction: none

? constraints

Absolute structure: Flack H D (1983), Acta Cryst.
A39, 876-881

Primary atom site location: structure-invariant
direct methods

Flack parameter: 0.086 (84)

Fractional atomic coordinates and isotropic or equivalent isotropic displacement parameters (\AA^2)

	<i>x</i>	<i>y</i>	<i>z</i>	$U_{\text{iso}}^*/U_{\text{eq}}$	Occ. (<1)
Cl1	0.5000	0.27670 (17)	0.0000	0.0676 (3)	
Cl2	0.5000	0.35382 (18)	0.5000	0.0840 (4)	
O1	0.24128 (12)	0.4655 (5)	0.2897 (4)	0.0697 (9)	0.85
O2	0.27380 (11)	0.7586 (5)	0.1995 (4)	0.0743 (10)	0.85
O1'	0.2421 (7)	0.522 (2)	0.3181 (15)	0.042 (4)*	0.15
O2'	0.2680 (9)	0.703 (3)	0.168 (2)	0.065 (6)*	0.15
N	0.46572 (8)	0.5504 (3)	0.2311 (2)	0.0474 (4)	
H1N	0.4741 (12)	0.460 (4)	0.172 (3)	0.053 (7)*	
H2N	0.4728 (12)	0.477 (4)	0.314 (3)	0.052 (7)*	
C1	0.35631 (9)	0.4916 (4)	0.2672 (2)	0.0503 (5)	
H11	0.3668	0.4596	0.3622	0.060*	
H12	0.3584	0.3640	0.2159	0.060*	
C2	0.40263 (9)	0.6391 (4)	0.2187 (2)	0.0444 (4)	
H2	0.3918	0.6721	0.1229	0.053*	
C3	0.41135 (13)	0.8335 (5)	0.2977 (4)	0.0737 (8)	
H31	0.3814	0.9365	0.2644	0.088*	
H32	0.4063	0.8105	0.3938	0.088*	
C4	0.47526 (16)	0.9024 (5)	0.2764 (4)	0.0857 (10)	
H41	0.4746	1.0066	0.2054	0.103*	
H42	0.4942	0.9620	0.3595	0.103*	
C5	0.51016 (12)	0.7236 (5)	0.2354 (3)	0.0730 (9)	
H51	0.5446	0.6969	0.3014	0.088*	
H52	0.5264	0.7450	0.1468	0.088*	
C6	0.18566 (12)	0.5803 (5)	0.2511 (4)	0.0539 (7)	0.85
C7	0.20961 (11)	0.7981 (5)	0.2251 (3)	0.0562 (7)	0.85
C8	0.15606 (16)	0.4774 (7)	0.1282 (4)	0.0819 (11)	0.85
H81	0.1486	0.3341	0.1475	0.099 (8)*	0.85

H82	0.1836	0.4873	0.0555	0.099 (8)*	0.85
H83	0.1173	0.5438	0.1012	0.099 (8)*	0.85
C9	0.14402 (17)	0.5651 (9)	0.3645 (5)	0.0918 (13)	0.85
H91	0.1635	0.6121	0.4494	0.102 (8)*	0.85
H92	0.1326	0.4222	0.3729	0.102 (8)*	0.85
H93	0.1074	0.6460	0.3420	0.102 (8)*	0.85
C10	0.1824 (2)	0.8973 (9)	0.0989 (6)	0.0837 (14)	0.85
H101	0.1882	0.8143	0.0197	0.103 (9)*	0.85
H102	0.2027	1.0284	0.0894	0.103 (9)*	0.85
H103	0.1387	0.9192	0.1075	0.103 (9)*	0.85
C11	0.2079 (2)	0.9389 (7)	0.3437 (5)	0.0948 (13)	0.85
H111	0.2288	1.0667	0.3266	0.142 (12)*	0.85
H112	0.2283	0.8720	0.4215	0.142 (12)*	0.85
H113	0.1654	0.9669	0.3614	0.142 (12)*	0.85
C6'	0.1887 (8)	0.646 (3)	0.2935 (15)	0.053 (5)*	0.15
C7'	0.2034 (7)	0.722 (2)	0.1519 (14)	0.049 (3)*	0.15
C8'	0.1931 (13)	0.794 (4)	0.406 (2)	0.093 (7)*	0.15
H81'	0.1831	0.7278	0.4894	0.139*	0.15
H82'	0.1633	0.9014	0.3840	0.139*	0.15
H83'	0.2339	0.8533	0.4174	0.139*	0.15
C9'	0.1335 (10)	0.512 (4)	0.271 (3)	0.083 (6)*	0.15
H91'	0.1409	0.4247	0.1949	0.125*	0.15
H92'	0.0969	0.5935	0.2507	0.125*	0.15
H93'	0.1277	0.4278	0.3499	0.125*	0.15
C10'	0.1880 (16)	0.943 (4)	0.144 (3)	0.075 (9)*	0.15
H10'	0.2049	1.0168	0.2227	0.113*	0.15
H11'	0.1436	0.9581	0.1370	0.113*	0.15
H12'	0.2051	0.9974	0.0638	0.113*	0.15
C11'	0.1799 (9)	0.591 (3)	0.0407 (17)	0.066 (4)*	0.15
H13'	0.1912	0.4496	0.0581	0.099*	0.15
H14'	0.1977	0.6372	-0.0410	0.099*	0.15
H15'	0.1354	0.6026	0.0298	0.099*	0.15
B	0.28920 (10)	0.5747 (4)	0.2525 (3)	0.0466 (5)	

Atomic displacement parameters (\AA^2)

	U^{11}	U^{22}	U^{33}	U^{12}	U^{13}	U^{23}
Cl1	0.0680 (5)	0.0812 (6)	0.0557 (5)	0.000	0.0198 (4)	0.000
Cl2	0.1045 (8)	0.0811 (7)	0.0616 (5)	0.000	-0.0315 (5)	0.000
O1	0.0341 (11)	0.0523 (17)	0.122 (3)	-0.0038 (11)	0.0031 (13)	0.0171 (18)
O2	0.0307 (10)	0.0633 (18)	0.129 (3)	0.0006 (12)	0.0048 (12)	0.030 (2)
N	0.0304 (8)	0.0604 (12)	0.0514 (10)	-0.0036 (8)	0.0024 (7)	-0.0053 (9)
C1	0.0335 (9)	0.0578 (12)	0.0593 (12)	0.0003 (9)	0.0002 (8)	0.0107 (10)
C2	0.0318 (9)	0.0538 (12)	0.0474 (10)	0.0008 (8)	0.0004 (8)	0.0021 (9)
C3	0.0554 (14)	0.0601 (17)	0.106 (2)	-0.0030 (12)	0.0046 (14)	-0.0200 (16)
C4	0.0709 (18)	0.066 (2)	0.121 (3)	-0.0237 (16)	0.0126 (18)	-0.0092 (18)
C5	0.0421 (12)	0.082 (2)	0.094 (2)	-0.0238 (13)	0.0046 (13)	-0.0013 (16)
C6	0.0313 (12)	0.0541 (17)	0.077 (2)	0.0001 (12)	0.0044 (12)	0.0011 (17)
C7	0.0351 (12)	0.0571 (17)	0.0762 (18)	0.0039 (12)	0.0025 (11)	0.0048 (15)
C8	0.0561 (18)	0.083 (2)	0.105 (3)	-0.0031 (17)	-0.0118 (18)	-0.015 (2)
C9	0.063 (2)	0.117 (3)	0.099 (3)	-0.016 (2)	0.031 (2)	0.010 (3)
C10	0.069 (2)	0.094 (3)	0.087 (3)	0.009 (2)	-0.004 (2)	0.028 (3)
C11	0.103 (3)	0.071 (2)	0.109 (3)	-0.004 (2)	-0.002 (3)	-0.021 (2)
B	0.0309 (10)	0.0550 (14)	0.0538 (13)	-0.0028 (10)	0.0012 (9)	0.0039 (11)

Geometric parameters (\AA , $^\circ$)

O1—B	1.349 (4)	C7—C10	1.515 (5)
O1—C6	1.470 (4)	C8—H81	0.9815
O2—B	1.359 (4)	C8—H82	0.9812
O2—C7	1.475 (4)	C8—H83	0.9816
O1'—B	1.310 (16)	C9—H91	0.9807
O1'—C6'	1.44 (2)	C9—H92	0.9804
O2'—B	1.270 (19)	C9—H93	0.9806
O2'—C7'	1.43 (2)	C10—H101	0.9809
N—C5	1.503 (3)	C10—H102	0.9806
N—C2	1.504 (3)	C10—H103	0.9806
N—H1N	0.87 (3)	C11—H111	0.9808
N—H2N	0.97 (3)	C11—H112	0.9804

C1—C2	1.512 (3)	C11—H113	0.9805
C1—B	1.573 (3)	C6'—C8'	1.494 (18)
C1—H11	0.9899	C6'—C9'	1.508 (18)
C1—H12	0.9900	C6'—C7'	1.559 (16)
C2—C3	1.514 (4)	C7'—C11'	1.476 (17)
C2—H2	1.0000	C7'—C10'	1.499 (19)
C3—C4	1.506 (4)	C8'—H81'	0.9799
C3—H31	0.9901	C8'—H82'	0.9800
C3—H32	0.9900	C8'—H83'	0.9800
C4—C5	1.480 (5)	C9'—H91'	0.9799
C4—H41	0.9900	C9'—H92'	0.9800
C4—H42	0.9900	C9'—H93'	0.9801
C5—H51	0.9900	C10'—H10'	0.9800
C5—H52	0.9900	C10'—H11'	0.9802
C6—C9	1.510 (5)	C10'—H12'	0.9800
C6—C8	1.517 (5)	C11'—H13'	0.9801
C6—C7	1.558 (4)	C11'—H14'	0.9800
C7—C11	1.512 (5)	C11'—H15'	0.9800
B—O1—C6	107.7 (3)	O2—C7—C10	105.2 (3)
B—O2—C7	107.9 (2)	C11—C7—C10	111.4 (4)
B—O1'—C6'	115.2 (13)	O2—C7—C6	101.8 (2)
B—O2'—C7'	116.8 (16)	C11—C7—C6	114.1 (3)
C5—N—C2	107.5 (2)	C10—C7—C6	114.7 (3)
C5—N—H1N	112.1 (18)	O1'—C6'—C8'	103.3 (16)
C2—N—H1N	116.6 (17)	O1'—C6'—C9'	109.5 (16)
C5—N—H2N	106.8 (16)	C8'—C6'—C9'	120.5 (18)
C2—N—H2N	111.3 (15)	O1'—C6'—C7'	97.1 (13)
H1N—N—H2N	102 (2)	C8'—C6'—C7'	118.3 (16)
C2—C1—B	113.2 (2)	C9'—C6'—C7'	105.4 (14)
C2—C1—H11	109.0	O2'—C7'—C11'	109.5 (14)
B—C1—H11	109.0	O2'—C7'—C10'	107.9 (18)
C2—C1—H12	108.9	C11'—C7'—C10'	117.5 (17)
B—C1—H12	108.9	O2'—C7'—C6'	97.8 (13)

H11—C1—H12	107.7	C11 ['] —C7 ['] —C6 [']	114.8 (13)
N—C2—C1	111.14 (19)	C10 ['] —C7 ['] —C6 [']	107.5 (18)
N—C2—C3	101.61 (18)	C6 ['] —C8 ['] —H81 [']	110.3
C1—C2—C3	116.2 (2)	C6 ['] —C8 ['] —H82 [']	107.0
N—C2—H2	109.1	H91—C8 ['] —H82 [']	111.2
C1—C2—H2	109.0	H81 ['] —C8 ['] —H82 [']	109.5
C3—C2—H2	109.4	C6 ['] —C8 ['] —H83 [']	111.2
C4—C3—C2	105.7 (2)	H81 ['] —C8 ['] —H83 [']	109.5
C4—C3—H31	110.7	H82 ['] —C8 ['] —H83 [']	109.5
C2—C3—H31	110.2	C6 ['] —C9 ['] —H91 [']	106.7
C4—C3—H32	110.3	C6 ['] —C9 ['] —H92 [']	110.7
C2—C3—H32	111.2	H91 ['] —C9 ['] —H92 [']	109.5
H31—C3—H32	108.7	C6 ['] —C9 ['] —H93 [']	111.0
C5—C4—C3	107.7 (2)	H91 ['] —C9 ['] —H93 [']	109.5
C5—C4—H41	109.6	H92 ['] —C9 ['] —H93 [']	109.5
C3—C4—H41	110.0	C7 ['] —C10 ['] —H11 [']	108.9
C5—C4—H42	110.6	H10 ['] —C10 ['] —H11 [']	109.5
C3—C4—H42	110.4	C7 ['] —C10 ['] —H12 [']	107.7
H41—C4—H42	108.5	H10 ['] —C10 ['] —H12 [']	109.5
C4—C5—N	105.4 (2)	H11 ['] —C10 ['] —H12 [']	109.5
C4—C5—H51	110.1	C7 ['] —C11 ['] —H13 [']	110.4
N—C5—H51	110.6	C7 ['] —C11 ['] —H14 [']	108.2
C4—C5—H52	111.1	H13 ['] —C11 ['] —H14 [']	109.5
N—C5—H52	110.8	C7 ['] —C11 ['] —H15 [']	109.8
H51—C5—H52	108.7	H13 ['] —C11 ['] —H15 [']	109.5
O1—C6—C9	107.6 (3)	H14 ['] —C11 ['] —H15 [']	109.5
O1—C6—C8	106.9 (3)	O2 ['] —B—O1 [']	104.3 (13)
C9—C6—C8	109.5 (3)	O1—B—O2	113.9 (2)
O1—C6—C7	103.6 (2)	O2 ['] —B—C1	126.7 (10)
C9—C6—C7	114.6 (4)	O1 ['] —B—C1	128.9 (8)
C8—C6—C7	114.1 (3)	O1—B—C1	122.2 (2)
O2—C7—C11	108.6 (3)	O2—B—C1	123.8 (2)
C5—N—C2—C1	-157.6 (2)	B—O1 ['] —C6 ['] —C7 [']	25.2 (15)

C5—N—C2—C3	-33.3 (3)	B—O2'—C7'—C11'	-94.3 (18)
B—C1—C2—N	-178.34 (19)	B—O2'—C7'—C10'	136.8 (19)
B—C1—C2—C3	66.1 (3)	B—O2'—C7'—C6'	25.5 (19)
N—C2—C3—C4	33.1 (3)	O1'—C6'—C7'—O2'	-26.4 (15)
C1—C2—C3—C4	153.9 (2)	C8'—C6'—C7'—O2'	83 (2)
C2—C3—C4—C5	-21.6 (4)	C9'—C6'—C7'—O2'	-138.9 (16)
C3—C4—C5—N	0.7 (4)	O1'—C6'—C7'—C11'	89.3 (15)
C2—N—C5—C4	20.7 (3)	C8'—C6'—C7'—C11'	-161.4 (18)
B—O1—C6—C9	-138.0 (4)	C9'—C6'—C7'—C11'	-23 (2)
B—O1—C6—C8	104.5 (3)	O1'—C6'—C7'—C10'	-138.0 (19)
B—O1—C6—C7	-16.3 (4)	C8'—C6'—C7'—C10'	-29 (2)
B—O2—C7—C11	100.3 (4)	C9'—C6'—C7'—C10'	109 (2)
B—O2—C7—C10	-140.4 (4)	C7'—O2'—B—O1'	-11.1 (18)
B—O2—C7—C6	-20.4 (4)	C7'—O2'—B—C1	165.8 (10)
O1—C6—C7—O2	21.8 (4)	C6'—O1'—B—O2'	-11.1 (15)
C9—C6—C7—O2	138.7 (3)	C6'—O1'—B—C1	172.1 (8)
C8—C6—C7—O2	-94.0 (3)	C6—O1—B—O2	3.8 (5)
O1—C6—C7—C11	-94.9 (3)	C6—O1—B—C1	-175.0 (3)
C9—C6—C7—C11	22.0 (4)	C7—O2—B—O1	11.6 (4)
C8—C6—C7—C11	149.3 (3)	C7—O2—B—C1	-169.7 (3)
O1—C6—C7—C10	134.9 (4)	C2—C1—B—O2'	27.2 (11)
C9—C6—C7—C10	-108.3 (4)	C2—C1—B—O1'	-156.7 (8)
C8—C6—C7—C10	19.1 (4)	C2—C1—B—O1	179.7 (3)
B—O1'—C6'—C8'	-96.2 (17)	C2—C1—B—O2	1.1 (4)
B—O1'—C6'—C9'	134.3 (15)		

Hydrogen-bond geometry (Å, °)

<i>D</i> —H... <i>A</i>	<i>D</i> —H	H... <i>A</i>	<i>D</i> ... <i>A</i>	<i>D</i> —H... <i>A</i>
N—H1N...Cl1	0.87 (3)	2.21 (3)	3.072 (2)	170 (2)
N—H2N...Cl2	0.97 (3)	2.09 (3)	3.045 (2)	170 (2)

